A STUDY OF HOST-CHLAMYDIAL INTERACTIONS MEDIATED BY

INTERFERON-GAMMA AND NITRIC OXIDE

Krithika Rajaram

Submitted to the faculty of the University Graduate School

in partial fulfillment of the requirements

for the degree

Doctor of Philosophy

in the Department of Biology

Indiana University

February 2015

Accepted by the Graduate Faculty, Indiana University, in partial fulfillment of

the requirements for the degree of Doctor of Philosophy.

Doctoral Committee

David E. Nelson, Ph.D.

Melanie M. Marketon, Ph.D.

Cheng C. Kao, Ph.D.

Justin P. Kumar, Ph.D.

October 23rd, 2014

ACKNOWLEDGEMENTS

I have a reputation for making bad decisions. Having said that, I congratulate my twenty-one-year old self for deciding to arrive at Indiana University to pursue biology. Graduate school forced me to initiate independent thought, outfitted me with a wonderful set of friends, and provided a stimulating environment to immerse myself in. I have had the immense fortune of being supported by numerous people during my years at university; to them, I owe enormous debts of gratitude.

My mentor David Nelson possesses an enviable talent for proposing bold ideas with skillful incorporation of colorful analogies. He challenged me to confront scientific questions from untraditional angles and allowed me freedom to explore my ideas. And when they failed, he did not admonish, but expertly guided me out of my scientific crises. He has demonstrated immense patience in dealing with my tardiness, carelessly worded criticisms and a general defiance of policies. It has been a privilege to work with this phenomenal scientist and I am indebted to him for his support and encouragement.

My committee members Justin Kumar, Cheng Kao and Melanie Marketon teamed up to provide a valuable compass that steered me when I was faced with an impasse and cajoled me into killing bad projects. I thank them for their gracious donations of time and knowledge. Joe Pomerening recognized that I would enjoy teaching and invited me to direct his supplemental instruction

classes. I am deeply obliged to him for giving me the opportunity to learn while instructing.

My time in school would have no doubt doubled if not for my lab mates. Bao provided kinship and kind instruction. Jasmine was my first collaborator and together, we battled many challenges. Evelyn brought structure to the lab and expertise in techniques that were completely alien to me. Liam, Brent and Lindsey washed our dishes and made our mess magically disappear while providing much needed entertainment. Shuai's constant optimism and good humor were greatly appreciated, especially in times of despair. Amanda was forced to learn in a month, what had taken me a year to master so she could tackle *Chlamydia* with me. Julie served as our in-house biochemist and answered my naïve questions about proteins while keeping the eye rolling to a minimum. Matt became our fix-it man, and has saved us a lot of dollars and frustration. It has been a joy to collaborate with Bob Suchland at the University of Washington and Sandra and Rick Morrison at the University of Arkansas. Bob can trick *Chlamydia* into doing pretty much anything for him, and Sandra and Rick know more about the ways of mice than I can hope to learn in a lifetime.

Bloomington became my home away from home, importantly because of the people it drew. My cohorts Velocity, Carrie, Brynn and Lesley provided companionship and commiseration. Vid set a very high benchmark for future roommates. Meeting Vikas was like meeting an old friend for the first time. Jelling clothed and fed me and allowed me to torment her. Deepak and Anoop could always be counted on to engage me in amusing conversations over lunch or

iv

dinner. Dear friends from India – Shreyas, Anirudh, Balaji, Ramya, Prithvi, Priyanka, Vishnu, Sindhuri and Abhinav – ensured that I wasn't completely lost in a new land.

I have come to the conclusion that my partner in life and crime, Brent, is a superhero in disguise. Over the last several months, he has juggled many roles with extraordinary ease and little complaint. I could not have emerged out of this whole ordeal without his motivation.

I would have accomplished but little without the support of my family. My parents had to resign themselves to seeing their daughter once in a grand while so she could do what she wanted to do. My sister had to deal with an absentee sibling. Parvathi, who I am humbled to call family, taught me that I don't need much to be content. Thank you for your love and for the ridiculous amounts of faith you have in me.

Krithika Rajaram

A STUDY OF HOST-CHLAMYDIAL INTERACTIONS MEDIATED BY INTERFERON-GAMMA AND NITRIC OXIDE

The host response towards chlamydial infection mobilizes elements of both innate and adaptive immunity, culminating in the production of the Th1 cytokine interferon-gamma (IFN-γ). IFN-γ induces a variety of anti-chlamydial programs, many of which are unique to either humans or mice. Consequently, the human pathogen *Chlamydia trachomatis* and its near-identical murine relative *C. muridarum* have evolved to survive and cause disease in their respective hosts. Understanding the mechanisms that contribute to chlamydial niche specificity will facilitate the creation of improved mouse models for the study of human chlamydial disease. To this end, we examined a small chlamydial genomic region of extreme divergence called the Plasticity Zone (PZ) in *C. muridarum* for its alleged roles in host specificity and virulence. Using a newly adapted reverse genetic technique, we determined that much of the PZ is in fact dispensable in the murine genital tract. We concomitantly embarked on a screen for *C. muridarum* mutants that were no longer resistant to IFN-γ and uncovered a gain-of-function mutation in an ORF outside the PZ that led to dramatic attenuation in mice.

IFN-γ is secreted by multiple cell types including macrophages, which participate in innate as well as adaptive immune responses. IFNγ-dependent and -independent defense mechanisms mounted by macrophages contribute

significantly to bacterial clearance. Specifically, the amount of nitric oxide (NO) produced by macrophages in response to different infectious doses determines infection outcome in mice. We discovered that the *in vivo* regulation of infection by NO is also replicated in cell culture. Murine macrophage cell lines infected at high multiplicities of infection cause chlamydial death because of a massive NO response that is triggered by elevated levels of reactive oxygen species (ROS) and lysosomal cathepsin B activity.

Taken together, our work elucidates the mechanisms behind important host and chlamydial defense strategies, offering insight into the evolutionary adaptations that are a consequence of the relentless host-pathogen arms race.

David E. Nelson, Ph.D.

Melanie M. Marketon, Ph.D.

Cheng C. Kao, Ph.D.

October 23rd, 2014   Justin P. Kumar, Ph.D.

TABLE OF CONTENTS

Curriculum vitae

Chapter 4: Chlamydia muridarum infection of RAW 264.7 macrophages elicits bactericidal nitric oxide production via reactive oxygen species and Cathepsin B

LIST OF TABLES

CHAPTER 1

INTRODUCTION

Now, here, you see, it takes all the running you can do, just to keep in the same place. **The Red Queen in Lewis Carroll's Alice in Wonderland.**

About 2 billion years ago, seas of bacteria witnessed the arrival of predatory eukaryotes that immediately imposed upon them an enormous evolutionary challenge. Protozoan ancestors drove their prey to acquire or evolve genes that allowed survival within the predator and sometimes even exploitation of the new host, thus paving the way for the emergence of intracellular bacteria. The genomes of both host and intracellular bacterium have since been continually shaped by their association. Microorganisms of the phylum Chlamydiae are obligate intracellular bacteria that have their beginnings in the cytoplasm of primordial amoebae. While many of them still maintain endosymbiotic relationships with free-living amoebae, the best-known chlamydial species are important pathogens of humans and animals. In this chapter, I will introduce prominent members of the Chlamydiae, their exclusive lifestyle within eukaryotic cells, and the defense and counter-defense strategies evolved by the host and pathogen, respectively.

1.1 A brief history of Chlamydiae

Chlamydia trachomatis bears the distinction of being the first identified species of the phylum Chlamydiae. Originally discovered as the causative agent

of a blinding disease called trachoma, *C. trachomatis* has since also been recognized as a leading cause of human sexually transmitted disease (STD). The earliest mention of trachoma dates back to ancient China in 2600 B.C. and was discussed in the Hippocratic Corpus around 5 B.C. (1). By the nineteenth century, the disease was pandemic in the New World and Europe. However, the agent of trachoma was identified only in 1907 when Halberstaedter and Prowazek, on a scientific expedition in Java, discovered inclusion bodies within the cytoplasm of conjunctival epithelial cells from apes and humans with trachoma. In the following years, similar inclusion bodies were observed in patients suffering from urogenital infections, thus linking trachoma and sexually transmitted disease. Due to its small size and inability to grow outside of living cells, *Chlamydia trachomatis* was thought to be a virus for several decades. The discovery that it contained both DNA and RNA and was susceptible to antibiotics in the 1960s led to its reclassification as a bacterium (1).

The sequencing revolution in the 1990s brought with it an explosion of data with many sequences bearing considerable similarity to *C. trachomatis* (Fig. 1.1) (2, 3). The number of chlamydial families has increased from 1 to 8 in the last two decades. 16S rRNA phylogenetic analysis of chlamydial species revealed that these organisms are a deeply branching group within the phylogenetic tree of eubacteria, with only very remote relationships to other taxa (3). *Chlamydia*-like organisms have been recovered from various hosts including protists, birds, fish, reptiles and mammals. Regardless of origin, all characterized species appear to lead strict intracellular lifestyles.

1.2 *Chlamydia trachomatis* and its relatives

C. trachomatis is grouped into 15 serovars based on antigenic variation of the major outer membrane protein (MOMP) (4). The serovars exhibit unique tissue tropisms and varying disease presentation (5). Ocular serovars A - C are endemic in developing regions of the world where poor hygiene and poverty prevail. Repeat infections of the conjunctival epithelium can lead to scarring of the eye and trichiasis, and the resulting corneal damage can cause blindness. Infection of columnar epithelial cells in the genital tract by sexually transmitted serovars D - K can be asymptomatic or can lead to urethritis, cervicitis and epididymitis. Complications in women typically arise from untreated or persistent infections and reinfections to cause pelvic inflammatory disease (PID). Patients with PID are at increased risk for infertility, miscarriage and ectopic pregnancy. Serovars L1 – L3 are also sexually transmitted, but can invade the mucosal epithelia to attack lymphatic tissues resulting in a serious, systemic disease referred to as lymphogranuloma venereum (LGV) (5). Laboratory studies of *C. trachomatis* infections often employ primate models, or alternatively, utilize the *C. trachomatis* mouse agent of pneumonitis, recently renamed *C. muridarum*, in a mouse genital tract (GT) model of infection (6). *Chlamydia pneumoniae* is another ubiquitous pathogen that is a common cause of human and animal respiratory infections and is increasingly associated with a number of chronic illnesses including asthma, chronic obstructive pulmonary disease (COPD), atherosclerosis and Alzheimer's disease (7). On rare occasions, other species of *Chlamydia* that are primarily animal pathogens, such as *C. psittaci* and *C.*

abortus, can be zoonotically transmitted to humans. *C. psittaci,* acquired from feral birds and domestic poultry, can cause life-threatening pulmonary respiratory infections (8) and is classified as a CDC biothreat agent.

1.3 Intracellular life of *Chlamydia*

1.3.1 *Developmental cycle*

All recognized *Chlamydia* spp. exhibit a biphasic developmental cycle (Fig. 1.2) where the organism alternates between the elementary body (EB) and the reticulate body (RB) (Fig. 1.3) (9). The EB are small, extracellular infectious particles protected by a cysteine-rich protein coat. They have a highly condensed nucleus and were long thought to be metabolically inactive. Recent studies have challenged this dogma by demonstrating that EB are capable of moderate levels of respiratory activity and glucose metabolism (3, 10). To establish an intracellular infection, unknown EB ligands bind to receptors on target epithelial cells to facilitate endocytosis of the pathogen. Upon entry, the EB-containing phagosome dissociates from the endocytic pathway and remains in the cytosol as a parasitophorous vacuole referred to as an 'inclusion'. At 2 to 3 hours post infection, the EB begins its transformation into the larger, reticulate body concomitant with decondensation of the chromosome and reduction of the outer membrane disulfide bonds. During the replicative stage, RB undergo repeated divisions by binary fission while decorating the inclusion membrane with chlamydial proteins that are presumably involved in nutrient trafficking and immune evasion. At around 18 to 24 hours post infection, the RB begin their

differentiation to EB. The cellular signals that initiate these developmental transitions have not been identified. Between 24 to 48 hours depending on the chlamydial species, the mature inclusion primarily contains EB. The EB escape the host cell either by rupturing the inclusion and host cell membranes, or by extrusion of the inclusion, and they then proceed to infect neighboring cells (9).

1.3.2 *Subversion of host metabolism*

Chlamydiae modulate multiple host cellular pathways in order to secure their residence in the cytosol. Entry into host cells is facilitated by the recruitment of host actin cytoskeleton or alternatively by lipid raft-mediated processes (11-13). Within the first several minutes, chlamydial endosomes are stripped of early endocytic markers and they avoid fusion with the phagolysosomal trafficking pathway (14). Many of these initial events are mediated by EB proteins that are translocated into the host cytosol upon invasion (13). Among the early effectors are a subset of chlamydial inclusion membrane proteins (Incs) that localize to the nascent inclusion membrane via a Type III secretion system-dependent mechanism (14). The inclusion utilizes host microtubules to migrate to the perinuclear region where its proximity to the host secretory system allows it to exploit a rich supply of host nutrients (15). To support the growing inclusion, chlamydiae acquire several host lipids by recruiting lipid-laden vesicles and lipid droplets to the inclusion and possibly via IncD interaction with the cytosolic lipid transfer protein (CERT) (16, 17). *Chlamydia* also appears to depend on lysosomal protein degradation for amino acids (18). Electron microscopic

observation has revealed that chlamydial inclusions also associate with mitochondria (19). The pathogens have limited ATP synthesizing capabilities and might acquire mitochondrial ATP to supplement their energy requirements (2). *Chlamydia* spp. are incapable of *de novo* nucleotide synthesis and contain ATP/ADP translocases that facilitate the transport of host dNTPs across the chlamydial cell membrane (20). dNTPs are converted into other nucleotide intermediates by chlamydial ribonucleotide reductase and salvage enzymes (21).

1.3.3 *Host response to chlamydial infection*

Regardless of host tissue or chlamydial species, the epithelial cell is a primary target of chlamydial infection. The epithelial cell barrier is equipped with an array of innate defense mechanisms and can detect chlamydial products by means of pattern recognition receptors (PRRs) located on the cell surface and in the cytosol. Chlamydial ligands of these PRR include lipopolysaccharide (LPS), heat shock protein 60 (Hsp60), macrophage infectivity potentiator (Mip), MOMP and chlamydial nucleic acid metabolites (22-25). PRR-ligand interaction triggers a cellular signaling cascade that culminates in the activation of NF-$\kappa\beta$, IRF3 or mitogen activated protein kinase (MAPK) pathways (26, 27). The ensuing production of inflammatory cytokines and Type I interferons facilitates the recruitment of neutrophils and macrophages to the site of infection. These innate responders drive tissue-damaging inflammation while also inducing adaptive immunity. The complete resolution of chlamydial infection usually depends on the

production of the pro-inflammatory cytokine IFN-γ by innate cells and CD4⁺ Th1 cells (28).

Interestingly, many of the anti-chlamydial responses induced by IFN-γ appear to be host-specific. IFN-γ in human cells upregulates the expression of indoleamine 2, 3-deoxygenase (IDO), a host enzyme that depletes intracellular pools of tryptophan by catalyzing the first step in its degradation to N-formylkynurenine. It was observed that the treatment of human cell lines with IFN-γ completely inhibited the development of *Chlamydia* spp. (29). Growth could be restored to sexually transmitted serovars of *C. trachomatis*, but not ocular strains or *C. muridarum*, by the addition of exogenous indole (30, 31). That this pro-survival adaptation was specific to *C. trachomatis* STD strains suggested that tryptophan starvation was induced by IFN-γ in the female urogenital tract. Vaginal microbiome studies have revealed that patients with chlamydial STD have abnormally high levels of indole-producing bacteria that presumably supply *C. trachomatis* with this essential intermediate (32). The IFN-γ-mediated IDO response is also conserved in guinea pigs. The guinea pig-adapted species *Chlamydia caviae*, like genital *C. trachomatis*, is completely refractory to the effects of IFN-γ in human cells (33).

In murine cells, IFN-γ does not induce IDO upon chlamydial infection. Instead, it stimulates defense mechanisms that target *C. trachomatis* while leaving mouse-adapted *C. muridarum* largely unaffected (30). The observed *in vitro* susceptibility of *C. trachomatis* to IFN-γ is reflected in its rapid resolution from genital tract infections of mice. In contrast, *C. muridarum* is more virulent in

the mouse model and much of its clearance is executed by an IFN-γ-independent mechanism (28). Why *C. trachomatis* and *C. muridarum* display such remarkable differences in their susceptibilities to murine IFN-γ is unknown. Unlike the primarily IDO-dependent inhibition of chlamydiae in human cells, it appears that multiple IFN-γ-regulated pathways contribute to pathogen destruction in murine cells. This includes the production of nitric oxide (NO) by inducible nitric oxide synthase (iNOS), an enzyme that is highly upregulated in response to IFN-γ and chlamydial infection in murine epithelial cells and macrophages. In the absence of NO, chlamydiae persist in IFN-γ-treated cell lines and mice (34, 35). Apart from a failure to prevent chlamydial dissemination, iNOS $^{-/-}$ mice also exhibit excessive pathology. However, the addition of an iNOS inhibitor to IFN-γ-treated murine cells did not rescue *C. trachomatis* growth, implying that other effector mechanisms contributed to chlamydial species-specific inhibition (30). A microarray gene expression study of murine cells treated with IFN-γ discovered a cluster of upregulated genes that encoded GTPases of the Guanylate Binding Protein (GBP) and the Immunity Related GTPase (IRG) families (30). GBP and IRG proteins bind to the phagosomal membranes of many pathogens including *Toxoplasma gondii* and *Mycobacterium tuberculosis*. Once they are docked on the phagosome surface, the GTPases orchestrate the recruitment of various immune effectors including autophagic components and NADPH oxidase (36). Several IRG proteins including Irga6 and Irgb10 localize specifically to *C. trachomatis* inclusions to facilitate their elimination from murine epithelial cells (30, 37, 38). These studies suggest that the coordinated action of several IRGs,

nitric oxide and other unidentified mechanisms might be necessary for the prompt resolution of *C. trachomatis* infection from the mouse genital tract. It was recently revealed that unlike *C. muridarum*, clearance of *C. trachomatis* infection from the mouse GT can be achieved entirely by innate immune responses (39). The distinct behaviors of chlamydiae that naturally infect mice and humans has called into question the suitability of the mouse model for the study of adaptive immunity and vaccine development (28, 39). These difficulties might be partially overcome by genetically engineering humanized mice that lack mouse-specific anti-chlamydial pathways (40). Identification and characterization of mouse defense mechanisms is thus critical for improved investigation of human genital chlamydial disease in mice.

Several studies examining *C. pneumoniae* lung infections in human patients and mice have revealed that the organisms are not restricted to epithelia, but can infect and disseminate via monocytes and macrophages (7). While chlamydial growth within macrophages is severely limited and species dependent (41, 42), their survival as persistent, viable forms in these mobile cell populations can facilitate their transfer to more permissive endothelial and epithelial cells in distant sites of the host. In spite of their role in assisting the systemic spread of *C. pneumoniae*, macrophages are required for the eventual resolution of murine lung infection (43). Aside from IFN-γ secretion, macrophages are potent producers of oxidative radicals via iNOS and the phagocyte NADPH oxidase (phox) pathways. By direct association with the phagosomal membrane, phox can deliver reactive oxygen species (ROS) to bacteria within the

phagosome, thereby minimizing damage to the host. NO can interact with ROS to produce reactive nitrogen species (RNS) such as ONOO⁻, NO_2, and N_2O_3 (44). ROS and RNS act upon a variety of bacterial targets including thiols, lipids, DNA and enzyme metal centers. The importance of macrophage-derived NO in mice was confirmed in a recent study where the ability to limit *C. psittaci*-mediated respiratory disease was dependent on the amount of NO produced by the macrophages (45).

1.3.4 *Chlamydial adaptations to counter host immunity*

Comparative genome sequence analysis of diverse chlamydial species revealed a remarkable degree of genetic conservation (46). Various serovars of *C. trachomatis* and *C. muridarum* were found to differ by less than 1% in gene content (47). This meant that only a handful of genes and single nucleotide polymorphisms (SNPs) dictate differences in host/tissue specificity and disease sequelae. It has been hypothesized that differential host immune responses govern biological and pathological phenotypes of *Chlamydia*, and that species-specific chlamydial genes and alleles may have evolved to combat the defenses mounted by their respective hosts (46, 48).

Among genes with a high degree of polymorphism are *ompA* (MOMP) and a family of genes encoding polymorphic membrane proteins (*pmp*) (2, 49). MOMP, a cysteine-rich surface protein, is also the most abundant protein present in EB and RB. Multiple studies have suggested that MOMP plays a role in attachment at the chlamydial-host interface (50, 51). Infectivity potential and

tissue tropism have also been ascribed to MOMP (52, 53). However, a large phylogenetic analysis of MOMP sequences from various serovars and isolates of *C. trachomatis* found no correlation between MOMP and chlamydial phenotypes (54). Thus, the variations observed in MOMP may have simply accumulated in response to host immune selection.

Chlamydia spp. possess varying numbers of *pmp* genes, ranging from 9 in *C. trachomatis* to 21 in *C. pneumoniae* (55). Many roles have been attributed to chlamydial Pmps including host cell entry, virulence and tissue tropism (56). Support for a role in antigenic variation was provided by a recent study that discovered variable expression of Pmps within subpopulations of chlamydial inclusions (57).

Inclusion membrane protein genes (*inc)*, described in an earlier section, also belong to a polymorphic multigene family that arose by gene duplication (14). Variations in the Incs helped to separate *C. trachomatis* isolates into ocular, genital and LGV biovars (58). Many Incs have roles in inclusion fusion and trafficking as well as lipid transport (17, 59).

Finally, a small hypervariable region referred to as the 'plasticity zone' (PZ) has been identified near the replication terminus in all sequenced *Chlamydia* spp. (2, 46, 60). In the following section, I will briefly describe the various genes and gene families encoded by the PZ.

1.3.5 *The Plasticity Zone*

The chlamydial plasticity zone contains a collection of poorly conserved genes encoding incomplete metabolic pathways, pseudogenes and uncharacterized ORFs (Fig. 1.4) (46). Understanding why certain PZ genes have been left intact in one species but have been lost from another could provide insight into the distinct host selective pressures that *Chlamydia* spp. encounter in their unique niches. For instance, several species possess a tryptophan biosynthesis (*trp*) operon in the PZ that allows them to evade IDO-mediated tryptophan starvation in their host cells. *C. trachomatis* STD serovars contain a partial *trp* operon (*trpRBA*) that encodes a functional tryptophan synthase. This enzyme catalyzes the final step in tryptophan synthesis by utilizing indole as a substrate. In contrast, IDO-susceptible ocular serovars have accumulated inactivating mutations in *trpA* and cannot synthesize tryptophan from indole (Fig. 1.5) (31).

Why ocular strains of *C. trachomatis* have lost tryptophan synthase is a subject of much speculation (31). Unlike the female urogenital tract which supports an abundant indole-producing microflora, the more sterile environment of ocular tissues may not be able to supply chlamydiae with exogenous indole. An indole-poor niche would offer little reason for ocular strains to retain functional tryptophan synthase. That the mouse pathogen *C. muridarum* lacks a *trp* operon is explained by the absence of an IDO response in murine epithelial cells (30, 47). Finally, *C. caviae*, *C. felis* and *C. pecorum* contain an almost complete *trp* operon (*trpABFCDR*, *kynU*, *prsA*) which should theoretically allow these

organisms to convert host kynurenine to tryptophan via several intermediate steps (46, 61, 62). Interestingly, the *trp* gene cluster in *C. pecorum* is situated outside the PZ, but whether the location of the operon bears any significance in terms of its function or regulation is unknown.

While the *trp* operon offers a compelling argument for the role of the PZ in mediating tropism, the function of other PZ ORFs is unclear. A family of putative cyotoxins has generated considerable interest because of their homology to clostridial toxin TcdB and *E. coli* Efa1/LifA (Fig. 1.6 A) (63, 64). The cytotoxin ORFs are either present as full length copies in several chlamydial species or have undergone frameshifts and deletions as observed in different strains of *C. trachomatis* and are completely absent from *C. pneumoniae* and *C. abortus* genomes (60). Elementary bodies of *C. muridarum* and *C. trachomatis* serovar D are cytotoxic in cultured cells and induce dramatic alterations in actin cytoskeletal morphology. However, cells infected with EB of *C. trachomatis* serovar L2 display no cytotoxicity. These results correlate with the presence of three intact cytotoxin genes in *C. muridarum* (*tc0437–tc0439*), a partial ORF (*ct166*) in *C. trachomatis* serovar D and an almost complete deletion of the toxin ORFs in serovar L2 (Fig. 1.6 B) (64). Comparison of a representative *C. muridarum* cytotoxin TC0438 with TcdB and Efa1/LifA shows that the three proteins are of similar length and share a UDP glucose-binding domain as well as a glucosyltransferase domain (Fig. 1.6 A) (63). TcdB and Efa/LifA toxins utilize UDP-glucose as a substrate to inactivate Rho/Ras GTPases by glucosylation (65). The yersinial YopT cysteine protease domain (CPD) present in TC0438 and Efa1/LifA also inactivates Rho GTPases

by proteolytic cleavage. Active Rho/Ras GTPases regulate cytoskeletal dynamics by directly or indirectly affecting the polymerization of F-actin (66). The actin rearrangements observed in cells infected with cytotoxic EB suggest that chlamydial toxins also target Rho/Ras GTPases. In support of this, a recent study showed that ectopic expression of CT166 in HeLa cells induced cytoskeletal collapse in a Rac1 GTPase-dependent manner (67). CT166 lacks the YopT motif, implying that the observed cytotoxicity is likely mediated by the UDP glucose-binding and glucosyltransferase domains. Neither of these domains are retained in the truncated *C. trachomatis* serovar L2 cytotoxin ORF. Whether the chlamydial cytotoxins promote virulence and confer niche-specific advantages has not yet been determined.

A *guaBA-add* operon predicted to encode enzymes that catalyze the interconversion of AMP and GMP has been retained by *C. muridarum*, *C. psittaci* and *C. felis*. *C. pneumoniae* human strains contain inactivating mutations in *guaB* and the operon is entirely absent from animal isolates of *C. pneumoniae* and *C. trachomatis*. Similarly, *C. abortus* contains only a *guaB* pseudogene (60). Presence of this nucleotide synthesis pathway in only some *Chlamydia* spp. could indicate that purine nucleotides are a limiting nutrient in certain niches. This idea is supported by the observation that *guaB* and *guaA* null mutants of other pathogenic organisms including *F. tularensis*, *B. burgdorferi* and *S. typhimurium* are severely attenuated in mice (68-70).

Multiple phospholipase D (PLD) homologs are present in the PZs of *C. trachomatis*, *C. muridarum* and *C. pecorum* (61, 71). All pzPLDs contain HKD

(His-Lys-Asp) catalytic motifs that have shown to be important for their localization to vesicular membranes (72). The recent finding that CT156, a *C. trachomatis* pzPLD, associates with lipid droplets near the chlamydial inclusion implicates the PLDs in lipid acquisition and modification (16). Finally, many chlamydial PZs encode a protein with homology to eukaryotic membrane attack complex/perforin (MACPF) domains (71, 73). In eukaryotes, MAC and perforin (PF) perform critical functions in defense against microbial invaders. Components of the complement cascade (C5b, C6, C7, C8 and C9) form a lytic pore called the MAC on the surface of bacteria and protozoan parasites. Perforin, produced by cytotoxic T lymphocytes and natural killer cells, similarly lyses bacterial membranes by pore formation (74). Proteins containing MACPF domains have been found in many species of bacteria and function as virulence factors that promote host cell invasion. While a role for chlamydial MACPF has not been defined, their pore-forming capability could facilitate chlamydial exit from cells. Furthermore, these proteins might block host complement function by molecular mimickry (71).

In addition to the ORFs described here, chlamydial PZs encode other conserved and unique proteins of unknown function. Characterization of the PZ and its alleged roles in chlamydial infection and pathogenesis might reveal novel cognate host immune responses as well as improve our understanding of chlamydial biology.

1.4 Genetics in *Chlamydia*

Molecular dissection of the interactions between chlamydiae and their host cells has been hindered by a lack of genetic tools. The inability of chlamydiae to replicate in axenic media combined with their complex developmental cycle has rendered many traditional genetic methods unusable (75). The field has therefore relied heavily on comparative genomics between reference and clinical chlamydial strains to find correlations between species-specific alleles and pathogenesis (31, 60). Analysis of sequences from different reference serovars of *C. trachomatis* revealed frequent occurrence of horizontal DNA transfer between chlamydiae (56, 76). Extensive recombination events that have since been described in multiple clinical strains does not appear to be restricted to genomic 'hot spots' and is rather promiscuous (77). DeMars et al. and others applied these observations to cell culture infections and successfully generated intraspecies and interspecies recombinants between different antibiotic-resistant strains (78-80). Recombined regions appear to vary greatly in size, ranging from less than 15 bp to several thousand bp (80) (unpublished observations). Lateral gene transfer has since been used in combination with chemical mutagenesis methods to backcross mutants to a wild-type genome (81).

The use of ethyl methanesulfonate (EMS) as a chemical mutagen has gained popularity in chlamydial research in recent years (81, 82). The mutation rate elicited by EMS treatment can be approximated by calculating the frequency of rifampin-resistant chlamydial mutants recovered in response to different doses of the mutagen. EMS-generated mutant chlamydial libraries have been utilized in

both forward and reverse genetic approaches. Kari et al. established a reverse genetic system in chlamydiae by borrowing a technique from plant biologists called Targeting Induced Local Lesions IN Genomes (TILLING) (82). TILLING combines EMS mutagenesis with a PCR based screen to isolate induced point mutations within genes of interest. Chlamydial RB are exposed to an optimized dose of EMS and the surviving population is arrayed in 96-well plates in pools of roughly 10 EB per well. After a few passages in cell culture, the final harvest is subjected to genome extraction and PCR amplification for a 1kb region from the gene of interest. PCR products are then incubated briefly with the mismatch-specific endonuclease CEL1. The presence of multiple alleles in a given subpopulation leads to the formation of PCR heterodimers that are recognized and cleaved by CEL1. Wells containing a mixture of wild type and mutant alleles can be identified by gel electrophoretic separation of the digested PCR products. The nature of the mutation is finally determined by capillary sequencing and desired mutants are isolated from corresponding wells in storage plates by plaque cloning. As proof of principle, Kari et al. employed TILLING to recover a *trpB* null mutant of *C. trachomatis* serovar D that could no longer utilize indole (82).

Many chlamydial genes are poorly annotated or have no assigned function, making forward genetic approaches invaluable in the identification of new pathway components. In a recent study, Nguyen and Valdivia screened an EMS-generated mutant *C. trachomatis* library to identify mutants with abnormal glycogen metabolism and defective type II secretion (81). Phenotypic screens

have also been launched in our laboratory to identify chlamydial genes involved in development and immune resistance. The generation of single nucleotide polymorphisms by EMS mutagenesis has advantages over insertional gene inactivation in that gain-of-function mutants and conditional mutants can be recovered. However, a significant limitation of EMS when used at higher doses is that mutations in close proximity to one another on a genome may not be resolved by backcrossing, thus making it difficult to link phenotype to genotype.

Numerous attempts to transform chlamydiae were met with little success until a few years ago when Binet and Maurelli generated recombinants of *C. psittaci* with mutated 16S rRNA alleles by electroporation (83). Wang et al. further advanced chlamydial transformation techniques by optimization of a simple calcium chloride protocol. An *E. coli* shuttle vector carrying the endogenous chlamydial plasmid and a β-lactamase gene was used to transform *C. trachomatis* serovar L2 EB under penicillin selection (84). The transformation procedure has since been reproduced by several groups with various strains and species of *Chlamydia* (85-87). Chlamydial transformation has also been used successfully in conjunction with a technology called TargeTron™ to inactivate genes (88). TargeTron™ employs mobile group II introns that insert themselves into specific DNA sequences by means of an RNA: protein recognition complex. By altering the RNA target sequence to match sequences within the gene of interest, the intron can be re-targeted to insert itself in specific sites. Finally, a dendrimer-based approach that delivers DNA complexed with highly-branched

polymers to cells has been shown to efficiently transform chlamydiae and can also knock-down target gene expression (89, 90).

The rapid advances in chlamydial genetics over the past decade have already enabled researchers to investigate questions that were previously impossible to explore. Whereas past research focused on manipulation of the host to determine its impact on chlamydial survival, the field can now directly examine chlamydial gene function and its contribution to infection and disease.

1.5 Summary and Thesis Overview

Reductive evolutionary processes that forced Chlamydiae to lead obligate intracellular lives caused the pathogens to shed the bulk of their ancestral genome, leaving intact only the most vital machineries. Different chlamydial species have fine-tuned this small core genome to combat the defenses mounted by their respective hosts. Understanding how different hosts respond to chlamydiae and how the pathogens in turn have evolved host-specific adaptations has been the primary focus of my research.

To this end, we investigated a small, variable genomic region within the mouse pathogen *C. muridarum* in Chapter 2. Referred to as the 'plasticity zone', the locus is present in all chlamydial species and is hypothesized to play important roles in niche adaptation and evasion of host defenses. By employing a newly available reverse genetic tool, we found that much of the PZ appears to be dispensable *in vitro* as well as in a murine genital tract model of infection.

In Chapter 3, we conducted a forward genetic screen to determine why *C. muridarum*, but not *C. trachomatis*, is resistant to IFN-γ in murine cells. We identified a gain-of-function mutation within a small putative *C. muridarum* membrane protein that resulted in increased IFN-γ susceptibility. Inactivation of the mutated protein rescued the mutant in IFN-γ-treated cell lines as well as in the murine genital tract.

Finally, a serendipitous observation lead to the investigation of macrophage innate responses against *C. muridarum* in Chapter 4. We discovered that the ability of *C. muridarum* to survive within cells of the RAW 264.7 macrophage line depended on the multiplicity of infection. An iNOS-dependent mechanism was crucial for restriction of chlamydial growth in macrophages at higher infectious doses. Reactive oxygen species and lysosomal cathepsin B were found to modulate iNOS expression.

A brief discussion of our results and how they impact our current understanding of chlamydial-host interactions is presented in Chapter 5. We identify future research questions for the continued exploration of host and chlamydial adaptations.

Fig. 1.1. 16S rRNA phylogenetic tree of identified members within the phylum Chlamydiae. Different families are distinguished by color coding (Figure reproduced from Horn, 2008).
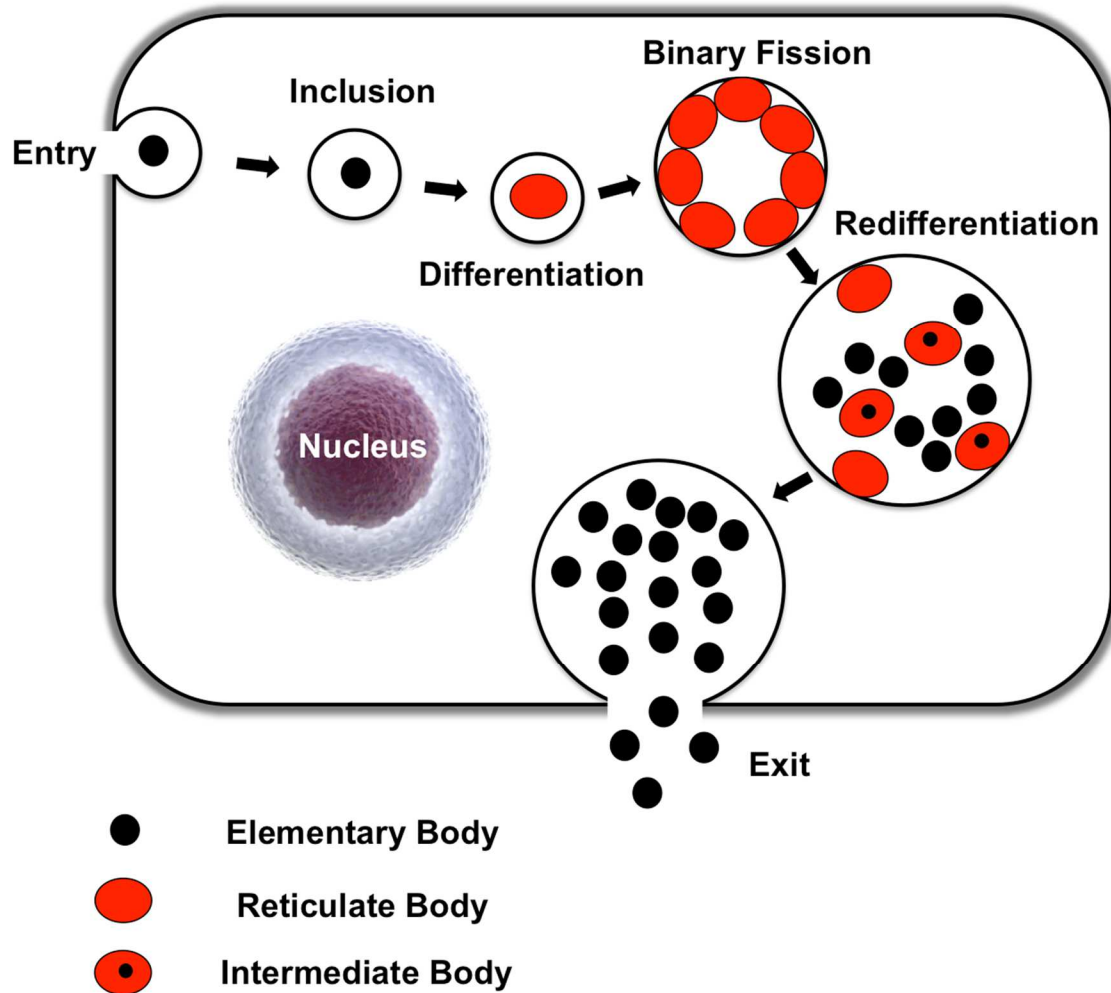
Fig. 1.2. Developmental cycle of *Chlamydia*. The diagram illustrates the invasion of a eukaryotic cell by an elementary body (EB). All intracellular forms of *Chlamydia* are enveloped by a lipid membrane called the inclusion. The EB differentiates into a bigger reticulate body (RB) that undergoes several rounds of multiplication. Towards the end of the cycle, RB differentiate into EB. EB are released from the host cell by lysis or extrusion.
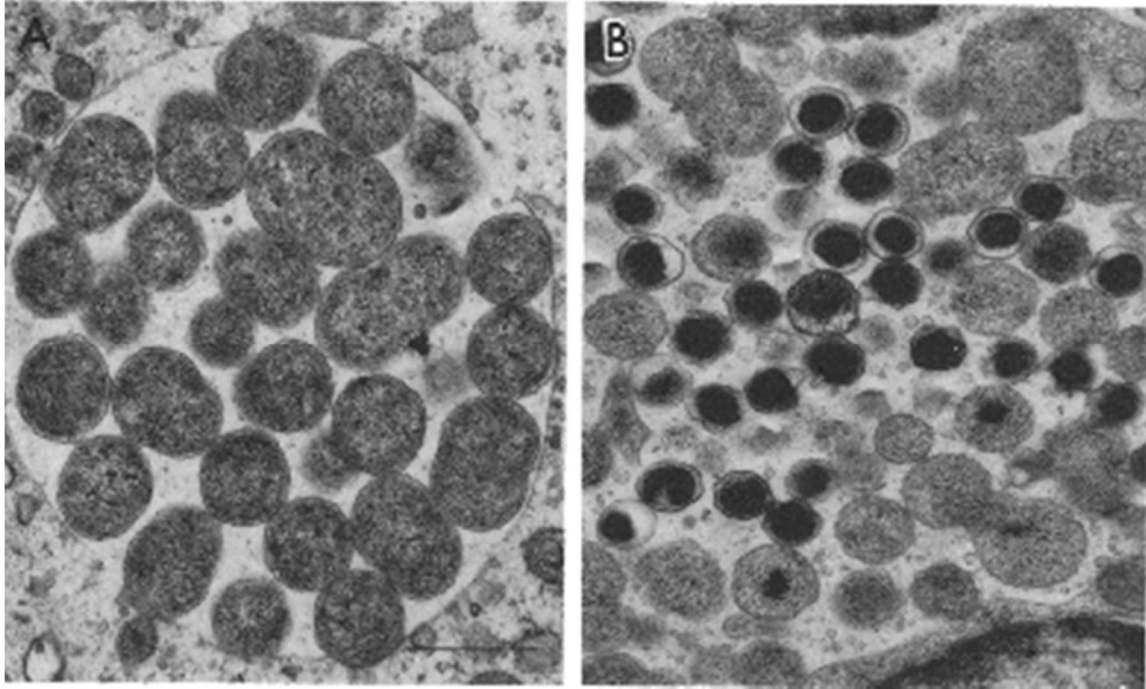
Fig. 1.3. Electron microscope images of *C. psittaci* developmental forms. (A) Chlamydial inclusion packed with RB at 24 hours post infection in the cytoplasm of L cells. Several RB are in the midst of binary fission. (B) EB, RB and intermediate forms in an inclusion at 48 hours post infection. Magnification: 16,000X (Images reproduced from Matsumoto and Manire, 1970 (91)).
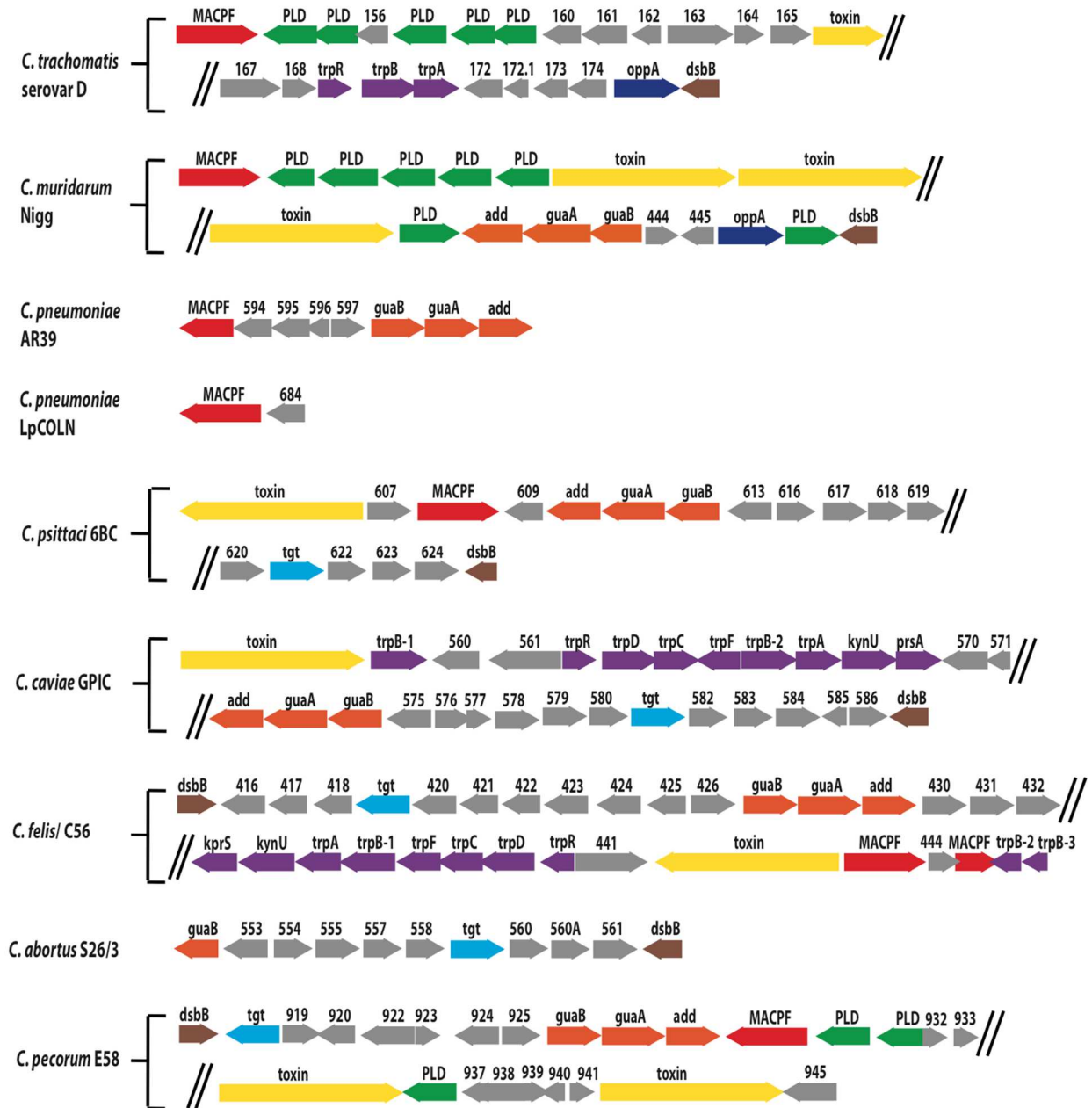
Figure 1.4. Map of plasticity zones from different species of *Chlamydia*. The plasticity zones (PZ) typically extend from *dsbB* or disulfide bond formation protein (brown) to MACPF (red). Other PZ genes are color-coded as follows: Phospholipase D, green; cytotoxin, yellow; nucleotide interconversion, orange; tryptophan synthesis, purple; *oppA* or ABC transporter, navy blue; *tgt* or queuine tRNA-ribosyl transferase, light blue; hypothetical, gray.
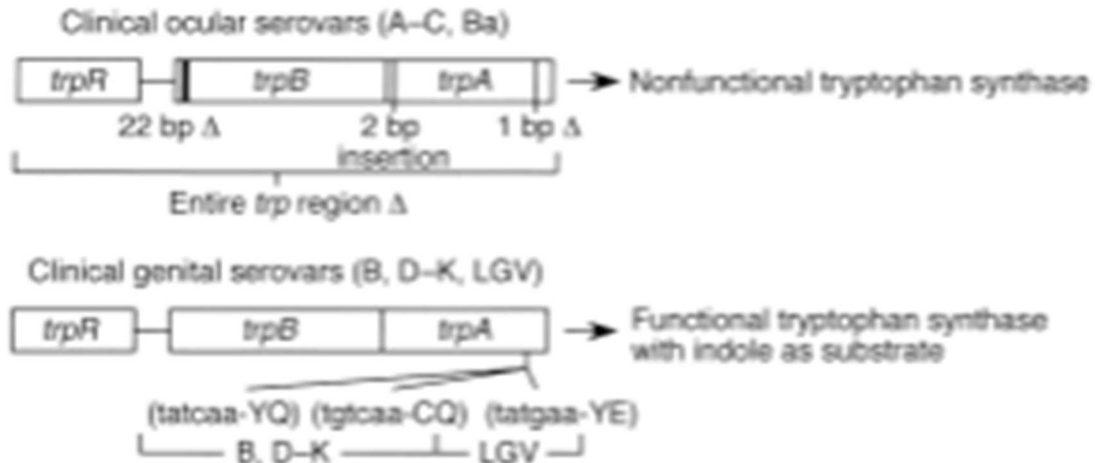
Fig. 1.5. Mutations in the *trpRBA* operon of *C. trachomatis*. A 1 bp deletion in the *trpA* gene of *C. trachomatis* ocular serovars results in a nonfunctional TrpA protein. All sequenced genital serovars encode a functional tryptophan synthase that contain serovar-specific polymorphisms in *trpA*. (Figure reproduced from Caldwell et al., 2003).

A.
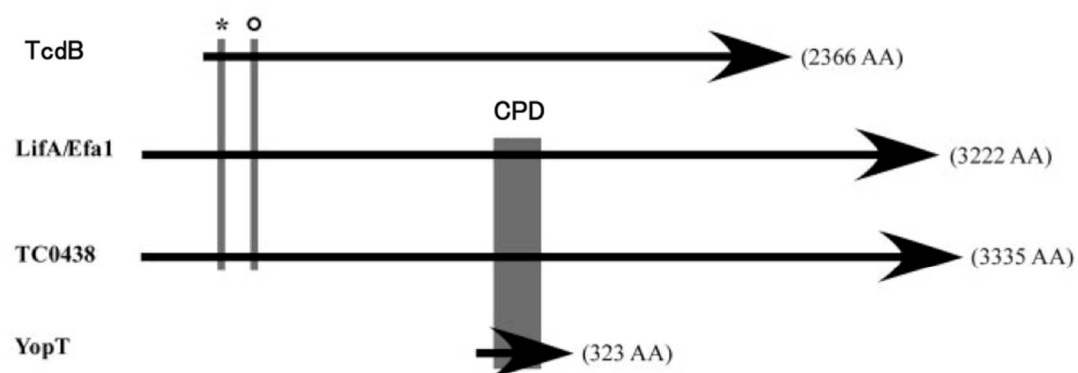
B.
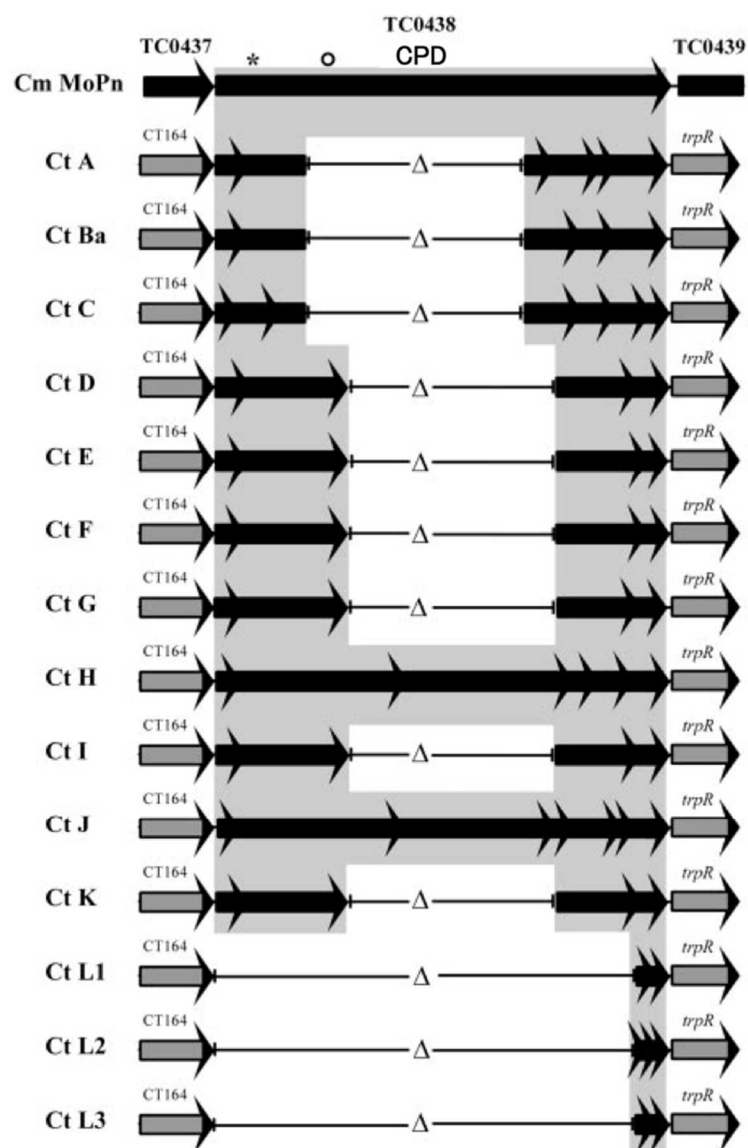
Fig.1.6. Distribution of active domains in chlamydial cytotoxins. (A) Full-length *C. muridarum* putative cytotoxin TC0438 and *E. coli* Efa1/LifA contain a UDP-glucose binding domain (*), a glucosyltransferase domain (°) and a YopT cysteine protease domain (CPD). CPD is absent from *Clostridium difficile* TcdB. (B) Schematic diagram of TC0438 aligned to homologous regions from all 15 serovars of *C. trachomatis*. *C. trachomatis* genital serovars D – K contain UDP-glucose binding domains (*) and glucosyltransferase domains (°). CPD is absent from serovars J and K due to frameshift mutations and from other *C. trachomatis* serovars due to deletion mutations. Ocular serovars A – C possess only the UDP-glucose binding domain. LGV serovars L1 – L3 lack all three domains. (Figure modified from Carlson et al., 2004).

1.6 References

1. **Alrifai KMJ.** 1988. Trachoma through history. International Ophthalmology **12:**9-14.

2. **Stephens RS, Kalman S, Lammel C, Fan J, Marathe R, Aravind L, Mitchell W, Olinger L, Tatusov RL, Zhao QX, Koonin EV, Davis RW.** 1998. Genome sequence of an obligate intracellular pathogen of humans: *Chlamydia trachomatis*. Science **282:**754-759.

3. **Horn M.** 2008. Chlamydiae as symbionts in eukaryotes, p. 113-131, Annu. Rev. Microbiol., vol. 62.

4. **Yuan Y, Zhang YX, Watkins NG, Caldwell HD.** 1989. Nucleotide and deduced amino acid sequences for the four variable domains of the major outer membrane proteins of the 15 Chlamydia trachomatis serovars. Infect. Immun. **57:**1040-1049.

5. **Schachter J.** 1990. Chlamydial infections Western J. Med. **153:**523-534.

6. **Woodland RM, Johnson AP, Tuffrey M.** 1983. Animal models of chlamydial infection. Br. Med. Bull. **39:**175-180.

7. **Blasi F, Centanni S, Allegra L.** 2004. *Chlamydia pneumoniae*: crossing the barriers? Eur. Respir. J. **23:**499-500.

8. **Vanrompay D, Ducatelle R, Haesebrouck F.** 1995. *Chlamydia psittaci* infections: A review with emphasis on avian chlamydiosis. Vet. Microbiol. **45:**93-119.

9. **Moulder JW.** 1991. Interaction of Chlamydiae and host cells *in vitro*. Microbiol. Rev. **55:**143-190.

10. **Omsland A, Sager J, Nair V, Sturdevant DE, Hackstadt T.** 2012. Developmental stage-specific metabolic and transcriptional activity of *Chlamydia trachomatis* in an axenic medium. PNAS **109:**19781-19785.

11. **Carabeo RA, Grieshaber SS, Fischer E, Hackstadt T.** 2002. *Chlamydia trachomatis* induces remodeling of the actin cytoskeleton during attachment and entry into HeLa cells. Infect. Immun. **70:**3793-3803.

12. **Jutras I, Abrami L, Dautry-Varsat A.** 2003. Entry of the lymphogranuloma venereum strain of *Chlamydia trachomatis* into host cells involves cholesterol-rich membrane domains. Infect. Immun. **71:**260-266.

13. **Clifton DR, Fields KA, Grieshaber SS, Dooley CA, Fischer ER, Mead DJ, Carabeo RA, Hackstadt T.** 2004. A chlamydial type III translocated protein is tyrosine-phosphorylated at the site of entry and associated with recruitment of actin. PNAS **101:**10166-10171.

14. **Bannantine JP, Rockey DD, Hackstadt T.** 1998. Tandem genes of *Chlamydia psittaci* that encode proteins localized to the inclusion membrane. Mol. Microbiol. **28:**1017-1026.

15. **Hackstadt T, Rockey DD, Heinzen RA, Scidmore MA.** 1996. *Chlamydia trachomatis* interrupts an exocytic pathway to acquire endogenously synthesized sphingomyelin in transit from the Golgi apparatus to the plasma membrane. EMBO J. **15:**964-977.

16. **Kumar Y, Cocchiaro J, Valdivia RH.** 2006. The obligate intracellular pathogen *Chiamydia trachomatis* targets host lipid droplets. Curr. Biol. **16:**1646-1651.

17. **Derre I, Swiss R, Agaisse H.** 2011. The lipid transfer protein CERT interacts with the *Chlamydia* inclusion protein IncD and participates to ER-*Chlamydia* inclusion membrane contact sites. PLoS Pathog. **7**.

18. **Ouellette SP, Dorsey FC, Moshiach S, Cleveland JL, Carabeo RA.** 2011. *Chlamydia* species-dependent differences in the growth requirement for lysosomes. PloS One **6**.

19. **Peterson EM, Delamaza LM.** 1988. *Chlamydia* parasitism: ultrastructural characterization of the interaction between the chlamydial cell envelope and the host cell. J. Bacteriol. **170:**1389-1392.

20. **Tjaden J, Winkler HH, Schwoppe C, Van der Laan M, Mohlmann T, Neuhaus HE.** 1999. Two nucleotide transport proteins in *Chlamydia trachomatis*, one for net nucleoside triphosphate uptake and the other for transport of energy. J. Bacteriol. **181:**1196-1202.

21. **Roshick C, Iliffe-Lee ER, McClarty G.** 2000. Cloning and characterization of ribonucleotide reductase from *Chlamydia trachomatis*. J. Biol. Chem. **275:**38111-38119.

22. **Heine H, Muller-Loennies S, Brade L, Lindner B, Brade H.** 2003. Endotoxic activity and chemical structure of lipopolysaccharides from *Chlamydia trachomatis* serotypes E and L-2 and *Chlamydophila psittaci* 6BC. Euro. J. Biochem. **270:**440-450.

23. **da Costa CUP, Wantia N, Kirschning CJ, Busch DH, Rodriguez N, Wagner H, Miethke T.** 2004. Heat shock protein 60 from *Chlamydia pneumoniae* elicits an unusual set of inflammatory responses via Toll-like receptor 2 and 4 *in vivo*. Euro. J. Immunol. **34:**2874-2884.

24. **Bas S, Lief L, Vuillet M, Spenato U, Seya T, Matsumoto M, Gabay C.** 2008. The proinflammatory cytokine response to *Chlamydia trachomatis* elementary bodies in human macrophages is partly mediated by a lipoprotein, the macrophage infectivity potentiator, through TLR2/TLR1/TLR6 and CD14. J. Immunol. **180:**1158-1168.

25. **Barker JR, Koestler BJ, Carpenter VK, Burdette DL, Waters CM, Vance RE, Valdivia RH.** 2013. STING-dependent recognition of cyclic di-AMP mediates type I interferon responses during *Chlamydia trachomatis* infection. mBio **4**.

26. **Buchholz KR, Stephens RS.** 2006. Activation of the host cell proinflammatory interleukin-8 response by *Chlamydia trachomatis*. Cell. Microbiol. **8:**1768-1779.

27. **Buchholz KR, Stephens RS.** 2007. The extracellular signal-regulated kinase/mitogen-activated protein kinase pathway induces the inflammatory factor interleukin-8 following *Chlamydia trachomatis* infection. Infect. Immun. **75:**5924-5929.

28. **Perry LL, Su H, Feilzer K, Messer R, Hughes S, Whitmire W, Caldwell HD.** 1999. Differential sensitivity of distinct *Chlamydia trachomatis* isolates to IFN-gamma-mediated inhibition. J. Immunol. **162:**3541-3548.

29. **Beatty WL, Morrison RP, Byrne GI.** 1994. Persistent Chlamydiae: From cell culture to a paradigm for chlamydial pathogenesis Microbiol. Rev. **58:**686-699.

30. **Nelson DE, Virok DP, Wood H, Roshick C, Johnson RM, Whitmire WM, Crane DD, Steele-Mortimer O, Kari L, McClarty G, Caldwell HD.** 2005. Chlamydial IFN-gamma immune evasion is linked to host infection tropism. PNAS **102:**10658-10663.

31. **Caldwell HD, Wood H, Crane D, Bailey R, Jones RB, Mabey D, Maclean I, Mohammed Z, Peeling R, Roshick C, Schachter J, Solomon AW, Stamm WE, Suchland RJ, Taylor L, West SK, Quinn TC, Belland RJ, McClarty G.** 2003. Polymorphisms in *Chlamydia trachomatis* tryptophan synthase genes differentiate between genital and ocular isolates. J. Clin. Invest. **111:**1757-1769.

32. **Romanik M, Martirosian G, Wojciechowska-Wieja A, Cieslik K, Kazmierczak W.** 2007. Co-occurence of indol-producing bacterial strains in the vagina of women infected with *Chlamydia trachomatis*. Ginekol. Pol. **78:**611-615.

33. **Wood H, Roshick C, McClarty G.** 2004. Tryptophan recycling is responsible for the interferon-gamma resistance of *Chlamydia psittaci* GPIC in indoleamine dioxygenase-expressing host cells. Mol. Microbiol. **52:**903-916.

34. **Cotter TW, Ramsey KH, Miranpuri GS, Poulsen CE, Byrne GI.** 1997. Dissemination of *Chlamydia trachomatis* chronic genital tract infection in gamma interferon gene knockout mice. Infect. Immun. **65:**2145-2152.

35. **Ramsey KH, Miranpuri GS, Sigar IM, Ouellette S, Byrne GI.** 2001. *Chlamydia trachomatis* persistence in the female mouse genital tract: Inducible nitric oxide synthase and infection outcome. Infect. Immun. **69:**5131-5137.

36. **Haldar AK, Saka HA, Piro AS, Dunn JD, Henry SC, Taylor GA, Frickel EM, Valdivia RH, Coers J.** 2013. IRG and GBP host resistance factors target aberrant, "non-self" vacuoles characterized by the missing of "self" IRGM proteins. PLoS Pathog. **9**.

37. **Coers J, Bernstein-Hanley I, Grotsky D, Parvanova I, Howard JC, Taylor GA, Dietrich WF, Starnbach MN.** 2008. *Chlamydia muridarum* evades growth restriction by the IFN-gamma-inducible host resistance factor Irgb10. J. Immunol. **180:**6237-6245.

38. **Al-Zeer MA, Al-Younes HM, Braun PR, Zerrahn J, Meyer TF.** 2009. IFN-gamma-inducible Irga6 mediates host resistance against *Chlamydia trachomatis* via autophagy. PloS One **4**.

39. **Sturdevant JL, Caldwell HD.** 2014. Innate immunity is sufficient for the clearance of *Chlamydia trachomatis* from the female mouse genital tract. Pathog. Dis. **72:** 70-73.

40. **Coers J, Starnbach MN, Howard JC.** 2009. Modeling infectious disease in mice: Co-adaptation and the role of host-specific IFN gamma responses. PLoS Pathog. **5**.

41. **Yong EC, Chi EY, Kuo CC.** 1987. Differential antimicrobial activity of human mononuclear phagocytes against the human biovars of *Chlamydia trachomatis*. J. Immunol. **139:**1297-1302.

42. **Kuo CC.** 1978. Cultures of *Chlamydia trachomatis* in mouse peritoneal macrophages: factors affecting organism growth. Infect. Immun. **20:**439-445.

43. **Rothfuchs AG, Kreuger MR, Wigzell H, Rottenberg ME.** 2004. Macrophages, CD4(+) or CD8(+) cells are each sufficient for protection against *Chlamydia pneumoniae* infection through their ability to secrete IFN-gamma. J. Immunol. **172:**2407-2415.

44. **Wink DA, Mitchell JB.** 1998. Chemical biology of nitric oxide: Insights into regulatory, cytotoxic, and cytoprotective mechanisms of nitric oxide. Free Radic. Biol. Med. **25:**434-456.

45. **Huang J, DeGraves FJ, Lenz SD, Gao DY, Feng P, Li D, Schlapp T, Kaltenboeck B.** 2002. The quantity of nitric oxide released by macrophages regulates *Chlamydia*-induced disease. PNAS **99:**3914-3919.

46. **Read TD, Myers GSA, Brunham RC, Nelson WC, Paulsen IT, Heidelberg J, Holtzapple E, Khouri H, Federova NB, Carty HA, Umayam LA, Haft DH, Peterson J, Beanan MJ, White O, Salzberg SL,**

Hsia RC, McClarty G, Rank RG, Bavoil PM, Fraser CM. 2003. Genome sequence of *Chlamydophila caviae* (*Chlamydia psittaci* GPIC): examining the role of niche-specific genes in the evolution of the Chlamydiaceae. Nuc. Ac. Res. **31:**2134-2147.

47. **Read TD, Brunham RC, Shen C, Gill SR, Heidelberg JF, White O, Hickey EK, Peterson J, Utterback T, Berry K, Bass S, Linher K, Weidman J, Khouri H, Craven B, Bowman C, Dodson R, Gwinn M, Nelson W, DeBoy R, Kolonay J, McClarty G, Salzberg SL, Eisen J, Fraser CM.** 2000. Genome sequences of *Chlamydia trachomatis* MoPn and *Chlamydia pneumoniae* AR39. Nuc. Ac. Res. **28:**1397-1406.

48. **Fehlner-Gardiner C, Roshick C, Carlson JH, Hughes S, Belland RJ, Caldwell HD, McClarty G.** 2002. Molecular basis defining human *Chlamydia trachomatis* tissue tropism - A possible role for tryptophan synthase. J. Biol. Chem. **277:**26893-26903.

49. **Stephens RS, Sanchezpescador R, Wagar EA, Inouye C, Urdea MS.** 1987. Diversity of *Chlamydia trachomatis* major outer membrane protein genes J. Bacteriol. **169:**3879-3885.

50. **Hackstadt T, Caldwell HD.** 1985. Effect of proteolytic cleavage of surface-exposed proteins on infectivity of *Chlamydia trachomatis*. Infect. Immun. **48:**546-551.

51. **Su H, Watkins NG, Zhang YX, Caldwell HD.** 1990. *Chlamydia trachomatis*-host cell interactions: role of the chlamydial major outer membrane protein as an adhesin. Infect. Immun. **58:**1017-1025.

52. **Su H, Raymond L, Rockey DD, Fischer E, Hackstadt T, Caldwell HD.** 1996. A recombinant *Chlamydia trachomatis* major outer membrane protein binds to heparan sulfate receptors on epithelial cells. FASEB J. **10:**A1094.

53. **Brunham RC, Plummer FA, Stephens RS.** 1993. Bacterial antigenic variation, host immune response, and pathogen-host coevolution. Infect. Immun. **61:**2273-2276.

54. **Stothard DR, Boguslawski G, Jones RB.** 1998. Phylogenetic analysis of the *Chlamydia trachomatis* major outer membrane protein and examination of potential pathogenic determinants. Infect. Immun. **66:**3618-3625.

55. **Kalman S, Mitchell W, Marathe R, Lammel C, Fan L, Hyman RW, Olinger L, Grimwood L, Davis RW, Stephens RS.** 1999. Comparative genomes of *Chlamydia pneumoniae* and *C. trachomatis*. Nat. Genet. **21:**385-389.

56. **Gomes JP, Nunes A, Bruno WJ, Borrego MJ, Florindo C, Dean D.** 2006. Polymorphisms in the nine polymorphic membrane proteins of *Chlamydia trachomatis* across all serovars: Evidence for serovar Da recombination and correlation with tissue tropism. J. Bacteriol. **188:**275-286.

57. **Tan C, Hsia RC, Shou HZ, Carrasco JA, Rank RG, Bavoil PM.** 2010. Variable expression of surface-exposed polymorphic membrane proteins in *in vitro*-grown *Chlamydia trachomatis*. Cell. Microbiol. **12:**174-187.

58. **Almeida F, Borges V, Ferreira R, Borrego MJ, Gomes JP, Mota LJ.** 2012. Polymorphisms in Inc proteins and differential expression of *inc* genes among *Chlamydia trachomatis* strains correlate with invasiveness and tropism of lymphogranuloma venereum isolates. J. Bacteriol. **194:**6574-6585.

59. **Hackstadt T, Scidmore-Carlson MA, Shaw EI, Fischer ER.** 1999. The *Chlamydia trachomatis* IncA protein is required for homotypic vesicle fusion. Cell. Microbiol. **1:**119-130.

60. **Voigt A, Schofl G, Saluz HP.** 2012. The *Chlamydia psittaci* genome: A comparative analysis of intracellular pathogens. PloS One **7**.

61. **Sait M, Livingstone M, Clark EM, Wheelhouse N, Spalding L, Markey B, Magnino S, Lainson FA, Myers GSA, Longbottom D.** 2014. Genome sequencing and comparative analysis of three *Chlamydia pecorum* strains associated with different pathogenic outcomes. BMC Genomics **15**.

62. **Azuma Y, Hirakawa H, Yamashita A, Cai Y, Rahman MA, Suzuki H, Mitaku S, Toh H, Goto S, Murakami T, Sugi K, Hayashi H, Fukushi H, Hattori M, Kuhara S, Shirai M.** 2006. Genome sequence of the cat pathogen, *Chlamydophila felis*. DNA Res. **13:**15-23.

63. **Carlson JH, Hughes S, Hogan D, Cieplak G, Sturdevant DE, McClarty G, Caldwell HD, Belland RJ.** 2004. Polymorphisms in the *Chlamydia trachomatis* cytotoxin locus associated with ocular and genital isolates. Infect. Immun. **72:**7063-7072.

64. **Belland RJ, Scidmore MA, Crane DD, Hogan DM, Whitmire W, McClarty G, Caldwell HD.** 2001. *Chlamydia trachomatis* cytotoxicity associated with complete and partial cytotoxin genes. PNAS **98:**13984-13989.

65. **Voth DE, Ballard JD.** 2005. *Clostridium difficile* toxins: Mechanism of action and role in disease. Clin. Microbiol. Rev. **18:**247-263.

66. **Sit S-T, Manser E.** 2011. Rho GTPases and their role in organizing the actin cytoskeleton. J. Cell Sci. **124:**679-683.

67. **Thalmann J, Janik K, May M, Sommer K, Ebeling J, Hofmann F, Genth H, Klos A.** 2010. Actin re-organization induced by *Chlamydia trachomatis* serovar D - Evidence for a critical role of the effector protein CT166 targeting Rac. PloS one **5**.

68. **Santiago AE, Cole LE, Franco A, Vogel SN, Levine MM, Barry EM.** 2009. Characterization of rationally attenuated *Francisella tularensis* vaccine strains that harbor deletions in the *guaA* and *guaB* genes. Vaccine **27:**2426-2436.

69. **Jewett MW, Lawrence KA, Bestor A, Byram R, Gherardini F, Rosa PA.** 2009. GuaA and GuaB are essential for *Borrelia burgdorferi* survival in the tick-mouse infection cycle. J. Bacteriol. **191:**6231-6241.

70. **Fields PI, Swanson RV, Haidaris CG, Heffron F.** 1986. Mutants of *Salmonella typhimurium* that cannot survive within the macrophage are avirulent. PNAS **83:**5189-5193.

71. **Taylor LD, Nelson DE, Dorward DW, Whitmire WM, Caldwell HD.** 2010. Biological characterization of *Chlamydia trachomatis* plasticity zone MACPF domain family protein CT153. Infect. Immun. **78:**2691-2699.

72. **Jang YH, Min DS.** 2012. The hydrophobic amino acids involved in the interdomain association of phospholipase D1 regulate the shuttling of phospholipase D-1 from vesicular organelles into the nucleus. Exp. Mol. Med. **44:**571-577.

73. **Ponting CP.** 1999. Chlamydial homologues of the MACPF (MAC/peforin) domain. Curr. Biol. **9:**R911-R913.

74. **Rosado CJ, Kondos S, Bull TE, Kuiper MJ, Law RHP, Buckle AM, Voskoboinik I, Bird PI, Trapani JA, Whisstock JC, Dunstone MA.** 2008. The MACPF/CDC family of pore-forming toxins. Cell. Microbiol. **10:**1765-1774.

75. **Heuer D, Kneip C, Maeurer AP, Meyer TF.** 2007. Tackling the intractable - Approaching the genetics of Chlamydiales. Int. J. Med. Microbiol. **297:**569-576.

76. **Gomes JP, Bruno WJ, Borrego MJ, Dean D.** 2004. Recombination in the genome of *Chlamydia trachomatis* involving the polymorphic membrane protein C gene relative to *ompA* and evidence for horizontal gene transfer. J. Bacteriol. **186:**4295-4306.

77. **Harris SR, Clarke IN, Seth-Smith HMB, Solomon AW, Cutcliffe LT, Marsh P, Skilton RJ, Holland MJ, Mabey D, Peeling RW, Lewis DA, Spratt BG, Unemo M, Persson K, Bjartling C, Brunham R, de Vries**

HJC, Morre SA, Speksnijder A, Bebear CM, Clerc M, de Barbeyrac B, Parkhill J, Thomson NR.** 2012. Whole-genome analysis of diverse *Chlamydia trachomatis* strains identifies phylogenetic relationships masked by current clinical typing. Nat. Genet. **44:**413-U221.

78. **DeMars R, Weinfurter J, Guex E, Lin J, Potucek Y.** 2007. Lateral gene transfer *in vitro* in the intracellular pathogen *Chlamydia trachomatis*. J. Bacteriol. **189:**991-1003.

79. **DeMars R, Weinfurter J.** 2008. Interstrain gene transfer in *Chlamydia trachomatis in vitro*: Mechanism and significance. J. Bacteriol. **190:**1605-1614.

80. **Suchland RJ, Sandoz KM, Jeffrey BM, Stamm WE, Rockey DD.** 2009. Horizontal transfer of tetracycline resistance among *Chlamydia* spp. *in vitro*. Antimicrob. Agents Chemother. **53:**4604-4611.

81. **Nguyen BD, Valdivia RH.** 2012. Virulence determinants in the obligate intracellular pathogen *Chlamydia trachomatis* revealed by forward genetic approaches. PNAS **109:**1263-1268.

82. **Kari L, Goheen MM, Randall LB, Taylor LD, Carlson JH, Whitmire WM, Virok D, Rajaram K, Endresz V, McClarty G, Nelson DE, Caldwell HD.** 2011. Generation of targeted *Chlamydia trachomatis* null mutants. PNAS **108:**7189-7193.

83. **Binet R, Maurelli AT.** 2009. Transformation and isolation of allelic exchange mutants of *Chlamydia psittaci* using recombinant DNA introduced by electroporation. PNAS **106:**292-297.

84. **Wang YB, Kahane S, Cutcliffe LT, Skilton RJ, Lambden PR, Clarke IN.** 2011. Development of a transformation system for *Chlamydia trachomatis*: Restoration of glycogen biosynthesis by acquisition of a plasmid shuttle vector. PLoS Pathog. **7**.

85. **Xu S, Battaglia L, Bao X, Fan H.** 2013. Chloramphenicol acetyltransferase as a selection marker for chlamydial transformation. BMC Res. Notes **6:**377-377.

86. **Song L, Carlson JH, Zhou B, Virtaneva K, Whitmire WM, Sturdevant GL, Porcella SF, McClarty G, Caldwell HD.** 2014. Plasmid-mediated transformation tropism of chlamydial biovars. Pathog. Dis. **70:**189-193.

87. **Gong S, Yang Z, Lei L, Shen L, Zhong G.** 2013. Characterization of *Chlamydia trachomatis* plasmid-encoded open reading frames. J. Bacteriol. **195:**3819-3826.

88. **Johnson CM, Fisher DJ.** 2013. Site-specific, insertional inactivation of *incA* in *Chlamydia trachomatis* using a group II intron. PloS one **8**.

89. **Kannan RM, Gerard HC, Mishra MK, Mao GZ, Wang SX, Hali M, Whittum-Hudson JA, Hudson AP.** 2013. Dendrimer-enabled transformation of *Chlamydia trachomatis*. Microb. Pathog. **65:**29-35.

90. **Mishra MK, Gerard HC, Whittum-Hudson JA, Hudson AP, Kannan RM.** 2012. Dendrimer-enabled modulation of gene expression in *Chlamydia trachomatis*. Mol. Pharm. **9:**413-421.

91. **Matsumoto A, Manire GP.** 1970. Electron microscopic observations on effects of penicillin on morphology of *Chlamydia psittaci*. J. Bacteriol. **101:**278-285.

CHAPTER 2

MUTATIONAL ANALYSIS OF THE *CHLAMYDIA MURIDARUM* PLASTICITY ZONE

2.1 Abstract

Pathogenically diverse *Chlamydia* spp. can have surprisingly similar genomes. *C. trachomatis* isolates that cause trachoma, sexually transmitted genital tract infections (chlamydia) and invasive lymphogranuloma venereum (LGV), and the murine strain *C. muridarum* share 99% of their gene content. A region of high genomic diversity between *Chlamydia* spp. termed the Plasticity Zone (PZ) may encode niche-specific virulence determinants that dictate pathogenic diversity. We hypothesized that PZ genes might mediate the greater virulence and IFN-γ resistance of *C. muridarum* compared to *C. trachomatis* in the murine genital tract. To test this hypothesis, we isolated and characterized a series of *C. muridarum* PZ nonsense mutants. Strains with nonsense mutations in chlamydial cytotoxins, *guaBA-add* and a phospholipase D homolog developed normally in cell culture. Two of the cytotoxin mutants were less cytotoxic than wild-type suggesting that the cytotoxins are functional. However, none of the PZ nonsense mutants exhibited increased IFN-γ sensitivity in cell culture or were profoundly attenuated in a murine genital tract infection model. Our results suggest that *C. muridarum* PZ genes are transcribed and some may produce functional proteins, but are dispensable for infection of the murine genital tract.

2.2 Introduction

Acquisition of genetic islands encoding the machinery necessary to invade eukaryotic cells was a key event in the evolution of many bacterial pathogens from free-living ancestors. For those pathogens that subsequently lost the ability to replicate outside host cells, a dearth of foreign microbial genetic material and Muller's ratchet may have tilted the balance of niche adaptation towards genomic decay. Reductive evolution appears to have played an especially pivotal role in niche adaptation of the obligate intracellular bacterial pathogens in the family *Chlamydiaceae* (1). Understanding why extant *Chlamydia* spp. retained different combinations of the metabolic pathways encoded by their common ancestors could reveal insights into chlamydial pathogenesis and cognate immune defenses against these intracellular pathogens.

Whole genome comparisons provided early clues concerning the importance of genomic streamlining in chlamydial evolution but less insight into how loss of specific genes and metabolic pathways is adaptive (2-5). What is clear is that the genomes of pathogenically diverse *Chlamydia* spp. are small, have limited biosynthetic capacity, and are remarkably similar. For example, the murine pathogen *C. muridarum* and pathogenically diverse *C. trachomatis* isolates share 99% gene content (4). Various hypotheses have been put forth to explain this paradox which was recently described as "divergence without difference" (6). One idea is that polymorphisms in conserved genes are key chlamydial virulence determinants. Some *C. trachomatis* trachoma strains have no obvious novel genes that differentiate them from genital strains (7) and some

trachoma strains that vary in their sensitivity to IFN-γ differ by only a few polymorphisms in conserved "core" genes (8) Alternately, but not exclusively, ORFs which have accumulated in a variable genomic region termed the plasticity zone "PZ" may be determinants of chlamydial pathogenic diversity (4). Comparative genomic and biochemical studies implicated that a partial tryptophan operon in the PZ of some *C. trachomatis* strains could reflect niche adaptation to immune-regulated tryptophan availability (9-12). Functionality of chlamydial tryptophan synthase, the product of this operon, in cell culture was recently confirmed using a reverse genetic strategy (13). Whether other PZ ORFs similarly mediate chlamydial niche adaptation, or if the PZ primarily houses inactive and decaying genes, remains unclear.

The PZ is consistently located near the region of replication termination in *Chlamydia* spp*.* but varies considerably in size and gene content (4). Some PZ ORFs have no homologs outside *Chlamydia* whereas others have been grouped into families based upon the homology of their predicted protein products to characterized bacterial and mammalian proteins. Some *Chlamydia* spp. encode a protein that resembles eukaryotic membrane attack complex (MAC) proteins and perforin (MACPF) in the PZ (4, 14). Various functions have been ascribed to chlamydial MACPFs including immune evasion by molecular mimicry, protein secretion and bacterial entry/exit (14, 15). Chlamydial MACPF is also purported to assist in lipid modification because of its proximity to a cluster of phospholipase D (PLD)-like genes (14, 16). Indirect evidence also suggests that PZ PLDs, like their mammalian homologs, are sensitive to primary alcohols and

play roles in lipid acquisition or transfer (17, 18). The *C. muridarum* PZ contains three putative cytotoxins that have similarity to the large clostridial toxins (LCTs) and yersinial YopT (4). The cytotoxin ORFs of *C. trachomatis* serovars are truncated, disrupted or absent altogether (2, 19, 20). A *guaBA-add* operon found in *C. muridarum,* but not *C. trachomatis,* could render the mouse pathogen less dependent on host nucleotides (4). These purine interconversion genes are replaced by *trpRBA* in *C. trachomatis* (2, 4). However, a lack of genetic tools and limitations of available animal models has prevented testing hypotheses concerning the functions of PZ ORFs in chlamydial virulence and tropism.

Determining functions of PZ ORFs could provide insight into the molecular basis of chlamydial host and tissue tropism and direct design of improved animal models of human chlamydial disease. *C. muridarum* infection of the murine genital tract (GT) is a leading model for the study of adaptive immunity to genital infection because innate immunity is sufficient to clear murine genital infection with human strains of *C. trachomatis* (21). We and others have speculated that *C. muridarum* PZ genes play roles analogous to *C. trachomatis* tryptophan synthase in circumvention of niche-specific innate immune responses (4, 22). If correct, this also implies that specific effectors were retained by *C. muridarum* because the cognate targets are relevant barriers during the natural course of infection. Murine modeling of *C. trachomatis* human urogenital tract infection might be improved by use of *C. muridarum* PZ null mutants and mice lacking the corresponding target of these effectors (23). Alternately, if PZ ORFs are dispensable for GT infection, this would suggest that either these ORFs do not

encode functional proteins or that the appropriate targets of these proteins are not relevant during experimental GT infection.

In this study, we used a combination of transcriptional profiling, reverse genetic analysis and mouse modeling to assess if *C. muridarum* PZ ORFs are expressed and necessary for murine GT infection. Our results suggest that although PZ ORFs are transcribed, they are dispensable for infection of the murine GT.

2.3 Materials and Methods

2.3.1 *Cell lines, chlamydial culture and infection*

C. muridarum and *C. trachomatis* serovar L2 (434/Bu) were kind gifts from Harlan Caldwell (Rocky Mountain Laboratories, NIAID, Hamilton, MT). Chlamydia were routinely propagated in McCoy mouse fibroblast cells (American Type Culture Collection CRL-1696) and infectious elementary bodies (EB) were purified by density gradient centrifugation (24). McCoy cells and HeLa human cervical epithelial cells (American Type Culture Collection CCL-2) were maintained in DMEM-high glucose medium containing HEPES, glutamine and sodium pyruvate (Hyclone), supplemented with 10% fetal bovine serum albumin (Atlanta Biologicals) and 100 μM non-essential amino acids (Gibco). Infections were performed in tissue culture flasks or plates with appropriate dilutions of chlamydial stock in SPG buffer (0.25 M sucrose, 10 mmol/L phosphate, 5 mmol/L L-glutamic acid; pH 7.2). Flask infections were rocked for 2 h at 37°C whereas plate infections were centrifuged at room temperature (RT) for 1 h followed by rocking at 37°C for 30 min. During large-scale propagation experiments SPG was

replaced with fresh DMEM containing 0.5 µg/mL cycloheximide. In some experiments, DMEM containing 20 U/ml murine IFN-γ (R&D Systems; catalog # 485-MI) was added to McCoy cells 24 h prior to and post infection. Cycloheximide was excluded from the cell culture media in experiments where IFN-γ was added.

2.3.2 *Recoverable Inclusion Forming Unit (rIFU) assays*

McCoy cells in 24-well plates were infected with *C. muridarum* or PZ mutants at a multiplicity of infection (MOI) of 0.25. The infected cell monolayers were frozen in 500 µl SPG at various intervals post-infection. Upon thawing, cells were scraped using a pipette tip and EB were harvested by bead-beating the cell suspension in microfuge tubes. Inclusion forming unit (IFU) assays were performed using serial dilutions of the harvests to infect confluent McCoy cell monolayers in 96-well plates. Cells were fixed with methanol and stained with anti-chlamydial LPS mAB (EVIH1) followed by a secondary Alexa Fluor488-conjugated anti-mouse IgG mAB (Life Technologies) at 24 hours post infection (hpi). Chlamydial inclusions were imaged and enumerated using an EVOS FL Auto Cell Imaging System (Life Technologies).

2.3.3 *RT-PCR and qRT-PCR*

McCoy cells in six-well plates were infected with *C. muridarum* at an MOI of 1. Total RNA was extracted at 0, 6, 12, 18, 24, and 30 hpi using TRISure reagent (Bioline), treated with DNAse I (Qiagen) for 15 min and then purified on

GeneJET RNA purification columns (Thermo Scientific). RT-PCR reactions were performed using 100 ng of total RNA and gene-specific primers (Table 1) using the MyTaq one-step RT-PCR kit (Bioline). For quantitative RT-PCR (qRT-PCR) experiments, total RNA was converted to cDNA using the Maxima H Minus First strand cDNA synthesis kit (Thermo Scientific). The qRT-PCR reactions were performed in an Eppendorf Realplex[4] thermocycler using SensiFAST SYBR No-ROX master mix (Bioline) using gene-specific primers (Table 2). The amplification cycle included a 2 min step at 95°C followed by 40 cycles of 95°C for 5 sec, 60°C for 10 sec, and 72°C for 20 sec. Absolute transcript copy numbers were calculated by normalizing to standard curves of *C. muridarum* genomic DNA amplified in parallel with experimental samples. Control reactions lacking RT were run in parallel with all RT-PCR and qRT-PCR experiments.

2.3.4 *PZ Cloning and β-galactosidase assays*

Overlapping 500 bp-1 kb regions of the *C. muridarum* PZ were PCR amplified from *C. muridarum* genomic DNA and were cloned upstream of the *lacZ* gene in pAC-lacZ, between the NruI and EagI sites of the vector (25). Sequences of the PCR primers and the genomic coordinates of the cloned PZ regions are in Table 3. The resulting plasmids were transformed into *E. coli* DH5α and the inserts and cloning junctions were confirmed by DNA sequencing. For β-galactosidase activity assays, triplicate samples from overnight cultures of *E. coli* strains carrying various PZ and control plasmids were grown in Luria-Bertani broth containing 50 µg/ml chloramphenicol, then were diluted 1:100 in

fresh broth and grown at 37°C until they reached mid-log phase ($OD_{600} \approx 0.6$). β-galactosidase expression analysis was performed as described previously, (26, 27) with the following modifications. Cells were diluted in a total volume of 500 µl Z-buffer (60 mM Na_2HPO_4, 40 mM $NaH_2PO_4 \cdot H2O$, 10 mM KCl, 1 mM $MgSO_4 \cdot 7H2O$) followed by the addition of 50 µl of chloroform and 50 µl of 0.1% sodium dodecyl sulfate. The solution was vortexed for 5 seconds, and the reactions were equilibrated by incubation at room temperature for 5 min prior to the addition of 100 µl of *ortho*-nitrophenyl-β-galactoside (4 mg/ml). The reactions were stopped by adding 250 µl of 1 M Na_2CO_3 and then were centrifuged at 14,000 rpm for 5 min in an Eppendorf microcentrifuge to separate the cell pellet and the supernatant. The initial OD_{600} of the cells and the OD_{420} supernatant were measured and used to calculate β–galactosidase activity.

2.3.5 *Preparation of CEL1 endonuclease extract*

CEL1 extract was prepared from celery as described previously (28). Fresh celery stalks (25 kg) were washed, chopped to remove leaves and juiced to yield approximately 10 L of celery juice. Subsequent steps were carried out at 4°C. 500 mL of Buffer A containing 2 M Tris-HCl (pH 7.7) and 0.1 M phenylmethanesulfonyl fluoride (PMSF) was added to the celery juice and the solution was centrifuged to remove plant debris. Protein was precipitated from the supernatant by ammonium sulfate fractionation in the 25-80% saturation range. The protein pellet was resuspended in 100 mL Buffer B (0.1 M Tris-HCl, pH 7.7; 0.5 M KCl; 100 µM PMSF; 0.01% Triton X-100) and was dialyzed

overnight against a large volume of Buffer B. The final CEL1 extract was stored in small aliquots at -80°C.

2.3.6 *EMS mutagenesis and library construction*

Confluent McCoy cells in a T-75 flask were infected with *C. muridarum* at an MOI of 0.5. At 16 hpi, culture media was replaced with 5 mL of DMEM containing 8 μg/ml ethyl methanesulfonate (EMS) (Sigma). The cells were exposed to EMS for 1 h and were then washed several times with 1X PBS, after which fresh DMEM without mutagen was added. EB were bead-harvested from the cells at 28 hpi and resuspended in 2 mL of SPG. An infection forming unit (IFU) assay estimated chlamydial survival after EMS treatment at less than 0.1% of untreated control. Half of the harvest was stored at -80°C and the remainder was used to infect a fresh T-75 flask of cells. Four rounds of EMS mutagenesis were performed in total and the final harvest yielded 9×10^5 EB. These EB were divided into small aliquots and stored at -80°C. To constuct mutant libraries, 96-well plates of McCoy cells were infected with 10 EB per well of the mutagenized stock. Mutant chlamydiae were scaled up by four rounds of passaging in 96-well plates. Plates from the third passage were stored at -80°C to serve as the library. Genomic DNA was extracted from the final plates by adding 75 μl of alkaline lysis buffer to each well (0.2 mM EDTA, 25 mM NaOH; pH 12.0) and incubating at 95°C for 10 min, after which the lysis buffer was neutralized by adding an equal volume of 40 mM Tris-HCl (pH 5.0). Genomic DNA plates were stored at 4°C.

2.3.7 *TILLING*

Targeting Induced Local Lesions IN Genomes (TILLING) was used to identify specific mutants in the library and was performed as described previously (13). Specific primers (Table 4) were used to amplify targeted PZ genes from template genomic DNA plates, which were extracted from the mutant libraries. These PCR products were annealed slowly ($80°C$, 7 seconds, 60X; decrease by $0.3°C$ every cycle) then were digested with CEL1 endonuclease. Digestions were performed for 10 min at $45°C$ using an empirically determined volume of CEL1 extract (range 0.1 to 1 μl) diluted in 1X CEL1 buffer (0.01 M $MgSO_4$; 0.01 M HEPES, pH 7.5; 0.02 M KCl; 0.005% Triton X-100; 2 μg/mL bovine serum albumin). Digestions were stopped by adding 10 μl EDTA (0.15 M, pH 8.0). The digested products were separated on 2% agarose TBE gels, stained with Midori Green (Bulldog Bio) and visualized using a ChemiDoc XRS+ device (BioRad Laboratories, Inc., Hercules, CA)).

2.3.8 *Cytotoxicity assays*

McCoy cells seeded on coverslips in 24-well plates were infected with *C. trachomatis*, *C. muridarum* or cytotoxin mutants at an MOI of 10 or 250 in the presence of 0.1 μg/mL rifampin. Cells were fixed in 3.7% formaldehyde at 3 hpi and then permeabilized with 1% Triton X-100. Following staining with AlexaFluor 488-phalloidin and AlexaFluor 594 WGA (Invitrogen) for visualization of actin filaments and host plasma membrane, respectively, coverslips were mounted on slides using ProLong Gold antifade reagent with DAPI (Life Technologies). Cells

were imaged using a Nikon Eclipse Ni-E fluorescent microscope (Nikon Instruments, Melville, NY).

Lactate Dehydrogenase (LDH) assays were performed according to the manufacturer's instructions (OPS Diagnostics). McCoy cells were infected with various strains at a range of MOI (10, 25, 100 and 500) in the presence of rifampin. To determine maximal LDH release, cells in control wells were lysed with 10% Triton X-100 10 min prior to supernatant collection. Supernatants were removed from wells 3 hpi after brief centrifugation of the plates to remove debris. 25 μl of the supernatants were mixed with 75 μl of the dye/buffer solution. The A_{490} was measured after 15 min incubation at 37°C.

2.3.9 *Animal experiments*

C57BL/6J mice were obtained from Jackson Laboratories (Bar Harbor, ME). All animal experiments were approved by the Institutional Animal Care and Use Committees of the University of Arkansas for Medical Sciences and Indiana University. Female mice between 6-10 weeks old were treated with 2.5 mg Depo-Provera diluted in 100 μl PBS at 10 and 3 days prior to infection. Prior to infectious challenge, the vaginal vault was swabbed to remove excess mucus. Mice were inoculated vaginally with *C. muridarum* or PZ mutants at a concentration of 5×10^4 IFU in 5 μl SPG. The infections were monitored by enumeration of IFU from cervical swabs collected at various time points.

2.3.10 *Sequencing Library Construction and Whole Genome Sequencing*

Gradient-purified EB were treated with DNase I (NEB) at 37 °C for 1 h and then 5 mM EDTA was added and the mixtures were incubated at 75 °C for 10 min to halt digestion. Total DNA was extracted using the DNeasy Blood & Tissue kit (Qiagen) and DNA concentrations were determined using the Quant-It High Sensitivity dsDNA assay (Life Technologies Corp.) The dsDNA fragments were generated by treating 1 µg of genomic DNA with NEBNext dsDNA Fragmentase (NEB). DNA sequencing libraries were prepared using the TruSeq Nano DNA sample preparation kit according to the manufacturer's protocols (Illumina Inc.). Samples were multiplexed using TruSeq Single Index sequencing primers. Equimolar concentrations of indexed libraries were combined into a single pool and submitted for Illumina HiSeq sequencing at Tufts University Genomics Core Facility. Paired-end 100 bp sequencing was performed on the Illumina HiSeq 2500 platform.

2.3.11 *Genome assembly and sequence analysis*

For single nucleotide polymorphisms (SNP), nucleotide insertion and deletion analysis (Indel), raw sequence data was mapped to the corresponding reference genome (GenBank: AE002160.2) using Bowtie2. Resulting SAM files were converted to a BAM file format and sorted. SNPs/Indels were called using a Samtools mpileup function. Remaining ambiguous sequences from the dataset and mutation calls with low quality scores were resolved by PCR and Sanger sequencing.

2.3.12 *Statistics*

Data was analyzed using Prism 6.0 software (GraphPad). For comparisons of multiple groups with more than one variable, two-way analysis of variance (ANOVA) followed by the Bonferroni posttest was used. Two-way ANOVA with Bonferroni posttest was also used to analyze the differences in chlamydial burden between groups of infected mice. Multiple comparisons for data with a single variable were analyzed by one-way ANOVA followed by the Dunnett's posttest. Differences were considered statistically significant when P< 0.05.

2.4 Results

2.4.1 *The C. muridarum Plasticity Zone is transcriptionally active*

The *C. muridarum* Plasticity Zone (PZ) is defined as the 50 kb locus between *tc0431* (MACPF) and *tc0448* (*dsbB*) (Fig. 2.1). The *C. muridarum* PZ is poorly characterized and the only evidence for gene activity in the region comes from a prior transcriptional study of the cytotoxin ORFs (*tc0437 – tc0439*) (19). To determine if and when other PZ ORFs were expressed, we examined the entire locus for transcriptional activity. RT-PCR analysis of RNA isolated from *C. muridarum*-infected McCoy cells at 24 hpi indicated that all the PZ genes were transcribed (Fig. 2.2 A). Next, we determined the transcriptional and temporal expression profiles of a subset of PZ ORFs (*tc0431*, *tc0436 – tc0443*) using qRT-PCR analysis at various time points post infection. The developmentally regulated genes, *euo*, *ompA* and *omcB* were analyzed as representative

chlamydial early, mid-late and late genes, respectively (19). Increased expression of *euo* was detected by 6 hpi, whereas *ompA* transcripts first increased between 6 and 12 hpi and *de novo omcB* expression was only detected at 12 hpi and did not peak until 18 hpi (Fig. 2.2 B). The expression trend for all of the PZ genes most closely resembled *ompA*, except that the absolute peak numbers of PZ ORF transcripts were 1 to 3 logs lower than those of *ompA* and *omcB*. Taken together, these results showed that expression of most PZ ORFs initiates mid to late developmental cycle and that they are expressed at low levels relative to known highly expressed chlamydial genes.

We next sought to identify the promoters of PZ genes. The ability of a series of overlapping cloned fragments of the *C. muridarum* PZ to drive expression of a promoterless *lacZ* gene was assayed in *E. coli* to identify promoters. Only two of the constructs exhibited strong promoter activity. One promoter locus (GenBank coordinates: 515330-515896) was situated near the 3' end of *tc0437* and was in the correct position and orientation to drive expression of *tc0438-tc0440*. The other locus (GenBank coordinates: 542868-542368) was located immediately upstream of *guaB* (Table 5). This gene is predicted to lie in an operon along with *guaA* and *add*. No promoter likely to drive expression of the predicted PZ PLD operon *tc0436-tc0432* or the cytotoxin ORF *tc0437* was identified although regions immediately upstream of *tc0436* and *tc0437* were represented in the PZ clone library (Table 5). Failure to identify other promoters for PZ genes whose expression was confirmed by RT-PCR could indicate that

some PZ promoters were not functional in *E. coli* or were located outside the regions interrogated in the assay.

2.4.2 *Members of three PZ gene families are dispensable for C. muridarum survival and proliferation in vitro*

Since little is known about the potential functions of most PZ ORFs*,* we tested if they were dispensable using a reverse genetic approach. An EMS-mutagenized *C. muridarum* library was screened by TILLING for isolates that had nonsense mutations in eight *C. muridarum*-specific PZ ORFs: *tc0437*, *tc0438*, *tc0439*, *tc0440*, *guaA (tc0441)*, *guaB (tc0442)*, *add (tc0443)* and MACPF (*tc0431*). (13). The TILLING library was constructed with a high mutation load to facilitate faster screening. To estimate the number of EMS-induced point mutations in a given gene that would have to be isolated in order to recover at least one nonsense mutation, we assumed a Poisson distribution described as P ($x \geq 1$) = 1 – P ($x = 0$) = $1 - e^{-a}$ where a = N·p; N is the number of mutations in gene X that need to be isolated and p is the probability of obtaining a nonsense mutation in gene X. The majority of mutations induced by EMS are GC->AT transitions. A total of 5 GC transitions in 4 amino acid codons (CAA, CGA, CAG, TGG) can yield a stop codon. We use *tc0442* as an example to illustrate how we arrived at an approximation of screen size (N). The probability p can be calculated as the number of possible nonsense GC transitions in the analyzed region of *tc0442* divided by the number of GC base pairs in the same region of *tc0442* (p = 19/585; = 0.032). For 95% screen saturation, screen size N was

determined as follows: P (x ≥ 1) = 0.95 = 1 - $e^{-0.032N}$ or N = 94. In other words, if *tc0442* is not essential, there is a 95% probability that at least one of 94 isolated mutants is a nonsense mutant. Screen sizes for other PZ genes were calculated by the same method (Table 6).

One or more nonsense mutants in *guaBA-add*, the *C. muridarum*-specific PZ PLD *tc0440* and the cytotoxins (*tc0437 – tc0439*) were isolated at anticipated frequencies, indicating that these ORFs are not essential for chlamydial survival *in vitro*. Despite isolating over 60 unique mutants with point mutations in *tc0431* (MACPF), none of these were nonsense (Table 6). *C. abortus* does not encode MACPF (29, 30), and the *C. caviae* and human *C. pneumoniae* MACPF genes contain frameshifts (5, 30, 31), so this result could indicate that MACPF plays an essential, species-specific role in *C. muridarum*.

2.4.3 *PZ mutants display mild in vitro growth defects*

The PZ nonsense mutants were initially characterized using temporal recoverable IFU assays. Since multiple independent mutants of *tc0440* and *guaA* were recovered by TILLING, we selected a representative mutant of each with a nonsense mutation located closest to the predicted 5' end of these ORFs for further analysis. Growth kinetics of most of the PZ mutants paralleled *C. muridarum*, with the sole exception of *guaB*, which attained maximal EB production at 18 hpi as opposed to 30 hpi. None of the mutants exhibited dramatic growth defects, although IFU production of most of the mutants was significantly reduced compared to *C. muridarum* (Fig. 2.3). Confocal microscopy

also failed to reveal obvious differences between the morphology of the mutant and *C. muridarum* inclusions (data not shown). These results implied that the presence of nonsense mutations in PZ ORFs did not hinder the ability of *C. muridarum* to form inclusions, complete development or produce infectious EB.

2.4.4 *Cytotoxicity of cytotoxin nonsense mutants is reduced*

Since none of the PZ mutants displayed pronounced growth or morphological defects, we focused on examining phenotypes that have been indirectly attributed to the chlamydial cytotoxins in previous studies. The *C. muridarum* LCT-like cytotoxins are purported to mediate multiplication-independent cytopathic effects of *C. muridarum* EB to host cells at high MOI (19). This phenomenon, referred to as "immediate cytotoxicity" (32), resembles the cytoskeletal collapse observed in cultured cells treated with clostridial TcdB (19).

To determine if the *C. muridarum* cytotoxin (*tc0437*, *tc0438* and *tc0439*) nonsense mutants were less cytotoxic, HeLa cells were infected with EB at an MOI of 250 in the presence of rifampin. Cells were fixed and stained with Phalloidin at 3 hpi and examined by fluorescent microscopy. HeLa cells infected with *C. trachomatis* serovar L2 (*C. trachomatis*), a cytotoxin negative strain, did not differ in morphology from uninfected cells. In contrast, cell rounding and alterations in actin filament morphology were observed in infections with *C. muridarum* and the cytotoxin mutants (Fig. 2.4 A). This implied that the single cytotoxin mutants retained some cytotoxic activity.

Microscopy could not distinguish small variations in cytotoxicity so we measured LDH release at 3 hpi from cells infected with *C. muridarum*, *C. trachomatis* and the mutants at various MOI. As expected, *C. trachomatis* elicited minimal LDH release even at an MOI of 500. In contrast, *C. muridarum* caused cells to release significantly more LDH at high MOIs. Interestingly, the *tc0437* and *tc0439* mutants elicited lower LDH release than *C. muridarum* at the highest MOI tested (Fig. 2.4 B). Wild-type cytotoxicity of the *tc0438* mutant implies that TC0438 may not be functional, or has a function different than the other two cytotoxins altogether.

2.4.5 *IFN-γ resistance is unaltered in C. muridarum PZ mutants*

While high multiplicity infections were important in associating a toxin-like activity to chlamydial EB, these doses may not be relevant in natural chlamydial disease. Roles for the chlamydial cytotoxins in host cell attachment, entry, vesicle trafficking and modification of host cell GTPases have been reported (33-35). The *C. muridarum* cytotoxins have also been proposed to mediate evasion of the inhibitory effects of IFN-γ responses in murine cells (12). To test the latter hypothesis, McCoy cells were treated with IFN-γ followed by infection with *C. trachomatis*, *C. muridarum* or cytotoxin mutants. Chlamydial survival was measured by IFU (Fig. 2.5 A) and rIFU (Fig. 2.5 B) assays. *C. trachomatis*, but not *C. muridarum*, was dramatically inhibited by IFN-γ. IFN-γ treatment did not significantly affect the survival of the cytotoxin mutants compared to *C. muridarum*. Parallel experiments with other PZ nonsense mutants indicated that

they were also similarly resistant to IFN-γ (Fig. 5). Thus, disruption of individual cytotoxin or other PZ ORFs did not confer IFN-γ sensitivity to *C. muridarum*.

2.4.6 *PZ mutants retain virulence in the mouse genital tract infection model*

Intravaginal inoculations of mice with human *C. trachomatis* isolates result in mild infections of short duration with minimal upper genital tract infection and pathology (36). In comparison, *C. muridarum* is more virulent in this model and the post-infection sequelae mimic human disease (37). To determine if the *C. muridarum* PZ genes were niche-specific virulence factors in mice, PZ mutants were analyzed in the murine genital tract infection model. Chlamydial burden in mice infected with the *tc0439* cytotoxin mutant was significantly lower at 3 days post infection in comparison to animals infected with *C. muridarum*. Infection trajectories in mice inoculated with the *tc0437* and *tc0438* mutants also trended lower during the first week of infection. However, chlamydial recoveries of all three cytotoxin mutants appeared identical to *C. muridarum* infection at later time points (Fig. 2.6 A). We also did not observe any significant deviation in bacterial loads of mice infected with the *tc0440* mutant compared to mice infected with *C. muridarum* (Fig. 2.6 B). Interestingly, the *guaA* nonsense mutant behaved identically to *C. muridarum*, whereas *guaB* and *add* mutants displayed reduced pathogen burdens at early data points (Fig. 2.6 C, D). The putative *guaBA-add* operon encodes products that function in the same purine biosynthetic pathway. Absence of phenotypes in the *guaA* mutant suggested that either the phenotypes of the *guaB* and *add* mutants were due to background mutations or that the

guaBA-add acts non-canonically in *C. muridarum*. Since none of the PZ mutants were completely attenuated *in vivo*, we conclude that these genes are dispensable for infection of the murine genital tract.

2.4.7 *PZ mutants contain multiple background mutations*

To identify a plausible explanation for the differing phenotypes of the purine pathway mutants, we sequenced the genomes of the parent strain and PZ mutants to an average coverage of 2075x on the Illumina HiSeq platform (Tables 7-14). Comparison to published *C. muridarum* genomes indicated that our parent most closely resembled a *C. muridarum* Weiss isolate that was recently sequenced by Ramsey *et al* (Table 7). On average, the PZ mutants contained 36.4 mutations, of which 66.67% were non-synonymous substitutions. Most (98.43%) of the mutations were GC->AT transitions consistent with EMS induced changes. Several synonymous and non-synonymous mutations were shared by some PZ mutant strains, which was a consequence of our serial mutagenesis strategy. These included mutations in *recA*, *alaS*, *tc0237*, *tc0283*, *tc0471*, *tc0490*, *rpoC*, *aroA*, *upp* and *tc0877* that were common to the *add*, *tc0437* and *tc0438* mutants. The *add* and *tc0437* mutant strains contained identical mutations in *tc0035*, *tc0069*, *tc0438*, *tc0575*, *tc0917* and *pfkA-2*. The *tc0438* mutant shared mutations in *murB*, *tc0330* and *tc0575* with the *add* mutant and a *pmpB/C-2* mutation with the *tc0437* mutant. Finally, mutations in *tc0054*, *tc0191*, *pmpD*, *tc0250*, *tc0290*, *tc0312*, *tc0600* and an intergenic region (GenBank genome position: 126188) were present in the *tc0439* and the *guaB* mutants.

Interestingly, multiple mutant strains had nonsense mutations in *tc0412*, an ortholog of *C. trachomatis ct135* which has been linked to virulence of *C. trachomatis* in the murine genital tract model (38). None of the *tc0412* mutants except *add* were significantly attenuated in the murine GT and an identical stop mutation was present in the *tc0437* mutant strain suggesting that attenuation of the *add* mutant was unlinked to this *tc0412* allele. No common mutations were present in the *guaB* and *add* mutants, which is consistent with the hypothesis that *guaB* and *add* might function in a non-canonical pathway independent of *guaA*.

2.5 Discussion

C. muridarum and *C. trachomatis* are genetically closely related and genital infection of their respective hosts, mice and humans respectively, have many similarities (4, 39). While T-cell immunity is critical for the resolution of chlamydial infection in both mice and humans, other aspects of immunity, most notably IFN-γ responses, appear to differ and are incompletely characterized (36). The results of our study suggest that although the PZ is the site of maximal divergence between the genomes of these pathogens, *C. muridarum* IFN-γ resistance determinants may not localize to this region.

We show that most PZ ORFs are transcribed mid to late developmental cycle and are expressed at relatively low levels. Although we identified two promoter regions that support our RT-PCR findings, and which could provide plausible explanations for how some PZ ORFs are transcribed, strong promoters

that could drive expression of one of the cytotoxin ORFs (*tc0437*) and an adjacent operon of PZ PLD (*tc0436-tc0432*) that is relatively conserved in *Chlamydia* spp. were not identified. The putative start sites of *tc0436* and *tc0437* are located less than 1000 bp apart in opposite strands of the *C. muridarum* genome, so perhaps our chosen cloning site disrupted two promoters in the same narrow region on opposing strands thus compromising their detection. Another possibility is that *E. coli* sigma factors cannot recognize the chlamydial promoters in this region. For example, the auxiliary *C. trachomatis* transcription factor GrgA, which is not conserved in *E. coli*, directs expression from some chlamydial σ^{66}-dependent promoters (40). Chlamydial σ^{28} also cannot complement an *E. coli* σ^{28} mutant, indicating that even conserved *E. coli* and chlamydial sigma factors are not completely interchangeable (41). We attempted to identify additional promoters using RNA-seq, but low expression of PZ ORFs relative to other highly expressed genes yielded insufficient coverage for mapping transcriptional start sites in this region. As costs of deep RNA-seq decrease further and methods for enrichment of chlamydial from host cell transcripts improve, it might make sense to re-visit this approach in the future. Better understanding of transcriptional organization could inform subsequent attempts to inactivate PZ operons.

Two of three cytotoxin mutants displayed reduced cytotoxicity *in vitro*, which suggests that these alleles are functional. The biological role of chlamydial cytotoxins is still largely a matter of speculation. Polymorphisms in the cytotoxins have been associated with differences in the ocular and genital tropisms of *C.*

trachomatis isolates (20). On the basis of their homology to LCTs and YopT, we have previously proposed that the cytotoxins may inactivate interferon regulated GTPases that inhibit *C. trachomatis*, but not *C. muridarum*, in IFN-γ-treated mouse cells (42). Finally, mutants of *E. coli efa1*, another chlamydial cytotoxin homolog, exhibit reduced adherence to epithelial cells and fail to colonize colonic tissue effectively in mice (43). The observed trend towards lower chlamydial burden during the first week of infection in mice inoculated with the chlamydial cytotoxin mutants argues for a possible role in adhesion and colonization. A future direction would be to evaluate IFN-γ resistance and virulence of double and triple cytotoxin mutants.

One of the most surprising findings of our study was that the *guaB* (IMP dehydrogenase) and *add* (adenosine deaminase) mutants were moderately attenuated in the GT while a *guaA* (GMP synthase) mutant was not. Genome sequencing confirmed that the phenotypes of the *guaB* and *add* mutants were not caused by a common background mutation. Thus, if unrelated background mutations were not responsible for the very similar GT phenotypes, our results suggest *C. muridarum* could encode an additional cryptic GMP synthase enzyme or that *C. muridarum* purine salvage acts non-canonically. The *guaBA-add* operon has been retained by several chlamydial species that cause respiratory illness including *C. psittaci*, *C. felis* and human isolates of *C. pneumoniae*, but it is unknown if they are functional (31, 44, 45). *guaA* and *gua*B are known virulence determinants in other pathogenic organisms like *B. burgdorferi* and *F. tularensis* during intraperitoneal and subcutaneous infection of mice, indicating

66

that one or more purine nucleoside monoposphates are limiting in certain mammalian niches (46, 47). Thus, an explanation of our results could be that NMP levels in the murine GT are sufficient to support chlamydial growth whereas other tissues like the lung are starved for purine nucleotides. We hope to differentiate these possibilities by constructing additional *guaA*, *guaB* and *add* nonsense mutants and comparing their virulence in murine GT and lung infection models.

Although we were unable to identify a role for individual PZ genes in IFN-γ resistance and murine genital infection, functional redundancy in the cytotoxin and PLD super family of proteins could have masked effects of the loss of a single family member. However, our data indicates that cytotoxin functions are not wholly redundant and true functional redundancy of these alleles is not consistent with the relatively low amino acid identity to one another (40-42%). While it would be possible to disrupt all members of the cytotoxin and *guaBA-add* operons sequentially, variable alleles including *tc0412* are a practical impediment to constructing isogenic strains by iterative TILLING (38, 48). Another possible explanation for the lack of phenotype of select PZ mutants is the emergence of suppressor mutations. Although this possibility is difficult to exclude, the fact that all of the PZ mutants were isolated from pools of mutants at expected frequencies indicates that this is unlikely to have been a significant issue. We are currently investigating the possibility of disrupting the putative PZ PLD (*tc0436-432*), cytotoxin (*tc0437-439*) and *guaBA-add* operons using polar transposon insertions by the Targetron® method developed by Fisher and colleagues (49).

In summary, our results imply that all examined PZ ORFs are non-essential for virulence in the mouse GT but we cannot rule out their importance in other niches. *C. muridarum* was originally isolated from the lungs of symptom-free laboratory mice. Disease was only observed upon inoculation of mice with serially passaged lung homogenates, indicating that very low levels of *C. muridarum* are typically present in pulmonary tissue (50). Later studies demonstrated that *C. muridarum* is transmitted through the oro-fecal route, which suggests that the gut is a reservoir and that small numbers of *C. muridarum* enter the lungs during feeding (51). Finally, it is notable that *guaBA-add* and cytotoxin homologs of other intracellular pathogens modulate infections of the lung and gastrointestinal tract, respectively (43, 46, 52). Thus, examination of *C. muridarum* PZ mutants in lung or gastrointestinal tract models of mouse infections is warranted. A positive implication of our study is that successful modeling of human disease in the murine GT does not appear to require much of the *C. muridarum* PZ. Future investigations of polymorphisms outside the PZ will be important in the identification of *C. muridarum* alleles that confer IFN-γ resistance and dictate virulence in the murine GT model.
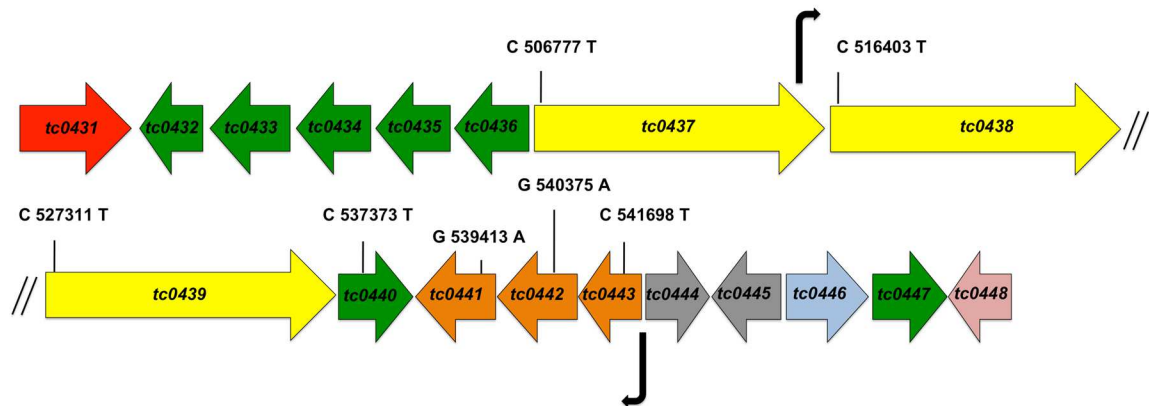
Fig. 2.1. Map of the *C. muridarum* Plasticity Zone. Diagram of PZ ORFs. ORFs are color-coded according to functional annotation: red, MACPF; green, phospholipase D (PLD); yellow, cytotoxin; orange, purine nucleotide synthesis; gray, conserved hypothetical; blue, peptide ABC transporter; pink, *dsbB*. Locations of promoters identified by β-galactosidase assays in this study are shown by arrows. The genomic location and nucleotide change of nonsense mutations discussed in this study are indicated in the corresponding ORFs. Figure is not drawn to scale.
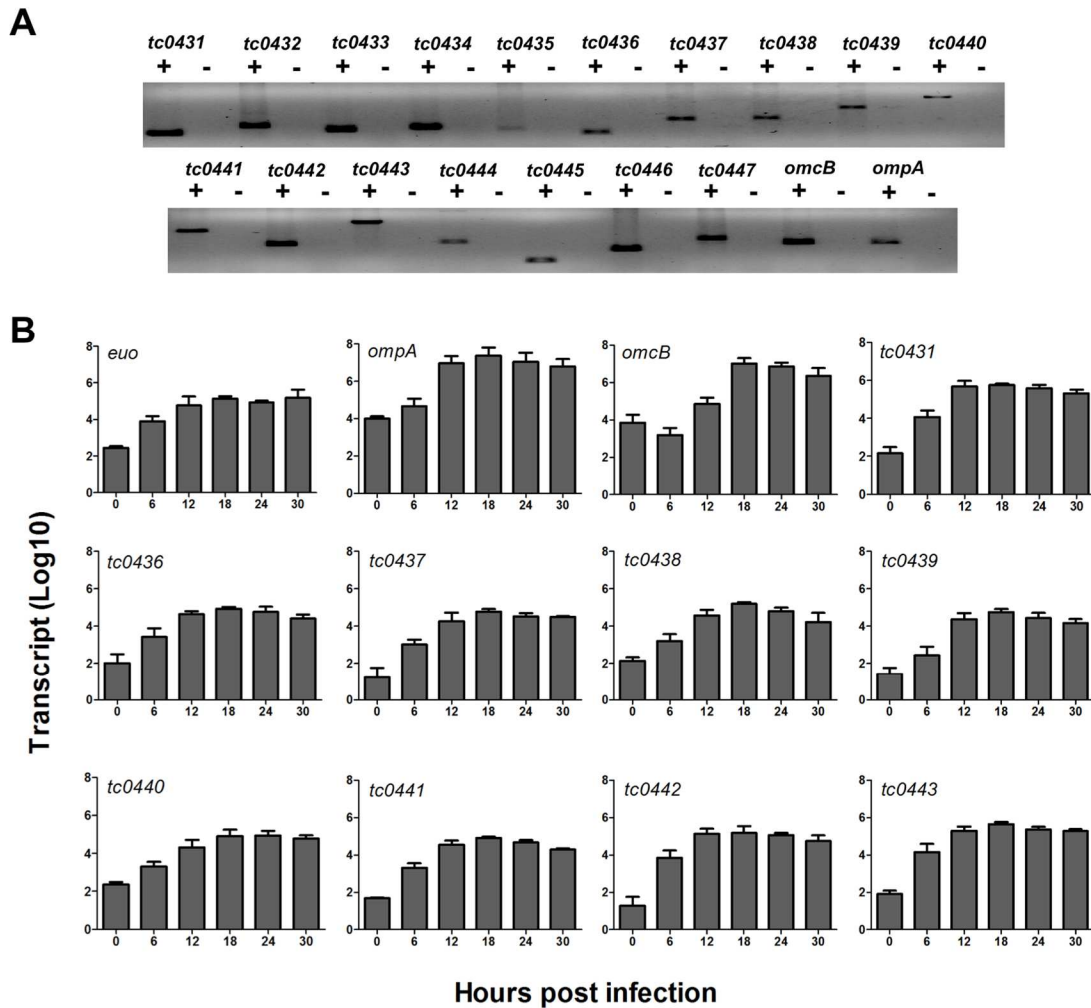
Fig. 2.2. Transcription of *C. muridarum* **PZ ORFs initiates mid-late developmental cycle.** Total RNA was isolated from *C. muridarum* infected McCoy cells at 0, 6, 12, 18, 24 and 30 hpi. A) RT-PCR at 24 hpi indicated that all genes in the PZ are transcribed, +/- symbols indicate amplifications performed with or without reverse transcriptase. B) Kinetics of transcription of select PZ ORFs was characterized by qRT-PCR. Transcript levels were normalized to standard curves of dilutions of *C. muridarum* chromosomes. Data represent the mean transcript levels (± SD) from three independent experiments. *euo, ompA* and *omcB* represent early, mid-late and late genes, respectively.
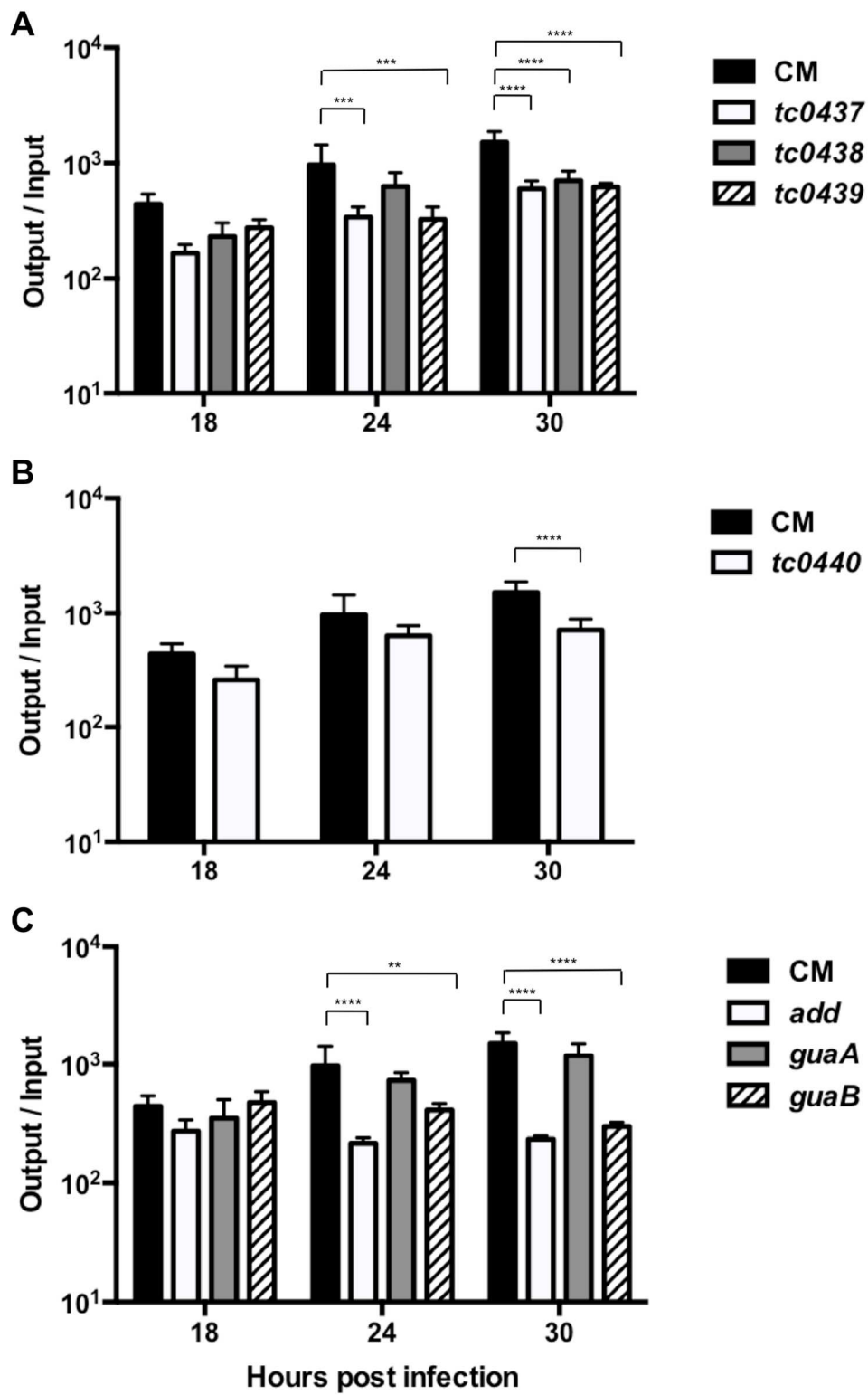
Fig. 2.3. *C. muridarum* **PZ mutants exhibit mild growth defects.** rIFU analysis was performed for *C. muridarum* WT (CM) and PZ mutants at various time intervals following infection of McCoy cells. Data in the panels are from experiments performed in parallel. Data represent the average ($\pm$ SD) ratios of input:output IFU from three independent experiments performed in triplicate. ****, $p < 0.0001$; ***, $p < 0.001$; **, $p < 0.01$ by two-way ANOVA with Bonferroni post hoc test.

Fig. 2.4. *tc0437* **and** *tc0439* **mutants have reduced cytotoxicity.** (A) HeLa cells were infected at an MOI of 250 in the presence of rifampin and were fixed 3 hpi. Cell morphology and actin structure were visualized by staining with AlexaFluor 488-phalloidin (green), DAPI (blue) and AlexaFluor 594 WGA (red). Overlays of fluorescent micrographs of cells that are mock-infected or infected with *C. muridarum* (CM), *C. trachomatis* serovar L2 (CTL), *tc0437*, *tc0438* or *tc0439* are depicted. Images are representative of three independent experiments. B) LDH in supernatants of HeLa cells infected at various MOI, indicated below the X axis, in the presence of rifampin. *C. muridarum* (black), *C. trachomatis* serovar L2 (gray), *tc0437* (hatched), *tc0438* (white) or *tc0439* (cross-hatched). Triton X-100 treated cells were used as positive controls for LDH release. Data show the mean percent of positive control ($\pm$ SD) of three independent experiments performed in triplicate. ****, $p < 0.0001$; **, $p < 0.01$ by one-way ANOVA with Dunnett's post hoc test.
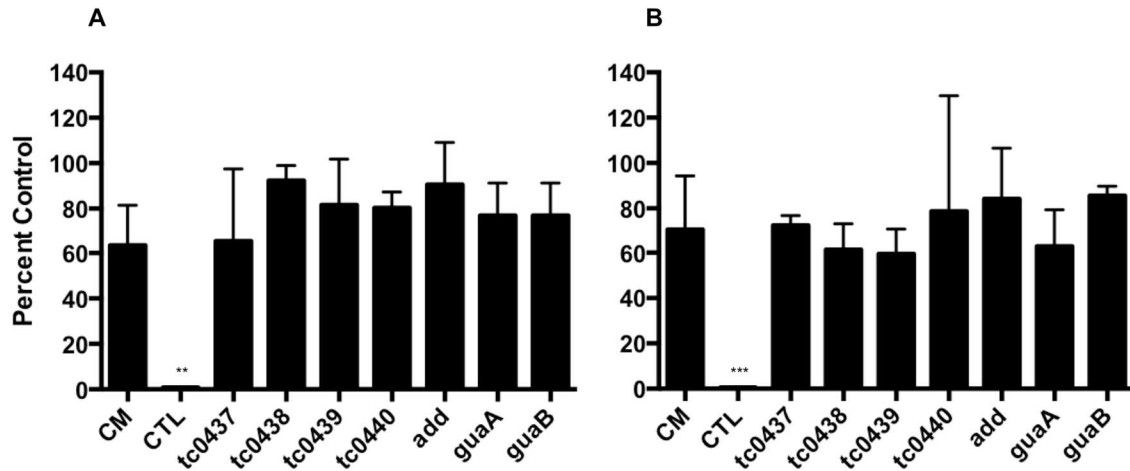
Fig. 2.5. PZ mutants are resistant to IFN-γ. Sensitivity to IFN-γ treatment of *C. muridarum* (CM), *C. trachomatis* serovar L2 (CTL) and various PZ mutants was assessed by A) IFU assay and B) rIFU assay. Data are represented as the average (± SD) percent of untreated (no IFN-γ) infected controls from three independent experiments performed in triplicate. ***, $p < 0.001$; **, $p < 0.01$ by one-way ANOVA with Dunnett's post hoc test.
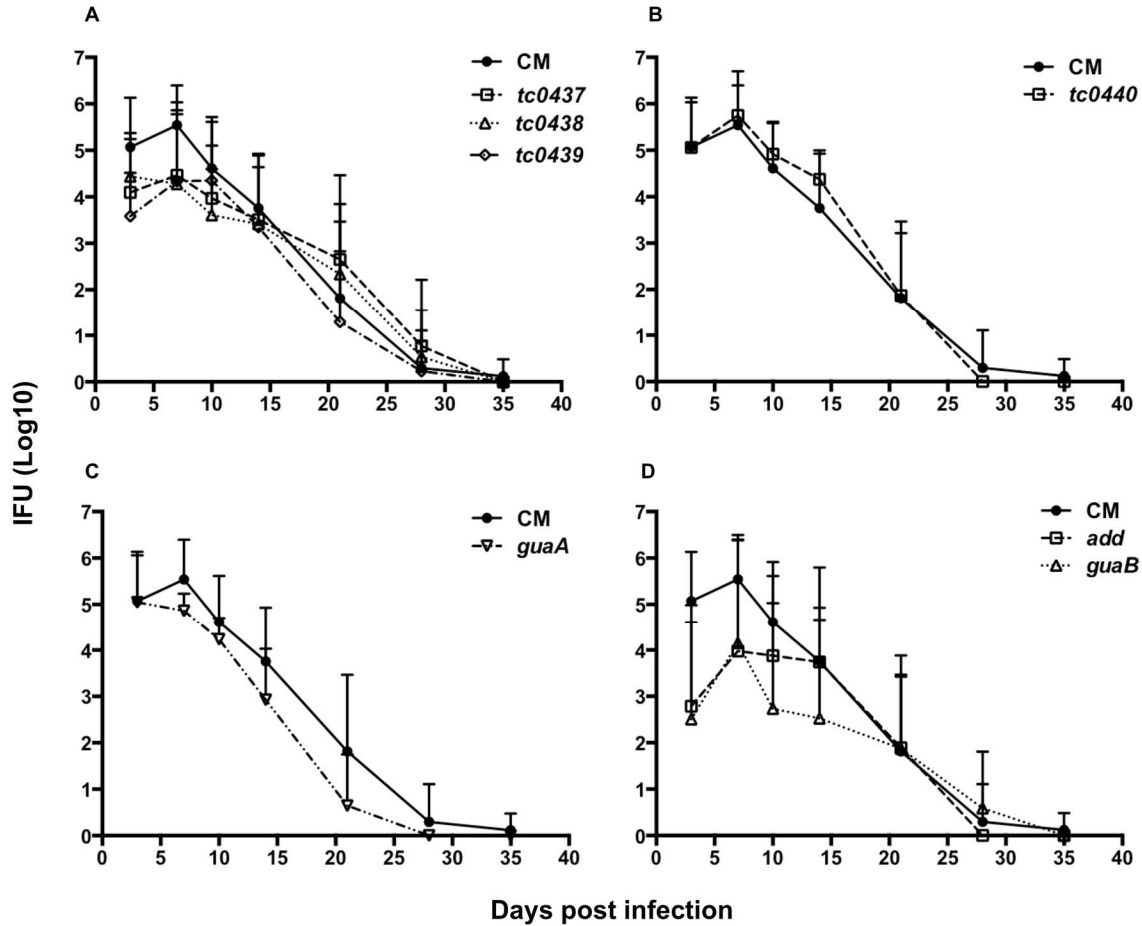
Fig. 2.6. Mouse genital tract infections with *C. muridarum* PZ mutants. Groups of mice were challenged intravaginally with 50,000 IFU of WT *C. muridarum* (CM) or various PZ mutants. The infection curve for WT *C. muridarum* infected mice (n=30) is reproduced in each panel for comparison. (A) Lower genital tract shedding of IFU by mice infected with *C. muridarum* (CM) differed significantly from that of mice infected with the *tc0439* mutant (n=8) at day 3 post infection (p < 0.01), but not those infected with *tc0437* (n=8) or *tc0438* (n=8). IFU shedding from mice infected with CM did not vary significantly from mice infected with mutants of (B) *t0440* (n=12) or (C) *guaA* (n=16). (D) Shedding by mice infected with *add* (n=8) mutant was significantly lower than with *C. muridarum* at 3 days (p < 0.0001) and 7 days (p < 0.01) post infection. IFU shedding from mice infected with *add* (n=8) mutant was also significantly reduced at 3 days (p < 0.0001), 7 days (p < 0.05) and 10 days (p < 0.001) post infection. Data are presented as mean IFU (± SD) for mice per group. Statistical differences were analyzed by two-way ANOVA with Bonferroni post hoc test.

76

TABLE 2.1. Primers for RT-PCR

Gene ID	Forward primer sequence (5' to 3')	Reverse primer sequence (5' to 3')	Product size (bp)
tc0431	ATG CCC CAC TCT CCT TTT TTA TAT GTT	CAA GTA GCT ACG CAG GCA GAT AG	272
tc0432	GTC AGT CAT TTG TAA GCT TAT GAA CCA GG	GCT ACT CGA GTC GCC AAC ATA GC	342
tc0433	GTG CTC TCC TTG TTC ACG TCA TAT C	GCT CTC AGT CCT ACG TGC TTT AAG G	292
tc0434	ATG ACC GCA CCT TTA ATA ACT ACC AC	GTT GCA GAG AGA ATG GCG TGT TC	317
tc0435	GGT CTC TCC TTT AAT AAC TAC CAC CTC	GAA GAC GGA ACA ACG TTC TTC AGA ACG	291
tc0436	CGA TAC AAG GTG TGT CCG TAA GC	CTC CAT TAA ACT AGC GAG ATG CAT G	251
tc0437	CCC CCT TCA GCA ATT TCA	TCT GAA GAA ACT GTA GGC TGT TTA C	399
tc0438	CCT GTT TCC GGT TCA ATT GTT GCA T	CGT ATC TTT AGA AGT GAA GCG A	406
tc0439	GTT AGG CAA GCC AAA ATT CTA G	CTA CTC CTT TGA GCT GGC AGT AG	550
tc0440	GTC ACT GAC TGC CCA ACT TG	GAT AGT GCG AAC TGC TAA TCG G	816
tc0441	GAA GCT CGC TTA CGA TTG TAC GAT C	CGC TGA GCT TAT GGT CTC TAA ATA ATG C	574
tc0442	GAA CTC GGA CTC CTA AAC CAG G	GCG CTT ATT CCC ACT CAA TAG TTG C	339
tc0443	ATG CGC GAA GCT CTG ACT TTT GAT G	GAG AAC CCA TAC CTC GAT ACA TCT TGT	781
tc0444	ATG GGC GCC AAT AAG ATA C	TTA TTC GAT TTT TGG AGA AAA AAT GTT C	363
tc0445	ATG GGC GCC AAT AAG ATA CAC GC	CCC TGT AAC CTC TGC ATT CGG ATT C	153
tc0446	GGC TTA ACG TCT TGT CAC CAG AAA G	GAT GTA CAA AAC TGG TAG CAA TGC	269
tc0447	CAG CTG CTT CAT CCT ATC TCC GC	CTG TGA CAA CGG ATT AGT TCT G	400
euo	ATG GAA TGC TTA CAA CAA GAT AC	CTA AGA AAC AAA ATC CTC TGA GTC	345
omcB	ATG AAA AAA CTC TTG AAA TCG GTA TTA GC	CTT GCA TAT GCT TGC CAT AAG C	340
ompA	ATG CGA ATA GGA GAT CCT ATG AAC	GCA CGA TTT CTA CAT TAC GAT CAT C	340

TABLE 2.2. Primers for qRT-PCR

Gene ID	Forward primer sequence (5' to 3')	Reverse primer sequence (5' to 3')	Product size (bp)
tc0431	GAG AGC GGC ACC CTA TTA CTT TAG ATT TC	GAT TCC CTA GAC AAG ACA TAA GAG GCT TC	140
tc0436	GGA CCC GAT TCG AGG GTT TC	CAC GAG AGG AAA CGC TCT TGT AAT ACG	117
tc0437	CGC CTC GCG CTT AAA GTT GAC TG	GGA CTG TTT GAC TAG CAG ATC CTT GTC C	123
tc0438	CTC AAG TTC CTT TTA CAA CCT CTC CTG C	CTC GGA TGG GTT GTA TAG TCG AAG G	116
tc0439	CGA ATA CAG CCT CTT CCA CAG TTT C	CTA TTG CTT TGA GCA ACA GGG TGA G	89
tc0440	CCT ATA GTC ACT GAC TGC CCA AC	GCT GCT GCT GTT GTC GAT GAG AG	77
tc0441	GAT GCG GCT TCA TCG AGC CAA CTC	CCT GAG TCA AGG AAT TAC CCT TCG	122
tc0442	GGA AGT CCA CCT ACA TTA TGG	CAT AGG AGC CGC CTT TAT CG	158
tc0443	GAG AAC CCA TAC CTC GAT ACA TCT TGT	CGC ATT GTG TTA TGC TCG GTA G	107
euo	GAG CAG CAA GAA GAG GAG AAT GC	GCG ACA TAG ATA GCC TGA CGA GTC	104
omcB	GCA TCA AGA GAG AAT CCC GCT TAT G	CCG CTA GTT GCT CCC AAT GTA C	128
ompA	GTG CTT GTC CAG AGA TCC GTT CG	CTG TTG CTG TTC CTT GGT TGA CTA C	138

TABLE 2.3. Primers for cloning PZ fragments into the pAC-lacZ vector

Construct	Forward primer sequence (5' to 3')	Reverse primer sequence (5' to 3')	Genbank Coordinates flanking Construct
1	ATA ATA TCG CGA ACC AAT GCG AAC AAC ATC TTC TGT	GCT CTT CGG CCG GTA ATA CGA AAA GGT GTG TTT C	506506-505406
2	TAA TAA TCG CGA ATG GAC CCG ATT CGA GGG TTT CAC CAG	AAG TGC CGG CCG CAC CAA GTG CAC AAA TC	505479-504381
3	ATC ATA TCG CGA AAA CTG TTA TCA TCG GCT CCG CTA ATT GGT CCG	GAT TAG CGG CCG CAT TTT GTC TGC GGG TAG GCC	504505-503381
4	ACA AAC TCG CGA AAT ACA CCC TTG AAA AGC TAT CCT CTC AC	CAG CGA CGG CCG GTT CTG GGC TAT TTA CTC GC	503476-502487
5	CGT TCA TCG CGA CTA TTT CAC AAA AAA ACT CTT ATC ATT GAT AAA C	GTT TTG CGG CCG CTA GAA GTC TCT AAC GAA TGA	502509-501488
6	GAA GAT TCG CGA TTG TTT ATC GTT CGA AAT CTA ACA GCA C	AGA GAT CGG CCG GGT TGT TGT TGC AGG ATA ATC	500724-499715
7	ACA ACC TCG CGA ATC TCT ATT CCA CAG AAA ATC GCT GG	GGC AGA CGG CCG TAG TTT GGG TTC TAG AAC GG	499715-498724
8	TTT ATT TCG CGA GAA AAC CTA CCT TTA GAA ATT TTT GGA GCC	GGC TTG CGG CCG CTG AAA ACG CTG CTG	498833-497707
9	ATA ATA TCG CGA GTT CCA ATG TAG TTT GGA TGA CC	ATA ATA CGG CCG CAA CAA TCC ATC CAC AAC GTT C	497801-496846
10	CAT AGG TCG CGA TTC TTT ACC TAT TCG ACA AAA GAT TTT TGG C	GCT GAG CGG CCG TAG AAT TAT GGG AAT TCT TAT TG	496910-495810
11	CCT GAA TCG CGA GCT CCG GTA ATC GCA ACC TCT CC	GAG CCT CGG CCG CGC TCT CTG TCT CAG TAC ATT	495919-494389
12	ATC ATA TCG CGA GTG CTC TTG AAC ATC TGG AG	ATC ATA CGG CCG GTT GTG TAA TAG TGC GTG G	505999-504971
13	ATCATA TCGCGA GTC CAA AAC AAC TAT AGA GCT AAT CCA G	ATC ATA CGG CCG GTC TTA TGA GGG CAA TGT ATG	504984-503936
14	ATC ATA TCG CGA GAA CGT TGT TCC GTC TTC TAA ATC	ATC ATA CGG CCG GTG GTA GTT ATT AAA GGT GC	503977-503108
15	CTG ATA TCG CGA GTA AGT TAG ATA GGC TGC G	ATA ATA CGG CCG GAA GAG TCA GCG TTT TCG	503120-501964
16	GTG GTC TCG CGA GTG AGA ATA GTA CTG CTA TAA C	ATA ATA CGG CCG GAT GGA AGA CAA TGG AGA G	501974-501177
17	ATA ATA TCG CGA CGC TGG TTG TTG ATC ACA GAA TG	ATA ATA CGG CCG GTC TCT AAC GAA TGA CGA TTG C	501231-500093
18	GTG GTA TCG CGA GAT CTC TCC CAT CGA GTT ATT TAT G	ATA GTA CGG CCG CTG ATA AGG ATT GGC ATT GAG	500098-499295
19	ATA GTA TCG CGA GGA TCT TCT AAT TGG TCA TTC GTA GG	ATA ATA CGG CCG GTC ACA AGA ATT TCC TGC TGT C	499340-498170
20	GTA GTA TCG CGA CTT TTT GTG TAC CAC CTC TTA CC	ATA ATA CGG CCG GAC ACT TTC AGA CCA ATC TTT AAA ATC	498229-497370
21	ATA ATA TCG CGA CAG CAC GGA ATC TGG CTA CTC TAC	ATA ATA CGG CCG GAT GAA CCT TCT GGG AAC CTG	497473-496327
22	ATA ATA TCG CGA CAG CTA ACT CTC GAT CAT GAG TTA CG	ATA ATA CGG CCG GCT TGT TCC AAT ATT GTG ACC	497415-495248
23	GTA CGA TCG CGA TTC CTG CTT GAT TTT TC	GAT ATA CGG CCG GTG TTT ACT TGA TCT AG	504810-505810
24	ATA CAG TCG CGA GAA CCT TAA TTG GGC	TAA ATA CGG CCG GTT CCA AGA GAA AAC GGC TTA	525699-526699
25	CTC ACG TCG CGA ATA AAA GCT TAT CAA TTG	ATA TTA CGG CCG GAA CAA TGC TTG GC	525199-526199
26	ATA CGA TCG CGA ATG CAA CAA CAC TAA AAT T	ATA TTA CGG CCG CTT GTC TTT AGA TGT GC	524699-525699
27	ATA TAA TCG CGA ACC CAA GAA TAG CGA AG	ATC CGA CGG CCG TGT TTT TTA TTT TAA CAA AG	535815-536815
28	ATT TAT TCG CGA CTA GCA ACC CAT CGG C	ATA CTA CGG CCG CGT TCT TCT TCT GTT GTC	535315-536315
29	TAT TCG CGG CCG TGC TCT TTC TAA ACC TTG	CGC AGG CGG CCG TAA ATC CCT TAA AAT AAG	541942-542942
30	TAT TCG CGG CCG TGC TCT TTC TAA ACC TTG	CGC AGG CGG CCG TAA ATC CCT TAA AAT AAG	542942-541942

TABLE 2.3. Cont.

Construct	Forward primer sequence (5' -> 3')	Reverse primer sequence (5' -> 3')	Genbank Coordinates flanking Construct
31	TTA TTA CGG CCG TAG CGT TCA GCA CTA CC	ATA TGC CGG CCG GTC GAT TTA ATT TCC	541442-542442
32	TTA TTA CGG CCG TAG CGT TCA GCA CTA CC	ATA TGC CGG CCG GTC GAT TTA ATT TCC	542442-541442
33	GTG CTA CGG CCG CGA AAA TAA AAG TTA ATA A	ATT CGA CGG CCG AAA CTT TTT TTT AGG CAT AAA G	543885-542868
34	TTA ATA CGG CCG TAG GTT GGA GGG ATT GTA ATG	CGC AGA CGG CCG ACT TTA GTA AAA AAA AGG	542368-543368
35	TTA ATA CGG CCG TAG GTT GGA GGG ATT GTA ATG	CGC AGA CGG CCG ACT TTA GTA AAA AAA AGG	543368-542368
36	GTA CGA TCG CGA GTT GTA GGG TTT GAT AAT GG	ATT CGA CGG CCG AAA CTT TTT TTT AGG CAT AAA G	542868-542368
37	GCA TGA TCG CGA ATC CAA GAA AAT AGT GAT GAA	GCA TGA CGG CCG ATT ATC TCC TAT TTC CCT CG	505347-506310
38	GCA TGA TCG CGA GAG ATA ATA TGC CCC CTT CA	GCA TGA CGG CCG CTA CCC AAA ATA AAA AAT CAA AC	506322-507296
39	GCA TGA TCG CGA GAG TAA AAA TTG ACA GTC	GCA TGA CGG CCG ACT TGA TTT TTG TTT ATT CTC	507174-508174
40	GCA TGA TCG CGA GGT TTC AGA TGG GGT TTT GAG	GCA TGA CGG CCG CAC ACA CTT GAT TAC GAA GAA	508021-509021
41	GCA TGA TCG CGA CGA GTT GCT AGA TCG ATT	GCA TGA CGG CCG CTA ATC TAG CAG ATG GAG	508915-509906
42	GCA TGA TCG CGA TTT AAC AGA GAT CAC TCG GTA	GCA TGA CGG CCG CCT CAT CTT CTA TGG ACA TAT	509812-510803
43	AAG TAT TCG CGA ACT TTG TTA TCT TGG CCA GAA	TGC CTC CCG CCG AAG AAA TTG AAA TAG AGA TGC	510635-511648
44	AAA CAT TCG CGA GTT TTA GAT TCT GAA ACG GTA	ATA ATT CGG CCG TAA AAG AAA ATT TCC TAA AAC	511514-512566
45	CTT TAC TCG CGA CCT CTT TGA TGC TAG CTG TGG	TTC CTC CGG CCG TTC CTT TAC CTG AAT AAA TAG	512355-513353
46	GTA GAA TCG CGA CAA GAT GTT CCG CTG ATA AGG	CCA TAA CGG CCG GAT TCC AAT AAC TTG GGT TTC	513179-514220
47	TAA GTT TCG CGA CCA TTC TAC CAA CTC TTA TAT	CTT GTC CGG CCG AAC TAA AAT CGC TAA ATT GAG	514008-514987
48	ATG GGA TCG CGA TTA ATT AAT CCT GCA TAT AGA	TCC TAA CGG CCG AGG TTT CAA GAA TGC GTC TAA	514913-515896
49	ATG GGA TCG CGA TTA ATT AAT CCT GCA TAT AGA	GTA CTA CGG CCG GAT TCA CCA ACA CTA TG	514913-515353
50	GTA CTA TCG CGA CTT CAC ATA GTG TTG GTG	TCC TAA CGG CCG AGG TTT CAA GAA TGC GTC TAA	515330-515896
51	GCA TGA TCG CGA GTA TTC CTA TAG CTT TAA	GCA TGA CGG CCG ATT GTA ATT AGT AAT AGC	515787-516852
52	CTC AAT TCG CGA CAG CCT CGG TCT TAG TC	GCC CAT CGG CCG TCC TGA TCG AAT CCC	542301-541321
53	CTG AAA TCG CGA TTG GTG TGG ACG CTG	CTT TGG CGG CCG GCA TTC TAT AGC GGC	541784-540688
54	CAC TGT TCG CGA CCC ATT GCC GCT ATA G	GGA GTG CGG CCG TCA TCG CTC AAC TCA G	540720-539541
55	GGT AAA TCG CGA GTT CTG GGT TTG CCG	CAA CTC CGG CCG GCA GCC TCT TCA G	540044-538928
56	CGT ACA TCG CGA GGG GCA TAG ACA TCC	CGA GTG CGG CCG GAA TAA GTA GCG CAG G	539248-538082
57	GCT CCG TCG CGA GCT ATT AAC CTG GTA C	GGA CTT CGG CCG CCG ATT AGC AGT TCG C	538633-537603
58	GTC TTG TCG CGA CGA GCA GTT GTT CAA G	GAT CCT CGG CCG GGA CAA TGG GTT CAG	545014-545939

TABLE 2.4. Identification of promoter elements in the *C. muridarum* PZ

Construct	Genbank Coordinates flanking Construct	Average β-galactosidase activity (Miller Units)	± SD
1	506506-505406	0	0
2	505479-504381	31.28	1.04
3	504505-503381	30.78	0.74
4	503476-502487	8.66	0.99
5	502509-501488	14.21	0.67
6	500724-499715	0	0
7	499715-498724	52.49	2.06
8	498833-497707	0	0
9	497801-496846	2.79	0.15
10	496910-495810	12.3	0.7
11	495919-494389	0	0
12	505999-504971	0	0
13	504984-503936	0	0
14	503977-503108	0	0
15	503120-501964	39.46	1.44
16	501974-501177	0	0
17	501231-500093	0	0
18	500098-499295	0	0
19	499340-498170	0	0
20	498229-497370	105.1	2.23
21	497473-496327	150.83	9.75
22	497415-495248	0	0
23	504810-505810	7.3	7.3
24	525699-526699	0	0
25	525199-526199	8.3	0.26
26	524699-525699	88.64	2.82
27	535815-536815	27.63	0.58
28	535315-536315	157.17	7.64
29	541942-542942	82.87	2.42
30	542942-541942	89.2	2.32
31	541442-542442	156.1	13
32	542442-541442	0	0
33	543885-542868	188.76	27.14
34	542368-543368	95.77	2.3
35	543368-542368	3175.467	995.4
36	542868-542368	3470.29	115.87
37	505347-506310	5.1	2.33
38	506322-507296	8.57	3.43
39	507174-508174	49.13	1.17
40	508021-509021	103.7	4.68
41	508915-509906	10.37	1.3
42	509812-510803	12.96	2.84
43	510635-511648	4.88	1.53
44	511514-512566	185.98	24.8
45	512355-513353	3.69	1.2
46	513179-514220	7.87	0.96
47	514008-514987	27.6	2.32

TABLE 2.4. Cont.

Construct	Genbank Coordinates flanking Construct	Average β-galactosidase activity (Miller Units)	± SD
48	514913-515896	1320.84	459.73
49	514913-515353	59.03	6.59
50	515330-515896	1172.97	132.06
51	515787-516852	86.12	1
52	542301-541321	6.75	0.27
53	541784-540688	19.85	3.77
54	540720-539541	70.37	4.96
55	540044-538928	32.84	1.04
56	539248-538082	9.36	0.87
57	538633-537603	19.56	0.71
58	545014-545939	9.43	1.06
lacZ vector (-) control	-	111.04	39.65
dnaK (+) control	-	518.9	82.39

TABLE 2.5. Primers for TILLING

Gene ID	Forward primer Sequence (5' to 3')	GenBank Coordinates	Reverse primer sequence (5' to 3')	GenBank Coordinates
tc0431	ATG CCC CAC TCT CCT TTT TTA TAT GTT	498629	ATC AAT TAA CAC GGC TGC AAT TGT ATG	497607
tc0437	TCT ACG ACG CCT CAA GTC A	506363	AAT TTA GCC GCT CCA AAA GC	507325
tc0438	CCT GTT TCC GGT TCA ATT GTT GCA T	516121	GGC TCA TAT ACT GTT CTA TGC CCT C	517124
tc0439	GAA CAA GCA TTG TGT ACT ATG ACT C	526702	GCT GCA TCA AAA GCA ATT CG	527714
tc0440	ATG TGT TCC CCC TGT CCA CGT C	536815	GTG GAG CAC CAG GCT TGC G	537841
tc0441	GTT AGA GGT GAA GAT GTC ACA TGA G	538405	CCA CCG GCA ACT ATT GAG TG	539652
tc0442	GCG CTT ATT CCC ACT CAA TAG TTG C	539628	GCG TGA AGC ATA TTT GCC AGA C	540609
tc0443	GCA AGT TAT GGA TGT GGC TTT CAG	541225	CTC AAT CAG CCT CGG TCT TAG TCA	542301

83

TABLE 2.6. Summary of TILLING screen size and isolated mutants

Gene ID	Estimated Screen Size (N)	Total no. of mutants	No. of silent mutants	No. of missense mutants	No. of nonsense mutants
tc0431 (MACPF)	64	68	13	55	0
tc0437	33	20	4	14	2
tc0438	55	30	9	20	1
tc0439	36	47	8	37	2
tc0440 (PLD)	48	43	11	28	4
tc0441(add)	42	13	3	9	1
tc0442(guaA)	94	12	0	10	2
tc0443(guaB)	94	8	1	6	1

TABLE 2.7. Polymorphisms in *C. muridarum* parent strain

Gene ID	Description	Position	*C. muridarum* used in study	*C. muridarum* Nigg	*C. muridarum* Weiss
tc0007	exodeoxyribonuclease V, beta chain, putative	10505	A	-	-
tc0007	exodeoxyribonuclease V, beta chain, putative	10558	A,C	-	-
tc0007	exodeoxyribonuclease V, beta chain, putative	10564	A	-	-
tc0027	Conserved hypothetical protein	32915	G	-	-
tc0052	major outer membrane protein, porin; ompA	58882	T	-	-
tc0052	major outer membrane protein, porin; ompA	58904	T	-	-
tc0052	major outer membrane protein, porin; ompA	59065	C	C	T
tc0107	lipoprotein	126406	G	G	-
tc0107	lipoprotein	126416	-	-	A
-	intergenic	126383	G	-	-
-	intergenic	126436	A	-	-
-	intergenic	126475	-	A	-
tc0124	transcription-repair-coupling factor; trcF	151212	T	T	-
tc_r05	rRNA-23S ribosomal RNA	158800	G	-	-
tc0138	phospho-N-acetylmuramoylpentapeptide transferase; mraY	169451	TTTT	T	T
tc0168	ribosomal protein L34; rpmH	200671	C	G	C
tc0301	methionyl tRNA synthetase; metG	358414	T	-	-
tc0338	ABC transporter, periplasmic substrate binding protein	401302	G	-	-
tc0341	ABC transporter, permease protein	403623	-	T	-
tc0341	ABC transporter, permease protein	403624	C	A	A
tc0341	ABC transporter, permease protein	403626	-	-	C
tc0341	ABC transporter, permease protein	403652	C,G	T	C
tc0341	ABC transporter, permease protein	403714	G	-	-
tc0342	ABC transporter, permease protein	404473	T	-	-
tc0342	ABC transporter, permease protein	404884	A	A	-
tc0343	1-deoxy-D-xylulose 5-phosphate reductoisomeras; dxr	405819	G	-	-
tc0359	hypothetical protein	419119	C	-	-
tc0408	hypothetical protein	468932	T	G	T
tc0412	hypothetical protein	473118	A	A	-
tc0437	adherence factor	515204	A	C	C
tc0493	phenylacrylic acid decarboxylase; ubiX	600435	A	C	C
tc0708	translation elongation factor; tuf	712587	C	-	-
tc0708	hypothetical protein	846475	G	G	-
tc0727	outer membrane protein; omcB	866121	T	G	T
tc0832	DNA polymerase III alpha subunit; dnaE	967487	A	A	-
tc0879	hypothetical protein	1022529	A	-	-
tc0879	hypothetical protein	1022551	A	-	-
tc0893	groEL-2	1035913	A	-	-

C. muridarum Nigg isolate accession number: AE002160.2

C. muridarum Weiss isolate accession number: ACOW00000000

TABLE 2.8. SNPs in *C. muridarum tc0437* mutant

Gene ID	Description	Nucleotide Position	Nucleotide Change	Amino acid Change
tc008	exodeoxyribonuclease V, gamma subunit	13703	G → A	Thr → Ile
tc0019	recA	26275	G → A	Glu → Lys
tc0035	hypothetical protein	40681	G → A	Leu → Leu
tc0069	endonuclease III	80096	C → T	Pro → Ser
tc0074	preprotein translocase SecA subunit; secA	85403	C → T	Arg → Cys
tc0096	ribosomal large subunit pseudouridine synthase B; rluB	115068	G → A	Gly → Gly
tc0120	hypothetical protein	144193	C → T	Arg → Cys
tc0125	alanyl-tRNA synthetase	153963	G → A	Ala → Val
tc0137	murF	168334	C → T	Leu → Leu
tc0159	primosomal protein N	193263	G → A	Arg → Arg
tc0172	conserved hypothetical protein	202909	G → A	Gly → Glu
tc0213	CDP-diacylglycerol--serine O-phosphatidyltransferase	252676	C → T	Met → Ile
tc0218	UDP-N-acetylenolpyruvoylglucosamine reductase; murB	260165	G → A	Ser → Phe
tc0237	hypothetical protein	277523	G → A	Arg → Cys
tc0283	PhoH-related protein	338843	C → T	Gly → Arg
tc0290	hypothetical protein	349249	C → T	Arg → Lys
tc0330	protein export protein, FHIPEP family protein	391857	C → T	Arg → Trp
tc0383	A/G-specific adenine glycosylase	444982	A → G	Thr → Ala
tc0412	conserved hypothetical protein	473585	C → T	Gln → STOP
tc0424	conserved hypothetical protein	487908	C → T	Ala → Val
tc0437	adherence factor	506777	C → T	Gln → STOP
tc0438	adherence factor	520769	G → A	Arg → Gln
tc0453	hypothetical protein	551457	G → A	Arg → Arg
tc0460	thymidylate kinase	558168	C → T	Glu → Lys
tc0469	hypothetical protein	569879	C → T	Ala → Val
tc0471	peptide ABC transporter, periplasmic peptide-binding protein	572022	C → T	Thr → Ile
tc0479	pfkA-2, beta subunit	581345	G → A	Glu → Lys
tc0490	Rep helicase family protein; uvrD	596078	G → A	Ser → Ser
tc0501	sodium:dicarboxylate symporter family protein	607577	C → T	Ser → Phe
tc0544	hypothetical protein	654353	G → A	Ile → Ile
tc0575	serine/threonine kinase protein	684627	G → A	Ala → Ala
tc0588	DNA-directed RNA polymerase, beta subunit; rpoC	702107	G → A	Leu → Phe
tc0635	hypothetical protein	761471	C → T	Glu → Gln
tc0645	3-phosphoshikimate 1-carboxyvinyltransferase; aroA	772383	G → A	Lys → Phe
tc0694	polymorphic membrane protein B/C family protein; pmpB/C-1	829608	C → T	Asn → Asn
tc0694	polymorphic membrane protein B/C family protein; pmpB/C-1	831869	C → T	Ser → Phe
tc0733	secDF protein	872206	G → A	Asp → Asp
tc0810	ribosomal protein, L22; rplV	945533	C → T	Gly → Arg
tc0816	hypothetical protein	949915	C → T	Thr → Thr
tc0833	uracil phosphoribosyltransferase; upp	969350	G → A	Gly → Arg
tc0842	branched-chain amino acid transport system carrier protein	977030	G → A	Gly → Glu
tc0864	DNA mismatch repair protein MutL	1001277	G → A	Leu → Phe
tc0877	regulatory protein	1016507	C → T	His → Tyr
tc0917	geranylgeranyl pyrophosphate synthase	1069215	G → A	Leu → Leu

TABLE 2.9. SNPs in *C. muridarum tc0438* mutant

Gene ID	Description	Nucleotide Position	Nucleotide Change	Amino acid Change
tc0019	recA	26275	G → A	Glu → Lys
tc0064	phosphate permease family protein	74467	G → A	Arg → Lys
tc0121	protoporphyrinogen oxidase; hemY	146183	G → A	Ser → Phe
tc0125	alanyl-tRNA synthetase	153963	G → A	Ala → Val
tc0137	murF	168503	G → A	Gly → Arg
tc0147	tRNA delta-2-isopentenylpyrophosphate transferase	179316	G → A	Glu → Lys
tc0186	ribosomal protein L9	218818	G → A	Glu → Lys
tc0214	ribonucleoside-diphosphate reductase, alpha subunit	255549	C → T	His → His
tc0218	UDP-N-acetylenolpyruvoylglucosamine reductase; murB	260165	G → A	Ser → Phe
tc0237	hypothetical protein	277523	G → A	Arg → Cys
tc0283	PhoH-related protein	338843	C → T	Gly → Arg
tc0294	signal recognition particle protein	352693	G → A	Asp → Asn
tc0330	protein export protein, FHIPEP family protein	391857	C → T	Arg → Trp
tc0404	adenylate kinase; adk	464247	G → A	Thr → Thr
tc0412	hypothetical protein	473585	C → T	Gln → STOP
tc0425	monooxygenase-related protein	491242	G → A	Ser → Phe
tc0438	adherence factor	516403	C → T	Gln → STOP
tc0438	adherence factor	519122	C → T	Ser → Phe
tc0438	adherence factor	520769	G → A	Arg → Gln
tc0438	adherence factor	525326	G → A	Arg → Lys
tc0450	hypothetical protein	549083	C → T	Arg → STOP
tc0471	peptide ABC transporter, periplasmic peptide-binding protein	572022	C → T	Thr → Ile
tc0575	serine/threonine kinase protein	684627	G → A	Ala → Ala
tc0580	ATP synthase subunit D; atpD	693778	G → A	Leu → Phe
tc0588	DNA-directed RNA polymerase, beta subunit; rpoC	702107	G → A	Leu → Phe
tc0635	hypothetical protein	761916	C → T	Glu → Lys
tc0644	hypothetical protein	771460	C → T	Asp → Asn
tc0645	3-phosphoshikimate 1-carboxyvinyltransferase; aroA	772383	G → A	Lys → Phe
tc0666	hypothetical protein	795149	G → A	Arg → Gln
tc0671	hypothetical protein	800641	C → A	Gly → Asp
tc0681	sodium:dicarboxylate symporter family protein	813777	G → A	Pro → Ser
tc0694	polymorphic membrane protein B/C family; pmpB/C-1	828687	C → T	Ser → Ser
tc0694	polymorphic membrane protein B/C family; pmpB/C-1	828944	G → A	Gly → Asp
tc0833	uracil phosphoribosyltransferase, upp	969350	G → A	Gly → Arg
tc0877	regulatory protein, putative	1016507	C → T	His → Tyr

TABLE 2.10. SNPs in *C. muridarum tc0439* mutant

Gene ID	Description	Nucleotide Position	Nucleotide Change	Amino acid Change
tc0044	serine/threonine protein kinase	50222	G → A	Val → Val
tc0054	penicillin-binding protein	62823	G → A	Gly → Glu
TC0084	hypothetical protein	101889	G → A	Asp → Asn
-	intergenic	126188	C → T	-
tc0191	hypothetical protein	224779	G → A	Gly → Gly
tc0197	polymorphic membrane protein; pmpD	233168	G → A	Glu → Lys
tc0226	hypothetical protein	265848	G → A	Cys → Cys
tc0230	polyribonucleotide nucleotidyltransferase; pnpA	273825	G → A	Ser → Ser
tc0244	fumarate hydratase; fumC	284699	G → A	Glu → Lys
tc0249	penicillin tolerance protein; lytB	291424	C → T	Arg → Trp
tc0250	hypothetical protein	292616	C → T	Val → Ile
tc0290	hypothetical protein	349120	G → A	Ser → Phe
tc0312	glycosyl hydrolase	369812	G → A	Ser → Phe
tc0390	hypothetical protein	455441	G → A	Glu → Lys
tc0414	hypothetical protein	474899	C → T	Ser → Leu
tc0439	adherence factor	527311	C → T	Gln → STOP
tc0472	peptide ABC transporter, permease protein	573799	C → T	Pro → Leu
tc0521	chromosomal replication initiator protein; dnaA	630193	C → T	Val → Val
tc0521	chromosomal replication initiator protein; dnaA	630703	G → A	Phe → Phe
tc0576	valyl-tRNA synthetase	687755	C → T	Lys → Lys
tc0588	DNA-directed RNA polymerase, beta subunit; rpoC	702342	G → A	Asn → Asn
tc0600	hypothetical protein	716734	G → A	Ser → Phe
tc0600	hypothetical protein	717761	G → A	Gln → STOP
tc0695	polymorphic membrane protein B/C family; pmpB/C-2	837382	G → A	Thr → Thr
tc0716	serine hydroxymethyltransferase; glyA	853750	C → T	Val → Val
-	intergenic	869958	C → T	-
tc0732	ssDNA-specific exonuclease; recJ	870022	C → T	Gln → His
-	intergenic	920321	C → T	-

TABLE 2.11. SNPs in *C. muridarum tc0440* mutant

Gene ID	Description	Nucleotide Position	Nucleotide Change	Amino acid Change
tc0076	GTP-binding protein EngA; yfgk	88283	C → T	Gly → Ser
tc0108	sodium/alanine symporter family protein	127881	G → A	Val → Val
tc0124	transcription-repair coupling factor; trcF	150150	G → A	Asp → Asp
tc0192	glycerol-3-phosphate acyltransferase	225336	G → A	Asp → Asp
tc0212	hypothetical protein	251161	C → T	Met → Ile
tc0286	hypothetical protein	342465	G → A	Thr → Ile
tc0322	coproporphyrinogen III oxidase	380857	G → A	Leu → Phe
tc0355	hypothetical protein	415946	C → T	Pro → Leu
tc0408	hypothetical protein	469557	G → A	Arg → Cys
tc0437	adherence factor/cytotoxin	508662	C → T	Ser → Leu
tc0440	putative phospholipase D	537373	C → T	Gln → STOP
tc0464	hypothetical protein	564839	G → A	Ser → Leu
tc0477	diphosphate-fructose-6-phospahte 1-phosphotransferase; pfkA-1	580008	G → A	Arg → Gln
tc0532	DNA polymerase III subunit epsilon	643156	G → A	Val → Ile
tc0535	ABC transporter ATP-binding protein	645392	C → T	Leu → Leu
tc0554	glycine cleavage system protein H; gcvH	663397	C → T	Gly → Asp
tc0561	hypothetical protein	672063	C → T	Ile → Ile
tc0575	serine/threonine-protein kinase; pknD	686396	G → A	Pro → Ser
tc0579	V-type ATP synthase subunit I	692340	G → A	Thr → Thr
tc0579	V-type ATP synthase subunit I	692683	C → T	Arg → Gln
tc0588	DNA-directed RNA polymerase subunit beta; rpoC	701622	C → T	Arg → Arg
tc0602	helicase	721695	G → A	Thr → Ile
tc0605	exodeoxyribonuclease VII large subunit; xseA	724506	G → A	Gly → Glu
tc0610	excinuclease ABC subunit A; uvrA	735281	C → T	Leu → Phe
tc0617	hypothetical protein	740043	C → T	Ser → Ser
tc0635	hypothetical protein	762982	G → A	Arg → Arg
tc0650	hypothetical protein	777433	C → T	Ala → Val
tc0676	VacB/Rnb family exoribonuclease	809172	C → T	Ser → Ser
tc0690	sodium/alanine symporter family protein	820643	C → T	Ser → Ser
tc0697	ABC transporter ATP-binding protein	839505	C → T	Asp → Asp
tc0706	hemolysin	845268	C → T	Arg → Arg
tc0733	preprotein translocase subunit SecD/SecF	875842	G → A	Arg → Arg
-	intergenic	876181	C → T	-
tc0737	cytidylate kinase; cmk	879394	C → T	Ser → Ser
tc0814	50S ribosomal protein L4; rplD	947444	C → T	Arg → Lys
-	intergenic	953298	C → T	-
tc0864	DNA mismatch repair protein; mutL	1000005	G → A	Gln → STOP
tc0873	hypothetical protein	1011011	C → T	Leu → Phe
tc0886	ExbD/TolR family protein	1030795	C → T	Ser → Phe
tc0911	hypothetical protein	1057937	C → T	Val → Ile

TABLE 2.12. SNPs in *C. muridarum add* mutant

Gene ID	Description	Nucleotide Position	Nucleotide Change	Amino acid Change
tc0019	recA protein	26275	G → A	Glu → Lys
tc0035	hypothetical protein	40681	G → A	Leu → Leu
tc0069	endonuclease III; nth	80096	C → T	Ala → Thr
tc0098	BirA-related protein	116059	C → T	Leu → Phe
tc0120	hypothetical protein	144193	C → T	Arg → Cys
tc0125	alanyl-tRNA synthetase; alaS	153963	G → A	Ala → Val
-	intergenic	183496	T → C	-
-	intergenic	227658	C → T	-
tc0218	UDP-N-acetylenolpyruvoylglucosamine reductase; murB	260165	G → A	Ser → Phe
tc0226	hypothetical protein	266168	G → A	Pro → Ser
tc0237	hypothetical protein	277523	G → A	Arg → Cys
tc0252	type III secretion chaperone	295119	G → A	Leu → Leu
tc0283	PhoH-related protein	338843	C → T	Gly → Arg
tc0306	hypothetical protein	364225	G → A	Phe → Phe
tc0330	protein export protein, FHIPEP family	391857	C → T	Arg → Trp
tc0409	hypothetical protein	470580	G → A	Ile → Ile
tc0412	hypothetical protein	473585	C → T	Gln → STOP
tc0413	serine esterase	474570	C → T	Ser → Phe
tc0424	hypothetical protein	487580	C → T	Leu → Phe
tc0438	adherence factor	520769	G → A	Arg → Gln
tc0440	phospholipase D family protein	538075	G → A	Gly → Arg
tc0441	adenosine deaminase; add	539413	G → A	Gln → STOP
tc0466	magnesium transporter; mgtE	567943	G → A	Ser → Ser
tc0471	peptide ABC transporter, periplasmic peptide-binding protein	572022	C → T	Thr → Ile
tc0477	pfkA-1, beta subunit	579586	G → A	Glu → Glu
tc0479	pfkA-2, beta subunit	581345	G → A	Glu → Lys
tc0490	UvrD/REP helicase family protein	596078	G → A	Ser → Ser
tc0490	UvrD/REP helicase family protein	596953	C → T	Asp → Asn
tc0492	4-hydroxybenzoate octaprenyltransferase; ubiA	599868	C → T	Pro → Leu
tc0575	serine/threonine protein kinase	684627	G → A	Ala → Ala
tc0588	DNA-directed RNA polymerase, beta` subunit; rpoC	702107	G → A	Leu → Phe
tc0603	N-(5'-phosphoribosyl)-anthranilate isomerase; trpF	723235	C → T	Gly → Ser
tc0629	hypothetical protein	753985	G → A	Glu → Lys
tc0645	3-phosphoshikimate 1-carboxyvinyltransferase; aroA	772383	G → A	Lys → Lys
tc0649	3-dehydroquinate dehydratase/shikimate 5-dehydrogenase	776683	C → T	Gly → Ser
tc0674	grpE protein	804884	C → T	Pro → Leu
tc0699	GTP-binding protein, GTP1/Obg family	841076	C → T	Ala → Ala
tc0715	ATP-dependent Clp protease, proteolytic subunit; clpP-2	853202	C → T	Leu → Leu
tc0828	peptidyl-prolyl cis-trans isomerase; mip	959089	C → T	Glu → Lys
tc0833	uracil phosphoribosyltransferase; upp	969350	G → A	Gly → Arg
tc0877	regulatory protein	1016507	C → T	His → Tyr
tc0917	geranylgeranyl pyrophosphate synthase	1069215	G → A	Leu → Leu

TABLE 2.13. SNPs in *C. muridarum guaA* mutant

Gene ID	Description	Nucleotide Position	Nucleotide Change	Amino acid Change
tc0001	delta-aminolevulinic acid dehydratase; hemB	576	G → A	Cys → Tyr
tc0024	hypothetical protein	31399	G → A	Pro → Ser
tc0032	DNA gyrase, subunit B; gyrB-1	36506	G → A	Pro → Leu
tc0059	aminotransferase, class V	69061	G → A	Val → Ile
tc0089	hypothetical protein	108562	G → A	Leu → Leu
tc0108	sodium/alanine symporter family protein	128662	G → A	Ala → Pro
tc0112	cell division protein FtsK, putative	131865	G → A	Ile → Ile
tc0123	uroporphyrinogen decarboxylase; hemE	148454	G → A	Pro → Pro
tc0124	transcription-repair coupling factor; trcF	151261	C → T	Gly → Glu
-	intergenic	182756	G → A	-
tc0193	ribonuclease G; cafA	226211	G → A	His → Tyr
tc0196	fatty acid/phospholipid synthesis protein; plsX	229357	G → A	Val → Met
-	intergenic	239576	G → A	-
tc0284	hypothetical protein	340204	C → T	Leu → Phe
tc0322	oxygen-independent coproporphyrinogen III oxidase; HemN	380626	G → A	Pro → Ser
tc0333	6-phosphogluconate dehydrogenase, decarboxylatin; pgd	395612	G → A	Thr → Thr
tc0383	A/G-specific adenine glycosylase; mutY	445590	G → A	Asp → Asn
tc0442	GMP synthase; guaA	540375	G → A	Gln → STOP
tc0527	hypothetical protein	637749	G → A	Val → Ile
tc0550	NADH:ubiquinone oxidoreductase, subunit B	659443	C → T	Pro → Pro
-	intergenic	667975	G → A	-
tc_t24	tRNA	712252	C → T	-
tc0610	excinuclease ABC, subunit A; uvrA	734634	C → T	Ser → Ser
tc0623	protease, Lon family	747850	C → T	Ser → Ser
tc0651	hypothetical protein	778747	C → T	Ser → Phe
-	intergenic	816010	G → A	
tc0694	polymorphic membrane protein B/C family; pmpB/C-1	830732	C → T	Ser → Phe
tc0721	translation elongation factor G; fusA	859591	G → A	Pro → Ser
tc0733	secDF protein, putative	874619	G → A	Pro → Leu
tc0759	hypothetical protein	899994	C → T	Asp → Asp
tc0764	peptide ABC transporter, permease protein	907437	C → A	Val → Val
tc0791	hypothetical protein	934794	C → T	Asp → Asn
tc0823	DNA polymerase III, epsilon subunit	955910	C → T	Gly → Glu
tc0842	branched-chain amino acid transport system carrier protein	976805	C → T	Pro → Leu
tc0843	helicase, Snf2 family	981172	T → G	Ser → Ala
tc0903	folK/P	1046666	G → A	His → Tyr
tc0906	hypothetical protein	1049784	G → A	Ser → Leu
tc0916	hypothetical protein	1067874	C → T	Ala → Val

TABLE 2.14. SNPs in *C. muridarum guaB* mutant

Gene ID	Description	Nucleotide Position	Nucleotide Change	Amino acid Change
tc0054	penicillin-binding protein	62823	G → A	Gly → Glu
tc0092	hypothetical protein	110539	C → T	Glu → Lys
-	intergenic	126188	C → T	-
tc0125	alanyl-tRNA synthetase; alaS	152652	C → T	Gly → Glu
tc0181	glycogen synthase; glgA	214991	G → A	Ala → Val
tc0191	hypothetical protein	224779	G → A	Gly → Gly
tc0197	polymorphic membrane protein D family; pmpD	233168	G → A	Glu → Lys
tc0228	MesJ/Ycf62 family protein	268437	G → A	Glu → Lys
tc0250	hypothetical protein	292616	C → T	Val → Ile
tc0263	polymorphic membrane protein G family; pmpG-1	312471	G → A	Asp → Asn
tc0285	hypothetical protein	341031	C → T	Ser → Phe
tc0290	hypothetical protein	349120	G → A	Ser → Phe
tc0312	glycosyl hydrolase family protein	369812	G → A	Ser → Phe
tc0319	hypothetical protein	376782	C → T	Ser → Phe
tc0331	RNA polymerase sigma factor, sigma-70 family	392203	C → T	His → His
tc0410	hypothetical protein	471306	C → T	Thr → Thr
tc0415	dipeptidase	475870	C → T	Val → Val
tc0439	adherence factor	536039	G → A	Gly → Asp
tc0443	inosine-5`-monophosphate dehydrogenase	541698	G → A	Gln → STOP
tc0473	peptide ABC transporter, permease protein	573799	C → T	Pro → Leu
tc0504	hypothetical protein	610197	C → T	Pro → Leu
tc0511	recombination protein RecR	617540	C → T	Phe → Phe
tcC0553	NADH:ubiquinone oxidoreductase, subunit E	662309	C → T	Ser → Phe
tc0600	hypothetical protein	717761	G → A	Gln → STOP
tc0610	excinuclease ABC, subunit A; uvrA	732712	G → A	Pro → Pro
tc0676	exoribonuclease, VacB/Rnb family	808732	G → A	Ile → Ile
-	intergenic	866802	G → A	-
tc0777	hypothetical protein	918927	G → A	Gly → Glu
tc0909	hypothetical protein	1052698	C → T	Gly → Gly

2.6 References

1. **Zomorodipour A, Andersson SGE.** 1999. Obligate intracellular parasites: *Rickettsia prowazekii* and *Chlamydia trachomatis*. FEBS Lett. **452:**11-15.

2. **Stephens RS, Kalman S, Lammel C, Fan J, Marathe R, Aravind L, Mitchell W, Olinger L, Tatusov RL, Zhao QX, Koonin EV, Davis RW.** 1998. Genome sequence of an obligate intracellular pathogen of humans: *Chlamydia trachomatis*. Science **282:**754-759.

3. **Kalman S, Mitchell W, Marathe R, Lammel C, Fan L, Hyman RW, Olinger L, Grimwood L, Davis RW, Stephens RS.** 1999. Comparative genomes of *Chlamydia pneumoniae* and *C. trachomatis*. Nat. Genet. **21:**385-389.

4. **Read TD, Brunham RC, Shen C, Gill SR, Heidelberg JF, White O, Hickey EK, Peterson J, Utterback T, Berry K, Bass S, Linher K, Weidman J, Khouri H, Craven B, Bowman C, Dodson R, Gwinn M, Nelson W, DeBoy R, Kolonay J, McClarty G, Salzberg SL, Eisen J, Fraser CM.** 2000. Genome sequences of *Chlamydia trachomatis* MoPn and *Chlamydia pneumoniae* AR39. Nuc. Ac. Res. **28:**1397-1406.

5. **Read TD, Myers GSA, Brunham RC, Nelson WC, Paulsen IT, Heidelberg J, Holtzapple E, Khouri H, Federova NB, Carty HA, Umayam LA, Haft DH, Peterson J, Beanan MJ, White O, Salzberg SL, Hsia RC, McClarty G, Rank RG, Bavoil PM, Fraser CM.** 2003. Genome sequence of *Chlamydophila caviae* (*Chlamydia psittaci* GPIC): examining

the role of niche-specific genes in the evolution of the Chlamydiaceae. Nuc. Ac. Res. **31:**2134-2147.

6. **Stephens RS, Myers G, Eppinger M, Bavoil PM.** 2009. Divergence without difference: phylogenetics and taxonomy of *Chlamydia* resolved. FEMS Immunol. Med. Mic. **55:**115-119.

7. **Carlson JH, Porcella SF, McClarty G, Caldwell HD.** 2005. Comparative genomic analysis of *Chlamydia trachomatis* oculotropic and genitotropic strains. Infect. Immun. **73:**6407-6418.

8. **Kari L, Whitmire WM, Carlson JH, Crane DD, Reveneau N, Nelson DE, Mabey DCW, Bailey RL, Holland MJ, McClarty G, Caldwell HD.** 2008. Pathogenic diversity among *Chlamydia trachomatis* ocular strains in nonhuman primates is affected by subtle genomic variations. J. Infect. Dis. **197:**449-456.

9. **Thomas SM, Garrity LF, Brandt CR, Schobert CS, Feng GS, Taylor MW, Carlin JM, Byrne GI.** 1993. IFN-gamma-mediated antimicrobial response. indoleamine 2,3-dioxygenase-deficient mutant host cells no longer inhibit intracellular *Chlamydia* spp. or *Toxoplasma* growth J. Immunol. **150:**5529-5534.

10. **Fehlner-Gardiner C, Roshick C, Carlson JH, Hughes S, Belland RJ, Caldwell HD, McClarty G.** 2002. Molecular basis defining human *Chlamydia trachomatis* tissue tropism - A possible role for tryptophan synthase. J. Biol. Chem. **277:**26893-26903.

11. **Caldwell HD, Wood H, Crane D, Bailey R, Jones RB, Mabey D, Maclean I, Mohammed Z, Peeling R, Roshick C, Schachter J, Solomon AW, Stamm WE, Suchland RJ, Taylor L, West SK, Quinn TC, Belland RJ, McClarty G.** 2003. Polymorphisms in *Chlamydia trachomatis* tryptophan synthase genes differentiate between genital and ocular isolates. J. Clin. Invest. **111:**1757-1769.

12. **Nelson DE, Virok DP, Wood H, Roshick C, Johnson RM, Whitmire WM, Crane DD, Steele-Mortimer O, Kari L, McClarty G, Caldwell HD.** 2005. Chlamydial IFN-gamma immune evasion is linked to host infection tropism. PNAS **102:**10658-10663.

13. **Kari L, Goheen MM, Randall LB, Taylor LD, Carlson JH, Whitmire WM, Virok D, Rajaram K, Endresz V, McClarty G, Nelson DE, Caldwell HD.** 2011. Generation of targeted *Chlamydia trachomatis* null mutants. PNAS **108:**7189-7193.

14. **Ponting CP.** 1999. Chlamydial homologues of the MACPF (MAC/peforin) domain. Curr. Biol. **9:**R911-R913.

15. **Rosado CJ, Kondos S, Bull TE, Kuiper MJ, Law RHP, Buckle AM, Voskoboinik I, Bird PI, Trapani JA, Whisstock JC, Dunstone MA.** 2008. The MACPF/CDC family of pore-forming toxins. Cell. Microbiol. **10:**1765-1774.

16. **Taylor LD, Nelson DE, Dorward DW, Whitmire WM, Caldwell HD.** 2010. Biological characterization of *Chlamydia trachomatis* plasticity zone MACPF domain family protein CT153. Infect. Immun. **78:**2691-2699.

17. **Nelson DE, Crane DD, Taylor LD, Dorward DW, Goheen MM, Caldwell HD.** 2006. Inhibition of chlamydiae by primary alcohols correlates with the strain-specific complement of plasticity zone phospholipase D genes. Infect. Immun. **74:**73-80.

18. **Kumar Y, Cocchiaro J, Valdivia RH.** 2006. The obligate intracellular pathogen *Chlamydia trachomatis* targets host lipid droplets. Curr. Biol. **16:**1646-1651.

19. **Belland RJ, Scidmore MA, Crane DD, Hogan DM, Whitmire W, McClarty G, Caldwell HD.** 2001. *Chlamydia trachomatis* cytotoxicity associated with complete and partial cytotoxin genes. PNAS **98:**13984-13989.

20. **Carlson JH, Hughes S, Hogan D, Cieplak G, Sturdevant DE, McClarty G, Caldwell HD, Belland RJ.** 2004. Polymorphisms in the *Chlamydia trachomatis* cytotoxin locus associated with ocular and genital isolates. Infect. Immun. **72:**7063-7072.

21. **Sturdevant JL, Caldwell HD.** 2014. Innate immunity is sufficient for the clearance of *Chlamydia trachomatis* from the female mouse genital tract. Path. Dis. **72:** 70-73.

22. **McClarty G, Caldwell HD, Nelson DE.** 2007. Chlamydial interferon gamma immune evasion influences infection tropism. Curr. Opin. Microbiol. **10:**47-51.

23. **Coers J, Starnbach MN, Howard JC.** 2009. Modeling infectious disease in mice: Co-adaptation and the role of host-specific IFN gamma responses. PLoS Pathog. **5**: e1000333. doi: 0.1371/journal.ppta.1000333.

24. **Caldwell HD, Kromhout J, Schachter J.** 1981. Purification and partial characterization of the major outer membrane protein of Chlamydia trachomatis. Infect. Immun. **31:**1161-1176.

25. **Hefty PS, Stephens RS.** 2007. Chlamydial type III secretion system is encoded on ten operons preceded by sigma 70-like promoter elements. J. Bacteriol. **189:**198-206.

26. **Miller JH.** 1992. A short course in bacterial genetics: A laboratory manual and handbook for *Escherichia coli* and related bacteria. Cold Spring Harbor Laboratory Press, Plainview, N.Y.

27. **Miller JH.** 1972. Experiments in molecular genetics. Cold Spring Harbor Laboratory Press, Plainview, N.Y.

28. **Greene EA, Till BJ, Henikoff JG, Taylor NE, Henikoff S, Reynolds SH, Burtner C, Codomo CA, Enns LC, Johnson JE, Odden AR, Young K, Comai L.** 2003. High-throughput TILLING for functional genomics. Methods Mol Biol. **236:**205-220.

29. **Thomson NR, Yeats C, Bell K, Holden MTG, Bentley SD, Livingstone M, Cerdeno-Tarraga AM, Harris B, Doggett J, Ormond D, Mungall K, Clarke K, Feltwell T, Hance Z, Sanders M, Quail MA, Price C, Barrell BG, Parkhill J, Longbottom D.** 2005. The *Chlamlydophila abortus*

genome sequence reveals an array of variable proteins that contribute to interspecies variation. Genome Res. **15:**629-640.

30.   **Voigt A, Schofl G, Saluz HP.** 2012. The *Chlamydia psittaci* genome: A comparative analysis of intracellular pathogens. PloS One **7**: e35097. doi: 10.1371/journal.pone.0035097.

31.   **Mitchell CM, Hovis KM, Bavoil PM, Myers GSA, Carrasco JA, Timms P.** 2010. Comparison of koala LPCoLN and human strains of *Chlamydia pneumoniae* highlights extended genetic diversity in the species. BMC Genomics **11:** 442.

32.   **Moulder JW, Hatch TP, Byrne GI, Kellogg KR.** 1976. Immediate toxicity of high multiplicities of *Chlamydia psittaci* for mouse fibroblasts (L cells). Infect. Immun. **14:**277-289.

33.   **Thalmann J, Janik K, May M, Sommer K, Ebeling J, Hofmann F, Genth H, Klos A.** 2010. Actin re-organization induced by *Chlamydia trachomatis* serovar D - Evidence for a critical role of the effector protein CT166 targeting Rac. PloS One **5:** e9887. doi: 10.1371/journal.pone.0009887.

34.   **Schramm N, Wyrick PB.** 1995. Cytoskeletal requirements in *Chlamydia trachomatis* infection of host cells. Infect. Immun. **63:**324-332.

35.   **Davis CH, Wyrick PB.** 1997. Differences in the association of *Chlamydia trachomatis* serovar E and serovar L2 with epithelial cells *in vitro* may reflect biological differences *in vivo*. Infect. Immun. **65:**2914-2924.

36. **Perry LL, Su H, Feilzer K, Messer R, Hughes S, Whitmire W, Caldwell HD.** 1999. Differential sensitivity of distinct *Chlamydia trachomatis* isolates to IFN-gamma-mediated inhibition. J. Immunol. **162:**3541-3548.

37. **Morrison RP, Feilzer K, Tumas DB.** 1995. Gene knockout mice establish a primary protective role for major histocompatibility class II-restricted responses in *Chlamydia trachomatis* genital tract infection. Infect. Immun. **63:**4661-4668.

38. **Sturdevant GL, Kari L, Gardner DJ, Olivares-Zavaleta N, Randall LB, Whitmire WM, Carlson JH, Goheen MM, Selleck EM, Martens C, Caldwell HD.** 2010. Frameshift mutations in a single novel virulence factor alter the *in vivo* pathogenicity of *Chlamydia trachomatis* for the female murine genital tract. Infect. Immun. **78:**3660-3668.

39. **Barron AL, White HJ, Rank RG, Soloff BL, Moses EB.** 1981. A new animal model for the study of *Chlamydia trachomatis* genital infections: infection of mice with the agent of mouse pneumonitis. J. Infect. Dis. **143:**63-66.

40. **Bao X, Nickels BE, Fan H.** 2012. *Chlamydia trachomatis* protein GrgA activates transcription by contacting the nonconserved region of sigma(66). PNAS **109:**16870-16875.

41. **Shen L, Li MX, Zhang YX.** 2004. *Chlamydia trachomatis* sigma(28) recognizes the *fliC* promoter of *Escherichia coli* and responds to heat shock in chlamydiae. Microbiology **150:**205-215.

42. **Nelson DE, Taylor LD, Shannon JG, Whitmire WM, Crane DD, McClarty G, Su H, Kari L, Caldwell HD.** 2007. Phenotypic rescue of *Chlamydia trachomatis* growth in IFN-gamma treated mouse cells by irradiated *Chlamydia muridarum*. Cell. Microbiol. **9:**2289-2298.

43. **Klapproth JMA, Sasaki M, Sherman M, Babbin B, Donnenberg MS, Fernandes PJ, Scaletsky ICA, Kalman D, Nusrat A, Williams IR.** 2005. *Citrobacter rodentium lifA/efa1* is essential for colonic colonization and crypt cell hyperplasia *in vivo*. Infect. Immun. **73:**3196-3196.

44. **Van Lent S, Piet JR, Beeckman D, van der Ende A, Van Nieuwerburgh F, Bavoil P, Myers G, Vanrompay D, Pannekoek Y.** 2012. Full genome sequences of all nine *Chlamydia psittaci* genotype reference strains. J. Bacteriol. **194:**6930-6931.

45. **Azuma Y, Hirakawa H, Yamashita A, Cai Y, Rahman MA, Suzuki H, Mitaku S, Toh H, Goto S, Murakami T, Sugi K, Hayashi H, Fukushi H, Hattori M, Kuhara S, Shirai M.** 2006. Genome sequence of the cat pathogen, *Chlamydophila felis*. DNA Res. **13:**15-23.

46. **Jewett MW, Lawrence KA, Bestor A, Byram R, Gherardini F, Rosa PA.** 2009. GuaA and GuaB are essential for *Borrelia burgdorferi* survival in the tick-mouse infection cycle. J. Bacteriol. **191:**6231-6241.

47. **Santiago AE, Cole LE, Franco A, Vogel SN, Levine MM, Barry EM.** 2009. Characterization of rationally attenuated *Francisella tularensis* vaccine strains that harbor deletions in the *guaA* and *guaB* genes. Vaccine **27:**2426-2436.

48. **Ramsey KH, Sigar IM, Schripsema JH, Denman CJ, Bowlin AK, Myers GAS, Rank RG.** 2009. Strain and virulence diversity in the mouse pathogen *Chlamydia muridarum*. Infect. Immun. **77:**3284-3293.

49. **Johnson CM, Fisher DJ.** 2013. Site-specific, insertional inactivation of *incA* in *Chlamydia trachomatis* using a group II intron. PloS One **8:** e83989. doi: 10.1371/journal.pone.0083989.

50. **Rank RG.** 2006. Chlamydial Diseases. The Mouse in Biomedical Research. Elsevier, San Diego, CA.

51. **Cotter TW, Ramsey KH, Miranpuri GS, Poulsen CE, Byrne GI.** 1997. Dissemination of *Chlamydia trachomatis* chronic genital tract infection in gamma interferon gene knockout mice. Infect. Immun. **65:**2145-2152.

52. **Stevens MP, Roe AJ, Vlisidou I, van Diemen PM, La Ragione RM, Best A, Woodward MJ, Gally DL, Wallis TS.** 2004. Mutation of *toxB* and a truncated version of the *efa-1* gene in *Escherichia coli* O157 : H7 influences the expression and secretion of locus of enterocyte effacement-encoded proteins but not intestinal colonization in calves or sheep. Infect. Immun. **72:**5402-5411.

CHAPTER 3

A GENETIC SCREEN REVEALS THAT *CHLAMYDIA MURIDARUM* IFN-γ

RESISTANCE IS A COMPLEX PHENOTYPE

3.1 Abstract

Some anti-chlamydial effector mechanisms controlled by the Th1 cytokine IFN-γ differ in mice and in humans and this can impact modeling of human chlamydial infections in mouse models. *C. muridarum,* a natural mouse pathogen, is highly resistant to IFN-γ in mice compared to *C. trachomatis* strains that infect humans. We screened a library of EMS-mutagenized *C. muridarum* strains to identify mutants sensitive to IFN-γ, with the goal being to identify and map *C. muridarum* IFN-γ resistance genes. 31 moderately to highly IFN-γ sensitive (*igs*) isolates were identified and genomes of four of these were sequenced. All *igs* strains contained multiple mutations, so revertants of *igs4*, the most sensitive mutant, were selected by serial passage in IFN-γ-treated mouse cells. Almost all of the revertants had intragenic suppressor mutations that were predicted to truncate a putative inclusion membrane protein (*inc*) allele of unknown function that was mutated in *isg4*. IFN-γ sensitivity of *igs4* was not reversed by an iNOS inhibitor or a scavenger of reactive oxygen species, indicating that *igs4* was susceptible to other IFN-γ-regulated antimicrobial effector pathways. *igs4* suppressor mutants behaved similarly to wild-type *C. muridarum* in mice whereas *igs4* was profoundly attenuated and its virulence was not restored in IFN-γ$^{-/-}$ mice. *igs4* was also sensitive to IFN-β in cell culture, suggesting that compensatory roles played by Type I IFNs might be sufficient to control *igs4* infection in mice. Overall, the data suggest that a gain-of-function missense mutation in a *C. muridarum*-specific Inc protein conferred IFN sensitivity to *C. muridarum in vitro* and accelerated its clearance from mice. This

mutant could be particularly useful in differentiating IFN-γ-dependent and independent pathways for control of *C. trachomatis* infection and disease in mice.

3.2 Introduction

The genus *Chlamydia* comprises a genetically similar, but pathogenically diverse, group of obligate intracellular bacterial pathogens, including the important human pathogen *C. trachomatis*. Acquisition and loss of chlamydial effectors that counter host immune defenses may have contributed to distinct host tropisms of some *Chlamydia* spp. (1-5). Identifying these bacterial effectors has been challenging because until recently, *Chlamydia* lacked a genetically tractable system (6).

The Th1 cytokine interferon-gamma (IFN-γ) is a key determinant of chlamydial tropism *in vitro* (7-9). For example, the mouse pathogen *C. muridarum* and the sexually transmitted human pathogen *C. trachomatis* serovar D can productively infect a variety of murine and human epithelial cell lines in the absence of IFN-γ. If mouse oviduct epithelial cells are exposed to IFN-γ, *C. trachomatis* serovar D, but not *C. muridarum*, is strongly inhibited (7). IFN-γ inhibits both *C. muridarum* and *C. trachomatis* serovar D in human epithelial cells in tryptophan-limiting conditions, but only the growth of *C. trachomatis* can be restored by adding an indole intermediate to the cell culture medium (2, 8, 10). Thus, it appears that *C. muridarum* and *C. trachomatis* have developed different strategies to circumvent IFN-γ regulated defenses that are relevant in cells of their natural host organisms.

More is known about how IFN-γ controls chlamydial infections than is known about the cognate bacterial effectors that these pathogens use to counteract the effects of this cytokine. In human epithelial cells, the tryptophan decyclizing enzyme indoleamine 2,3 dioxygenase (IDO) appears to be the most important IFN-γ-regulated pathway in chlamydial inhibition (7, 8, 11-14). This is based upon observations that IFN-γ inhibition of *C. trachomatis* and *C. muridarum* can be completely reversed by adding tryptophan in some human cell culture models (2, 8, 15). Although p65 family interferon inducible GTPase proteins (p65 IRG) may not be directly antimicrobial, there is evidence that these proteins potentiate IFN-γ inhibition of *C. trachomatis* in human epithelial cells (16). Since IDO may not be functional in anaerobic regions of the female genital tract in humans (17), it is unclear if these pathways are relevant to human *C. trachomatis* genital infection.

The role of IFN-γ in *C. trachomatis* infection and disease has been studied more extensively in mice. IFN-γ knockout mice are susceptible to *C. trachomatis* genital tract infection, and develop more severe pathology and disseminated infections (7, 18, 19). IDO is not regulated by IFN-γ in murine genital tract epithelial cells or fibroblasts (7, 8) and the course of *C. trachomatis* genital tract infection does not differ in wild type and IDO knockout mice (7). This suggests that different pathways control *C. trachomatis* infections in mice and humans. The role of p65 IRGs in *C. trachomatis* infection has not yet been evaluated in mice although there is evidence that some of these proteins contribute to control of this pathogen in murine fibroblasts (20, 21). Other IFN-γ regulated proteins and

pathways including inducible nitric oxide synthase (iNOS), the phagocyte oxidase complex (phox) and various interferon inducible p47 GTPase family members (p47 IRGs) clearly impact *C. trachomatis* infection or disease progression in mice. *inos*^{-/-} and *inos*^{-/-}/*phox*^{-/-} mice cannot efficiently clear *C. trachomatis* genital tract infections (22-25). Multiple p47 IRGs may restrict *C. trachomatis* growth in murine fibroblasts and epithelial cells (7, 26-28). Some p47 IRG knockout mice are more sensitive to intravenous challenge with *C. trachomatis* (26, 27, 29). Disentangling roles of the individual p47 IRGs in the murine models has proven challenging because loss of these proteins can trigger compensatory immune responses (29). It is clear however that *inos*^{-/-} (7), *inos*^{-/-}/*phox*^{-/-} (23) and some p47 IRG^{-/-} mice (29) are less susceptible to *C. trachomatis* genital tract infection than are IFN-γ^{-/-} mice (7), thus suggesting that the anti-chlamydial effects of these pathways may be additive or could work with unidentified IFN-γ pathways.

Discovery of chlamydial effectors that counteract IFN-γ has relied heavily upon genome sequencing. Comparison of *C. trachomatis* and *C. muridarum* genomes revealed a partial tryptophan biosynthesis operon that was only present in *C. trachomatis* (3, 30). Presence of intact tryptophan synthase genes was subsequently shown to separate *C. trachomatis* urogenital and trachoma biovar isolates (2, 5). Work from the McClarty group first showed that *C. trachomatis* tryptophan synthase was functional in *E. coli* (10) and a later reverse genetic study confirmed that tryptophan synthase is required for indole rescue of *C. trachomatis* in cell culture (31). It has been speculated that tryptophan synthase harvests indole from other urogenital microorganisms to make tryptophan and

circumvent tryptophan depletion mediated by host IDO (1, 2). Duplication and polymorphisms of *tyrP*, a putative tryptophan transporter, were linked to chlamydial IFN-γ resistance and tropism in other studies (32, 33). Even less is known about the genes that mediate *C. muridarum* IFN-γ resistance. We previously speculated that the *C. muridarum* cytotoxin family might inactivate IRGs based primarily on their homology to effectors of other bacteria that inactivate GTPases and their expansion in *C. muridarum* (1, 7). Some *C. muridarum* effectors that counter IFN-γ are pre-loaded in EB and may function *in trans* because metabolically inactive *C. muridarum* EB can partially restore *C. trachomatis* growth in IFN-γ treated mouse cells (34). The identity of these *C. muridarum* effectors is unknown.

In this study we identified IFN-γ sensitive *C. muridarum* mutants using a genetic screen. Genome sequencing of four of these IFN-γ sensitive (*igs*) mutants revealed that they shared no common mutations and that *C. muridarum* IFN-γ resistance is a complex phenotype. We determined that IFN-γ sensitivity of one mutant, *igs4*, was likely linked to a gain-of-function mutation in the putative inclusion membrane protein (Inc) TC0574 using genetic analysis. Virulence of *igs4*, but not *igs4* suppressor mutants, was severely attenuated in the murine genital tract infection model and *igs4* infection only provided partial protection against re-infection with virulent *C. muridarum* in C57/B6 mice. IFN-γ sensitivity of *igs4* was not reversed by inhibitors of iNOS and reactive oxygen species suggesting that it might be sensitive to IRG or other uncharacterized interferon-regulated antimicrobial pathways. Our results provide the first molecular insights

into the mechanisms of *C. muridarum* IFN-γ resistance and a powerful set of mutants for identification of chlamydial genes that counteract IFN-γ regulated defenses.

3.3 Methods

3.3.1 *Chlamydia and cell culture*

Chlamydia muridarum (*C. muridarum*) and *Chlamydia trachomatis* L2/434/Bu (*C. trachomatis*) were gifts from Dr. Harlan Caldwell (Rocky Mountain Laboratories, NIH-NIAID). The rifampin-resistant *C. trachomatis* L2/434/Bu isolate *rif*R (*C. trachomatis rif*R) was described previously (34). Chlamydiae were routinely propagated in HeLa229 (HeLa) or mouse McCoy cells and chlamydial elementary bodies (EB) were purified by density gradient centrifugation as described previously (34-36). Dulbecco's modified Eagle's medium (Hyclone) supplemented with 10% fetal bovine serum, sodium pyruvate (Atlanta Biologicals), non-essential amino acids (Gibco), and 5 μM HEPES buffer (Sigma) (DMEM-10) was used for cell culture and was supplemented with mouse recombinant IFN-γ (0.15 ng/U) (R&D systems) in some experiments. Unless stated otherwise, 20 U/ml IFN-γ was added to cell culture media for 24 hours prior to infection and to the infection media in IFN-γ treatment experiments. Cell culture was performed at 37°C in a 5% CO_2 atmosphere.

3.3.2 *Chemical mutagenesis*

Confluent 150 cm^2 flasks of Vero cells were infected with *C. muridarum* at a multiplicity of infection (MOI) of 2 in sucrose phosphate glutamic acid buffer

(0.25 M sucrose, 10 mM sodium phosphate, 5 mM L-glutamic acid, pH7.2) (SPG) by rocking for 1.5 h and were incubated in DMEM-10 supplemented with 100 µg/mL cycloheximide. The monolayers were washed 16 hours post infection (hpi) and were then treated with 10 mL DMEM-10 supplemented with 15 mg/ml ethyl methanesulfonate (EMS) for 1 h to mutagenize EB as described previously (31, 37). The monolayers were washed with phosphate buffered saline (PBS) to remove the mutagen and fresh DMEM-10 with cycloheximide was added. The media was aspirated and the infected cell monolayers were disrupted with 3 mm glass beads at 26 hpi in SPG. Aliquots of mutagenized EB stocks were stored at -80°C.

3.3.3 *Mutant library construction*

McCoy cell monolayers in 6-well cell culture plates were infected with mutagenized EB to isolate plaques (38). Well-isolated plaques were picked 10 days post infection using plugged pipette tips and were transferred into tubes containing 150 µl SPG and 3 mm glass beads. EB were released by agitation at 1400 rpm for 2 min in an Eppendorf Thermomixer (Eppendorf). Plaque lysates were arrayed in deep 96-well plates and archived at -80°C. 30 µL of each plaque isolate was used to infect McCoy cells in 96-well plates by centrifugation (168 x g for 1 h at room temp.) and rocking (30 min at 37°C) and the infected cells were frozen 26 hpi in SPG at -80°C. EB were harvested by thawing and transferred to 96-deep-well plates for use as working stocks in mutant screens.

3.3.4 *IFN-γ sensitive (igs) mutant screen*

McCoy cells were seeded in 96-well plates in DMEM-10 and were incubated until 90% confluent. The medium was then replaced with fresh DMEM-10 +/- IFN-γ and the plates were incubated for 24 h. Equal inoculums of mutant working stocks were used to infect the plates as described above and fresh DMEM-10 +/- IFN-γ was added. The monolayers were fixed 24 hpi in methanol at room temp. for 5 min, washed with PBS and then blocked in PBS with 1% bovine serum albumin (BSA) for 1 h at room temp. Inclusions were labeled with a murine monoclonal antibody (mAB) against chlamydial LPS (EVIH1), a gift from Harlan Caldwell, followed by a secondary Alexa 488 conjugated goat anti-mouse IgG (Life Technologies). Inclusions were imaged using an EVOS® FL Auto cell imaging microscope and counted using a custom macro written in Image J (39).

3.3.5 *Inclusion Forming Unit Assays*

Inclusion forming unit (IFU) and recoverable IFU (rIFU) inclusion assays were performed in McCoy cells in 24 or 96-well cell culture plates. Infections were performed by centrifugation and rocking as above and IFN-γ was added in some experiments. For IFU experiments, cells were fixed in methanol and inclusions were labeled with antibodies as described above. For rIFU assays, cell monolayers were harvested in SPG by scraping and EB were released by bead agitation. Serial dilutions of these lysates were used to infect McCoy cells and inclusions were visualized and counted 24 hpi as described for IFU. In some rIFU experiments, 2 mM of the iNOS inhibitor L-NMMA (L-NG-monomethyl arginine

citrate, Cayman Chemical) or 15 mM of the hydroxyl radical scavenger DMTU (Dimethylthiourea, Cayman Chemical) or both were added simultaneously with IFN-γ.

3.3.6 *Analysis of igs mutant inclusion morphology*

McCoy cells were seeded in 24-well tissue culture plates on glass coverslips overnight and then were incubated an additional 24 h +/- 20 U/ml IFN-γ. The cells were then infected with *C. muridarum, C. trachomatis* or *igs* mutants at an MOI of 0.1 by centrifugation and rocking and were overlaid with infection medium +/- 20 U/ml IFN-γ. At 24 hpi, the infected cells were fixed with methanol, rinsed with PBS, treated with 0.05% Evans Blue for 1 min and rinsed again with PBS. The fixed cells were blocked in 0.1% BSA for 1 h and then stained with the primary antibody EVI-H1 followed by a secondary DY488-conjugated goat anti mouse IgG antibody (Life Technologies). The coverslips were mounted in Prolong gold anti-fade reagent with DAPI (Life Technologies) and imaged using a Leica DMI6000B microscope with a 63X and 100X oil immersion objectives. At least 30 inclusions of each strain in each condition were imaged.

Inclusion morphology of chlamydial strains in HeLa cells was similarly analyzed. HeLa cells were grown on coverslips in tryptophan-free DMEM (trp-DMEM-10) (University of California at San Francisco, Cell Culture Facility, San Francisco, CA) supplemented with 10% dialyzed FBS (HyClone) or in media containing excess tryptophan (trp+ DMEM-10) by the addition of 128 mg/L tryptophan to trp- DMEM-10. 20 U/mL of human recombinant IFN-γ (R&D

Systems) was added to culture media 24 hours prior to infection and treatment continued throughout infection. Infected cells were fixed at 24 hpi with methanol, stained with EVI-H1 and imaged as described above.

3.3.7 *Isolation of igs suppressor mutants*

McCoy cell monolayers were incubated for 24 h in DMEM-10 + 20 U/ml IFN-γ, infected with the IFN-γ sensitive *C. muridarum* mutant *igs4* (described in the Results) at an MOI of 1.5 (3×10^6 total IFU) by centrifugation and rocking and were incubated for 24 h in DMEM-10 + 20 U/ml IFN-γ. The infections were harvested by scraping in SPG and EB were released by bead agitation. One-fifth of each harvest was used to infect a new well of IFN-γ-treated McCoy cells, and then the entire infection and harvest cycle was repeated 6-8 times. The number of chlamydia-infected cells declined to undetectable levels in most wells after 4 passages, whereas 23/96 wells became heavily infected by passage 6. Suppressor mutants (S1-S9) were isolated from the latter wells and were purified by two rounds of plaque cloning.

3.3.8 *Construction of tc0574::GII(bla)*

EB from a plasmid-cured isolate of *C. muridarum* (10^8 IFU), which was a gift from Harlan Caldwell (40), were transformed with a modified vector pFDTT3 containing an intron targeted to *tc0574* (7 μg) which was constructed similarly to an *incA* targeting intron plasmid recently described by Johnson et al (41). The TargeTron™ algorithm (Sigma) was used to design *tc0574*-specific primers

(supplemental table 3) for retargeting pDFTT3 between nucleotides 44 and 45 of *tc0574*. Transformation was performed as described previously (41, 42), except the infections were performed by centrifugation at 550 x g for 1 h at room temp, and were allowed to proceed 30 h before EB were harvested by bead agitation to generate Passage P_0. Additional passages were performed in 6-well tissue culture dishes, and the growth medium was supplemented with 5 µg/ml ampicillin from P_2-P_9. Clones from P_9 were purified by two rounds of plaque isolation as described above, except that the overlay medium was supplemented with 5 µg/ml ampicillin. Insertion of the intron in *tc0574*::GII(bla) was confirmed by PCR and Sanger sequencing.

3.3.9 *Co-infection rescue assays*

Co-infections of McCoy cells with *C. trachomatis rif^R* and *C. muridarum* or *igs4* was performed as described previously (34). Confluent cells in 24-well plates were infected with *C. trachomatis rif^R* at an MOI of 0.5 in SPG, +/- 20 U/mL IFN-γ, and sufficient rifampin (0.1 µg/mL) to completely inhibit *C. muridarum* inclusion development. Some wells were co-infected with *C. muridarum* or *igs4* EB. Following centrifugation and rocking, SPG was replaced by DMEM-10 containing rifampin, +/- 20 U/mL IFN-γ. Cells were harvested in SPG by scraping at 34 hpi and *C. trachomatis rif^R* EB were collected by bead agitation. Recoverable IFU assays were performed as above except that rifampin was included in the infection medium and the inclusions were visualized by labeling

with the *C. trachomatis* serovar L2 MOMP-specific monoclonal antibody (mAB) L21-45 which was a gift from Harlan Caldwell.

3.3.10 *Western blot analysis of iNOS expression and Griess Assay*

Expression of iNOS protein was analyzed by Western blot. Cells from the Griess assay experiments were washed with PBS and then incubated in 50 ml Lysis buffer (2% sodium dodecyl sulphate (SDS), 10% glycerol, 62 mM Tris, pH 6.8) supplemented with a Protease Inhibitor mini tablet (Pierce) for 10 min on ice. Cells were gently scraped and denatured at 95°C for 5 min. Protein samples were separated in 10% SDS-polyacrylamide gels and electrophoretically transferred to nitrocellulose membranes. The proteins were then labeled with a primary rabbit anti-mouse iNOS mAb (#2982S) or a rabbit anti-murine GAPDH mAb (#2118S), followed by a secondary anti-rabbit horse radish peroxidase-conjugated mAB antibody (#7074), all of which were purchased from Cell Signaling. Proteins were visualized by adding SuperSignal West Pico Chemiluminescent Substrate (Pierce) according to the manufacturer instructions.

Nitrite was measured using a commercial Griess assay kit (Biotium). 24-well plates containing uninfected or infected McCoy cells, +/- IFN-γ, were cultured for 24 h +/- 2 mM L-NMMA. 150 μl volumes of the culture supernatants were incubated with 20 μL Griess reagent (0.05% N-(1-naphthyl)ethylenediamine dihydrochloride, 0.5% sulfanilic acid, 2.5% phosphoric acid) in a 96-well plate for 30 min at room temp. Absorbance was measured at 540 nm and nitrite levels were calculated against a sodium nitrite standard curve.

3.3.11 *Sequencing Library Construction and Genome Sequencing*

C. muridarum isolates were expanded in McCoy cells. Genomic DNA was isolated from 30% Renocal gradient-purified EB. EB were treated with DNase I (NEB) at 37°C for 1 hour followed by treatment with 5mM EDTA and incubated at 75°C for 10 min to halt digestion. Total DNA was extracted from EB using the DNeasy Blood & Tissue kit (Qiagen) and genomic DNA was quantified using the Quant-It High Sensitivity dsDNA assay (Life Technologies Corp.). 1 µg aliquots of purified genomic DNAs were subjected to NEBNext dsDNA Fragmentase (NEB) treatment to generate dsDNA fragments for multiplex Illumina sequencing. The TruSeq Nano DNA sample preparation kit was used to prepare DNA sequencing libraries according to the manufacturer's protocols (Illumina Inc.). Samples were multiplexed using TruSeq Single Index Sequencing primers. Equimolar concentrations of indexed libraries were combined into a single pool and were sequenced at Tufts University Genomics Core. Paired-end 100 bp sequencing was performed on the Illumina HiSeq 2500 platform.

3.3.12 *Genome assembly and analysis*

Single nucleotide polymorphisms (SNP), nucleotide insertions and deletions analysis (Indel), were mapped from raw sequence data to the corresponding reference genome accession number (AE002160.2) using Bowtie2. Resulting SAM files were converted to BAM file format and sorted. SNPs/Indels were called using a Samtools mpileup function. Ambiguous sequences and mutation calls with low quality scores were resolved by PCR and Sanger sequencing.

3.3.13 *Taqman quantitative real time PCR (q-PCR)*

McCoy cells were plated at 0.5×10^6 cells per well in twenty four-well plates in DMEM-10 +/- IFN-γ and the plates were incubated for 24 h. Equal inoculums of WT and *igs4* were then used to infect the plates as above and fresh DMEM-10 +/- IFN-γ was added. Following infection, the cell monolayers were disrupted via cell scraping at 2, 18, 24, 30, and 36 hpi, and total DNA was extracted using the IBI gMax Mini Kit. The DNA was re-suspended in 50 µl of elution buffer. Taqman quantitative real time-PCR (q-PCR) was performed in an Eppendorf Realplex^4 thermocycler using the FastStart Taqman Probe master mix (Roche). The amplification cycle included 10 min at 95°C, followed by 40 cycles of 95°C for 20 s, 60°C for 1 min and 68°C for 20 s. Taqman primer-probe sets were designed using PrimerQuest software (Integrated DNA Technologies). The sequences of the primers and probes were: 16S Forward (5'-GTAGCGGTGAAATGCGTAGA-3'); 16S Reverse (5'-CGCCTTAGCGTCAGGTATAAA-3'); 16S Taqman probe (5'- / 56-FAM / ATGTGGAAG / ZEN / AACAACAGTGGCGAA / 3IABkFQ / -3'). Genome copy numbers were determined by comparison to standard curves of dilutions of a plasmid that contained a cloned copy of the *C. muridarum* 16S rRNA gene.

3.3.14 *Reverse transcriptase PCR (RT-PCR) analysis of tc0572-tc0574 expression*

McCoy cells were seeded in 6-well tissue culture plates and were allowed to adhere overnight. They were then incubated for an additional 24 h +/- 20 U/ml IFN-γ. The cells were infected at an MOI of 1 by centrifugation and rocking and were overlaid with infection medium +/- 20 U/ml IFN-γ. Total RNA was harvested 24 hpi using TRISure reagent (Bioline). The RNA was treated with DNAseI (Qiagen) for 15 min and then was purified on a GeneJET RNA purification column (Thermo scientific). RT-PCR reactions were performed with 100 ng of total RNA and gene specific primers (Table 3.3) using the Mytaq one-step RT-PCR kit (Bioline). RNA was harvested and processed similarly for semi-quantitative RT-PCR. 1 μg of total RNA was then converted to cDNA with random hexamers utilizing iscript select cDNA synthesis kit (Biorad).

3.3.15 *In vivo pathogenicity of C. muridarum mutants*

C. muridarum and various mutant strains were expanded in HeLa cells and EB were purified using Renocal gradients. 6-10 week old female C57BL/6J or B6.129S7-Ifnγ^{tm1Ts}/J (IFN-$\gamma^{-/-}$ mice) (Jackson laboratories, Bar Harbor, ME) were treated with 25 mg/mL Depo-Provera at 10 and 3 days prior to infection by subcutaneous injection of 100 μl (2.5 mg total) between the front shoulders. Mice were inoculated with *C. muridarum* wild-type or mutants by placing 5 μl of SPG containing 50,000 inclusion forming units (IFU) into the vaginal vault. At various time points following infectious challenge (day 3, 7, 10, 14 and weekly thereafter)

the vaginal vault was swabbed using a Calgiswab and the infections were monitored by counting IFU.

Fifty-nine days following primary infection, mice were treated daily for 11 days with 300 µg doxycycline/mouse given by intraperitoneal injection to assure infection cure, and then rested for 14 days prior to assessing protective immunity. To determine if primary infections induced protective immunity, mice were treated with Depo-Provera following the 14-day rest period, reinfected with 50,000 IFU of wild-type *C. muridarum*, and the infections were monitored as described above. Mice were euthanized at the termination of the secondary infection experiment and presence or absence of hydrosalpinx was recorded.

Nonparametric repeated measures analysis of variance (ANOVA) models were used to test whether the time trends between treatment groups were parallel and, if they were parallel, to determine whether the groups differ with respect to magnitude of response. An α-level of 0.05 was used to determine the statistical significance of each test. No adjustments for multiple comparisons were made. All analyses were performed using *R* (version 3.0.1, R Foundation for Statistical Computing, Vienna, Austria).

3.3.16 *Treatment with IFN-β and IFNAR-1 neutralizing antibody*

McCoy cells were incubated with 10 µM anti-mouse IFNAR-1 antibody (clone MAR-5A3) or an IgG1 isotype control antibody (BioLegend). At the time of antibody addition, some wells were treated with 250 U/mL IFN-β (R&D Systems).

Cells were infected after 1 hour with *C. muridarum* or *igs4* at an MOI of 0.5. IFN-$\beta \pm$ Ab treatment continued throughout the course of infection.

3.4 Results

3.4.1 *A phenotypic screen for IFN-γ sensitive C. muridarum mutants*

    C. trachomatis and *C. muridarum* can establish productive infections in McCoy murine fibroblast cells (McCoy cells). However, *C. trachomatis* infection of McCoy cells is profoundly inhibited by low doses of the Th1 cytokine interferon gamma (IFN-γ), while *C. muridarum* infection is only mildly affected (8, 34). We reasoned that *C. muridarum* IFN-γ resistance in murine cells is linked to genes that are either absent or non-functional in *C. trachomatis* and that these genes might be dispensable for infection of McCoy cells in the absence of IFN-γ (1, 7). We screened a library of 2976 moderately EMS-mutagenized and plaque-cloned *C. muridarum* isolates to identify mutants that could productively infect McCoy cells and were sensitive to IFN-γ.

    Numbers of inclusions that the library isolates formed in IFN-γ treated (10 U/ml 24 h pre- and post-infection) and untreated McCoy cells were counted and compared using an automated microscopic assay. The ratio of inclusions formed by the library wild type parent (*C. muridarum*) -/+ IFN-γ averaged 1.22 fold and 328/2976 library clones that yielded higher ratios were selected for secondary screening. The secondary screen was performed in triplicate and the IFN-γ concentration was increased to 20 U/ml to improve specificity. The ratio of inclusions formed by *C. muridarum* in -/+ 20 U/ml IFN-γ averaged 1.26 fold and

31/328 isolates that yielded ratios equal to or greater than 2 fold (range 2-7) were selected for further characterization. These isolates were plaque-cloned and the phenotypes of all 31 mutants were confirmed by an additional round of screening (in triplicate) in 20 U/ml IFN-γ. Four interferon gamma sensitive (*igs*) mutants were expanded for characterization and genome sequencing.

3.4.2 *Phenotypes of igs mutants can be differentiated by inclusion forming unit assays and morphology*

The ability of *C. muridarum* and the *igs* mutants to infect and replicate in McCoy cells was compared using IFU and rIFU assays (Fig. 3.1). Infection of McCoy cells with *C. muridarum* was robust and production of infectious EB neared maximum by 18 hpi (Fig. 3.1 A, B). In the absence of IFN-γ, IFU production from 3 of the 4 *igs* mutants (*igs*1-3) was nearly indistinguishable from *C. muridarum*, whereas peak *igs4* IFU production was slightly delayed (Fig. 3.1 C-J). Quantitative PCR (q-PCR) analysis showed that *igs4* genome copy number was reduced compared to *C. muridarum* at 18 hpi but was similar to *C. muridarum* by 24 hpi (Fig. 3.2).

The defining phenotype of *igs* mutants was that fewer inclusions were observed 24 hpi in the presence of IFN-γ and inclusion size and morphology of the mutants and parent were similar in untreated McCoy cells. It was unclear if IFN-γ sensitivity of these mutants was due to formation of fewer inclusions or lysis of inclusions prior to 24 hpi. Ratios of inclusions versus rIFU which were formed by *C. muridarum* and the *igs* mutants were compared to differentiate

these possibilities. An IFU/rIFU ratio was defined as (IFU+ IFN-γ/IFU- IFN-γ)/(rIFU+ IFN-γ/rIFU- IFN-γ) to express the results of the growth curves as a single number (Table 3.1). The IFU/rIFU ratio of *C. muridarum* ranged narrowly from 0.9 to 1.1 at 4 time points from 12 to 30 hpi. This indicated that *C. muridarum* formed slightly fewer inclusions in the presence of IFN-γ, but that once these inclusions formed they produced similar numbers of infectious EB in the presence or absence of IFN-γ. *igs3* followed a similar pattern indicating that their phenotypes were primarily because they initially formed fewer inclusions in the presence of IFN-γ (Fig. 3.1 G, H). In contrast, elevated IFU/rIFU ratios were observed in *igs1* and *igs2* suggesting that inclusions of these mutants yielded fewer infectious EB (Fig. 3.1 C-F). Interestingly, the IFU/rIFU ratio of *igs4* increased progressively from 0.7 at 12 hpi to 9.4 at 30 hpi indicating that this mutant not only produced fewer inclusions in the presence of IFN-γ, but that many of the chlamydiae failed to mature in the few remaining inclusions (Fig. 3.1 I, J). The genome copy number of *igs4* also failed to increase between 18 and 24 hpi in IFN-γ treated cells and subsequently decreased (Fig. 3.2). These results showed that the *igs* mutants could be separated into distinct phenotypic classes.

We previously reported that *C. trachomatis* is most sensitive to IFN-γ when the cytokine is added prior to or shortly after infection (34), so we tested if *igs4* exhibited a similar pattern. *C. trachomatis* and *igs4* yielded similar results in temporal IFN-γ addition assays (Fig. 3.3). Both strains were inhibited when IFN-γ was added prior to or shortly after infection, but were mostly unaffected when IFN-γ was added 12 h or later post-infection. This implied that the effectors that

inhibit *C. trachomatis* and *igs4* target nascent or early inclusions and are less effective against more mature inclusions.

3.4.3 IFN-γ causes lysis of igs4 inclusions in mouse cells

Inclusion morphology of the *igs* mutants and *C. muridarum* was compared using fluorescent microscopy (Fig. 3.4 A). Size and morphology of most of the inclusions formed by *C. muridarum* and the *igs* mutants were similar in McCoy cells in the absence of IFN-γ. Some lysed inclusions was observed in populations of *igs1* and *igs4*, although these never exceeded 10% (Fig. 3.4 B). In IFN-γ treated McCoy cells, the morphologies of most *C. muridarum* and *igs1-3* mutant inclusions were also similar, with the caveat that minor sub-populations of lysed inclusions were again observed with *igs1* (Fig. 3.4 B). In contrast, the vast majority of *igs4* inclusions had lysed by 24 hpi in IFN-γ treated McCoy cells (Fig. 3.4 A, B). These results indicated that the IFN-γ sensitivity of *igs4* was associated with premature inclusion lysis.

To determine if *igs4* was similarly sensitive to human IFN-γ, we examined the inclusion morphology of *igs4* and *C. muridarum* in HeLa cells in tryptophan-free DMEM (Trp- DMEM-10) -/+ 20 U/ml IFN-γ (Fig. 3.5). In untreated HeLa cells, no lysed inclusions were observed with *igs4* and *C. muridarum*. In the presence of cytokine, neither *igs4* nor *C. muridarum* inclusions developed due to tryptophan starvation. When HeLa cells were treated with IFN-γ in DMEM containing excess tryptophan (Trp+ DMEM-10), *igs4* and *C. muridarum* grew

normally and inclusions remained intact at 24 hpi. This implied that lysis of *igs4* inclusions was caused by mechanisms that were specific to mouse cells.

3.4.4 *IFN-γ sensitivity is a complex phenotype*

The *C. muridarum* parent isolate and the *igs* mutants were pair-end sequenced to an average coverage of 1511 fold (range 815 to 2894) on the Illumina HiSeq platform. The *igs* mutants differed by an average of 12.75 mutations (range 8 to 20) from our *C. muridarum* isolate and 49 of the 51 total mutations in the four mutants were GC-AT transitions, consistent with their being elicited by EMS (43).

All 4 *igs* strains had mutations in *tc0412*, the highly polymorphic (44) ortholog of *C. trachomatis ct135*, that were predicted to truncate TC0412 (364 amino acids, full length): a C-T mutation ($tc0412_{66(Am)}$) in *igs1* and *igs3*, a T-G mutation ($tc0412_{338(Op)}$) in *igs2* and frameshift mutations leading to a premature stop codon ($tc0412_{197(Oc)}$) in *igs4* (Table 3.2). To test if *tc0412* polymorphisms contributed to IFN-γ sensitivity, *tc0412* alleles of 10 library isolates with wild-type IFN-γ sensitivity, and 10 uncharacterized *igs* isolates from the secondary screen were sequenced. Four and five novel *tc0412* sequences were identified in the ten wild-type and ten *igs* isolates, respectively (data not shown). This suggested that there was no correlation between *tc0412* genotype and IFN-γ sensitivity *in vitro*, consistent with a previous study of a *C. trachomatis* isolate with a frameshift mutation in *ct0135* (45). The observation that no other common genes were

123

mutated in the *igs* mutants showed that our screen did not reach saturation and that *C. muridarum* IFN-γ resistance is a complex phenotype.

3.4.5 *A gain-of-function missense mutation in TC0574 is linked to IFN-γ sensitivity of igs4*

Since *igs4* produced few infectious EB in IFN-γ treated McCoy cells, we used a serial passage strategy to test if we could isolate IFN-γ resistant revertants. This was successful in 23 of 96 experiments in which inoculums of 3 x 10^6 *igs4* IFU were blindly passed 6 times in IFN-γ treated McCoy cells. Phenotypes of nine representative isolates (S1-S9) were characterized in single time point IFU and rIFU assays and two of the isolates (S1 and S5) were further characterized in temporal IFU and rIFU assays (Fig. 3.6). IFN-γ sensitivity of all of these isolates was similar to *C. muridarum* at 24 hpi (Fig. 3.7). Developmental kinetics and inclusion morphology in the presence and absence of IFN-γ were also similar to wild type (Fig. 3.8).

IFN-γ resistant revertants were isolated more frequently (7.9 x 10^{-6}) than was anticipated for true revertants, based upon a previous estimate of spontaneous mutation frequency in *C. trachomatis* (1.10×10^{-9} to 3.84×10^{-10}) (46). Therefore we tested if any of the mutant alleles that were present in the *igs4* parent had reverted or accumulated intragenic suppressors. Intragenic suppressor mutations in *tc0574* were identified in 22 of the 23 revertants, although only 8 unique *tc0574* genotypes were detected (Fig. 3.9), indicating that

some of the revertants may have been siblings in the original *igs4* stock. No mutations were identified in any of the *igs4* mutant alleles in S9.

The genomes of S1, S5 and S9 were sequenced. S1 contained no additional mutations aside from the missense mutation in *tc0574* identified by Sanger sequencing (Table 3.2). S5 contained a synonymous mutation in codon 204 of *tc0673*, which encodes the heat shock gene repressor HcrA. S9 had a T to C transition that changed the predicted start codon of *tc0573*, the gene immediately upstream of *tc0574*, from valine to alanine (Fig. 3.9). This ORF, like *tc0574,* is predicted to encode an Inc protein and is located immediately upstream of *tc0574* (47).

Five of the 9 unique *igs4* suppressor mutations were predicted to truncate mutant TC0574 of *igs4* (Fig. 3.9). A possible explanation for the phenotype of S9 was that translation of *tc0574* is coupled to *tc0573,* in which case the proteins would be transcribed from the same transcript (48). Consistent with this hypothesis, we determined that *tc0573* and *tc0574* were co-transcribed as part of an operon that originated upstream of tc0572 using RT-PCR. (Fig. 3.10 A, B). We also determined that *tc0574* transcript levels were similar in *C. muridarum*, *igs4* and the suppressor mutants S5 and S9 using semi-quantitative RT-PCR (Fig. 3.10 C). These results ruled out the alternate possibility that the phenotype of *igs4* was linked to destabilization of the larger polycistronic transcript detected by RT-PCR. Many of the mutations in the *igs4* suppressors were predicted to truncate TC0574 suggesting that the normal function of TC0574 was unrelated to IFN-γ resistance. To independently test this, we inserted an ~2kb intron in the 5'

prime end of *tc0574* to create *C. muridarum tc0574::GII(bla)* (41). IFN-γ resistance of the *tc0574::GII(bla)* mutant was indistinguishable from *C. muridarum* and the suppressor mutants (Fig. 3.7). Overall the results suggested that the IFN-γ sensitivity of *igs4* is caused by mutant TC0574 protein of altered function and that this phenotype can be suppressed by inactivating the mutant protein or by blocking its expression.

3.4.6 *igs4 EB can rescue C. trachomatis from IFN-γ*

Productive *C. trachomatis* infection in IFN-γ treated mouse cells can be partially rescued if the cells are co-infected with *C. muridarum* EB (34) and this blocks recruitment of the IRG proteins Irgb10 and Irga6 and to *C. trachomatis* inclusions (27). Rescue does not require *C. muridarum* replication or metabolic activity. We tested if *igs4* could similarly rescue *C. trachomatis* to differentiate if *C. trachomatis* and *igs4* had defects in the same or different pathways (Fig. 3.11). IFN-γ-treated McCoy cells were simultaneously infected with a rifampin resistant *C. trachomatis* isolate and *C. muridarum* or *igs4* EB in the presence of rifampin to inhibit growth of *C. muridarum*. *C. trachomatis* infection was rescued by *C. muridarum* in a dose-dependent manner up to a *C. muridarum* MOI of 4. Higher doses were not evaluated because of the immediate cytotoxic potential of *C. muridarum* EB (34, 49). Rescue with *igs4* EB was similar to *C. muridarum*, suggesting that the underlying mechanisms of IFN-γ sensitivity in *igs4* and *C. trachomatis* differ.

3.4.7 *IFN-γ sensitivity of igs4 is not reversed by inhibitors of nitric oxide or reactive oxygen*

We next interrogated the mechanism of *igs4* sensitivity to IFN-γ from the perspective of the stimulated host cell. Nitric oxide (NO) produced by inducible nitric oxide synthase (iNOS) and reactive oxygen species from the phagosome oxidase pathway (Phox) have been implicated in IFN-γ-mediated control of chlamydial infection in mice and mouse cells (22-24, 50, 51). We tested if *igs4* activated these pathways more robustly or was more sensitive to their products.

Levels of iNOS protein in lysates of mock-treated and *Chlamydia*-infected McCoy cells +/- IFN-γ, were compared by Western blot (Fig. 3.12 A). iNOS was below the limit of detection in the mock infected cells and infection with *C. muridarum*, *igs4*, S1 and S5 also failed to elicit detectable iNOS by 24 hpi. Robust iNOS expression was detected in *C. trachomatis* infected cells at 24 hpi. Similar and relatively low levels of iNOS were detected in lysates of IFN-γ treated cells that were infected with *C. muridarum* or the mutants. However, levels of iNOS appeared to be consistently higher in IFN-γ-treated *C. trachomatis*-infected McCoy cells. These results suggested that *igs4* IFN-γ sensitivity was not linked to elevated expression of iNOS.

A possible explanation for the above results was that *C. muridarum* and the suppressor mutants modulated iNOS activity, whereas *igs4* did not. This was tested by comparing nitrite levels in supernatants using the Griess assay (Fig. 3.12 B). Nitrite levels mirrored iNOS levels found by Western blotting. Elevated nitrite was almost completely reversed by addition of 2 mM L-NMMA indicating

127

that iNOS, not altered expression or activity of constitutive nitric oxide synthase (NOS), was the primary source of nitrite.

We also tested if *igs4* was more sensitive to nitrogen oxide radicals produced by NO and reactive oxygen species using the competitive iNOS inhibitor L-N^G-monomethyl Arginine citrate (L-NMMA) (52) and the oxygen radical scavenger dimethylthiourea (DMTU) (53) (Fig. 3.12 C). Neither compound, individually or in combination, rescued *C. trachomatis* or *igs4*, although the compounds effectively rescued *C. trachomatis* in IFN-g treated RAW 264.7 murine macrophages (Krithika Rajaram, Chapter 4). These results suggested that IFN-γ sensitivity of *igs4* was not due to enhanced production of NO or increased susceptibility to reactive nitrogen species.

3.4.8 *igs4 is attenuated in the murine genital tract*

Growth of *igs4* in cell culture was similar to its parent under normal growth conditions but was diminished in the presence of IFN-γ (Fig. 3.1). To determine if *igs4* had decreased pathogenicity *in vivo*, we used the murine genital infection model. The infection course of *igs4* and *C. muridarum* in C57BL/6 mice differed significantly with respect to both duration of infection and magnitude of chlamydiae shedding (Fig. 3.13 A, P<0.0001). Differences in the magnitude of chlamydiae shedding were clearly evident as early as 7-10 days post infection, which correlates with marked inflammation and CD4$^+$ T cell emigration to genital tract tissues (54). In contrast, the infections with the suppressor mutants S1 and S5 were indistinguishable from *C. muridarum* (P>0.05). These results suggested

that the suppressor mutations completely reversed the effects of the *tc0574* missense mutation in their *igs4* parent.

Next we tested if the decreased pathogenicity of *igs4* in mice was mediated by IFN-γ. Surprisingly, the course and magnitude of *igs4* infection was similar in C57BL/6 (IFN-$\gamma^{+/+}$) and the IFN-$\gamma^{-/-}$ animals (Fig. 3.13 A, C; p>0.05). This result suggested that anti-chlamydial mediators not regulated by IFN-γ were sufficient to control *igs4* infection.

C. muridarum infection of mice produces an adaptive immune response that robustly protects against reinfection (55, 56). To determine if *igs4* could similarly elicit protective immunity, C57BL/6 that had resolved primary genital infection were reinfected with wild type *C. muridarum*. Infection with *igs4* conferred partial protection against WT challenge in C57BL/6 mice (*C. muridarum* Fig. 3.13 A vs *igs4* primary infection-WT reinfection Fig. 3.13 B; p<0.0001), but the magnitude of immunity as measured by bacterial shedding and duration of infection was significantly less than that induced by primary infection with *C. muridarum* (Fig. 3.13 B; p<0.001). Also, although there was a significant difference in chlamydiae shedding and infection duration between *C. muridarum* and *igs4* in IFN-$\gamma^{-/-}$ mice (Fig. 3.13 C; P<0.0001), the degree of protective immunity conferred by primary WT and *igs4* infection in IFN-$\gamma^{-/-}$ mice was indistinguishable (Fig. 3.13 D; P>0.05). Thus, primary genital infection with *igs4* is much attenuated compared to *C. muridarum* infection, but nevertheless, significant protective immunity is elicited.

The development of hydrosalpinx following murine *C. muridarum* genital infection is used as a measure of upper genital tract immunopathology. We found that the proportion of C57BL/6 mice that developed hydrosalpinx following infection with *C. muridarum*, *igs4*, S1 or S5 and reinfected with *C. muridarum* was 9/9, 0/10, 10/10 and 7/9, respectively. Similarly, only 2/10 IFN-$\gamma^{-/-}$ mice infected with *igs4* and reinfected with *C. muridarum* developed hydrosalpinx, whereas 4/4 IFN-$\gamma^{-/-}$ mice challenged at both primary infection and reinfection with *C. muridarum* developed hydrosalpinx. Collectively, these data suggest that *igs4* produces an infection that is not only attenuated in chlamydial shedding and infection duration, but also in upper genital tract pathology as measured by hydrosalpinx. Furthermore, infection with *igs4* conferred immunity sufficient to protect against hydrosalpinx when challenged with *C. muridarum*.

3.4.9 *igs4 is sensitive to IFN-β*

The attenuated phenotype of *igs4* in IFN-$\gamma^{-/-}$ mice suggested that some of the IFN-γ anti-chlamydial pathways might also be regulated by innate immune interferons. For example, the type I interferons IFN-α/β and IFN-ϵ are expressed in the murine genital tract during *C. muridarum* infection (57-59). To determine if *igs4* was susceptible to type I interferons, inclusion morphology of *C. muridarum* and *igs4* was examined in McCoy cells $\pm$ 250 U/mL IFN-β (Table 3.4). *C. muridarum* inclusions at 24 hpi were similar in the presence or absence of cytokine. However, the percent of lysed *igs4* inclusions increased from 8.5% in untreated cells to over 80% in cells treated with IFN-β. *igs4* lysis induced by IFN-

β was reduced to basal levels (9.14%) when McCoy cells were incubated with an anti-IFNAR antibody. The antibody failed to significantly reduce *igs4* lysis in the absence of exogenous cytokine, but the addition of cycloheximide prior to infection abolished inclusion lysis (Table 3.4 and Amanda Rhoel, personal communication). Collectively, these results suggested that *C. muridarum* infection of McCoy cells was sufficient to induce the production of inhibitory factors, and their expression could be greatly increased by the addition of interferons.

3.5 Discussion

Chlamydia IFN-γ resistance is both strain and host-organism specific and few chlamydial genes that mediate this have been identified. We believe our study is the first to use a forward genetic approach to directly search for IFN-γ resistance genes. We previously speculated that plasticity zone (PZ) genes could be key determinants of *C. muridarum* IFN-γ resistance in mice (1, 34), but analysis of multiple nonsense mutants of *C. muridarum* PZ genes revealed no defect in resistance to IFN-γ *in vitro* or dramatic attenuation in mice (Krithika Rajaram, Chapter 2). Since none of the four *igs* mutants we sequenced had mutations in the same genes aside of the polymorphic *tc0412* ORF, our results imply that chlamydial IFN-γ resistance is a complex phenotype. This could reflect the importance of IFN-γ resistance in *C. muridarum* virulence, prolonged pathogen adaptation or the inability of a single chlamydial effector to counteract mechanistically distinct anti-chlamydial pathways controlled by interferons. If the

last hypothesis is correct, we expect that our collection of *igs* mutants would contain isolates that are sensitive to specific IFN-γ regulated effectors, such as iNOS, Phox and IRGs. One of the caveats of our screen is that it would not be expected to identify functionally redundant resistance genes. This could be relevant to phospholipase D and cytotoxin genes in the PZ which are present in multiple copies in *C. muridarum* (3). Requiring that *igs* mutants had near wild-type growth in the absence of IFN-γ probably also prevented identifying genes with crossover functions in housekeeping and IFN-γ resistance. Nonetheless, our results suggest that characterization of additional *igs* mutants could be a powerful approach for identification of chlamydial IFN-γ resistance genes.

We focused initial characterization on *igs4* due to the strong phenotype of this mutant in cells of mouse, but not human, origin. We hypothesize that the phenotype of *igs4* is caused by a gain-of-function *tc0574* allele, although we have not yet been able to confirm that either TC0574 or mutant TC0574 proteins are expressed. Gain of function is suggested by observations that 1) predicted missense, nonsense and frame-shift mutations throughout *tc0574* completely reversed *igs4* IFN-γ sensitivity as did 2) destruction of the predicted start codon of the upstream gene *tc0573* and 3) insertion of an ~ 2kb intron in the 5' prime end of *tc0574*. These results, and our observation that expression of the larger polycistronic transcript encoding *tc0574* was unaffected in *igs4* and suppressor mutants, rules out the possibility that the *igs4* phenotype is caused by nonsense-mediated decay of upstream genes. Confirming that the *igs4 tc0574* allele is gain-of-function will require allele swapping which may be challenging due to a

lack of systems for complementation at relevant gene dosage and the likely possibility that the mutant *tc0574* allele is dominant. Isolation of *igs4* genotypic revertants would also be difficult because phenotypic revertants arose >1,000 fold more frequently than would be predicted for revertants. We cannot exclude that *tc0574* suppressors are intergenic or bypass suppressor mutations of another mutant allele in *igs4*. However, with the relatively low degree of mutagenesis in *igs4,* the possibility that a random mutation serendipitously located to the same 381 bp gene as did 8 of 9 suppressors is unlikely. We hope to differentiate these possibilities using a lateral gene transfer approach we are developing for crossing *C. muridarum* strains (Amanda Roehl, personal communication).

Little can be gleaned from homology of TC0574 to other chlamydial proteins, although *in silico* structural modeling suggests how the missense mutation in TC0574 in *igs4* might alter this protein's function. Our results suggest *tc0574* is expressed as part of an operon with another putative Inc *tc0573* (47) and possibly *hemC*, which is flanked by *radA* and *pknD*. An orthologous operon in *C. suis* MD56 is organized similarly and encodes homologs with 47% and 55% amino acid identity to TC0573 and TC0574, respectively (60). CT300 of *C. trachomatis* shares 42% amino acid identity with TC0574, but the region between *hemC* and *ct300* in *C. trachomatis* contain numerous stops in all three frames. Why this operon was maintained in *C. muridarum* and *C. suis* but not *C. trachomatis* is unclear but seem consistent with a niche-specific function. Phyre2 modeling suggested that TC0574 contains two α-helices that are packed

together (Krithika Rajaram, Chapter 5). Interestingly, glycine 81, mutated to glutamate in TC0574 of *igs4*, is located at the interface between the helices in TC0574. Ronzone et al. recently reported that a core region between the two α-helices of IncA regulates homodimer formation and can block the SNARE-mediated fusion and homotypic inclusion fusion activities of IncA (61). Thus, we speculate the mutation in TC0574 might alter homo-oligomerization or interactions of this protein with host proteins. Instability of *igs4* inclusions also seems consistent with known functions of other Inc proteins in maintenance of inclusion morphology.

How a mutant Inc could confer IFN-γ sensitivity is unclear but our observation that *tc0574* frameshift and nonsense mutants were normal in this regard suggests that TC0574 does not directly mediate IFN-γ resistance. A trivial explanation could be that IFN-γ resistance is an indirect effect of the slight reduction in growth rate we observed between 18 and 24 hpi. We think this is unlikely because we have identified *C. muridarum* mutants with more severe growth defects in unrelated screens that have wild type IFN-γ resistance (David Nelson, unpublished observation). Alternately, mutation of TC0574 could lead to general inclusion instability that manifests IFN-γ sensitivity, although this still means that some direct or indirect effect of IFN-γ exacerbates inclusion instability. Our observation that inhibitors of iNOS and Phox cannot facilitate rescue argues against sensitivity of *igs4* to these IFN-γ-mediated anti-chlamydial mechanisms. Coers et al. reported that ectopically expressed Irgb10 inhibits growth of *C. trachomatis* and that both Iigp1 (Irg6a) and IrgB10 localize to *C.*

trachomatis, but not *C. muridarum,* inclusions (27, 29). Whether p47 IRG proteins are regulated similarly in McCoy cells is unknown, but similar experiments might be useful in determining if *igs4* is sensitive to IRG proteins. Differentiating these possibilities in IRG knockout cell lines and mice could be challenging because the effects of loss of individual IRG proteins may be masked by other IRG proteins at the cellular level (20), and by compensatory T-cell responses at the level of the organism (29). If IFN-γ sensitivity of *igs4* cannot be explained by susceptibility to IRG family proteins our results may indicate that Plac8 (25) or novel pathways not yet implicated in chlamydial IFN-γ resistance are key.

Our observation that *igs4* virulence was not completely restored in IFN-γ$^{-/-}$ mice suggests that clearance of this mutant is not solely regulated by this cytokine. We observed that *igs4* is sensitive to exogenous IFN-β in McCoy cells. Type I interferons modulate the course of *C. muridarum* infection and disease in the murine genital tract. The magnitude and duration of *C. muridarum* genital tract shedding was reduced in IFNAR$^{-/-}$ mice, possibly due to improved CD4 T-cell recruitment to local lymph nodes in these animals (57). In contrast, mice that lack the reproductive tract-specific and constitutively-expressed type I interferon IFN-ε shed more *C. muridarum* than wild type mice and this is most pronounced early in infection (58). Relevant to the design of our mutant screen, IFN-ε is not secreted by cells of fibroblastic lineage (59). Since expression of IRG proteins (62, 63) and iNOS (64) is also regulated by type I interferons, an immediate future direction would be to test if igs4 virulence is fully restored in mice that cannot respond to both Type I and Type II interferons.

Hours post infection

136
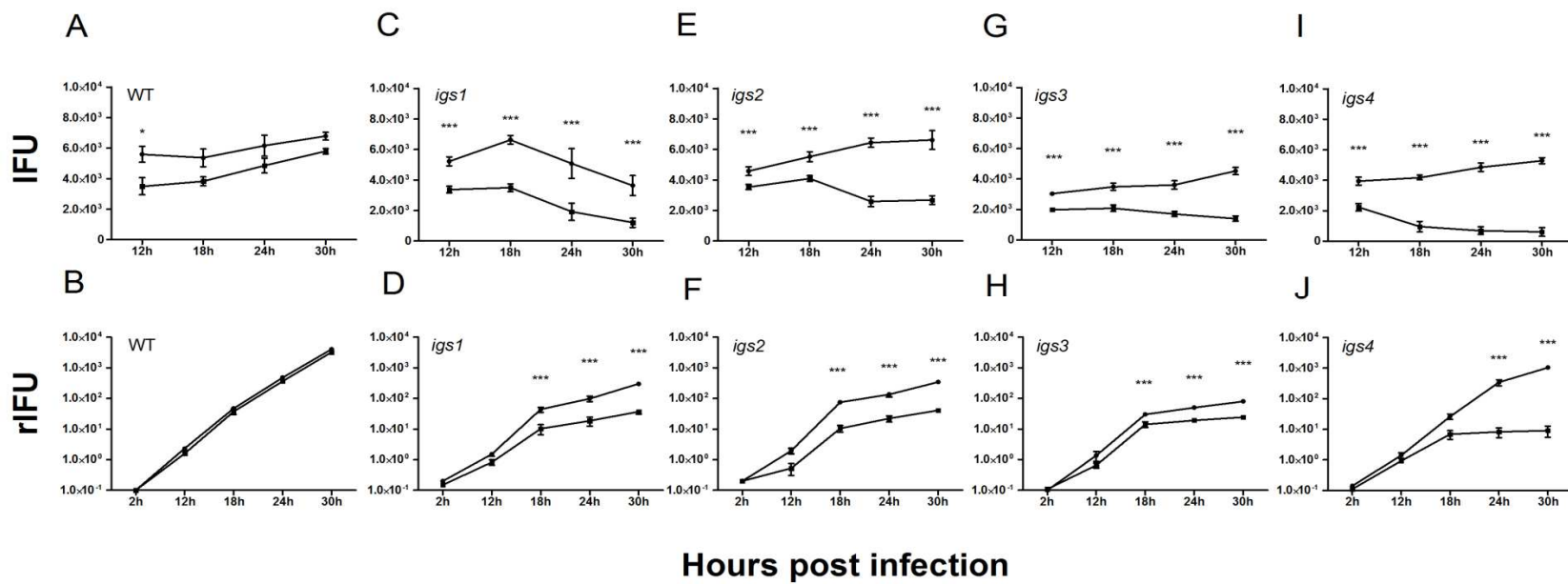
Fig. 3.1. Development of *igs* mutants is inhibited by IFN-γ. McCoy cells were infected at an MOI 1 with *C. muridarum* (WT) or *igs* mutants, +/- 20/ml IFN-γ, and numbers of IFU and rIFU were measured at multiple times post-infection. IFN-γ slightly decreased IFU and rIFU production of *C. muridarum*. In contrast, IFN-γ strongly and significantly inhibited IFU and/or rIFU production of the *igs* mutants at one or more points in the developmental cycle. The graphs show results of three experiments performed in triplicate. Error bars indicate standard deviation. IFN-γ treated specimens are indicated by squares, untreated by circles. Corresponding +/- IFN-γ samples were compared by two-way ANOVA with Bonferroni post test. *P<0.05, ***P<0.001.
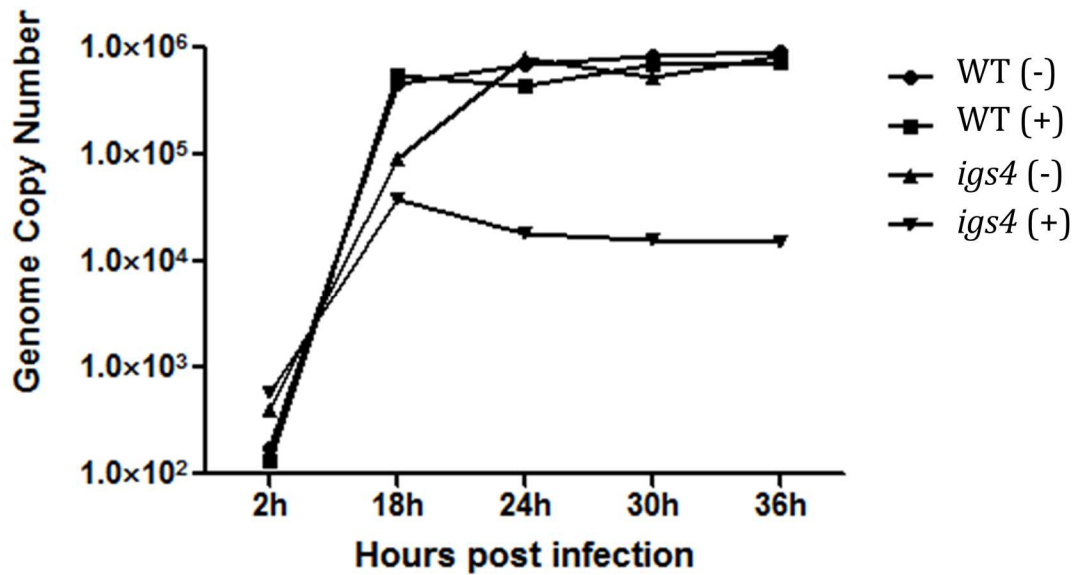
Fig. 3.2. Genome replication of *igs4* is inhibited by IFN-γ. IFN-γ treated or untreated McCoy cells were infected at an MOI of 1 with *C. muridarum* or *igs4* and DNA was harvested at various intervals post-infection. Quantitative real-time PCR was performed using a primer-probe set against the *C. muridarum* 16S rRNA gene and genome copy numbers were calculated by comparing the amplification curves to dilutions of a plasmid with a clone copy of *C. muridarum* 16S rRNA. Results of a representative experiment performed in triplicate are shown.
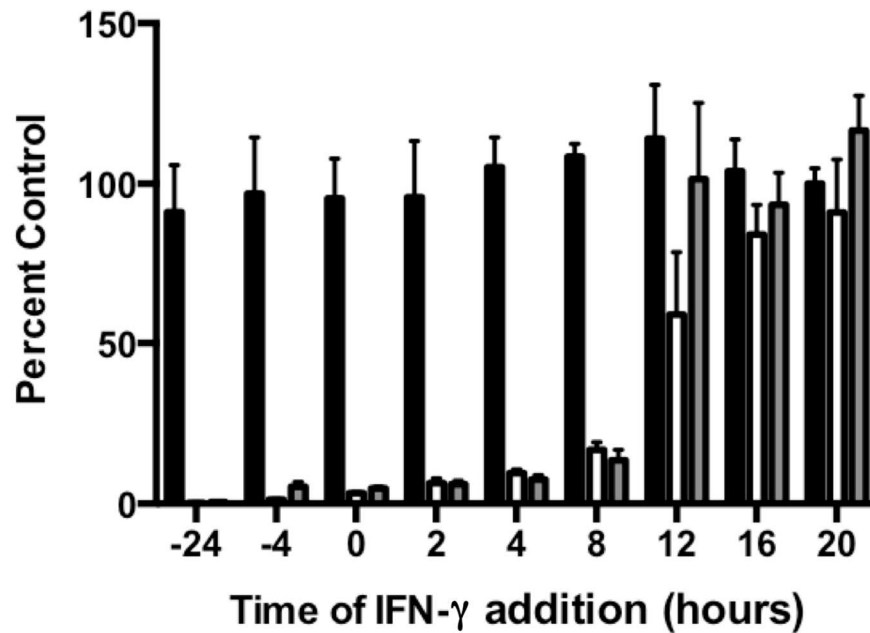
Figure 3.3. *igs4* **is most sensitive to IFN-γ early in its developmental cycle.**
McCoy cells infected with *C. muridarum* (black bars), *igs4* (white bars) or *C. trachomatis* serovar L2 (gray bars) were treated with 20 U/ml IFN-γ at different times relative to the start of infection. Times of IFN-γ addition are indicated on the Y-axis. Recoverable IFU are shown as percent of rIFU produced in the absence of IFN-γ. The graphs depict results of three experiments performed in triplicate. Error bars indicate standard deviation.

A

	C. muridarum	C. trachomatis	igs4
- IFN-γ			
+ IFN-γ			

30 µm

B

	- IFN-γ	+ IFN-γ
wt	0.0%	0.0%
igs1	2.6%	2.7%
igs2	0.0%	0. 0%
igs3	0.0%	0.0%
igs4	7.3%	83.9%
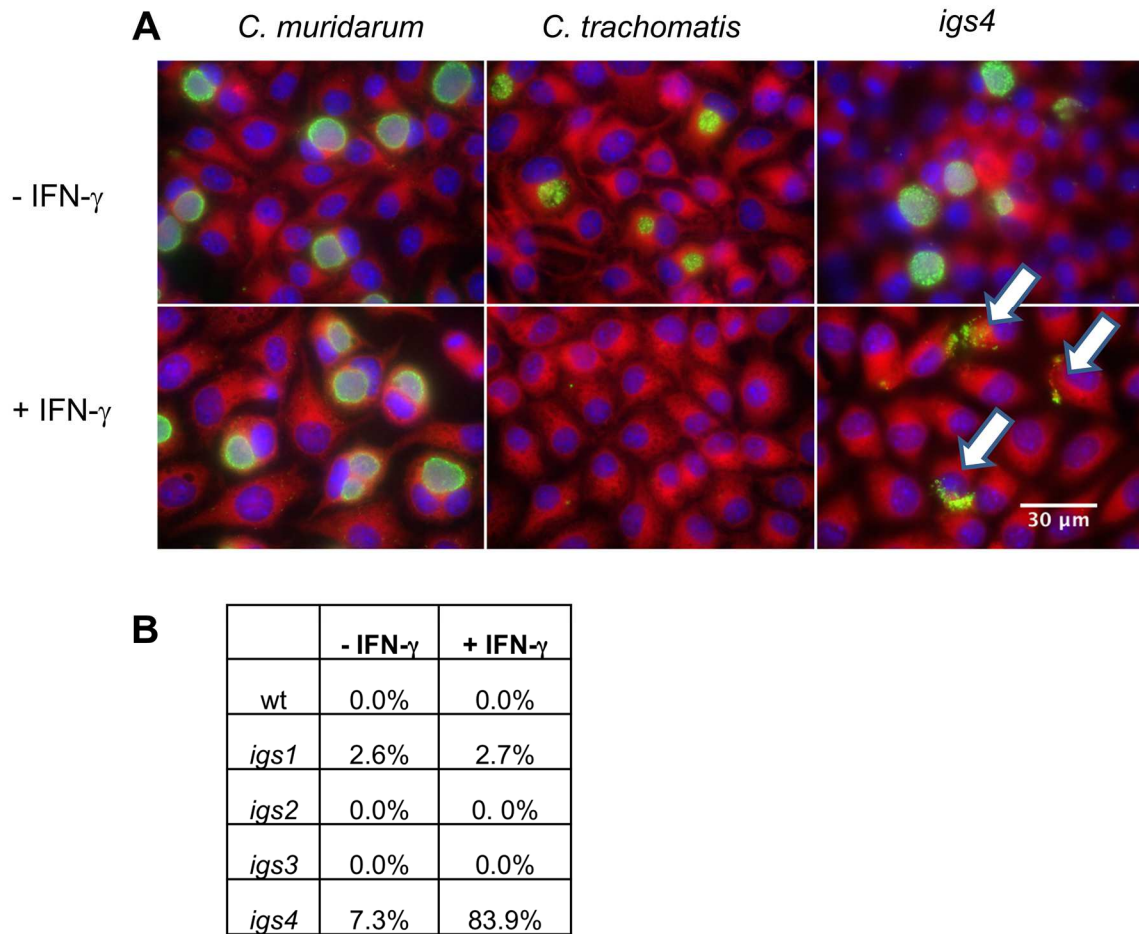
Fig. 3.4. IFN-γ treatment elicits lysis of *igs4* inclusions in McCoy cells. A) McCoy cell monolayers which were untreated or pre- and post-treated with 20U/ml IFN-γ were infected with *C. muridarum*, *C. trachomatis* L2 or *igs* mutants at an MOI of 0.1, and inclusions were fixed and stained with an antibody for chlamydial LPS and a green secondary fluorescent antibody at 24 hpi. Nuclei and host cytosol were stained with DAPI (blue) and Evans Blue (red), respectively. Representative lysed *igs4* inclusions are indicated by white arrows. B) Percentages of lysed inclusions, out of total inclusions, observed in the cultures infected with *C. muridarum* and *igs* mutants +/- IFN-γ. Lysed inclusions were rare except in IFN-γ-treated *igs4* cultures where they were dominant. The results indicate the averages of two independent experiments where at least 30 inclusions for each strain and condition were imaged.
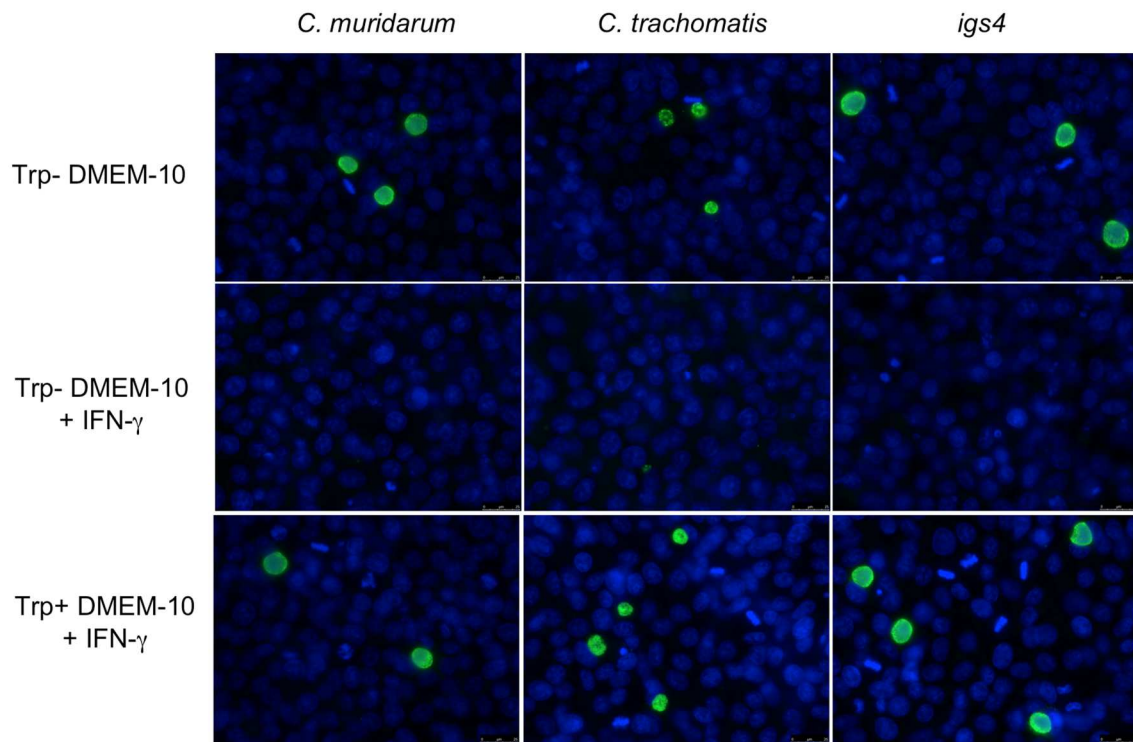
Fig. 3.5. IFN-γ treatment does not elicit lysis of *igs4* inclusions in HeLa cells. HeLa cells in Trp- DMEM-10 +/- 20U/mL IFN-γ or in Trp+ DMEM-10 with IFN-γ were infected with *C. muridarum*, *C. trachomatis* or *igs4* at an MOI of 0.1. Inclusions were fixed and stained with an antibody for chlamydial LPS (green) and DAPI (blue). All chlamydial strains grew normally in tryptophan-free DMEM-10 in the absence of IFN-γ, but the addition of cytokine resulted in complete inhibition of all three strains. In medium containing excess tryptophan, IFN-γ did not cause inhibition of any strain. *igs4* inclusions were identical in morphology to those of *C. muridarum*. The results indicate representative images from two independent experiments where at least 30 inclusions for each strain and condition were imaged.
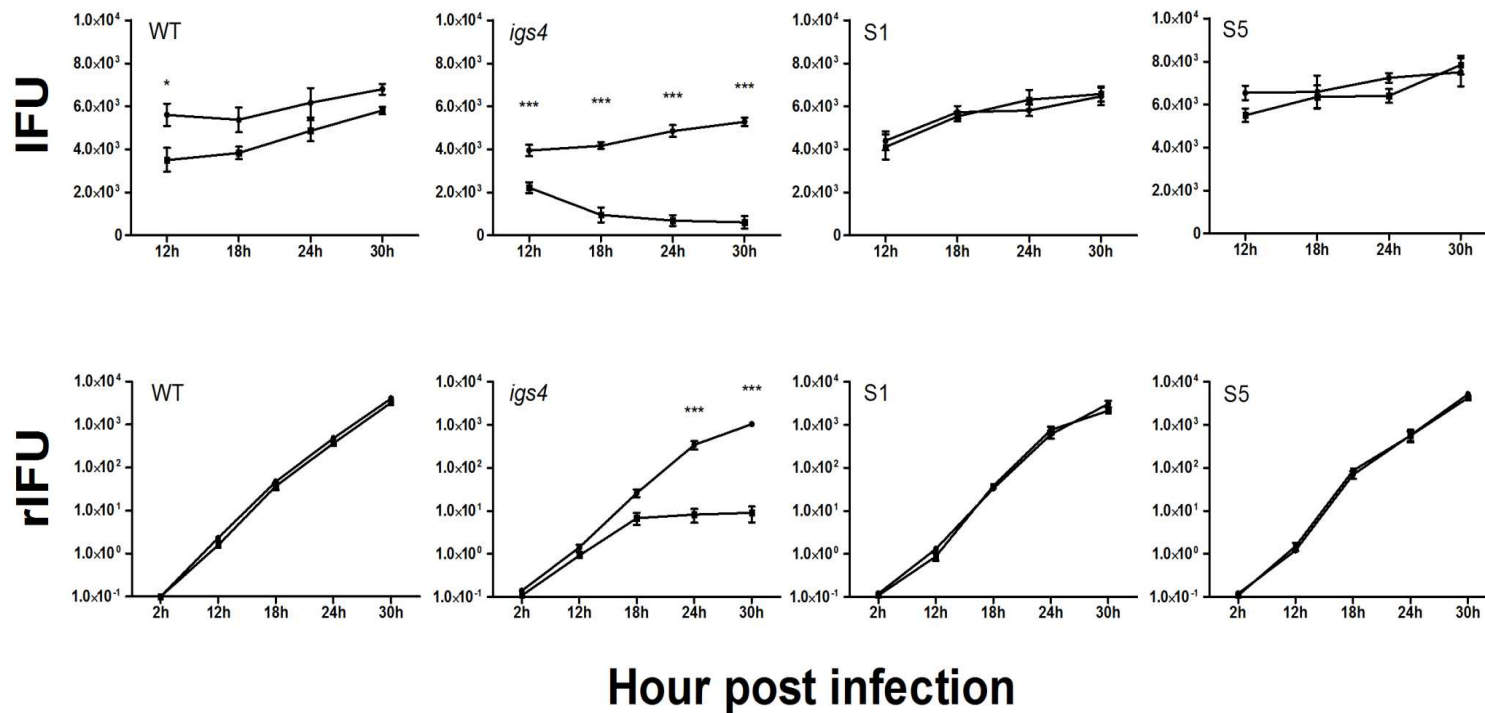
Fig. 3.6. Development of *igs4* suppressor mutants is unaffected by IFN-γ. McCoy cells were infected at an MOI of 1 with the *igs4* suppressor mutants S1 and S5, +/- 20/ml IFN-γ, and the numbers of IFU, and rIFU was measured at multiple intervals post-infection. IFN-γ slightly and similarly decreased IFU and rIFU production of *C. muridarum* and the suppressor mutants (Table 3.1). The graphs show results of three experiments performed in triplicate. Error bars indicate standard deviation of the experiments. Corresponding +/- IFN-γ samples were compared by two-way ANOVA with Bonferroni post test. *P<0.05, ***P<0.001. Results for *C. muridarum* (WT) and *igs4* are reproduced from Fig. 3.1.
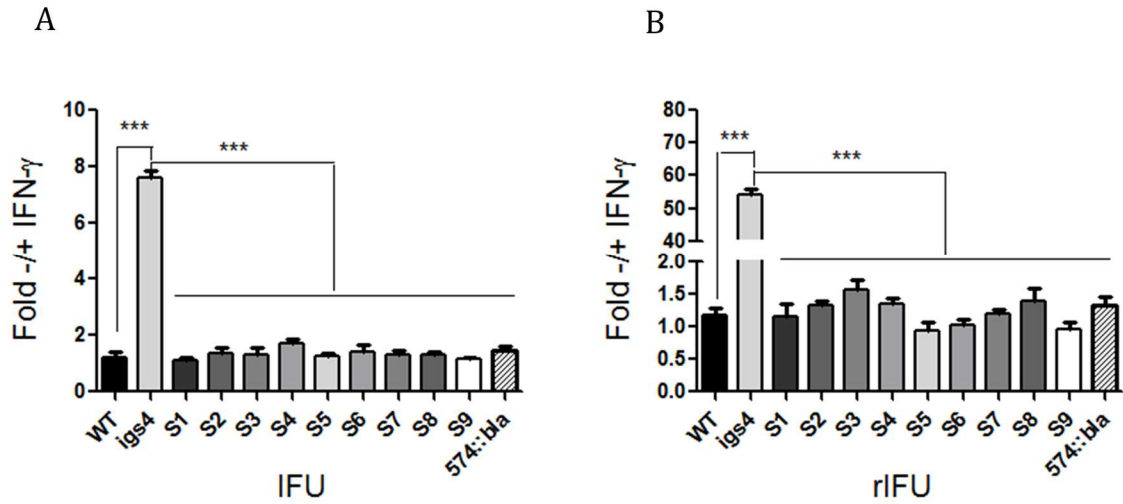
Fig. 3.7. *Suppressor mutants and a tc0574::GII(bla)* **mutant are IFN-γ resistant.** IFN-γ treated and untreated McCoy cells were infected with *C. muridarum*, *igs4,* various suppressor mutants or *C. muridarum tc0574::GII(bla)* and the fold change of A) IFU and B) rIFU +/- 20 U/ml IFN-γ was compared at 24 hpi. The graphs depict results of three independent experiments performed in triplicate. Error bars indicate standard deviation of the experiments. Values were compared to *igs4* by one-way ANOVA with Bonferroni post test. ***P<0.001.

	- IFN-γ	+ IFN-γ
WT	0.00%	0.00%
igs4	7.32%	83.93%
S1	0.00%	2.78%
S5	0.00%	1.33%
S9	1.29%	2.70%
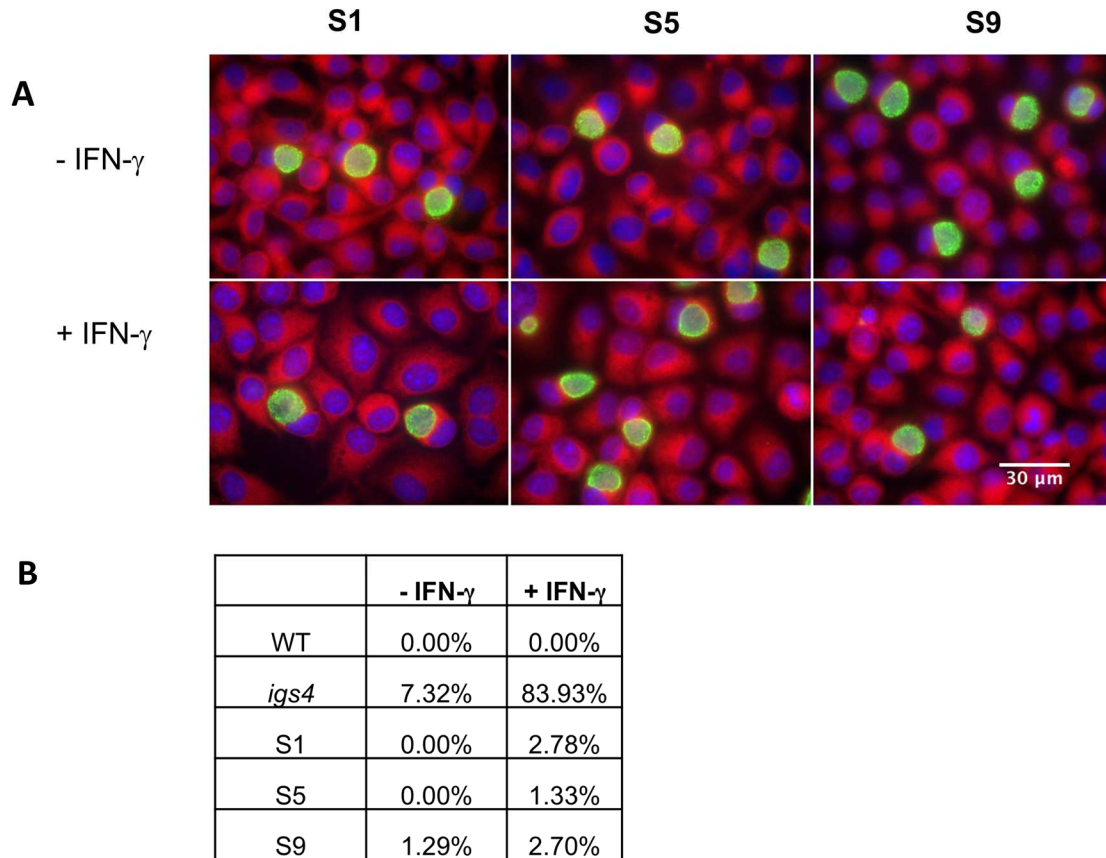
Fig. 3.8. Suppressor mutants resist IFN-γ-mediated lysis. A). Untreated or 20 U/ml IFN-γ pre- and post-treated McCoy cell monolayers were infected with *igs4* suppressor mutants at an MOI of 0.1 and were then fixed and labeled with EVI-H1 and a secondary fluorescent antibody at 24 hpi (green). Nuclei (blue) and host cytoplasm (red) were stained with DAPI and Evans Blue, respectively. B) Percentages of lysed inclusions, out of total inclusions, observed in the cultures infected with *C. muridarum, igs4* and the suppressor mutants S1, S5 and S9. Cross-sectional area for at least 30 inclusions per strain per condition were measured using ImageJ. Burst inclusions were excluded in cross-sectional area measurements. Graph represents cross sectional area average (μM^2) with standard deviation bars from two independent experiments. Results for *C. muridarum* (WT) and *igs4* are reproduced from Fig. 3.4 B.

145

Fig. 3.9. Diagram of *igs4* suppressor mutants. Approximate location and predicted effects of suppressor mutations on the expression of the 127 amino acid TC0574. All nine suppressor mutants retained the G81E mutation (black circle) which was present in *igs4* but not in the *C. muridarum* parent. Hatched areas indicate regions of TC0574 predicted not to be translated due to nonsense mutations (* asterisk in amino acid designations), out-of-frame insertions (ins) or single base deletions causing frame-shifts (deletions are marked by the delta symbol).

146

Fig.3.10. Organization and expression of *tc0572-tc0574*. A) Diagram of *tc0572-tc0574* genomic region (top) and amplicons amplified by RT-PCR (bottom). B) Total RNA from *C. muridarum* (left) or *igs4* (right) infected McCoy cells 24 hpi was reverse transcribed and then was PCR amplified with primers against various regions of *tc0572-tc0574* (indicated by numbered lines in panel A) and the amplicons were separated by gel electrophoresis. Corresponding control PCR reactions of each amplified region with no reverse transcriptase (RT) are labeled with asterisks (*). PCR products spanning *tc0572-tc0574* were detected in both *C. muridarum* and *igs4* infected cultures indicating that these genes are expressed in a single transcript and that the SNP in *tc0574* of *igs4* did not alter transcription of *tc0572-tc0574*. C) Semi-quantitative RT-PCR analysis of *tc0574* expression. One hundred µg of total RNA from McCoy cells infected with *C. muridarum*, *igs4* or S9 at an MOI of 1 was reverse transcribed and PCR amplified as above with primers against *tc0574* and 16S rRNA, except that the PCR products were analyzed by gel electrophoresis after various numbers of PCR cycles (indicated above the gel lanes). Similar quantities of *tc0574* transcripts were detected in *C. muridarum*, *igs4* and S9 infected McCoy cells.

147
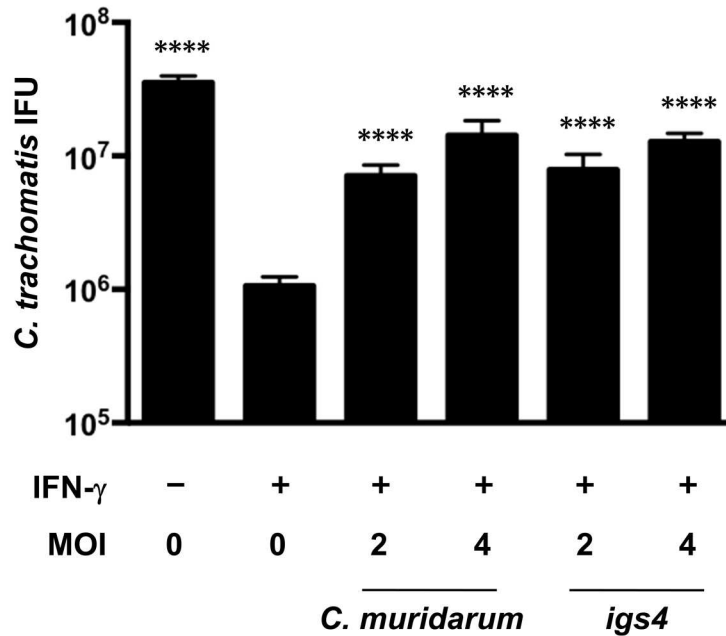
Fig. 3.11. *C. muridarum* **and** *igs4* **can rescue** *C. trachomatis* **from IFN-γ**. IFN-γ treated McCoy cells were co-infected with a rifampin-resistant *C. trachomatis* isolate at an MOI 1 and *C. muridarum* or *igs4* EB at an MOI of 2 or 4. The infection medium was supplemented with rifampin to inhibit the *C. muridarum* strains, and *C. trachomatis* rIFU were counted 24 hpi. *C. trachomatis* growth was inhibited in IFN-γ-treated cells but was partially and similarly restored by *C. muridarum* or *igs4* co-infection. The graphs depict results of three experiments performed in triplicate and the error bars indicate standard deviation. Values were compared to IFN-γ treated sample by one-way ANOVA with Bonferroni post test. ***P<0.001.
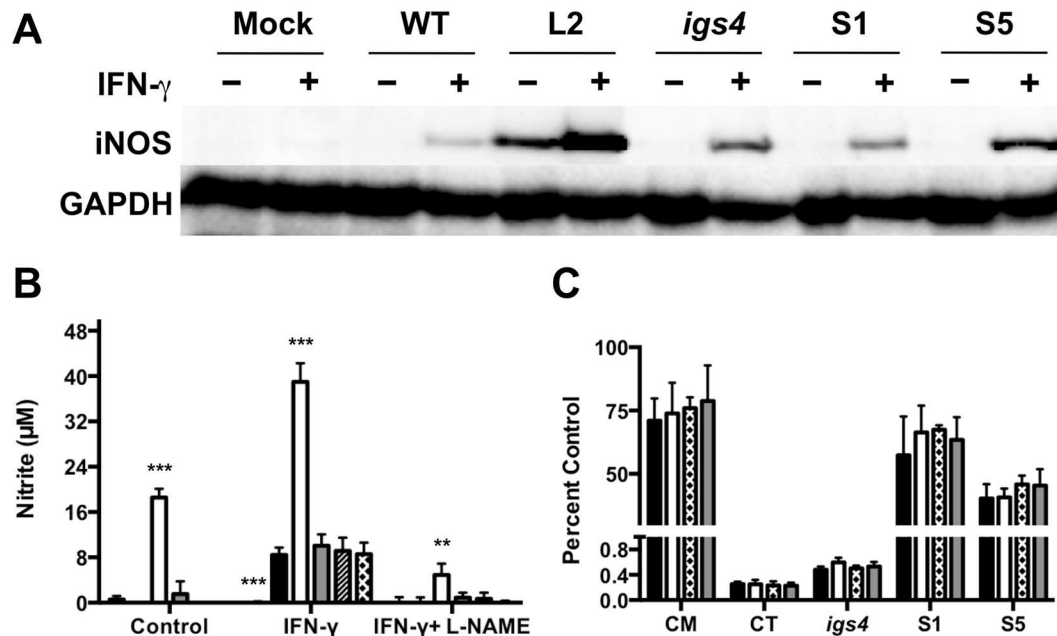
Fig. 3.12. *igs4* **IFN-γ sensitivity is unrelated to iNOS or Phox.** A) McCoy cells treated with IFN-γ and untreated controls were infected with *C. muridarum* (WT), *C. trachomatis* L2 (CT) or various mutant strains at an MOI of 1 and were harvested at 24 hpi. Equal amounts of protein from the samples were separated by SDS-PAGE and were immunoblotted with primary antibodies to the loading control GAPDH or iNOS. *C. muridarum*, *igs4* and the *igs* suppressor strains elicited similar levels of iNOS protein expression. B) McCoy cells treated with IFN-γ, IFN-γ and L-NAME, or untreated controls were infected with *C. muridarum* (black bars), *C. trachomatis* L2 (white bars), *igs4* (gray bars), S1 (hatched bars) or S5 (cross-hatched bars) at an MOI of 1. Nitrite in the cell culture supernatants was measured at 24 hpi by Griess assay. *C. muridarum*, *igs4* and *igs* suppressor mutants elicited similar levels of nitrite production. P-values were calculated by comparison to *C. muridarum* by two-way ANOVA with Bonferroni post test. **P<0.01, ***P<0.001. C). McCoy cells treated with IFN-γ (black bars), IFN-γ and L-NAME (white bars), IFN-γ and DMTU (hatched bars), IFN-γ L-NAME and DMTU (gray bars) or untreated controls were infected with *C. muridarum* (WT), *C. trachomatis* L2 (CT), *igs4* or the suppressor mutants S1 and S5 at an MOI of 1 (indicated below X-axis). The infections were harvested at 24 hpi and the rIFU produced by each strain in the various treatment conditions was compared to the control rIFU produced in untreated McCoy cells (Y axis). Inhibitors of iNOS and oxidative radicals did not reverse IFN-γ sensitivity of *C. trachomatis* or *igs4*. Western blotting experiments shown in panel A were performed multiple times and results of a single representative experiment are depicted. Experiments in panels B and C were repeated three times in triplicate and the error bars indicate standard deviation of the experiments.

149
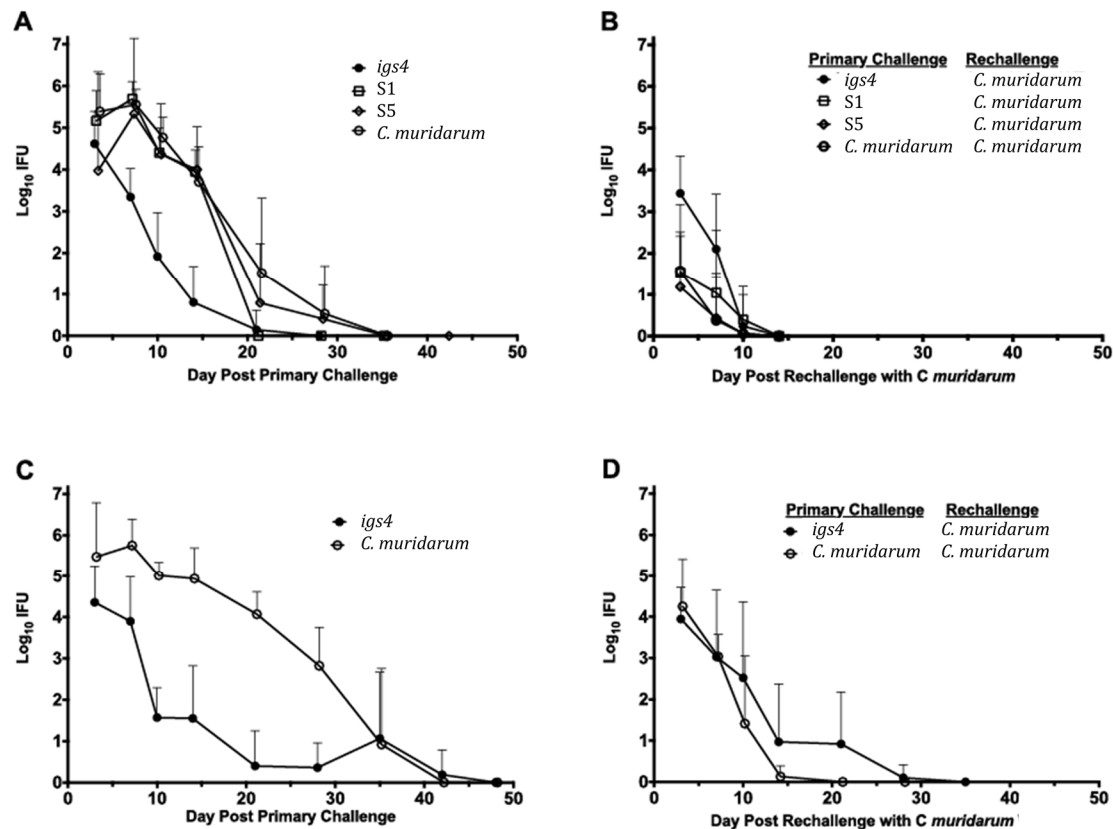
Figure 3.13. *igs4* is attenuated in the murine genital infection model. The course of primary genital infection (A, C) and reinfection (B, D) in female C57BL/6 (A, B) and IFN-$\gamma^{-/-}$ (C, D) mice was evaluated. For primary infections, mice were challenged intra-vaginally with 50,000 IFU of WT *C. muridarum* (C57BL/6 mice n=9; IFN-$\gamma^{-/-}$ mice n=4), *igs4* (C57BL/6 mice n=10; IFN-$\gamma^{-/-}$ mice n=10), S1 (C57BL/6 mice n=10) or S5 (C57BL/6 mice n=9). Immunity to reinfection was assessed following the resolution of primary infection by challenging mice with 50,000 IFU of WT. Infection was followed by enumerating IFU recovered from cervico-vaginal swabs. Data are presented as mean (log$_{10}$) IFU $\pm$ standard deviation. Data were analyzed by ANOVA (see Materials and Methods) and P values for various comparisons are noted in the Results.

TABLE 3.1. IFU/rIFU ratios of *C. muridarum* and *igs* mutants

	C. muridarum	igs1	igs2	igs3	igs4
12h	0.898 ± 0.162	1.136 ± 0.034	2.938 ± 0.139	1.39 ± 0.101	0.735 ± 0.149
18h	0.907 ± 0.061	2.30 5± 0.091	5.236 ± 0.304	1.138 ± 0.113	0.542 ± 0.176
24h	1.03 ± 0.037	2.759 ±0.122	2.319 ± 0.097	1.42± 0.161	4.1 ± 0.442
30h	1.08 ± 0.113	2.685 ± 0.156	3.441 ± 0.226	1.04 ± 0.133	9.4 ± 0.787

*Standard deviation of values is indicated after each value by ±

TABLE 3.2. Genome sequences of *igs* and *igs4* suppressor mutants

Strain	Gene ID	Chromosomal Position	Mutation	Amino Acid Change
igs 1	TC004	3413	CCT--> TCT	P--> S
igs 1	TC0090	108613	CTC--> TTC	L--> F
igs 1	TC0180	214411	TTG--> TTA	L--> L
igs 1	Intergenic	227381	G--> A	Substitution
igs 1	TC0243	281925	GAT--> AAT	D--> N
igs 1	TC0256	299426	CCC--> CCT	P--> P
igs 1	TC0271	325196	ATG--> ATA	M--> I
igs 1	TC0320	377362	ACT--> ATT	T--> I
igs 1	TC0412	472952	CAG--> TAG	Q--> Stop
igs 1	TC0439	532334	GCT--> GTT	A--> V
igs 1	TC0851	987831	GCT--> GTT	A--> V
igs 1	TC0862	997718	CGT--> TGT	R--> C
igs 1	TC0868	1005383	GGG--> AGG	G--> R

Strain	Gene ID	Chromosomal Position	Mutation	Amino Acid Change
igs 2	TC008	13782	CTG--> TTG	L--> L
igs 2	TC052	58829	AAA--> GAA	K--> E
igs 2	TC056	66042	GTA--> ATA	V--> I
igs 2	TC0197	230212	CAG--> CAA	Q to Q
igs 2	TC0412	473769	TTA--> TGA	L--> Stop
igs 2	TC0476	577763	AGT--> AAT	S--> N
igs 2	TC0481	585522	TTC--> TTT	F--> F
igs 2	TC0496	603314	AGC--> AGT	S--> R
igs 2	TC0671	800632	TCA--> TTA	S--> L
igs 2	TC0726	864375	GGA--> AGA	G--> R
igs 2	TC0820	952912	GAA--> AAA	E--> K

Strain	Gene ID	Chromosomal Position	Mutation	Amino Acid Change
igs 3	TC0090	108613	CTC--> TTC	L--> F
igs 3	TC0143	174709	TCG--> TTG	S--> L
igs 3	TC0243	281925	GAT--> AAT	D--> N
igs 3	TC0303	361136	AAC--> AAT	N--> N
igs 3	TC0412	472952	CAG--> TAG	Q--> Stop
igs 3	TC0414	474871	GTT--> ATT	V--> I
igs 3	TC0476	578503	CAG--> TAG	Q--> Stop
igs 3	TC0799	940807	GTG--> GTA	V--> V

igs 4	TC0094	112667	TCT--> TTT	S--> F
igs 4	TC0157	190522	GTG--> GCG	V--> A
igs 4	Intergenic	216687	G--> A	Substitution
igs 4	Intergenic	303555	C--> T	Substitution
igs 4	TC0412	473299-473303	Multiple indels	Frameshift
igs 4	TC0412	473349-473356	Multiple indels	Frameshift
igs 4	TC0425	491571	CAC--> CAT	H--> H
igs 4	TC0431	496343	GAT--> AAT	D--> N
igs 4	TC0431	497583	TCC--> TCT	S--> S
igs 4	TC0433	500955	TCC--> TTC	S--> F
igs 4	TC0461	561752	AGT--> AAT	S--> N
igs 4	Intergenic	565121	G--> A	Substitution
igs 4	Intergenic	647536	C--> T	Substitution
igs 4	TC0574	684336	GGA--> GAA	G--> E
igs 4	TC0610	730959	GGG--> GAG	G--> E
igs 4	TC0684	817790	AGC--> AGT	S--> S
igs 4	TC0692	823967	GCG--> GCA	A--> A
igs 4	TC0741	886389	ATG--> ATA	M--> I
igs 4	TC0769	911628	TCT--> TTT	S--> F
igs 4	TC0776	918129	TTG--> TTA	L--> L

Note: Only novel mutations in suppressor mutants are listed

S1	TC0574	684375	ACT--> AAT	T--> N

S5	TC0574	684200	CAA--> TAA	Q--> Stop
S5	TC0673	804307	TCC--> TCT	S--> S

S9	TC0573	683605	GTG--> GCG	V--> A

TABLE 3.3. Primers

Semi-quantitative RT-PCR

gene	Forward (5' to 3')	Reverse (5' to 3')
tc0574	GGGAAACGCTTTCAATAATCCC	CGAAAAGGAAATACAGCAAGGC
16s rRNA	TGGTTCAGATTGAACGCTGG	GATTCTCGACTGCAGCCTC
tc0727	ATGCGAATAGGAGATCCTATGAAC	GCACGATTTCTACATTACGATCATC

RT-PCR

Amplicon #	Forward (5' to 3')	Reverse (5' to 3')
1	CTGACTCATACGGGTCAATGAC	GCATTGTCTAGCACTGCAATAATG
2	GGGAAACGCTTTCAATAATCCC	CGAAAAGGA AATACAGCAAGGC
3	CTGACTCATACGGGTCAATGAC	CGAAAAGGAAATACAGCAAGGC
4	ATCCTGCCACCATATAGCAAG	GCATTGTCTAGCACTGCAATAATG
5	ATCCTGCCACCATATAGCAAG	CGAAAAGGAAATACAGCAAGGC

154

TABLE 3.4 *igs4* inclusions are susceptible to IFN-β

	C. muridarum	*igs4*
Untreated	0	8.5
IFNAR Ab	0	7.82
IgG1 Ab	0	8.17
IFN-β	0	81.62
IFN-β + IFNAR Ab	0	9.14
IFN-β + IgG1 Ab	0	82.49

3.6 References

1. **McClarty G, Caldwell HD, Nelson DE.** 2007. Chlamydial interferon gamma immune evasion influences infection tropism. Curr. Opin. Microbiol. **10:**47-51.

2. **Caldwell HD, Wood H, Crane D, Bailey R, Jones RB, Mabey D, Maclean I, Mohammed Z, Peeling R, Roshick C, Schachter J, Solomon AW, Stamm WE, Suchland RJ, Taylor L, West SK, Quinn TC, Belland RJ, McClarty G.** 2003. Polymorphisms in *Chlamydia trachomatis* tryptophan synthase genes differentiate between genital and ocular isolates. J. Clin. Invest. **111:**1757-1769.

3. **Read TD, Brunham RC, Shen C, Gill SR, Heidelberg JF, White O, Hickey EK, Peterson J, Utterback T, Berry K, Bass S, Linher K, Weidman J, Khouri H, Craven B, Bowman C, Dodson R, Gwinn M, Nelson W, DeBoy R, Kolonay J, McClarty G, Salzberg SL, Eisen J, Fraser CM.** 2000. Genome sequences of *Chlamydia trachomatis* MoPn and *Chlamydia pneumoniae* AR39. Nuc. Ac. Res. **28:**1397-1406.

4. **Read TD, Myers GS, Brunham RC, Nelson WC, Paulsen IT, Heidelberg J, Holtzapple E, Khouri H, Federova NB, Carty HA, Umayam LA, Haft DH, Peterson J, Beanan MJ, White O, Salzberg SL, Hsia RC, McClarty G, Rank RG, Bavoil PM, Fraser CM.** 2003. Genome sequence of *Chlamydophila caviae* (*Chlamydia psittaci* GPIC): examining the role of niche-specific genes in the evolution of the Chlamydiaceae. Nuc. Ac. Res. **31:**2134-2147.

5. **Shaw AC, Christiansen G, Roepstorff P, Birkelund S.** 2000. Genetic differences in the *Chlamydia trachomatis* tryptophan synthase alpha-subunit can explain variations in serovar pathogenesis. Microbes Infect. **2:**581-592.

6. **Heuer D, Kneip C, Maeurer AP, Meyer TF.** 2007. Tackling the intractable - Approaching the genetics of Chlamydiales. Int. J. Med. Microbiol. **297:**569-576.

7. **Nelson DE, Virok DP, Wood H, Roshick C, Johnson RM, Whitmire WM, Crane DD, Steele-Mortimer O, Kari L, McClarty G, Caldwell HD.** 2005. Chlamydial IFN-gamma immune evasion is linked to host infection tropism. PNAS **102:**10658-10663.

8. **Roshick C, Wood H, Caldwell HD, McClarty G.** 2006. Comparison of gamma interferon-mediated antichlamydial defense mechanisms in human and mouse cells. Infect. Immun. **74:**225-238.

9. **Morrison RP.** 2000. Differential sensitivities of *Chlamydia trachomatis* strains to inhibitory effects of gamma interferon. Infect. Immun. **68:**6038-6040.

10. **Fehlner-Gardiner C, Roshick C, Carlson JH, Hughes S, Belland RJ, Caldwell HD, McClarty G.** 2002. Molecular basis defining human *Chlamydia trachomatis* tissue tropism. A possible role for tryptophan synthase. J. Biol. Chem. **277:**26893-26903.

11. **Rapoza PA, Tahija SG, Carlin JP, Miller SL, Padilla ML, Byrne GI.** 1991. Effect of interferon on a primary conjunctival epithelial cell model of trachoma. Invest. Ophthalmol. Vis. Sci. **32:**2919-2923.

12. **Thomas SM, Garrity LF, Brandt CR, Schobert CS, Feng GS, Taylor MW, Carlin JM, Byrne GI.** 1993. IFN-gamma-mediated antimicrobial response. Indoleamine 2,3-dioxygenase-deficient mutant host cells no longer inhibit intracellular *Chlamydia* spp. or *Toxoplasma* growth. J. Immunol. **150:**5529-5534.

13. **Beatty WL, Belanger TA, Desai AA, Morrison RP, Byrne GI.** 1994. Tryptophan depletion as a mechanism of gamma interferon-mediated chlamydial persistence. Infect. Immun. **62:**3705-3711.

14. **Beatty WL, Belanger TA, Desai AA, Morrison RP, Byrne GI.** 1994. Role of tryptophan in gamma interferon-mediated chlamydial persistence. Ann. N. Y. Acad. Sci. **730:**304-306.

15. **Belland RJ, Nelson DE, Virok D, Crane DD, Hogan D, Sturdevant D, Beatty WL, Caldwell HD.** 2003. Transcriptome analysis of chlamydial growth during IFN-gamma-mediated persistence and reactivation. PNAS **100:**15971-15976.

16. **Tietzel I, El-Haibi C, Carabeo RA.** 2009. Human guanylate binding proteins potentiate the anti-chlamydia effects of interferon-gamma. PloS One **4:**e6499.

17. **Roth A, Konig P, van Zandbergen G, Klinger M, Hellwig-Burgel T, Daubener W, Bohlmann MK, Rupp J.** 2010. Hypoxia abrogates

antichlamydial properties of IFN-gamma in human fallopian tube cells *in vitro* and *ex vivo*. PNAS **107:**19502-19507.

18. **Cotter TW, Ramsey KH, Miranpuri GS, Poulsen CE, Byrne GI.** 1997. Dissemination of *Chlamydia trachomatis* chronic genital tract infection in gamma interferon gene knockout mice. Infect. Immun. **65:**2145-2152.

19. **Perry LL, Feilzer K, Caldwell HD.** 1997. Immunity to *Chlamydia trachomatis* is mediated by T helper 1 cells through IFN-gamma-dependent and -independent pathways. J. Immunol. **158:**3344-3352.

20. **Haldar AK, Saka HA, Piro AS, Dunn JD, Henry SC, Taylor GA, Frickel EM, Valdivia RH, Coers J.** 2013. IRG and GBP host resistance factors target aberrant, "non-self" vacuoles characterized by the missing of "self" IRGM proteins. PLoS Pathog. **9:**e1003414.

21. **Haldar AK, Piro AS, Pilla DM, Yamamoto M, Coers J.** 2014. The E2-like conjugation enzyme Atg3 promotes binding of IRG and Gbp proteins to *Chlamydia-* and *Toxoplasma*-containing vacuoles and host resistance. PloS One **9:**e86684.

22. **Ramsey KH, Miranpuri GS, Sigar IM, Ouellette S, Byrne GI.** 2001. *Chlamydia trachomatis* persistence in the female mouse genital tract: inducible nitric oxide synthase and infection outcome. Infect. Immun. **69:**5131-5137.

23. **Ramsey KH, Sigar IM, Rana SV, Gupta J, Holland SM, Byrne GI.** 2001. Role for inducible nitric oxide synthase in protection from chronic

Chlamydia trachomatis urogenital disease in mice and its regulation by oxygen free radicals. Infect. Immun. **69:**7374-7379.

24. **Igietseme JU, Perry LL, Ananaba GA, Uriri IM, Ojior OO, Kumar SN, Caldwell HD.** 1998. Chlamydial infection in inducible nitric oxide synthase knockout mice. Infect. Immun. **66:**1282-1286.

25. **Johnson RM, Kerr MS, Slaven JE.** 2012. Plac8-dependent and inducible NO synthase-dependent mechanisms clear *Chlamydia muridarum* infections from the genital tract. J. Immunol. **188:**1896-1904.

26. **Bernstein-Hanley I, Coers J, Balsara ZR, Taylor GA, Starnbach MN, Dietrich WF.** 2006. The p47 GTPases Igtp and Irgb10 map to the *Chlamydia trachomatis* susceptibility locus Ctrq-3 and mediate cellular resistance in mice. PNAS **103:**14092-14097.

27. **Coers J, Bernstein-Hanley I, Grotsky D, Parvanova I, Howard JC, Taylor GA, Dietrich WF, Starnbach MN.** 2008. *Chlamydia muridarum* evades growth restriction by the IFN-gamma-inducible host resistance factor Irgb10. J. Immunol. **180:**6237-6245.

28. **Al-Zeer MA, Al-Younes HM, Braun PR, Zerrahn J, Meyer TF.** 2009. IFN-gamma-inducible Irga6 mediates host resistance against *Chlamydia trachomatis* via autophagy. PloS One **4:**e4588.

29. **Coers J, Gondek DC, Olive AJ, Rohlfing A, Taylor GA, Starnbach MN.** 2011. Compensatory T cell responses in IRG-deficient mice prevent sustained *Chlamydia trachomatis* infections. PLoS Pathog. **7:**e1001346.

30. **Stephens RS, Kalman S, Lammel C, Fan J, Marathe R, Aravind L, Mitchell W, Olinger L, Tatusov RL, Zhao Q, Koonin EV, Davis RW.** 1998. Genome sequence of an obligate intracellular pathogen of humans: *Chlamydia trachomatis*. Science **282:**754-759.

31. **Kari L, Goheen MM, Randall LB, Taylor LD, Carlson JH, Whitmire WM, Virok D, Rajaram K, Endresz V, McClarty G, Nelson DE, Caldwell HD.** 2011. Generation of targeted *Chlamydia trachomatis* null mutants. PNAS **108:**7189-7193.

32. **Gieffers J, Durling L, Ouellette SP, Rupp J, Maass M, Byrne GI, Caldwell HD, Belland RJ.** 2003. Genotypic differences in the *Chlamydia pneumoniae tyrP* locus related to vascular tropism and pathogenicity. J. Infect. Dis. **188:**1085-1093.

33. **Kari L, Whitmire WM, Carlson JH, Crane DD, Reveneau N, Nelson DE, Mabey DC, Bailey RL, Holland MJ, McClarty G, Caldwell HD.** 2008. Pathogenic diversity among *Chlamydia trachomatis* ocular strains in nonhuman primates is affected by subtle genomic variations. J. Infect. Dis. **197:**449-456.

34. **Nelson DE, Taylor LD, Shannon JG, Whitmire WM, Crane DD, McClarty G, Su H, Kari L, Caldwell HD.** 2007. Phenotypic rescue of *Chlamydia trachomatis* growth in IFN-gamma treated mouse cells by irradiated *Chlamydia muridarum*. Cell. Microbiol. **9:**2289-2298.

35. **Caldwell HD, Kromhout J, Schachter J.** 1981. Purification and partial characterization of the major outer membrane protein of *Chlamydia trachomatis*. Infect. Immun. **31:**1161-1176.

36. **Liu X, Afrane M, Clemmer DE, Zhong G, Nelson DE.** 2010. Identification of *Chlamydia trachomatis* outer membrane complex proteins by differential proteomics. J. Bacteriol. **192:**2852-2860.

37. **Nguyen BD, Valdivia RH.** 2012. Virulence determinants in the obligate intracellular pathogen *Chlamydia trachomatis* revealed by forward genetic approaches. PNAS **109:**1263-1268.

38. **Matsumoto A, Izutsu H, Miyashita N, Ohuchi M.** 1998. Plaque formation by and plaque cloning of *Chlamydia trachomatis* biovar trachoma. J. Clin. Microbiol. **36:**3013-3019.

39. **Schneider CA, Rasband WS, Eliceiri KW.** 2012. NIH Image to ImageJ: 25 years of image analysis. Nat. Methods **9:**671-675.

40. **Song L, Carlson JH, Zhou B, Virtaneva K, Whitmire WM, Sturdevant GL, Porcella SF, McClarty G, Caldwell HD.** 2014. Plasmid-mediated transformation tropism of chlamydial biovars. Pathog. Dis. **70:**189-193.

41. **Johnson CM, Fisher DJ.** 2013. Site-specific, insertional inactivation of *incA* in *Chlamydia trachomatis* using a group II intron. PloS One **8:**e83989.

42. **Wang Y, Kahane S, Cutcliffe LT, Skilton RJ, Lambden PR, Clarke IN.** 2011. Development of a transformation system for *Chlamydia trachomatis*:

restoration of glycogen biosynthesis by acquisition of a plasmid shuttle vector. PLoS Pathog. **7:**e1002258.

43.   **Sega GA.** 1984. A review of the genetic effects of ethyl methanesulfonate. Mutat. Res. **134:**113-142.

44.   **Ramsey KH, Sigar IM, Schripsema JH, Denman CJ, Bowlin AK, Myers GA, Rank RG.** 2009. Strain and virulence diversity in the mouse pathogen *Chlamydia muridarum*. Infect. Immun. **77:**3284-3293.

45.   **Sturdevant GL, Kari L, Gardner DJ, Olivares-Zavaleta N, Randall LB, Whitmire WM, Carlson JH, Goheen MM, Selleck EM, Martens C, Caldwell HD.** 2010. Frameshift mutations in a single novel virulence factor alter the *in vivo* pathogenicity of *Chlamydia trachomatis* for the female murine genital tract. Infect. Immun. **78:**3660-3668.

46.   **Borges V, Ferreira R, Nunes A, Sousa-Uva M, Abreu M, Borrego MJ, Gomes JP.** 2013. Effect of long-term laboratory propagation on *Chlamydia trachomatis* genome dynamics. Infection, genetics and evolution:journal of molecular epidemiology and evolutionary genetics in infectious diseases **17:**23-32.

47.   **Lutter EI, Martens C, Hackstadt T.** 2012. Evolution and conservation of predicted inclusion membrane proteins in Chlamydiae. Comp. Funct. Genomics **2012:**362104.

48.   **Oppenheim DS, Yanofsky C.** 1980. Translational coupling during expression of the tryptophan operon of *Escherichia coli*. Genetics **95:**785-795.

49. **Belland RJ, Scidmore MA, Crane DD, Hogan DM, Whitmire W, McClarty G, Caldwell HD.** 2001. *Chlamydia trachomatis* cytotoxicity associated with complete and partial cytotoxin genes. PNAS **98:**13984-13989.

50. **Chen B, Stout R, Campbell WF.** 1996. Nitric oxide production: a mechanism of *Chlamydia trachomatis* inhibition in interferon-gamma-treated RAW264.7 cells. FEMS Immunol. Med. Microbiol. **14:**109-120.

51. **Igietseme JU, Uriri IM, Chow M, Abe E, Rank RG.** 1997. Inhibition of intracellular multiplication of human strains of *Chlamydia trachomatis* by nitric oxide. Biochem. Biophys. Res. Commun. **232:**595-601.

52. **Griffith OW, Kilbourn RG.** 1996. Nitric oxide synthase inhibitors: amino acids. Methods Enzymol. **268:**375-392.

53. **Fox RB.** 1984. Prevention of granulocyte-mediated oxidant lung injury in rats by a hydroxyl radical scavenger, dimethylthiourea. J. Clin. Invest. **74:**1456-1464.

54. **Morrison SG, Morrison RP.** 2000. In situ analysis of the evolution of the primary immune response in murine *Chlamydia trachomatis* genital tract infection. Infect. Immun. **68:**2870-2879.

55. **Morrison RP, Feilzer K, Tumas DB.** 1995. Gene knockout mice establish a primary protective role for major histocompatibility complex class II-restricted responses in *Chlamydia trachomatis* genital tract infection. Infect. Immun. **63:**4661-4668.

56. **Su H, Feilzer K, Caldwell HD, Morrison RP.** 1997. *Chlamydia trachomatis* genital tract infection of antibody-deficient gene knockout mice. Infect. Immun. **65:**1993-1999.

57. **Nagarajan UM, Prantner D, Sikes JD, Andrews CW, Jr., Goodwin AM, Nagarajan S, Darville T.** 2008. Type I interferon signaling exacerbates *Chlamydia muridarum* genital infection in a murine model. Infect. Immun. **76:**4642-4648.

58. **Fung KY, Mangan NE, Cumming H, Horvat JC, Mayall JR, Stifter SA, De Weerd N, Roisman LC, Rossjohn J, Robertson SA, Schjenken JE, Parker B, Gargett CE, Nguyen HP, Carr DJ, Hansbro PM, Hertzog PJ.** 2013. Interferon-epsilon protects the female reproductive tract from viral and bacterial infection. Science **339:**1088-1092.

59. **Hermant P, Michiels T.** 2014. Interferon-lambda in the context of viral Infections: production, response and therapeutic Implications. J. Innate Immun. **6:**563-574.

60. **Donati M, Huot-Creasy H, Humphrys M, Di Paolo M, Di Francesco A, Myers GS.** 2014. Genome sequence of *Chlamydia suis* MD56, isolated from the conjunctiva of a weaned piglet. GenomeA. **2**.

61. **Ronzone E, Wesolowski J, Bauler LD, Hackstadt T, Paumet F.** 2014. An alpha-helical core encodes the dual functions of the chlamydial protein IncA. J. Biol. Chem.

62. **Taylor GA, Feng CG, Sher A.** 2007. Control of IFN-gamma-mediated host resistance to intracellular pathogens by immunity-related GTPases (p47 GTPases). Microbes Infect. **9:**1644-1651.

63. **Shenoy AR, Kim BH, Choi HP, Matsuzawa T, Tiwari S, MacMicking JD.** 2007. Emerging themes in IFN-gamma-induced macrophage immunity by the p47 and p65 GTPase families. Immunobiol. **212:**771-784.

64. **Xie QW, Whisnant R, Nathan C.** 1993. Promoter of the mouse gene encoding calcium-independent nitric oxide synthase confers inducibility by interferon gamma and bacterial lipopolysaccharide. J. Exp. Med. **177:**1779-1784.

CHAPTER 4

CHLAMYDIA MURIDARUM INFECTION OF RAW 264.7 MACROPHAGES

ELICITS BACTERICIDAL NITRIC OXIDE PRODUCTION VIA REACTIVE

OXYGEN SPECIES AND CATHEPSIN B

4.1 Abstract

The ability of certain species of *Chlamydia* to inhibit the biogenesis of phagolysosomes permits their survival and replication within macrophages. Survival of macrophage-adapted chlamydiae correlates with the multiplicity of infection (MOI). Optimal chlamydial growth in macrophages occurs at MOI ≤ 1 while an MOI of 100 or higher induces "immediate cytotoxicity" resulting in the death of both the macrophage and pathogen. In this study, we examined the replicative capacity of *Chlamydia muridarum* in the RAW 264.7 murine macrophage cell line at different MOIs. *C. muridarum* productively infected these macrophages at low MOI but yielded few viable in EB when macrophages were infected at moderate (10) or high (100) MOI. While high MOIs caused cytotoxicity and host cell death, macrophages infected at the moderate MOI did not show signs of cytotoxicity until late in the infectious cycle. Inhibition of host protein synthesis rescued *C. muridarum* in macrophages infected at a moderate MOI, implying that chlamydial growth was blocked by activated defense mechanisms. Conditioned medium from these macrophages was anti-chlamydial and contained elevated levels of IL-1β, IL-6, IL-10 and IFN-β. Macrophage activation depended on TLR2 signaling and required live, transcriptionally active chlamydiae. A hydroxyl radical scavenger and inhibitors of iNOS and cathepsin B also reversed chlamydial killing. High levels of reactive oxygen species (ROS) led to an increase in cathepsin B activity, and pharmacological inhibition of ROS and cathepsin B reduced iNOS expression. Our results reveal a novel role for

cathepsin B in enhancing nitric oxide production and chlamydial inhibition in activated RAW 264.7 macrophages.

4.2 Introduction

Infection of host epithelia by *Chlamydia* spp. sets in motion a cascade of signaling events that recruit multiple innate immune effectors to the impacted site. Upon recognition of chlamydial pathogen-associated molecular patterns (PAMPs) and host danger signals, infiltrating leukocytes undergo transcriptional reprogramming to amplify the immune response by producing several cytokines and anti-microbial factors. The subsequent inflammatory process aids in bacterial clearance and primes elements of adaptive immunity while also contributing to the damaging pathology associated with chlamydial disease (1, 2).

Cells of the monocyte-macrophage lineage play critical roles in innate and adaptive immunity against chlamydial infections. Depletion of macrophages from mice prior to infection results in increased morbidity and pathogen burden (3, 4). Adoptive transfer of macrophages to IFN-γ-deficient mice has been shown to be sufficient for the control of *Chlamydia pneumoniae* in lung models of infection even in the absence of T and B cell responses (5). Some species of *Chlamydia* can survive and replicate in isolated macrophages. Studies examining intracellular survival of *C. trachomatis* strains determined that lymphogranuloma venereum (LGV) biovar, but not oculogenital, strains could productively infect macrophages (6-8). *C. pneumoniae* and *C. psittaci* have been similarly shown to replicate in macrophages by preventing maturation of the phagosome (9, 10).

Chlamydial persistence or replication within phagocytic cells correlates with infection resolution and disease outcome. For instance, LGV strains are highly invasive and cause systemic infections by dissemination through the lymphatic system (11). These strains also require a longer antibiotic regimen for effective treatment as compared to non-LGV *C. trachomatis* biovars (12). Persistent infection of macrophages by *C. pneumoniae* in several tissues has been associated with chronic inflammatory conditions including atherosclerosis, reactive arthritis and asthma (13, 14).

Intracellular replication of chlamydiae within macrophages *in vitro* is less efficient than in epithelial cells and is limited by the constitutive expression of perforin-2 in macrophages (15). Productive infection also appears to be contingent upon the macrophage activation state and multiplicity of infection (MOI). Macrophages "classically activated" by IFN-γ and LPS or other microbial PAMPs switch to an M1 polarized state. This correlates with increased bacterial killing via pro-inflammatory cytokines, production of reactive oxygen species (ROS) and upregulation of inducible nitric oxide synthase (iNOS) (16). Multiple types of immune cells secrete IFN-γ in response to chlamydial infection, likely favoring M1 polarization (17). M2 anti-inflammatory macrophages are activated by IL-4 or IL-10 and participate in wound-healing and fibrosis (16). All evaluated chlamydial species fail to survive in M1 macrophages *in vitro*, but whether they selectively replicate in M2 or resting macrophage (M0) reservoirs as opposed to M1 *in vivo* is unknown (18-21). Interestingly, a virulent strain of *C. psittaci* 6BC recruits M0 instead of activated macrophages in mice and this correlates with

increased morbidity (3). Other chlamydial species may also modulate macrophage activation state or possess alternative macrophage subversion strategies.

Early work with macrophages isolated from various hosts and tissues indicated that recovery of chlamydial infectious particles is also dictated by MOI (6, 10, 22). Optimal recoveries were obtained when macrophages were infected at an MOI of 1 or less. MOI in the order of 10 to 250 of *C. psittaci* and *C. trachomatis* L2/434/Bu led to decreased EB recovery, and this was attributed to host cell cytotoxicity occurring within the first 6 to 10 hours of infection.

In this study, we examined chlamydial recoveries from cells of the murine RAW 264.7 macrophage line (RAW) infected with the mouse pathogen *C. muridarum* at a range of MOI from 0.5 and 100. We observed a decrease in chlamydial survival with increasing MOI, consistent with previous studies (10, 22). Interestingly, a majority of cells infected at an MOI of 10 remained healthy but failed to support chlamydial development. However, these cells produced high levels of pro-inflammatory cytokines, iNOS-derived nitric oxide (NO) and ROS, indicative of M1 polarization. Induction of iNOS expression depended on an increase in cathepsin B activity and ROS accumulation. Blocking iNOS, ROS or cathepsin B restored chlamydial growth in moderately infected macrophages. Together, our results indicate a novel ROS and cathepsin B-dependent pathway for NO production and control of *C. muridarum* infection in RAW macrophages.

4.3 Materials and Methods

4.3.1 *Cell lines and chlamydial propagation*

The murine RAW 264.7 macrophage (RAW) cell line was a kind gift from Cheng Kao (Indiana University, Bloomington). RAW cells were maintained in low-adhesion 10 cm bacterial petri dishes (VWR) in RPMI-1640 medium containing 2 mM L-glutamine (Life Technologies), supplemented with 10% fetal bovine serum albumin (FBS) (Atlanta Biologicals), 10 mM HEPES (Gibco) and 1 mM sodium pyruvate. Only low passage macrophages ($\leq$ 4) were used for experiments. *C. muridarum* (a generous gift from Harlan Caldwell, NIAID, NIH) was propagated in McCoy mouse fibroblast cells (American Type Culture Collection CRL-1696) and elementary bodies (EB) were purified as previously described (23). McCoy cells were cultured in DMEM-high glucose medium containing 4 mM L-glutamine and 110 mg/L sodium pyruvate (Hyclone) and supplemented with 10% FBS, 10 mM HEPES and 100 μM non-essential amino acids (Gibco).

4.3.2 *Recoverable Inclusion Forming Unit (rIFU) assays*

RAW cells were seeded in 24-well cell culture plates (Thermo Scientific) 48 h prior to infection. Chlamydial infections were performed on confluent monolayers in sucrose phosphate glutamic acid (SPG) buffer and infections were performed by centrifugation at 168 $\times$ g at room temperature (RT) for 1 h. Following infection, SPG was replaced with fresh culture medium and the plates were incubated at 37°C in 5% CO_2. In some recoverable infection forming unit

(rIFU) experiments, RAW cells were treated at 30 minutes prior to infection with one or more of the following reagents: 1 mM L-NG-monomethyl Arginine citrate (L-NMMA) (Cayman Chemical), 2 mM L-NG-Nitroarginine methyl ester (L-NAME) (Cayman Chemical), 15 mM N,N′-Dimethylthiourea (DMTU) (Acros Organics), 50 or 100 ng/mL IL-1Ra (Peprotech), 25 μM Ac-YVAD-CHO (Peprotech), 25 μM Z-WEHD-FMK and 25 μM CA-074 Me (kind gifts of Stanley Spinola, Indiana University School of Medicine). Treatment continued throughout the course of infection. Infected monolayers were frozen in 500 μl SPG at 24 hours post infection (hpi). Upon thawing, cells were scraped from the wells and were agitated with 3 mm glass beads to harvest EB. An IFU assay was then performed by infecting McCoy cells in 96-well plates (Thermo Fisher) with serial dilutions of the harvests. At 24 hpi, cells were fixed with methanol and stained with mouse anti-chlamydial LPS mAB (EVIH1) followed by a secondary Alexa Fluor488-conjugated mAB (Life Technologies). Chlamydial inclusions were imaged and counted using an EVOS FL Auto Cell Imaging System (Life Technologies).

4.3.3 *Cytotoxicity assay*

Lactate Dehydrogenase (LDH) assays were performed according to the manufacturer's instructions (OPS Diagnostics). RAW cells were infected with *C. muridarum* at an MOI of 0.5, 10 or 100. Maximal LDH release was determined by treating cells in control wells with 10% Triton X-100 10 minutes prior to the assay. Supernatants were removed from wells at the indicated time points after a brief spin to remove debris. In a 96-well plate, 25 μl of the supernatants were mixed

with 75 μl of the dye/buffer solution. Following incubation at 37°C for 15 minutes, absorbance was measured at 490 nm.

4.3.4 *Immunofluorescence Microscopy*

RAW macrophages were grown on glass coverslips in 24-well plates. Cells were infected by centrifugation, fixed at 2 hpi with 4% formaldehyde and were then permeabilized with 0.05% Saponin. Cells were blocked in PBS containing 0.1% Bovine Serum Albumin (BSA) for 1 h and chlamydial inclusions were then stained with primary mAB EVIH1 followed by an anti-mouse Alexa Fluor488 secondary antibody (Life Technologies). The coverslips were mounted on glass slides using ProLong Gold antifade reagent with DAPI (Life Technologies) and images were captured using a Leica DMI6000 B inverted microscope with a 63X oil immersion objective.

4.3.5 *TLR2 and TLR4 neutralization experiments*

RAW macrophages were incubated for 1 h with antibody (10-30 μg/mL) and were stimulated with either *C. muridarum* (MOI 10) or 0.5 ng/mL *E. coli* LPS and *C. muridarum* EB (MOI 0.5). Anti-TLR4-MD2 (clone MTS510), anti-TLR2 (clone T2.5) and isotype-matched antibodies IgG2A and IgG1 were purchased from BioLegend (San Diego, CA). Supernatants were assayed for IFN-β levels at 24 hpi, and the cells were harvested for rIFU assays.

4.3.6 *C. muridarum EB heat and UV inactivation*

Heat-inactivated EB were prepared by incubating concentrated *C. muridarum* stocks at 56°C for 30 minutes. UV-inactivated EB were made by diluting stocks in SPG at a 1:10 ratio. Diluted EB solutions were pipetted onto a petri dish and exposed to 1,200 J/cm^2 twice in a UV-cross-linking cabinet (Spectralinker; Spectronics Corporation) (24, 25). Efficacy of the UV and heat treatments was confirmed by IFU assays.

4.3.7 *Cytokine analysis*

Culture supernatants were collected from infected RAW macrophages at indicated times and were centrifuged briefly to remove debris. The supernatants were assayed for IL-1β, IL-6, 1L-10, IL-12p40, TNF-α and IFN-γ (Milliplex) at the Bio-Plex core (IUPUI, Indianapolis) according to manufacturer's instructions. IFN-β levels were determined using a mouse IFN-β ELISA Kit according to manufacturer's instructions (BioLegend, San Diego, CA).

4.3.8 *Griess assay*

Nitrite concentrations in culture media were measured by a commercial Griess assay kit (Biotium). 150 μl of culture supernatant was removed from infected monolayers at 6, 12 and 24 hpi. The samples were incubated with 20 μL Griess reagent (0.05% N-(1-naphthyl) ethylenediamine dihydrochloride; 0.5% sulfanilic acid; 2.5% phosphoric acid) in a 96-well plate at room temperature for

30 minutes. Absorbance was measured at 540 nm and nitrite levels were calculated from a sodium nitrite standard curve.

4.3.9 *Western blot analysis*

RAW cells were treated with various reagents and were infected at an MOI of 0.5 or 10. Cells were washed with PBS at 6, 12 or 24 hpi and were then incubated in 50 μl Lysis buffer (2% sodium dodecyl sulphate (SDS); 10% glycerol; 62 mM Tris, pH 6.8) containing a Protease Inhibitor mini tablet (Pierce) for 10 minutes on ice. Cell lysates were boiled for 5 minutes. Protein samples were separated by SDS-PAGE and transferred to nitrocellulose membranes. Membranes were incubated at 4°C overnight with rabbit iNOS mAb or rabbit GAPDH mAb followed by incubation with a secondary anti-rabbit horse radish peroxidase conjugate for 1 h. Antibodies were purchased from Cell Signaling Technology (Danvers, MA). Proteins were visualized using SuperSignal West Dura Chemiluminescent Substrate (Pierce) according to the manufacturer's instructions.

4.3.10 *ROS assay*

ROS production from infected RAW cells in 96-well clear bottom black plates (Corning) was assayed using the fluorogenic dye 2', 7'-dichlorofluorescein diacetate (DCFDA) (Abcam). At indicated times, 20 μM DCFDA was mixed with culture media 45 minutes prior to measurement of fluorescence intensity (excitation/emission wavelengths: 485 nm/535 nm).

4.3.11 *Assay for cathepsin B activity*

RAW macrophages were cultured on coverslips in 24-well plates. Infections and pharmacological treatments of RAW macrophages were performed. At 10 hpi, reconstituted Magic Red cathepsin B substrate reagent MR-(RR) 2 (Immunochemistry Technologies) was added directly to the culture media in wells. After 30 minutes of treatment, nuclei were counterstained with Hoechst 33342 for 10 minutes. Coverslips were analyzed for cathepsin B activity by fluorescence microscopy (Leica DMI6000 B; 63X oil immersion objective). Fluorescence intensities were quantified from ten images obtained from each of three independent experiments using ImageJ software (26).

4.3.12 *Statistics*

Data was analyzed using Prism 6.0 software (GraphPad). For comparisons of multiple groups with two or more variables, data was subjected to log transformation and two-way analysis of variance (ANOVA) followed by the Bonferroni posttest was used. Multiple comparisons for data with a single variable were analyzed by one-way ANOVA followed by the Dunnett's posttest. Differences in values between two different groups were determined using Student's *t* test. Differences were considered statistically significant when $p < 0.05$.

4.4 Results

4.4.1 Productive C. muridarum infection of RAW macrophages is dependent on multiplicity of infection

The effects of multiplicity of infection (MOI) on *C. muridarum* infection forming unit (IFU) production were examined in RAW macrophages (Fig. 4.1 A). At the lowest MOI (0.5), we observed a 2-fold increase in IFU recovery over input, which is in agreement with previous reports (22). Maximal IFU recovery occurred when macrophages were infected at an MOI of 1. IFU recovery decreased at MOIs of 3 and higher. At moderate (10) and high (100) MOIs, IFU recoveries were approximately .001% and .0001% of input, respectively.

To determine if reduced IFU recovery at moderate and high MOIs could be explained by host cell death, infected macrophages were examined by light microscopy (Fig. 4.1 B-G). Cells infected at an MOI of 100 exhibited rounding and cytotoxicity (Fig. 4.1 G). However, most cells infected at an MOI of 10 had normal morphologies (Fig. 4.1 F). These macrophages also released basal levels of LDH until late in the chlamydial developmental cycle (Fig. 4.2). To test if low IFU recovery could be explained by reduced EB entry into macrophages, internalized EB were quantified by fluorescence microscopy at 2 hpi. The numbers of cytosolic EB correlated with input MOI (Fig. 4.1 H). Overall, these findings suggested that moderate MOI infection triggered macrophage activation which inhibited chlamydial EB production.

178

4.4.2 *Chlamydial inhibition in RAW macrophages requires de-novo host protein synthesis*

To elucidate the mechanism of *C. muridarum* inhibition in RAW macrophages, we initially tested if the anti-chlamydial factors were pre-formed. Infected macrophages were treated with cycloheximide to block protein synthesis. Cycloheximide increased IFU production of macrophages infected at an MOI of 0.5 by 3-fold, but did not increase IFU production of macrophages infected at an MOI of 100 (Fig. 4.2). In contrast, cycloheximide treatment increased IFU production of macrophages infected at an MOI of 10 by more than 10,000-fold. These results implied that moderate MOI of *C. muridarum* induced macrophage defenses, whereas higher MOIs caused macrophage death.

4.4.3 *Supernatants from RAW macrophages contain heat-sensitive anti-chlamydial factors*

Activated macrophages release cytokines that can stimulate neighboring cells (27) so we tested if conditioned supernatants from infected macrophages could inhibit *C. muridarum* infection of newly infected macrophages. Conditioned supernatants from RAW cells, infected at low or moderate MOIs, were collected at various intervals post infection. The fresh supernatants were then transferred onto macrophages that had just been infected with *C. muridarum* at an MOI of 0.5 by centrifugation. Supernatants from the MOI 0.5 infections failed to inhibit chlamydial growth (Fig. 4.4). In contrast, supernatants from the MOI 10 infections inhibited rIFU production. The degree of this inhibition varied from 4-fold with 4

hpi supernatants, to 1000-fold with 24 hpi supernatants and was completely abolished if the supernatants were heated at 95°C for 5 minutes.

4.4.4 *Multiple chlamydial antigens are required for induction of macrophage inhibitory responses*

Killed and viable EB elicit dissimilar cytokine responses (28, 29). We tested if the anti-chlamydial responses of macrophages that we had observed could be triggered by heat and UV-killed EB using co-infection assays. Macrophages were co-infected with live EB at an MOI of 0.5, and UV or heat-killed EB at MOIs of 9.5 (total MOI =10). To differentiate if chlamydial transcription was required to elicit cytokine responses, similar co-infection experiments were performed with rifampin-resistant *C. muridarum* EB at an MOI of 0.5, and wild type *C. muridarum* EB at an MOI of 9.5, in the presence of sufficient rifampin to block growth of the wild type *C. muridarum*. Heat-inactivated EB did not inhibit IFU production in the co-infection experiments (Fig. 4.5 A). In contrast, UV-inactivated EB (Fig. 4.5 A) and transcriptionally inactive EB (Fig. 4.5 B) dramatically reduced IFU production of *C. muridarum* and CM^{RifR}, respectively. This suggested that the chlamydial antigen(s) that stimulated the macrophage antimicrobial responses was present in EB and was not damaged by UV treatment. Failure of heat-inactivated EB to block chlamydial growth might be explained by reduced uptake of these EB by macrophages or destruction of the relevant antigens by heat (30).

Macrophages were also infected with wild-type EB in the presence of rifampin, or UV/heat-inactivated EB at an MOI of 10. Supernatants from these infections were collected 24 hpi and were transferred onto macrophages that had been infected at an MOI of 0.5 with CM^{RifR} or wild-type EB, respectively. None of the supernatants inhibited IFU production (Fig. 4.5 C, D). Collectively, the results of the co-infection and conditioned supernatant transfer experiments suggested that two anti-chlamydial pathways were activated by transcriptionally active chlamydiae: an endogenous pathway, and an exogenous pathway mediated by a trans-acting heat-labile factor.

4.4.5 *Cytokine secretion from RAW macrophages varies with C. muridarum EB dose and treatment*

To attempt to identify the trans-acting factor, we assayed cytokines in the conditioned supernatants of macrophages which had been infected at various MOI. Levels of most of most of the cytokines produced by moderately infected macrophages peaked by 3 hpi and were higher than those produced by the lowly infected macrophages (Fig. 4.6 A). High levels of TNF-α were detected at both MOI but this cytokine peaked earlier in supernatants from the macrophages infected at the higher MOI (Fig. 4.6 A). Cytokines in supernatants from macrophages which were infected with non-replicating chlamydia at MOIs of 10 (wild-type EB+rifampin or UV-inactivated) were also assayed. With the exception of TNF-α, cytokine levels were substantially lower than observed in experiments with viable *C. muridarum (*Fig. 4.6 B). Overall, the results of these experiments

suggested that most cytokine secretion required an antigen not present in EB and which was synthesized by *C. muridarum* in the host cell.

4.4.6 *Anti-chlamydial activity of RAW macrophages is mediated by TLR2 but not TLR4*

Chlamydial cell wall antigens and heat shock proteins induce Toll-like receptor 2 (TLR2), and to a lesser extent TLR4, signaling in phagocytes and epithelial cells (31, 32). To determine if TLR2 or TLR4 activation stimulated macrophage anti-chlamydial responses, we used mAbs to specifically block TLR2 (anti-TLR2) and TLR4 (anti-TLR4) responses. The neutralizing efficacy of anti-TLR2 was first determined by pre-treating macrophages with mAb followed by infection with *C. muridarum* at an MOI of 10. Anti-TLR2 treatment reduced IFN-β production of *C. muridarum*-infected RAW cells in a dose dependent manner (Fig. 4. 7 A). Anti-TLR4 increased rIFU production by 1000 fold in RAW macrophages that were infected with *C. muridarum* at an MOI of 0.5 and co-treated with *E. coli* LPS. These preliminary experiments established that both antibodies effectively blocked cognate TLR function. However, only anti-TLR2 partially restored *C. muridarum* IFU production in macrophages infected at an MOI of 10 (Fig. 4.7 C, D). This indicated that the anti-chlamydial response of macrophage infected at moderate MOIs is primarily mediated by TLR2.

4.4.7 Chlamydial inhibition at moderate MOIs is mediated by iNOS and ROS

Pro-inflammatory cytokines and bacterial products can upregulate expression of inducible nitric oxide synthase (iNOS), an enzyme which catalyzes nitric oxide (NO) formation (33-36). Activated leukocytes can also accumulate high levels of reactive oxygen species (ROS) via the phagocyte NADPH oxidase complex (phox) or damaged mitochondria.

To determine if iNOS was induced in RAW macrophages by *C. muridarum* infection we measured the quantity of nitrites in culture supernatants. Higher nitrite levels were observed in supernatants from macrophages infected at moderate MOI compared to macrophages infected at low MOI (Fig. 4.8 A). Levels of iNOS protein measured by Western blot correlated with these supernatant nitrite levels (Fig. 4.8 B). While iNOS was not detected in cells infected at low MOI, iNOS was detected by 6 hpi in macrophages infected at moderate MOI.

Macrophage ROS response was assessed by incubating infected cells with the fluorogenic dye 2', 7'-dichlorofluorescin diacetate (DCFDA). ROS production of mock-infected and low MOI infected macrophages was low and similar (Fig. 4.8 C). However, macrophages infected at moderate MOI produced strong fluorescence which was mostly reversed by the addition of the hydroxyl radical scavenger dimethylthiourea (DMTU).

To evaluate the chlamydicidal potential of macrophage-derived NO and ROS, infected macrophages were treated with the iNOS inhibitors L-NMMA and L-NAME or the hydroxyl radical scavenger DMTU. None of these compounds

affected chlamydiae recovery in low MOI infections (Fig. 4.8 D). However, both of the iNOS inhibitors and DMTU increased IFU production in the moderate MOI infected macrophages (39, 40). These results indicated that moderate MOI infections of RAW macrophages stimulated production of NO and reactive oxygen species that inhibited *C. muridarum*.

4.4.8 Ca-074Me, a cathepsin B inhibitor, rescues C. muridarum from anti-chlamydial macrophage responses

Macrophage IL-1β can stimulate caspase-1 dependent iNOS expression (35, 41) (42). We evaluated the roles of IL-1β and caspase-1 in chlamydial inhibition in macrophages using various inhibitors. Pre-treatment of the macrophages with IL-1Ra, an IL-1β antagonist, did not influence chlamydial recovery (Fig. 4.9 A). The caspase-1 inhibitor Ac-YVAD-CHO also failed to alter IFU production. However, the less specific caspase-1 inhibitor Z-WEHD-FMK increased IFU recovery in moderately infected macrophages approximately 10-fold. Z-WEHD-FMK can also inhibit lysosomal cathepsins (43), so we treated macrophages infected with the selective cathepsin B inhibitor Ca-074Me. Ca-074Me increased IFU production by 1000 fold in moderately infected macrophages (Fig. 4.9 B). Cathepsin B activity was also monitored in the infected cells using the fluorogenic substrate CV-(RR) 2. Analysis at 10 hpi indicated no difference in fluorescence intensity between mock-infected and low MOI infected cells (Fig. 4.9 C, D; Fig. 4.10). In contrast, cathepsin B activity was significantly increased in the moderate MOI-infected macrophages and this was

reversed by the addition of Ca-074Me (Fig. 4.9 E, F; Fig. 4.10). Together, these results indicated that cathepsin B activity influences chlamydial IFU production in RAW macrophages.

4.4.9 ROS and cathepsin B activity are necessary for maximal iNOS induction in C. muridarum-infected RAW macrophages

Pharmacological inhibition of ROS, iNOS and cathepsin B led to equal but non-additive chlamydial recoveries, suggesting that they functioned in the same inhibitory pathway or that they played cooperative roles in chlamydial killing (Fig. 4.11 A). To distinguish between these possibilities, we first analyzed iNOS protein and nitrite levels in moderately infected macrophages treated with L-NAME, DMTU or Ca-074Me. L-NAME interferes with iNOS activity, but not expression. Western blots showed equal quantities of iNOS protein in samples that were and were not treated with L-NAME, but that nitrite levels were reduced in the L-NAME treated cells (Fig. 4.11 B; Fig. 4.12). However, iNOS and nitrite levels were also substantially lower in cells treated with DMTU or Ca-074Me. This indicated that ROS and cathepsin B controlled iNOS expression.

We next investigated if ROS modulated cathepsin B activity or vice versa. Addition of DMTU to macrophages infected at an MOI of 10 decreased cathepsin B activity to levels lower than that of mock-infected cells (Fig. 4.11 C-E; Fig.4.13). Inhibition of cathepsin B with Ca-074Me in similarly infected macrophages also caused a small decrease in ROS levels (Fig. 4.14). The DCFDA probe can also detect peroxynitrite. Since nitric oxide production was inhibited in cells treated

with Ca-074Me, the slight reduction in DCFDA fluorescence could be due to an absence of nitrite intermediates. Indeed, the quantity of ROS did not differ in Ca-074Me and L-NMMA treated macrophages (Fig. 4.14). In summary, these results suggested that ROS production increased cathepsin B activity, which upregulated iNOS expression.

4.5 Discussion

Members of the family *Chlamydiaceae* differ in their capacity to survive within macrophages and this is largely dictated by the pathogen's ability to avoid phagolysosomal fusion inside these cells (10). The capacity to survive and replicate in macrophages has been linked to chlamydial dissemination leading to systemic disease, as well as persistence which can cause chronic inflammation and a delayed response to antibiotic treatment (11, 12). Thus, understanding the mechanisms that promote chlamydial survival in mononuclear phagocytes could have implications for the development of therapeutic strategies.

Chlamydial species that can evade phagosome-lysosome fusion within macrophages appear to do so only when host cells are infected at an optimal MOI. Several groups have reported reduced chlamydial recoveries from macrophages infected at MOIs of 100 or greater (10, 22). This correlated with immediate damage to the host cells and fusion of lysosomes with EB-containing phagosomes. In this study, we characterized the interactions of RAW 264.7 macrophages with *C. muridarum* and demonstrated that three different outcomes could be achieved in response to different MOIs. At an MOI of 1 or lower, RAW

cells supported chlamydial replication. An MOI of 100 conferred immediate cytotoxicity to the macrophages and few infectious chlamydial particles were recovered. Inhibition of host protein synthesis did not prevent chlamydial or host cell death. These results were consistent with findings from previous studies. However, when RAW macrophages were infected at an intermediate MOI of 10, they did not succumb to early death and cleared *C. muridarum* infection by a process that could be reversed by cycloheximide.

Consistent with previous studies, we found that macrophage activation and subsequent clearance of *C. muridarum* was predominantly mediated by TLR2 (44, 45). The cognate chlamydial ligands for TLR2 have not been identified, but several candidates have been proposed in recent years. Recombinant chlamydial MIP-like protein can induce cytokine production via TLR2/TLR1/TLR6 and CD14 in human macrophages (46). Chlamydial LPS is less active than classic endotoxins but can elicit TLR2 signaling *in vitro* (47). Chlamydial Hsp60 induces inflammatory responses in mice in a TLR2- and TLR4-dependent fashion (31). Plasmid-deficient strains of *C. trachomatis* and *C. muridarum* exhibit impaired TLR2 responses, implying that one or more TLR2 antigens are either encoded or regulated by the plasmid (48, 49). Signaling via TLR2 in epithelial cells also requires infection with live, transcriptionally active chlamydiae, indicating that the antigen is not present in EB (29). Our experiments with inactive EB demonstrated that more than one chlamydial antigen was necessary to elicit chlamydicidal responses of RAW macrophages. An EB antigen required for endogenous inhibition of chlamydiae was unaffected by UV

treatment. Interestingly, the inhibitory potential of conditioned supernatants from macrophage cultures depended on an antigen present in transcriptionally active chlamydiae but not in heat- or UV-inactivated EB.

Binding of microbial PAMPs to TLRs or other cytosolic PRRs triggers a series of cellular signals that culminate in the activation of NFκB, mitogen-activated protein kinase (MAPK) or IRF3 pathways (50, 51). These in turn regulate the expression of genes that encode pro-inflammatory cytokines and iNOS. Aside from the direct induction of iNOS by PRR signaling, several cytokines can also regulate iNOS expression. Protective effects of nitric oxide in chlamydial infections have been well documented. Nitric oxide promotes IFN-γ-mediated eradication of chlamydiae and protects mice from the development of hydrosalphinx and infertility (52). Interestingly, TLR2/4 double-deficient mice do not resolve *C. pneumoniae* lung infections because of their inability to induce iNOS in spite of elevated IFN-γ secretion in these animals (53). This suggests that nitric oxide production relies on signaling via TLR2/4 in the murine lung model of infection. We observed that moderately infected RAW macrophages produced more iNOS and nitrite compared to cells infected an MOI of 0.5 and that this negatively impacted chlamydial survival. Our results are reminiscent of a study by Huang et al. in which the outcome of low and high doses of intranasally inoculated chlamydiae in C57BL/6 mice was evaluated (54). Animals infected with higher numbers of *C. psittaci* remained healthy as opposed to those that were infected at low doses, and the accelerated bacterial clearance in heavily infected mice was linked to an increased NO production by macrophages.

Comparable observations have been reported with *C. muridarum* infections of the murine genital tract, where high infectious doses result in less disease severity and fewer viable organisms in the oviducts (55). We speculate that similar macrophage activation programs control NO production in response to higher doses of infectious chlamydiae in both mice and in cell culture.

We determined that iNOS induction in RAW macrophages was mediated by an increase in the production of ROS. Modulation of iNOS expression by ROS is not without precedent. High MOI infection of macrophages with *Propionibacterium acnes* increases ROS levels which in turn upregulate iNOS via NFκB/AP-1 activation (56). Similar dependence on ROS for nitric oxide production has also been observed in mouse endothelial cells stimulated with IFN-γ and LPS (57). Multiple sources of ROS exist within mammalian cells including the NADPH oxidase complex and mitochondria. If ROS generated by RAW macrophages in our study was mitochondria- or NADPH oxidase-derived was not determined. Several groups have reported a loss of mitochondrial membrane potential and integrity in cells invaded by pathogens (58). The subsequent mitochondrial ROS release can cause lysosomal membrane permeabilization (LMP) leading to the leakage of active lysosomal cathepsins into the cytosol. In agreement with these studies, we noted increased cathepsin B activity in moderately infected RAW cells that was abolished by an ROS scavenger. However, a significant proportion of this cathepsin B activity at 10 hpi appeared to localize to large vesicular structures. Labeling with specific markers will be required to determine if these vesicles are lysosomes or also include EB-

containing phagosomes that fused with lysosomes. Whether lysosomal cathepsin B leaks into the cytosol at later times due to ROS-mediated LMP requires further investigation. What is certain is that ROS affects cathepsin B activity in RAW macrophages. Surprisingly, the inhibition of cathepsin B led to a substantial decrease in iNOS and nitrite levels while also enabling chlamydial rescue. Pharmacological inhibition of iNOS did not greatly affect ROS levels or cathepsin B (Fig. 4. 10 and unpublished observations), indicating that chlamydial survival in RAW cells was dictated by the presence or absence of NO. We cannot rule out a direct role for ROS and cathepsin B in chlamydial inhibition because chlamydiae damaged by reactive nitrogen species might show increased susceptibility to lysosomal fusion and processing by cathepsin B.

In summary, we report that iNOS-derived nitric oxide leads to the inhibition of *C. muridarum* in RAW macrophages in an MOI-dependent manner. Elevated levels of reactive oxygen species and cathepsin B activity in moderately infected cells modulate iNOS expression to facilitate *C. muridarum* clearance. Future experiments will involve confirming these observations in primary macrophages isolated from wild-type and cathepsin B-knockout mice.
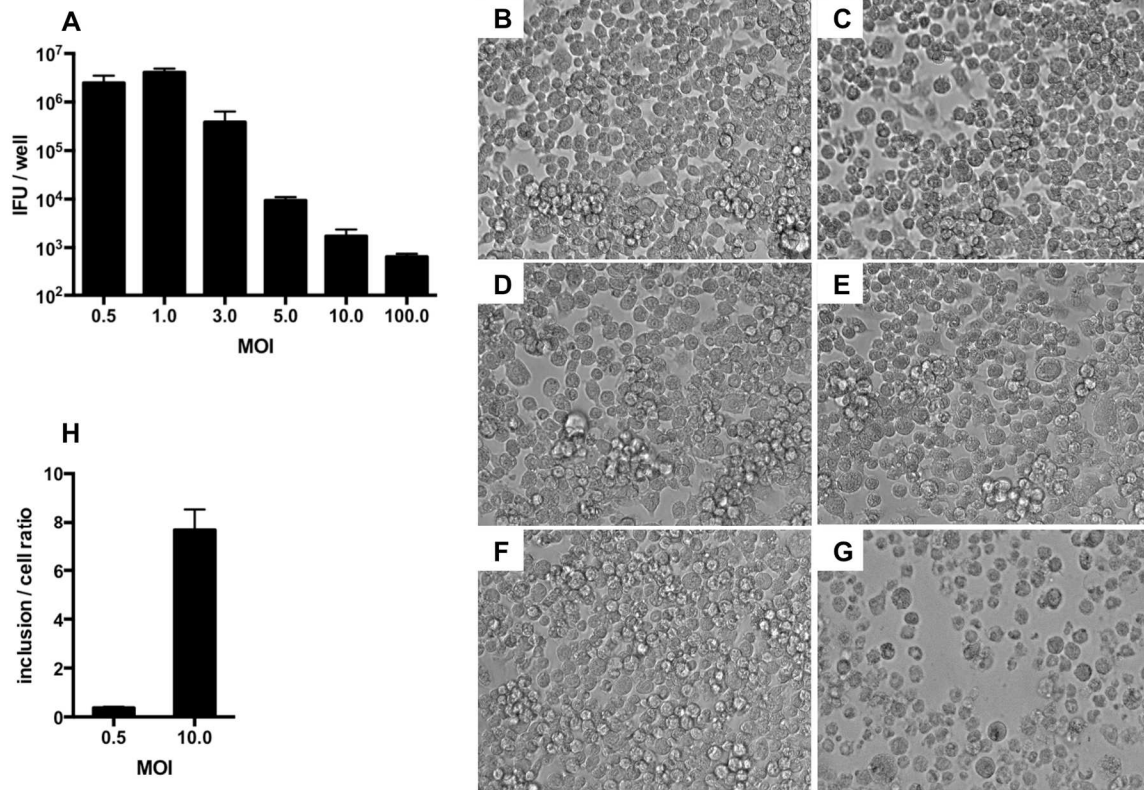
Fig. 4.1. ***C. muridarum* is inhibited in RAW macrophages infected at high MOI.** Macrophages were infected with *C. muridarum* at MOIs from 0.5 to 100. (A) Recoverable IFU (rIFU) assays performed at 24 hpi showed that EB recovery was decreased from macrophages infected at MOI 3 and higher. (B-G) Light microscopy at 18 hpi revealed that the infected macrophages exhibited normal cell morphology at all MOIs with the exception of MOI 100. (B) Mock-infected (C) MOI 0.5 (D) MOI 3 (E) MOI 5 (F) MOI 10 (G) MOI 100. (H) Immunofluorescence microscopy of infected RAW cells at 2hpi showed that chlamydial EB invasion of macrophages was not hindered at an MOI of 10.
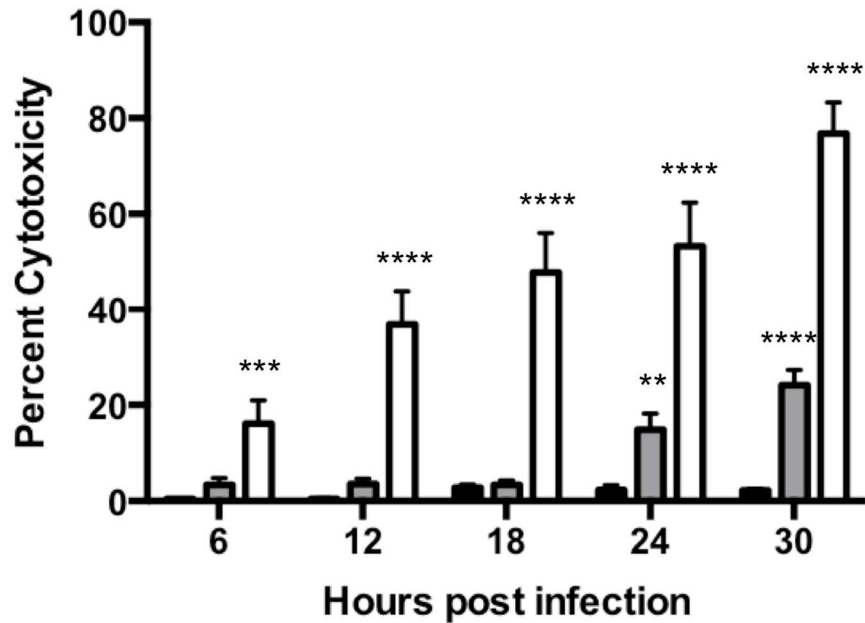
Fig. 4.2. High MOI induces macrophage cytotoxicity. Macrophages were infected at an MOI of 0.5, 10 or 100. An LDH assay for cytotoxicity demonstrated that macrophages infected at an MOI of 10 (gray bars) released low amounts of LDH comparable to macrophages infected at an MOI of 0.5 up to 18 hpi. At 24 and 30 hpi, LDH release increased significantly in supernatants of macrophages infected at an MOI of 10, indicating delayed cell death. RAW macrophages infected at an MOI of 100 exhibited cytotoxicity as early as 6 hpi. Error bars represent mean ± standard deviations (SD). (****, $P < 0.0001$; ***, $P < 0.001$; **, $P < 0.01$). P values were determined by two-way ANOVA with Bonferroni post hoc test.
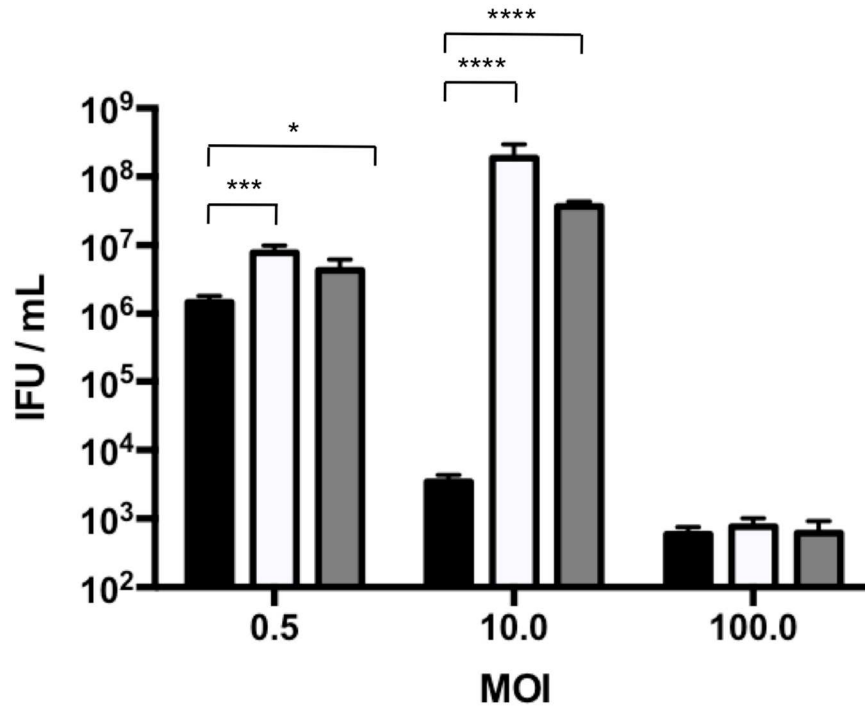
Fig. 4.3. Inhibition of host protein synthesis rescues chlamydial growth in moderately infected macrophages. RAW macrophages were treated with 0.5 µg/mL cycloheximide four hours prior to or at the time of infection. rIFU assays were performed at 24 hpi. Cycloheximide addition improved infectious EB recovery from macrophages infected at an MOI of 0.5 and completely reversed chlamydial inhibition in cells infected at an MOI of 10 but had no effect on chlamydial recovery from cells infected at an MOI of 100 (black bars, untreated; white bars, cycloheximide addition at -4 hpi; gray bars, cycloheximide addition at 0 hpi). Error bars represent mean ± SD. ****, (P < 0.0001; ***, P < 0.001; **, P < 0.01). P values were determined by two-way ANOVA with Bonferroni post hoc test.
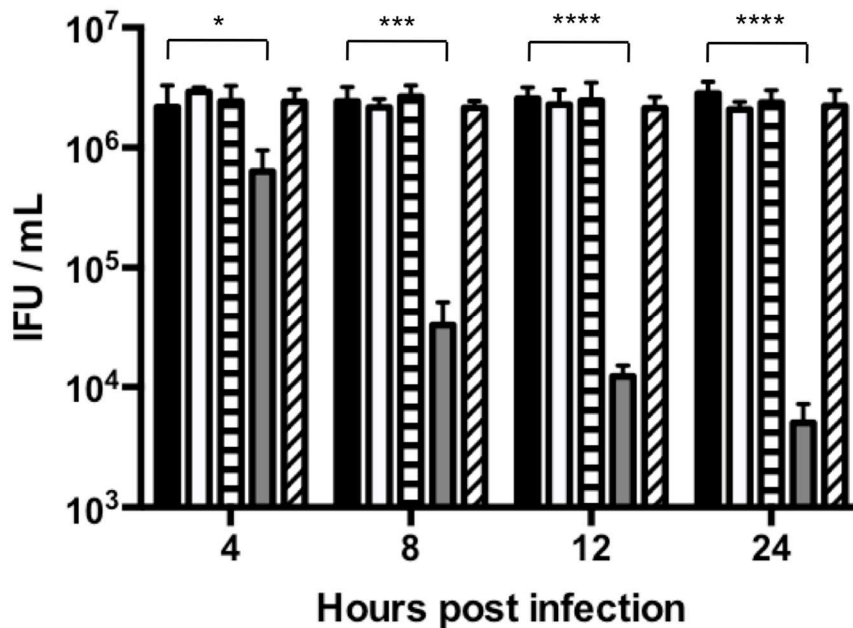
Fig. 4.4. Supernatants from moderately infected macrophages contain anti-chlamydial factors. RAW macrophages were infected with *C. muridarum* at an MOI of 0.5 or 10. Culture media was removed at 4, 8, 12 or 24 hpi and centrifuged briefly to remove debris. A new 24-well plate of macrophages was infected at an MOI of 0.5. At 1.5 hpi, the conditioned supernatants were transferred onto the newly infected cells. Some supernatants were heated at 95°C for 5 minutes prior to transfer. rIFU assays performed on the supernatant-treated macrophages at 24 hpi revealed that media from cells infected at an MOI of 0.5 (white bars, unheated; striped bars, heated) had no effect on rIFU when compared to mock-treated cells (black bars). In contrast, media from MOI 10-infected cells inhibited chlamydial recovery (gray bars). The inhibitory effect of supernatants from heavily infected macrophages increased with time and was abolished upon heat treatment (hatched bars). Error bars represent mean $\pm$ SD. (****, $P < 0.0001$; ***, $P < 0.001$; *, $P < 0.05$). P values were determined by two-way ANOVA with Bonferroni post hoc test.
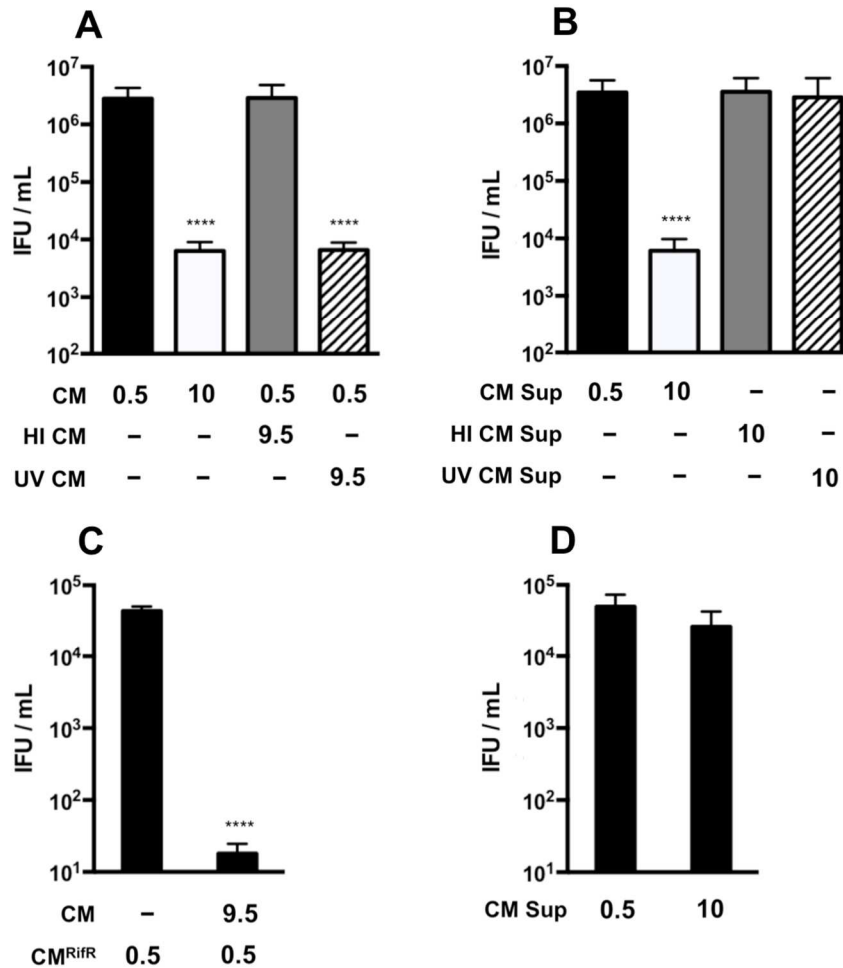
Fig. 4.5. RAW macrophage inhibitory response is mediated by at least two chlamydial antigens. rIFU was performed at 24 hpi from macrophages infected with live or inactive EB. (A) RAW macrophages were infected with *C. muridarum* (CM) at an MOI of 0.5 (black bars) or 10 (white bars). Some wells infected at an MOI of 0.5 were also incubated with heat-inactivated (HI) EB (hatched bars) or UV-inactivated EB (gray bars) at an MOI of 9.5. (B) Supernatants were collected at 24 hpi from RAW cells infected at an MOI of 0.5 (black bars) or 10 with live (white bars), HI (gray bars) or HI (hatched bars) EB. After a brief spin, supernatants were transferred to macrophages freshly infected with CM at an MOI of 0.5. (C) RAW cells were treated with 0.1 μg/mL rifampin and infected with *C. muridarum*[RifR] (CM[RifR]) at an MOI of 0.5 with or without CM at an MOI of 9.5. (D) Supernatants were collected from rifampin-treated cells that had been infected with CM at an MOI of 0.5 or 10 at 24 hpi. These were then transferred to macrophages freshly infected with CM[RifR] at an MOI of 0.5. Error bars represent mean ± SD. (****, P < 0.0001). P values were determined by one-way ANOVA with Dunnett's post hoc test.
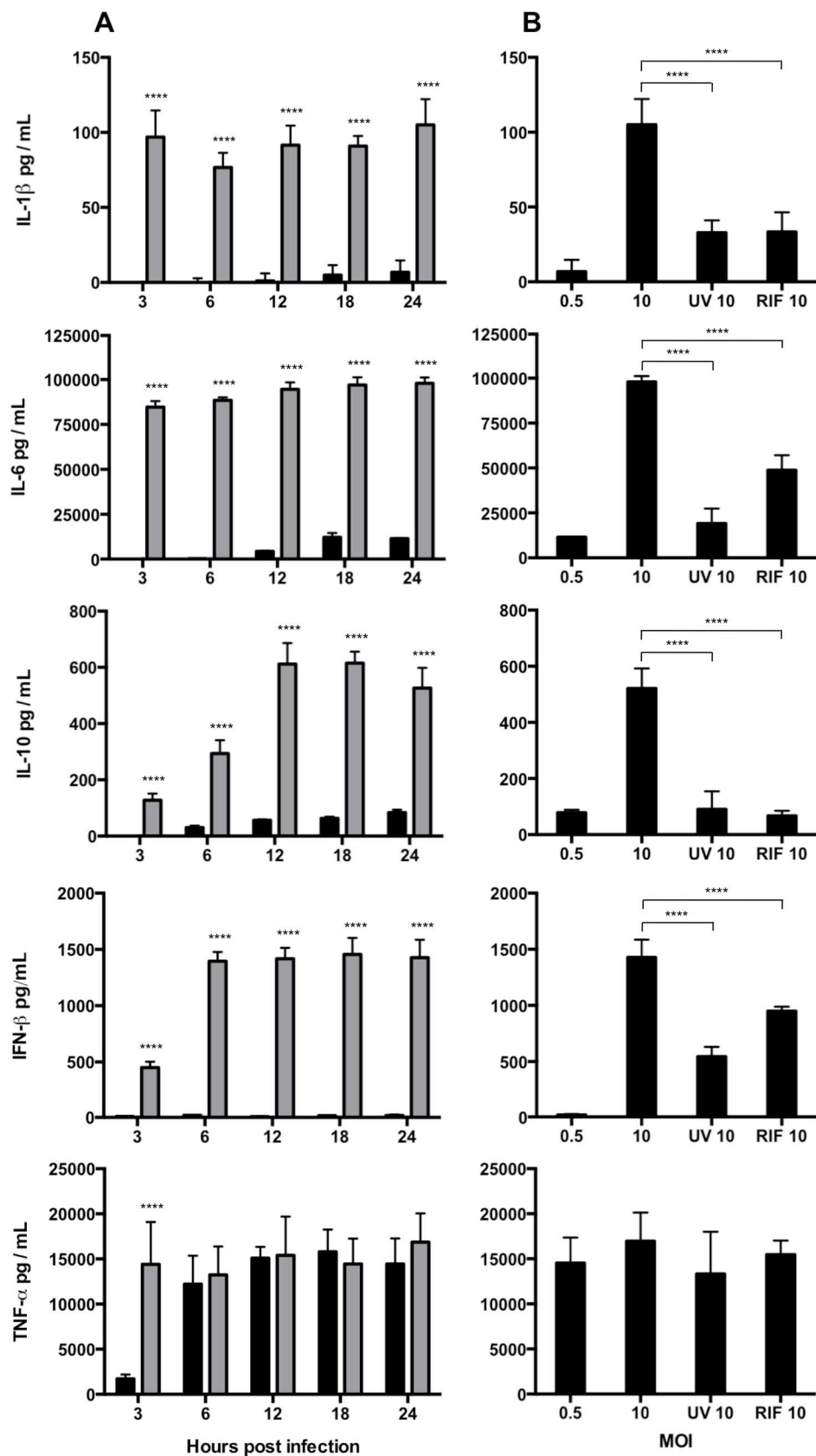
Fig. 4.6. Cytokine profiles from infected macrophages. (A) RAW macrophages were infected at an MOI of 0.5 (black bars) or 10 (gray bars). Supernatants were collected at 3, 6, 12, 18 and 24 hpi and assayed for cytokines. Levels of IL-1β, IL-6, L-10 and IFN-β were significantly higher in supernatants from MOI 10-infected cells at all time points. TNF-α amounts were low at 3 hpi in supernatants from MOI 0.5-infected macrophages but reached maximal levels between 6-12 hpi. (B) Supernatants were collected at 24 hpi from RAW cells infected at an MOI of 0.5 or 10 with live EB in the absence or presence of rifampin (RIF 10) or UV EB (UV 10). Cytokine analysis indicated that levels of IL-1β, IL-6, IL-10 and IFN-β were significantly lower in supernatants from UV 10- and RIF 10-infected cells vs cells infected with live EB at an MOI of 10. TNF-α levels were similar in all analyzed supernatants. Error bars represent mean $\pm$ SD. (****, $P < 0.0001$). P values were determined by one-way ANOVA with Dunnett's post hoc test.
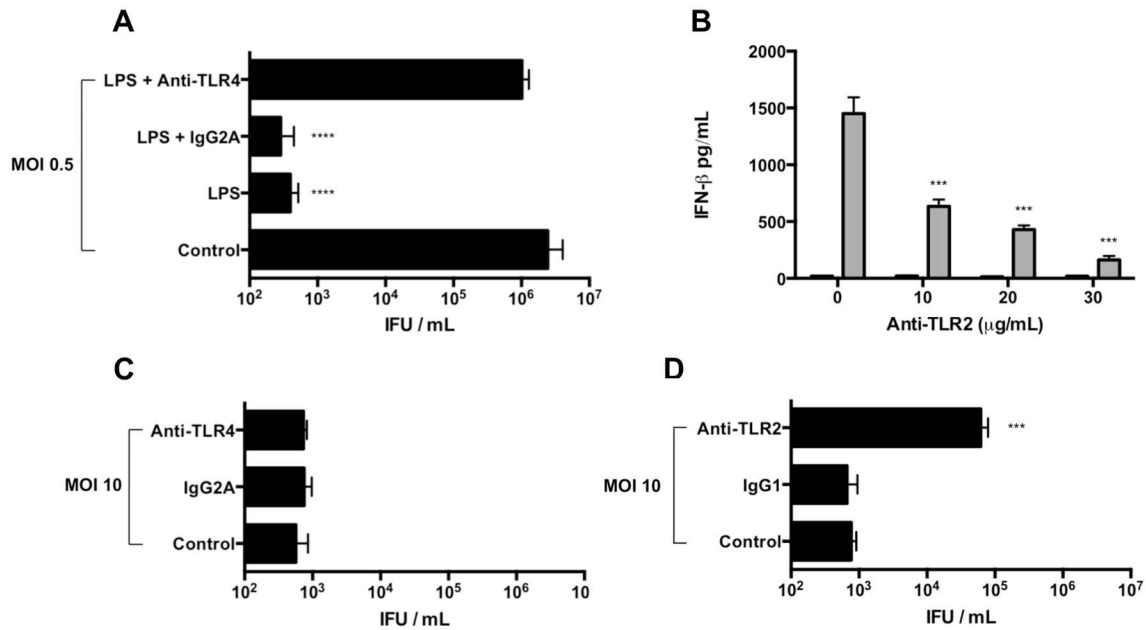
Fig. 4.7. TLR2, but not TLR4, mediates macrophage inhibition of *C. muridarum* at intermediate MOI. (A) Macrophages that were untreated or pre-treated with anti-TLR2 or isotype control Ab (IgG1) were infected at an MOI of 0.5 (black bars) or 10 (gray bars). ELISA measurement of IFN-β in supernatants collected from cells at 24 hpi showed significantly lower cytokine levels from moderately infected macrophages in the presence of anti-TLR2. (B) Macrophages infected with *C. muridarum* at an MOI of 0.5 produced significantly fewer rIFU when co-treated with *E. coli* LPS. Anti-TLR4, but not an isotype control Ab (IgG2A), completely reversed LPS-mediated inhibition. (C) Anti-TLR2 treatment (30 μg/mL) significantly increased rIFU yield from MOI 10-infected macrophages. (D) Anti-TLR4 did not prevent chlamydial inhibition in macrophages infected at an MOI of 10. Error bars represent mean ± SD. (****, P < 0.0001). P values were determined by one-way ANOVA with Dunnett's post hoc test for (A), (C) and (D), and by two-way ANOVA with Bonferroni post hoc test for (B).
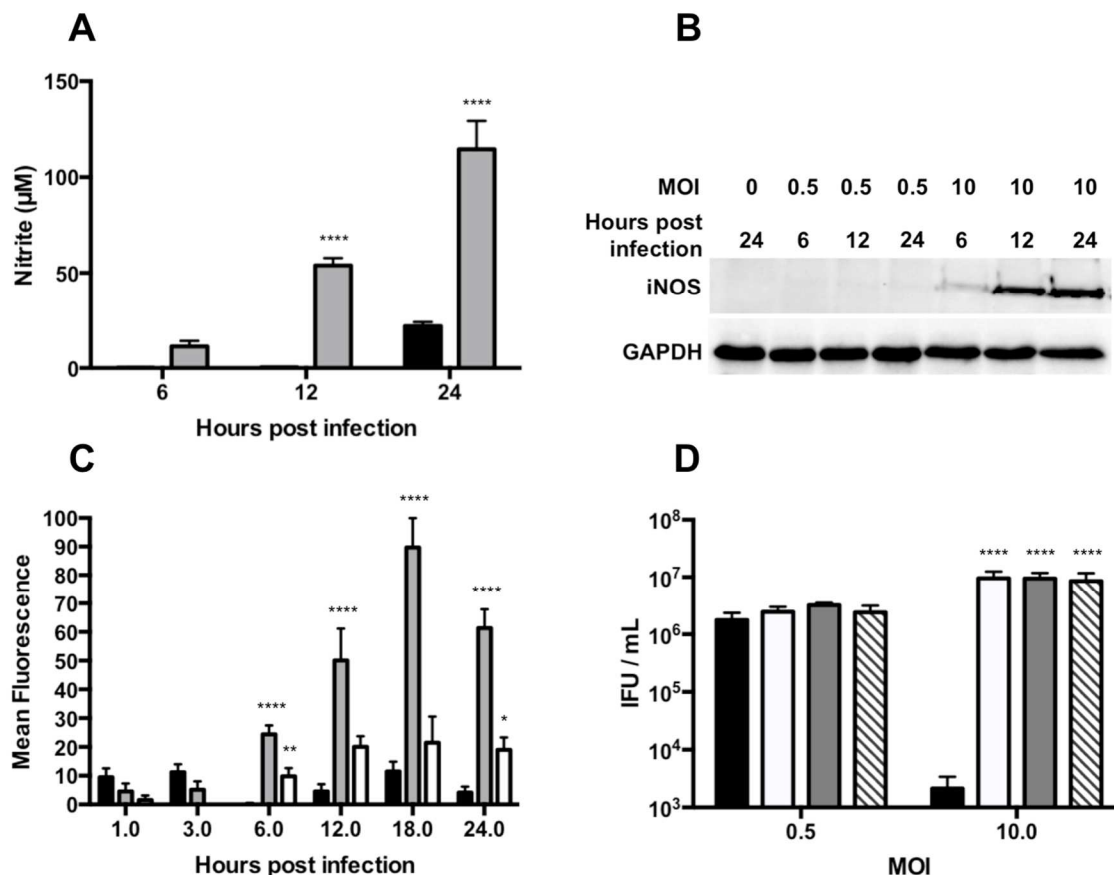
Fig. 4.8. Moderately infected RAW macrophages inhibit *C. muridarum* by producing nitric oxide and reactive oxygen species. (A) Supernatants were collected at 6, 12 or 24 hpi from RAW cells infected at an MOI of 0.5 (black bars) or 10 (gray bars). Nitrite levels were quantified by Griess assay. (B) Western blot for iNOS indicated that protein was absent from mock- or MOI 0.5-infected cells, but expressed at all analyzed time points in MOI 10-infected cells. (C) RAW cells infected at an MOI of 0.5 (black bars), 10 (gray bars) or 10 with DMTU (white bars) were assayed for ROS production at 1, 3, 6, 12, 18 and 24 hpi. ROS started to accumulate in cells infected at an MOI of 10 at 6 hpi. ROS levels decreased in the presence of the hydroxyl radical scavenger DMTU. (D) RAW cells infected at an MOI of 0.5 or 10 were left untreated (black bars) or treated with L-NMMA (white bars), L-NAME (gray bars) or DMTU (hatched bars). rIFU assay at 24 hpi revealed that inhibitors rescued chlamydial inhibition in moderately infected cells. Error bars represent mean ± SD. (****, $P < 0.0001$; **, $P < 0.01$; *, $P < 0.05$). P values were determined by two-way ANOVA with Bonferroni post hoc test.
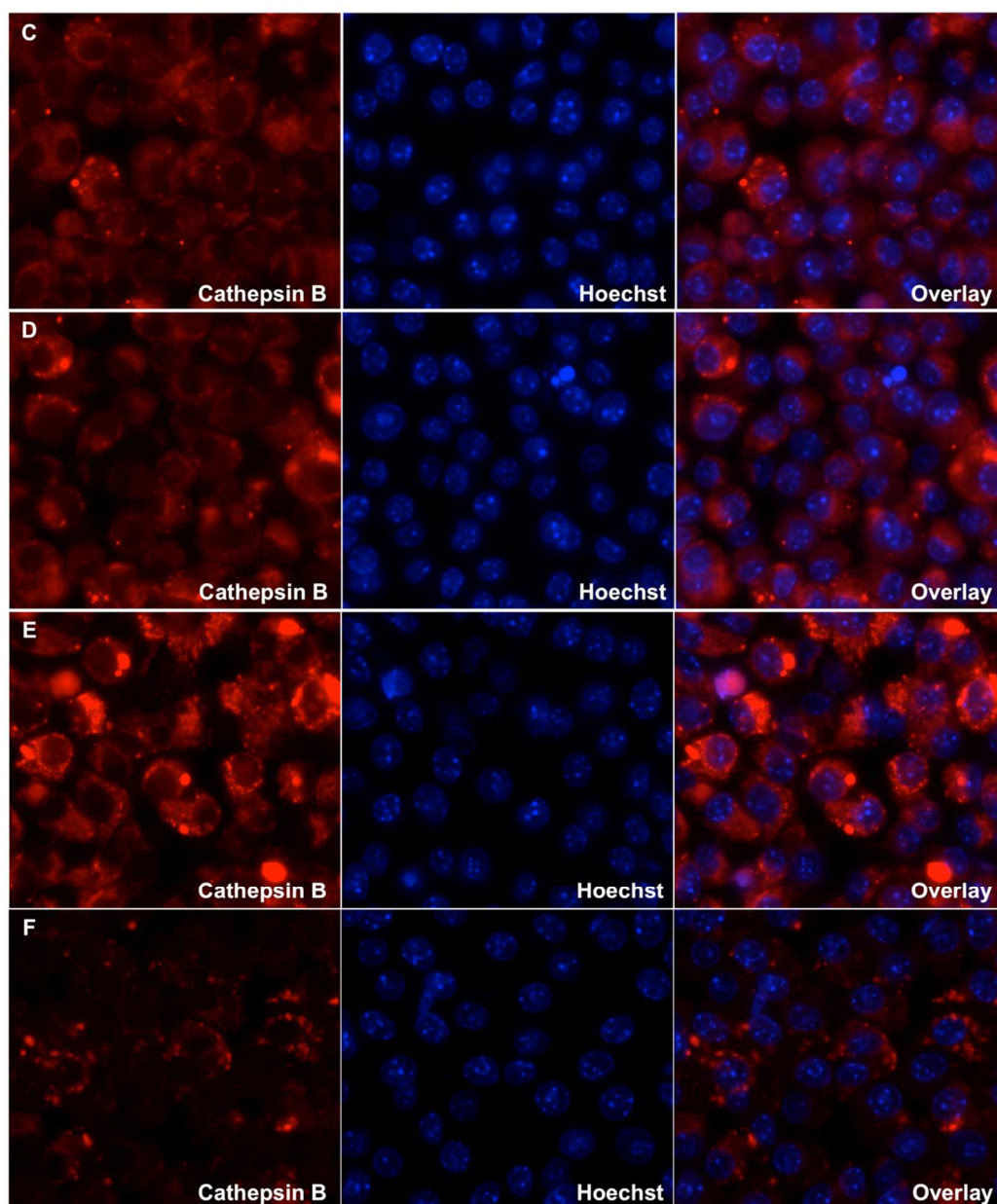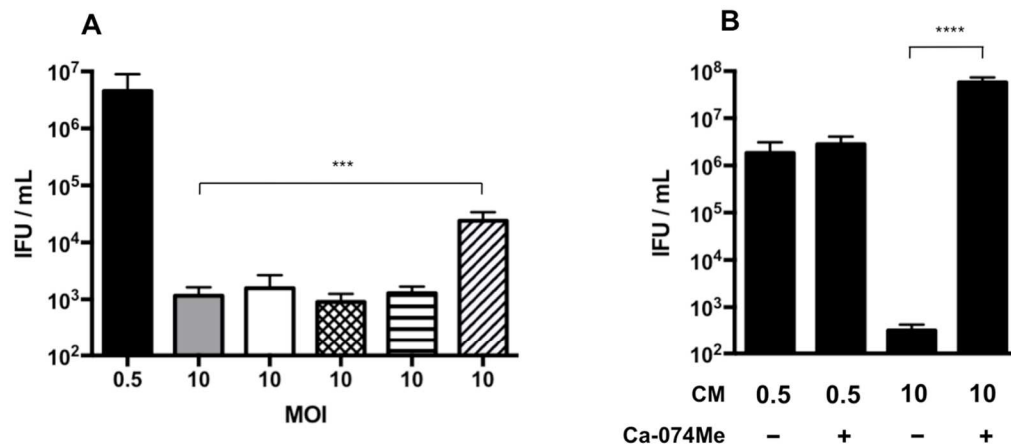
Fig. 4.9. Ca-074Me, a cathepsin B inhibitor, rescues *C. muridarum* from macrophage inhibition. (A) RAW macrophages were infected at an MOI of 0.5 (black bar) or 10 (gray bar). Some MOI 10-infected cells were treated with IL-1Ra at 50 µg/mL (white bar) or 100 µg/mL (cross-hatched bar), Ac-YVAD-CHO (striped bar) or Z-WEHD-FMK (hatched bar). Z-WEHD-FMK addition led to a partial increase in chlamydial output. Error bars represent mean ± SD. (****, P < 0.0001; ***, P < 0.001). P values were determined by one-way ANOVA with Dunnett's post hoc test. (B) Treatment of MOI 10-infected macrophages with CA-074Me blocked macrophage inhibition. Panels C-F represent live microscopy images of cells at 10 hpi treated with the cathepsin B indicator dye MR-(RR)2 (red channel) and nuclear stain Hoechst 33342 (blue channel). (C) Mock-infected (D) MOI 0.5 (E) MOI 10 (F) MOI 10 with Ca-074Me.
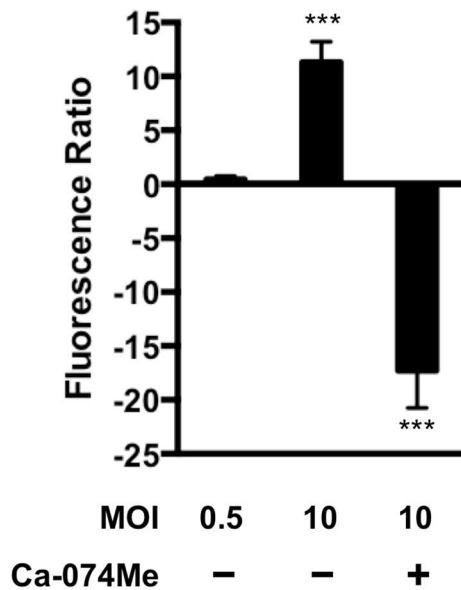
Fig. 4.10. Cathepsin B activity increases in moderately infected RAW macrophages. Mean red fluorescence intensity of activated cathepsin B in cells infected at an MOI of 0.5 or 10 was calculated from ten microscopy images obtained from three independent experiments. Intensity was normalized to mock-infected control. Cathepsin B activity significantly increased in cells infected at an MOI of 10 and was dramatically reduced in cells treated with Ca-074Me. Error bars represent mean ± SD. (***, P < 0.001). P values were determined by one-way ANOVA with Dunnett's post hoc test.

A

B

	1	2	3	4	5	6
iNOS						
GAPDH						

L-NAME	−	+	−	−	+	−	+	+
DMTU	−	−	+	−	+	+	−	+
Ca-074Me	−	−	−	+	−	+	+	+

C — Cathepsin B / Hoechst / Overlay

D — Cathepsin B / Hoechst / Overlay

E — Cathepsin B / Hoechst / Overlay

203

Fig. 4.11. iNOS expression in moderately infected macrophages is regulated by ROS and cathepsin B. (A) RAW macrophages were infected at an MOI of 10 and treated with one of more of the following chemicals: L-NAME, DMTU and Ca-074Me. All drugs and combinations rescued chlamydiae from macrophage inhibition to the same extent. Error bars represent mean ± SD. (****, $P < 0.0001$). P values were determined by one-way ANOVA with Dunnett's post hoc test. (B) Western blot for iNOS at 24 hpi from cells. (1) mock-infected (2) MOI 0.5 (3) MOI 10 (4) MOI 10 with L-NAME (5) MOI 10 with DMTU (6) MOI 10 with Ca-074Me. Panels C-E represent live microscopy images of cells at 10 hpi treated with the cathepsin B indicator dye MR-(RR)2 (red channel) and nuclear stain Hoechst 33342 (blue channel). (C) Mock-infected (D) MOI 10 (E) MOI 10 with DMTU.
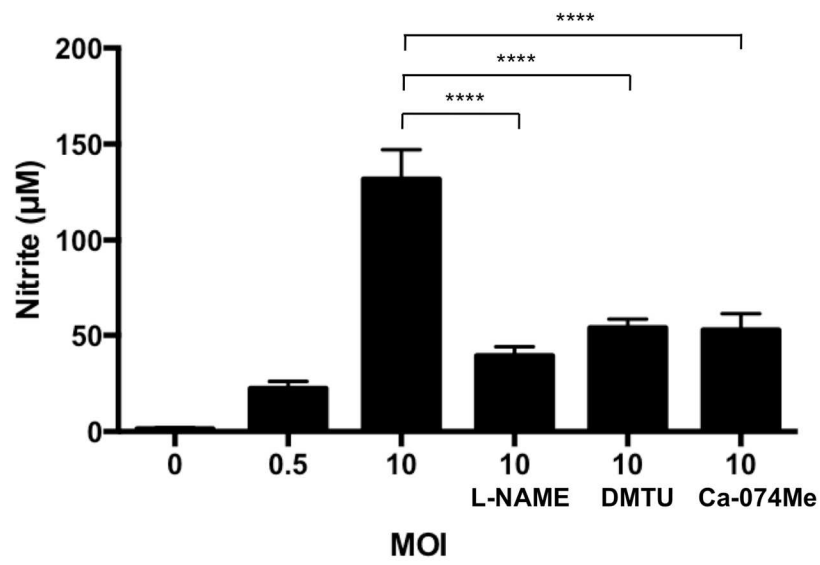
**Fig. 4.12. Nitrite levels in supernatants of moderately infected macrophages are reduced by DMTU and Ca-074Me.** RAW macrophages were infected at an MOI of 0.5 or 10. Some wells infected at an MOI of 10 were pre-treated with L-NAME, DMTU or Ca-074Me. Supernatant nitrite levels were measured at 24 hpi. All three compounds significantly decreased the amount of nitrites produced by moderately infected macrophages. Error bars represent mean $\pm$ SD. (****, $P < 0.0001$). P values were determined by one-way ANOVA with Dunnett's post hoc test.
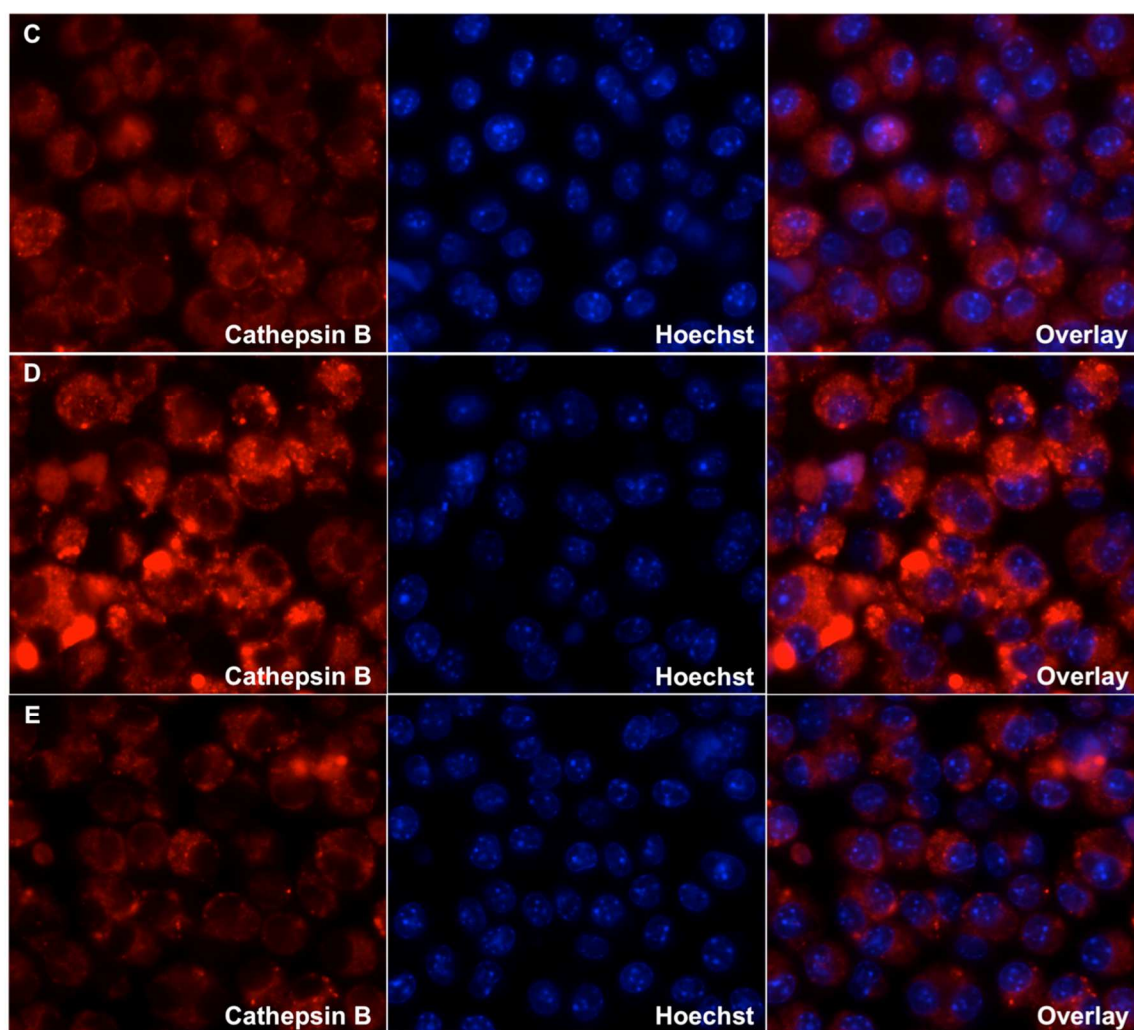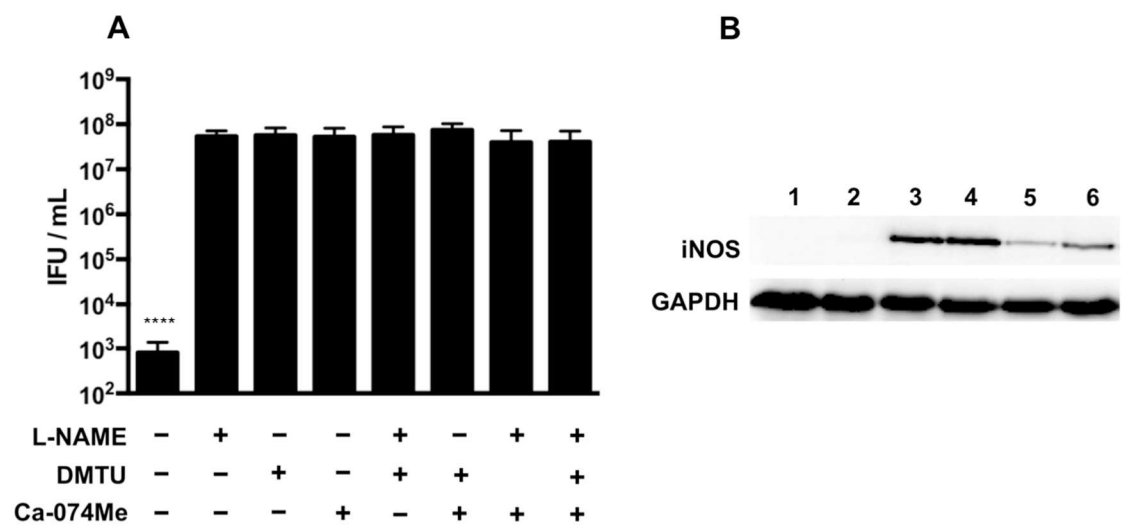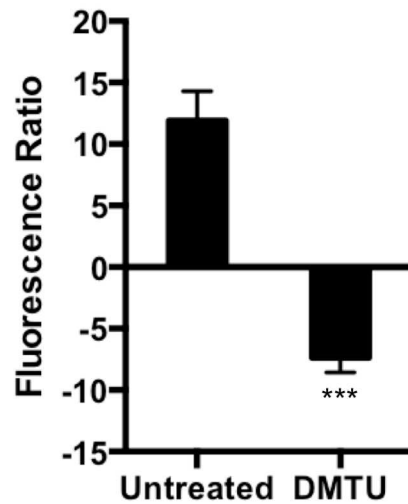
Fig. 4.13. Cathepsin B activity is regulated by reactive oxygen species.
Mean red fluorescence intensity of activated cathepsin B in cells infected at an MOI of 10 was calculated from ten microscopy images obtained from three independent experiments. Intensity was normalized to mock-infected control. The high level of cathepsin B activity in macrophages infected at an MOI of 10 was significantly reduced in DMTU-treated cells. Error bars represent mean $\pm$ SD. (***, $P < 0.001$). P values were determined by unpaired t-test.
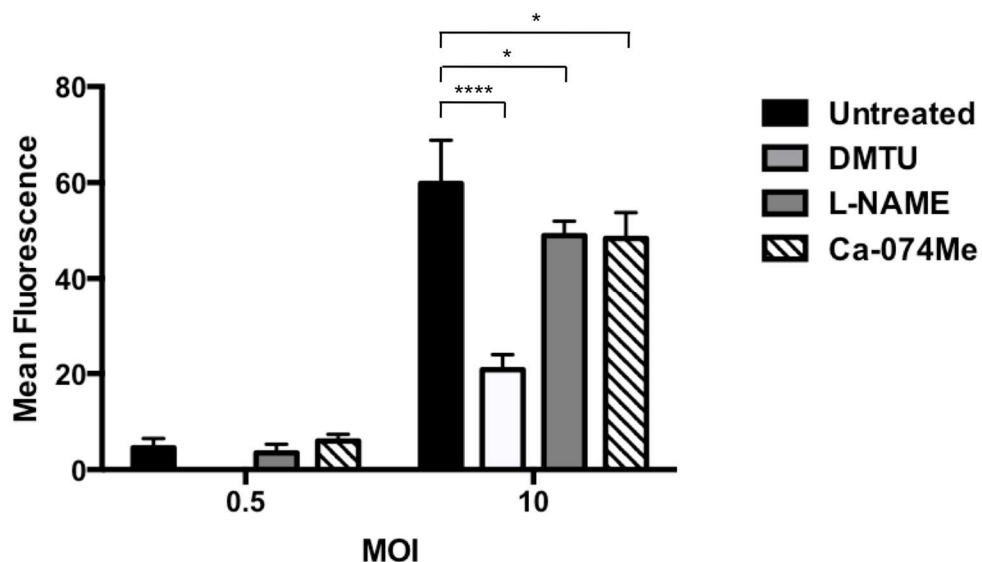
Fig. 4.14. Evaluation of DCFDA fluorescence in moderately infected macrophages. Untreated RAW cells or cells treated with DMTU, L-NAME or Ca074-Me were infected at an MOI of 0.5 or 10. Macrophages were incubated with DCFDA to measure ROS levels at 24 hpi. Low fluorescence intensity was recorded from cells infected at an MOI of 0.5 and was not significantly affected in the presence of inhibitors. Macrophages infected at an MOI of 10 displayed strong DCFDA fluorescence that was dramatically reduced by the addition of DMTU and moderately affected by L-NAME and Ca-074Me. Error bars represent mean $\pm$ SD. (****, $P < 0.0001$; *, $P < 0.05$). P values were determined by two-way ANOVA with Bonferroni post hoc test.

4.6 References

1. **Rusconi B, Greub G.** 2011. Chlamydiales and the innate immune response: friend or foe? FEMS Immunol. Med. Microbiol. **61:**231-244.

2. **Darville T, Hiltke TJ.** 2010. Pathogenesis of genital tract disease due to *Chlamydia trachomatis*. J. Infect. Dis. **202:**S114-S125.

3. **Miyairi I, Laxton JD, Wang X, Obert CA, Tatireddigari VRRA, van Rooijen N, Hatch TP, Byrne GI.** 2011. Chlamydia psittaci genetic variants differ in virulence by modulation of host immunity. J. Infect. Dis. **204:**654-663.

4. **Qiu H, Fan Y, Joyee AG, Wang S, Han X, Bai H, Jiao L, Van Rooijen N, Yang X.** 2008. Type I IFNs enhance susceptibility to *Chlamydia muridarum* lung infection by enhancing apoptosis of local macrophages. J. Immunol. **181:**2092-2102.

5. **Rothfuchs AG, Kreuger MR, Wigzell H, Rottenberg ME.** 2004. Macrophages, CD4(+) or CD8(+) cells are each sufficient for protection against *Chlamydia pneumoniae* infection through their ability to secrete IFN-gamma. J. Immunol. **172:**2407-2415.

6. **Kuo CC.** 1978. Cultures of *Chlamydia trachomatis* in mouse peritoneal macrophages: factors affecting organism growth. Infect. Immun. **20:**439-445.

7. **Yong EC, Chi EY, Kuo CC.** 1987. Differential antimicrobial activity of human mononuclear phagocytes against the human biovars of *Chlamydia trachomatis*. J. Immunol. **139:**1297-1302.

8. **Manor E, Schmitz E, Sarov I.** 1993. TNF and PGE(2) in human monocyte-derived macrophages infected with *C. tracohmatis*. Mediators Inflamm. **2:**367-371.

9. **Gold ES, Simmons RM, Petersen TW, Campbell LA, Kuo CC, Aderem A.** 2004. Amphiphysin IIm is required for survival of *Chlamydia pneumoniae* in macrophages. J. Exp. Med. **200:**581-586.

10. **Wyrick PB, Brownridge EA.** 1978. Growth of *Chlamydia psittaci* in macrophages. Infect. Immun. **19:**1054-1060.

11. **Blasi F, Centanni S, Allegra L.** 2004. *Chlamydia pneumoniae*: crossing the barriers? Eur. Respir. J. **23:**499-500.

12. **de Vries HJC, Smelov V, Middelburg JG, Pleijster J, Speksnijder AG, Morre SA.** 2009. Delayed microbial cure of Lymphogranuloma venereum proctitis with doxycycline treatment. Clin. Infect. Dis. **48:**E53-E56.

13. **Hoymans VY, Bosmans JM, Ieven MM, Vrints CJ.** 2007. *Chlamydia pneumoniae*-based atherosclerosis: a smoking gun. Acta Cardiol. **62:**565-571.

14. **Hammerschlag MR, Kohlhoff SA, Darville T.** 2009. *Chlamydia pneumoniae* and *Chlamydia trachomatis.* Sequelae and long-term consequences of infectious diseases pp. 27-52.

15. **Fields KA, McCormack R, de Armas LR, Podack ER.** 2013. Perforin-2 restricts growth of *Chlamydia trachomatis* in macrophages. Infect. Immun. **81:**3045-3054.

16. **Martinez FO, Gordon S.** 2014. The M1 and M2 paradigm of macrophage activation: time for reassessment. F1000prime reports **6:**13-13.

17. **Rottenberg ME, Gigliotti-Rothfuchs A, Wigzell H.** 2002. The role of IFN-gamma in the outcome of chlamydial infection. Curr. Opin. Immunol. **14:**444-451.

18. **Rothermel CD, Rubin BY, Murray HW.** 1983. Gamma-interferon is the factor in lymphokine that activates human macrophages to inhibit intracellular *Chlamydia psittaci* replication. J. Immunol.**131:**2542-2544.

19. **Shemer Y, Sarov I.** 1985. Inhibition of growth of *Chlamydia trachomatis* by human gamma interferon. Infect. Immun. **48:**592-596.

20. **Gracey E, Inman RD.** 2012. Chlamydia-induced ReA: immune imbalances and persistent pathogens. Nat. Rev. Rheumatol. **8:**55-59.

21. **Gracey E, Lin A, Akram A, Chiu B, Inman RD.** 2013. Intracellular survival and persistence of *Chlamydia muridarum* Is determined by macrophage polarization. PloS One **8**.

22. **Kuo CC.** 1978. Immediate cytotoxicity of *Chlamydia trachomatis* for mouse peritoneal macrophages. Infect. Immun. **20:**613-618.

23. **Caldwell HD, Kromhout J, Schachter J.** 1981. Purification and partial characterization of the major outer membrane protein of *Chlamydia trachomatis*. Infect. Immun. **31:**1161-1176.

24. **Jayarapu K, Kerr MS, Katschke A, Johnson RM.** 2009. *Chlamydia muridarum*-specific CD4 T-cell clones recognize infected reproductive

tract epithelial cells in an interferon-dependent fashion. Infect. Immun. **77:**4469-4479.

25. **Zhang DJ, Yang X, Berry J, Shen CX, McClarty G, Brunham RC.** 1997. DNA vaccination with the major outer-membrane protein gene induces acquired immunity to *Chlamydia trachomatis* (mouse pneumonitis) infection. J. Infect. Dis. **176:**1035-1040.

26. **Schneider CA, Rasband WS, Eliceiri KW.** 2012. NIH Image to ImageJ: 25 years of image analysis. Nat. Methods **9:**671-675.

27. **Arango Duque G, Descoteaux A.** 2014. Macrophage cytokines: involvement in immunity and infectious diseases. Front. Immunol. **5:**491-491.

28. **Dessus-Babus S, Knight ST, Wyrick PB.** 2000. Chlamydial infection of polarized HeLa cells induces PMN chemotaxis but the cytokine profile varies between disseminating and non-disseminating strains. Cell. Microbiol. **2:**317-327.

29. **O'Connell CM, Ionova IA, Quayle AJ, Visintin A, Ingalls RR.** 2006. Localization of TLR2 and MyD88 to *Chlamydia trachomatis* inclusions - Evidence for signaling by intracellular TLR2 during infection with an obligate intracellular pathogen. J. Biol. Chem. **281:**1652-1659.

30. **Kuo CC, Grayston JT.** 1976. Interaction of *Chlamydia trachomatis* organisms and HeLa 229 cells Infect. Immun. **13:**1103-1109.

31. **da Costa CUP, Wantia N, Kirschning CJ, Busch DH, Rodriguez N, Wagner H, Miethke T.** 2004. Heat shock protein 60 from *Chlamydia*

pneumoniae elicits an unusual set of inflammatory responses via Toll-like receptor 2 and 4 *in vivo*. Eur. J. Immunol. **34:**2874-2884.

32. **Ingalls RR, Rice PA, Qureshi N, Takayama K, Lin JS, Golenbock DT.** 1995. The inflammatory cytokine response to *Chlamydia trachomatis* infection is endotoxin mediated Infect. Immun. **63:**3125-3130.

33. **Yao SY, Ljunggren-Rose A, Stratton CW, Mitchell WM, Sriram S.** 2001. Regulation by IFN-beta of inducible nitric oxide synthase and interleukin-12/p40 in murine macrophages cultured in the presence of *Chlamydia pneumoniae* antigens. J. Interferon Cytokine Res. **21:**137-146.

34. **Rothfuchs AG, Gigliotti D, Palmblad K, Andersson U, Wigzell H, Rottenberg ME.** 2001. IFN-alpha beta-dependent, IFN-gamma secretion by bone-marrow-derived macrophages controls an intracellular bacterial infection. J. Immunol. **167:**6453-6461.

35. **Shimada K, Crother TR, Karlin J, Chen S, Chiba N, Ramanujan VK, Vergnes L, Ojcius DM, Arditi M.** 2011. Caspase-1 dependent IL-1 beta secretion Is critical for host defense in a mouse model of *Chlamydia pneumoniae* lung infection. PloS One **6**.

36. **Zhang Y, Wang H, Ren J, Tang X, Jing Y, Xing D, Zhao G, Yao Z, Yang X, Bai H.** 2012. IL-17A synergizes with IFN-gamma to upregulate iNOS and NO production and inhibit chlamydial growth. PloS One **7**.

37. **Wink DA, Hines HB, Cheng RYS, Switzer CH, Flores-Santana W, Vitek MP, Ridnour LA, Colton CA.** 2011. Nitric oxide and redox mechanisms in the immune response. J. Leukoc. Biol. **89:**873-891.

38. **Wink DA, Mitchell JB.** 1998. Chemical biology of nitric oxide: Insights into regulatory, cytotoxic, and cytoprotective mechanisms of nitric oxide. Free Radical Bio. Med. **25:**434-456.

39. **Parker NB, Berger EM, Curtis WE, Muldrow ME, Linas SL, Repine JE.** 1985. Hydrogen peroxide causes dimethylthiourea consumption while hydroxyl radical causes DMSO consumption *in vitro*. Free Radical Bio. Med. **1:**415-420.

40. **Boer R, Ulrich WR, Klein T, Mirau B, Haas S, Baur I.** 2000. The inhibitory potency and selectivity of arginine substrate site nitric-oxide synthase inhibitors is solely determined by their affinity toward the different isoenzymes. Mol. Pharmacol. **58:**1026-1034.

41. **Lima-Junior DS, Costa DL, Carregaro V, Cunha LD, Silva ALN, Mineo TWP, Gutierrez FRS, Bellio M, Bortoluci KR, Flavell RA, Bozza MT, Silva JS, Zamboni DS.** 2013. Inflammasome-derived IL-1 beta production induces nitric oxide-mediated resistance to *Leishmania*. Nat. Med. **19:**909-916.

42. **Kostura MJ, Tocci MJ, Limjuco G, Chin J, Cameron P, Hillman AG, Chartrain NA, Schmidt JA.** 1989. Identification of a monocyte specific pre-interleukin 1-beta convertase activity. PNAS **86:**5227-5231.

43. **Newman ZL, Leppla SH, Moayeri M.** 2009. CA-074Me protection against anthrax lethal toxin. Infect. Immun. **77:**4327-4336.

44. **Prebeck S, Kirschning C, Durr S, da Costa C, Donath B, Brand K, Redecke V, Wagner H, Miethke T.** 2001. Predominant role of toll-like

receptor 2 versus 4 in *Chlamydia pneumoniae*-induced activation of dendritic cells. J. Immunol. **167:**3316-3323.

45.   **Darville T, O'Neill JM, Andrews CW, Nagarajan UM, Stahl L, Ojcius DM.** 2003. Toll-like receptor-2, but not toll-like receptor-4, is essential for development of oviduct pathology in chlamydial genital tract infection. J. Immunol. **171:**6187-6197.

46.   **Bas S, Lief L, Vuillet M, Spenato U, Seya T, Matsumoto M, Gabay C.** 2008. The proinflammatory cytokine response to *Chlamydia trachomatis* elementary bodies in human macrophages is partly mediated by a lipoprotein, the macrophage infectivity potentiator, through TLR2/TLR1/TLR6 and CD14. J. Immunol. **180:**1158-1168.

47.   **Erridge C, Pridmore A, Eley A, Stewart J, Poxton IR.** 2004. Lipopolysaccharides of *Bacteroides fragilis*, *Chlamydia trachomatis* and *Pseudomonas aeruginosa* signal via Toll-like receptor 2. J. Med. Microbiol. **53:**735-740.

48.   **O'Connell CM, Ingalls RR, Andrews CW, Scurlock AM, Darville T.** 2007. Plasmid-deficient *Chlamydia muridarum* fail to induce immune pathology and protect against oviduct disease. J. Immunol. **179:**4027-4034.

49.   **O'Connell CM, AbdelRahman YM, Green E, Darville HK, Saira K, Smith B, Darville T, Scurlock AM, Meyer CR, Belland RJ.** 2011. Toll-Like receptor 2 activation by *Chlamydia trachomatis* Is plasmid dependent, and plasmid-responsive chromosomal loci Are coordinately regulated in

response to glucose limitation by *C. trachomatis* but not by *C. muridarum*. Infect. Immun. **79:**1044-1056.

50. **Buchholz KR, Stephens RS.** 2006. Activation of the host cell proinflammatory interleukin-8 response by *Chlamydia trachomatis*. Cell. Microbiol. **8:**1768-1779.

51. **Buchholz KR, Stephens RS.** 2007. The extracellular signal-regulated kinase/mitogen-activated protein kinase pathway induces the inflammatory factor interleukin-8 following *Chlamydia trachomatis* infection. Infect. Immun. **75:**5924-5929.

52. **Ramsey KH, Miranpuri GS, Sigar IM, Ouellette S, Byrne GI.** 2001. *Chlamydia trachomatis* persistence in the female mouse genital tract: Inducible nitric oxide synthase and infection outcome. Infect. Immun. **69:**5131-5137.

53. **Wantia N, Rodriguez N, Cirl C, Ertl T, Duerr S, Layland LE, Wagner H, Miethke T.** 2011. Toll-Like Receptors 2 and 4 regulate the frequency of IFN gamma-producing CD4(+) T-Cells during pulmonary infection with *Chlamydia pneumoniae*. PloS One **6**.

54. **Huang J, DeGraves FJ, Lenz SD, Gao DY, Feng P, Li D, Schlapp T, Kaltenboeck B.** 2002. The quantity of nitric oxide released by macrophages regulates *Chlamydia* induced disease. PNAS **99:**3914-3919.

55. **Maxion HK, Liu W, Chang MH, Kelly KA.** 2004. The infecting dose of *Chlamydia muridarum* modulates the innate immune response and ascending infection. Infect. Immun. **72:**6330-6340.

56. **Tsai H-H, Lee W-R, Wang P-H, Cheng K-T, Chen Y-C, Shen S-C.** 2013. *Propionibacterium acnes*-induced iNOS and COX-2 protein expression via ROS-dependent NF-kappa B and AP-1 activation in macrophages. J. Dermatol. Sci. **69:**122-131.

57. **Wu F, Tyml K, Wilson JX.** 2008. iNOS expression requires NADPH oxidase-dependent redox signaling in microvascular endothelial cells. J. Cell. Physiol. **217:**207-214.

58. **Boya P, Kroemer G.** 2008. Lysosomal membrane permeabilization in cell death. Oncogene **27:**6434-6451.

CHAPTER 5

DISCUSSION

A recurring theme in the evolutionary trajectories of intracellular pathogens is the degradation of the genome accompanied by niche restriction. A combination of host homeostasis and conserved host defense mechanisms have created relatively stable, predictable environments for obligate intracellular chlamydiae. So well-tuned are these bacteria to their respective hosts that human-adapted *Chlamydia trachomatis*, for instance, cannot survive in mice in spite of near-identity with the mouse pathogen *C. muridarum*. Much of this host-pathogen incompatibility appears to arise from the fact that the primary host immune mediator IFN-γ elicits different responses in humans and mice to chlamydial infection (Fig. 5.1) (1).

It is well established that tryptophan depletion in human cells is the basis of the antimicrobial effect of IFN-γ against many intracellular pathogens including *Toxoplasma* and *Chlamydia* (2). Work from several groups has revealed how genital serovars of *C. trachomatis* have evolved to overcome tryptophan starvation in human cells. *C. trachomatis* contains a tryptophan biosynthesis (*trp*) operon that it utilizes along with imported indole to make its own tryptophan, thereby no longer relying on the host for this essential amino acid (3-5). The *trp* operon of *C. trachomatis* is located in the Plasticity Zone (PZ) which is a highly variable locus between otherwise conserved chlamydial genomes (6, 7). The *C. muridarum* PZ lacks the *trp* operon, making the mouse pathogen extremely

217

susceptible to IFN-γ in human cells (8). However, *C. muridarum* can survive in mice without the *trp* gene cluster because IFN-γ does not induce tryptophan starvation in murine cells. Instead, it upregulates a family of murine GTPases that specifically localize to *C. trachomatis* inclusions but not to those of *C. muridarum* (9). The GTPases recruit autophagic machinery to the *C. trachomatis* inclusions which results in their eventual destruction (10). The factors that *C. muridarum* employs to block these immunity GPTases from docking on to its inclusions have not been identified. A clue as to the location and expression of these chlamydial IFN-γ resistance factors (IRF) was provided when Nelson et al. showed that inactive *C. muridarum* EB could partially rescue *C. trachomatis* from GTPase-mediated clearance (11). This implied that the *C. muridarum* IRF are pre-packaged into EB and are either surface-exposed or released into the host cell upon chlamydial invasion. Since the *trp* operon in the *C. trachomatis* PZ contributes to immune evasion, we asked if the *C. muridarum* PZ also conferred protection by harboring IRF genes.

We examined the *C. muridarum* PZ in Chapter 2 by employing a reverse genetic technique called Targeting Induced Local Lesions in Genomes (TILLING) adapted for chlamydial mutational analysis (5). We screened a *C. muridarum* mutant library generated by several rounds of EMS mutagenesis for nonsense mutations in select PZ genes (Fig. 5.2). Aside from *orf tc0431*, all other targeted genes were found to be non-essential. *tc0431* encodes a membrane attack complex/perforin (MACPF) domain-containing protein (8). MACPF has been

218

retained by only certain species of *Chlamydia*, and our inability to recover a *C. muridarum* MACPF nonsense mutant could indicate that the protein performs an essential function in the mouse pathogen (12). However, TILLING has its limitations in that very sick mutants may be lost from the EMS library. Thus, the indispensability of *C. muridarum* MACPF needs to be validated by other methods. Recent advances in chlamydial genetics now make it possible to transform chlamydiae and insertionally inactivate genes (13, 14). A technology called TargeTron, made commercially available by Sigma-Aldrich (St. Louis, MO) employs an intronII-based platform to insert mobile introns into specific sites within a target gene. Attempts will be made in the future to disrupt *C. muridarum* MACPF by TargeTron.

C. muridarum PZ genes that were found to be non-essential include putative cytotoxin *orfs tc0437 – tc0439*, a phospholipase D gene *tc0440* and a *guaBA – add* nucleotide synthesis operon *tc0443 – tc0441*. All isolated PZ mutants displayed mild growth defects, but whether these defects were caused by mutations in the PZ as opposed to background mutations could not be distinguished. Previous studies have suggested that cytotoxin *orfs* encode IFN-γ resistance factors and are also responsible for the cytotoxicity associated with *C. muridarum* EB at high multiplicities of infection (11, 15). An examination of the cytotoxic potential of the toxin mutants revealed that *tc0437*⁻ and *tc0439*⁻ did in fact induce less cell damage than the *C. muridarum* wild-type parent. However, none of the toxin mutants displayed any sensitivity to IFN-γ in murine cells. Other PZ mutants also retained wild-type resistance to the cytokine, implying that the

IRF were likely encoded by genes outside the PZ. The reduced cytotoxicity associated with *tc0437* ⁻ and *tc0439* ⁻ strongly indicate that these *orfs* are functional and induce cytopathic damage. Whether *tc0438* is non-functional or plays an unrelated role in chlamydial infection needs to be evaluated. Since infection with *tc0437* ⁻ and *tc0439* ⁻caused some cytotoxicity, whether the chlamydial cytotoxins have additive roles will need to be assessed by creating a mutant lacking all three toxins.

Infection of the mouse genital tract (GT) with *C. muridarum* PZ mutants revealed no dramatic differences in terms of infectious burden or duration of infection. These results, combined with the retention of resistance to IFN-γ *in vitro*, suggests that individual PZ genes do not confer survival advantages to *C. muridarum* in the GT. This does not necessarily imply that *C. muridarum* PZ genes are non-functional. Assuming they encode proteins with niche-specific roles, they might function only in the relevant host tissue. The *C. muridarum* mouse GT model is an artificial system that has been employed because of its close resemblance to human chlamydial disease (16). However, *C. muridarum* was originally isolated from mice lungs and studies suggest that it might be a gut pathogen (17, 18). Future work will involve the analysis of PZ mutants for their ability to infect and colonize the mouse lung and gut. Since we know that PZ genes are dispensable, PZ-null mutants will be generated by TargeTron to avoid the complication of EMS-induced background mutations.

Since the PZ genes targeted by TILLING did not appear to encode *C. muridarum* IRF, we embarked on a forward genetic screen described in Chapter 3 to identify putative IRF genes. 31 mutants with varying degrees of sensitivity to murine IFN-γ were isolated from an EMS-derived *C. muridarum* mutant library. Whole genome sequencing of four selected IFN-γ-sensitive mutants (*igs1 – igs4*) revealed multiple mutations in each strain. All four strains were found to carry inactivating mutations in *tc0412*; however, the gene was discovered to be polymorphic in the population. We therefore focused our efforts on *igs4* since it displayed the greatest sensitivity to IFN-γ. A suppressor screen yielded multiple revertants that restored IFN-γ resistance to *igs4*. Sequence analysis indicated that most revertants contained additional mutations in *tc0574* aside from the original missense mutation in *igs4*. Interestingly, many of the suppressor mutations were predicted to inactivate TC0574. This suggested that the original *tc0574* missense mutation in *igs4* was a deleterious gain-of-function mutation and that loss of the protein in the revertants allowed them to overcome IFN-γ-mediated inhibition.

As mentioned previously, IRF present in inactive *C. muridarum* wild-type EB can rescue *C. trachomatis* from IFN-γ responses in murine cells (11). Since *ig45* was nearly as sensitive to IFN-γ as *C. trachomatis*, we hypothesized that *igs4* EB would be unable to rescue *C. trachomatis* from inhibition in IFN-γ-treated murine cells. However, co-infection of inactive *igs4* EB with *C. trachomatis* caused a significant increase in *C. trachomatis* infectious yield that was comparable to the rescue observed with wild-type *C. muridarum* EB. This

indicates that *igs4* contains some intact IRF but is still sensitive to IFN-γ. These results imply that the IFN-γ resistance phenotype is more complex than previously envisioned. That no other sequenced *igs* mutant (*igs1 – ig3*) contained mutations in *tc0574* also supports the notion that multiple independent effectors contribute to *C. muridarum* IFN-γ resistance. Efforts are underway to conduct a saturating screen for additional chlamydial factors that mediate resistance to IFN-γ.

Examination of *igs4* infection course and duration in the mouse GT revealed severe attenuation of the mutant in comparison to wild-type *C. muridarum*. Shedding from mice infected with *igs4* revertants was similar to that from mice inoculated with wild-type *C. muridarum*, confirming that the *in vitro* suppressors also restored virulence to the *igs4* mutant *in vivo*. Surprisingly, *igs4* remained attenuated in IFN-γ $^{-/-}$ mice, implying that other host effectors were sufficient to control *igs4* infection in mice. That resolution of *igs4* occurs rapidly in mice suggests that IFN-γ-independent innate mechanisms may be sufficient for the clearance of *igs4*. Epithelial cells in the female urogenital tract produce type-1 interferons including IFN-β and IFN-ε that share the regulation of many pathways with IFN-γ (19-21). We found that *igs4* was equally sensitive to IFN-β in McCoy cells. Whether type-1 interferons are responsible for *igs4* attenuation in mice will be tested by infecting mice that are incapable of responding to both type I and type II interferons.

The mutated gene *tc0574* that confers IFN-γ sensitivity to *igs4* is predicted to lie in an operon with *tc0573*, and RT-PCR analysis in Chapter 4 indicated that

orfs tc0572 – tc0574 are expressed as part of a single transcript. Interestingly, an *igs4* revertant was found to contain a missense mutation in *tc0573* that abolished the start codon. Two possibilities exist to explain how a mutation that prevents *tc0573* translation affects the expression of *tc0574*:

1) Rho-dependent termination of RNA polymerase transcription:

If a large segment of mRNA remains unbound by ribosomes, a Rho factor can bind to *rut* (rho utilization) sites in the region. Upon binding, Rho uses its ATPase activity to move along the RNA until it subsequently catches up with RNA polymerase to terminate transcription.

2) Translational coupling:

When genes are translationally coupled, the translational efficiency of one gene is interdependent on another. While the exact mechanism is not well understood, a widely accepted theory is that when a gene is not being actively translated, it allows the formation of secondary mRNA structures that inhibit ribosomal binding to the downstream gene mRNA.

In the scenario of Rho-dependent termination, the mutation in *tc0573* would result in decreased levels of *tc0574* mRNA. However, we did not find any differences in *tc0574* mRNA levels between wild-type *C. muridarum*, *igs4* and the *tc0573* revertant. This suggests that *tc0573* and *tc0574* are translationally coupled. To confirm this, a comparison of TC0574 protein levels in wild-type, *igs4* and the *tc0573* revertant by western blotting is required.

TC0573 and TC0574 are predicted to contain Inc domains that would result in their localization to the chlamydial inclusion membrane (22). While no

223

function has been attributed to these proteins, our results indicate that TC0574 is not essential for growth in cell culture and virulence in mice. Interestingly, some *igs4* inclusions ruptured early during infection even in the absence of IFN-γ, and the addition of the cytotokine dramatically exacerbated this phenotype. This observation, combined with its dispensability, leads us to propose that wild-type TC0574 has a redundant function at the inclusion membrane, but the mutated protein in *igs4* leads to inclusion membrane instability, perhaps due to a conformational change. Interestingly, a BLAST search for homologous proteins in other species of *Chlamydia* returned only two proteins with very low identity scores, one found in *C. trachomatis* and the other in *C. caviae*. A Phyre2 structure prediction for TC0574 and the *C. trachomatis* serovar D homolog generated models where both proteins contained two α-helices in different spatial arrangements (23). The helices in TC0574 are packed together, with the glycine residue that is mutated in *igs4* located at the interacting surface. The glycine ⇒ glutamate substitution in *igs4* could cause the protein to adopt a conformation that is similar to the *C. trachomatis* protein. How these different predicted conformations alter protein function needs to be determined.

Future studies will focus on identifying the mechanism that contributes to the IFN-γ sensitivity displayed by *igs4*. It will also be important to confirm that *tc0574* is expressed and if it localizes to the inclusion membrane. We have determined the mutant is not sensitive to IFN-γ-induced nitric oxide or reactive oxygen species, but whether it can actively block the localization of IFN-γ-regulated GTPases to its inclusions requires investigation.

While IFN-γ-dependent adaptive cellular immunity is crucial for resolving chlamydial disease, innate phagocytic cells (neutrophils and macrophages) act as first responders at the site of infection and orchestrate the immune response against *Chlamydia*. Surprisingly, some species of *Chlamydia* are capable of survival and limited replication within the hostile environment of macrophages, a property that correlates with invasive disease and chronic inflammation. The parameters that contribute to chlamydial growth or persistence within macrophages have not been well defined.

Chapter 4 was born out of the observation that the survival of *C. muridarum* in RAW 264.7 macrophages depends on the multiplicity of infection (MOI). An MOI of 2 or lower was optimal for a productive infection; however, MOIs ranging from 3 to 100 resulted in a corresponding decrease in chlamydial yield from macrophages. *C. muridarum* could not be recovered from cells infected at an MOI of 100 because these high infectious doses resulted in immediate macrophage death. In contrast, chlamydial inhibition by macrophages infected at more moderate doses was found to occur because of macrophage activation. Activated RAW cells expressed high levels of inducible nitric oxide synthase (iNOS) and secreted inhibitory factors into culture supernatants. Accordingly, an inhibitor of iNOS fully restored chlamydial growth in infected cells. We found that TLR2, but not TLR4, was required for the activation of macrophages by *C. muridarum*; however, the cognate chlamydial antigen has not been identified. Complete chlamydial inhibition by macrophages required the

225

presence of live, transcriptionally active *C. muridarum*, indicating that at least one antigen was present only in replicating chlamydiae.

A new pathway of iNOS regulation was discovered in RAW macrophages when an inhibitor of cathepsin B and a hydoxyl radical scavenger were found to rescue *C. muridarum* by blocking iNOS induction. Further investigation revealed that reactive oxygen species (ROS) controlled cathepsin B activation. Our current model of chlamydial inhibition in RAW macrophages can be described as follows: an intermediate multiplicity of infection is not immediately cytotoxic, but instead provides enough chlamydial antigen for macrophage activation. Once activated, increased accumulation of macrophage ROS either directly or indirectly enhances lysosomal cathepsin B activity. Active cathepsin B, in turn, upregulates iNOS expression. The resulting production of nitric oxide effectively eradicates intracellular chlamydiae.

Several questions regarding macrophage chlamydial inhibition need to be addressed. Firstly, is the described mechanism of iNOS regulation in infected RAW cells conserved in primary macrophages? Second, what are the intermediate steps between ROS production, cathepsin B activation and iNOS induction? Finally, can this observation in macrophages be extrapolated to chlamydial infection in mice and humans? Past research has indicated that disease outcome in murine and lung models of chlamydial infection is linked to the inoculating dose and the quantity of nitric oxide released by macrophages, thus lending support to our *in vitro* findings.

In summary, our genetic and immunological studies have examined important host immune mechanisms that control chlamydial infection in cell culture and mice. We find that both host and pathogen have evolved multiple defense strategies that allow coexistence. Further genetic investigation on the biology of chlamydiae will reveal new adaptive mechanisms to assist in the design of effective therapeutics against these pathogens.
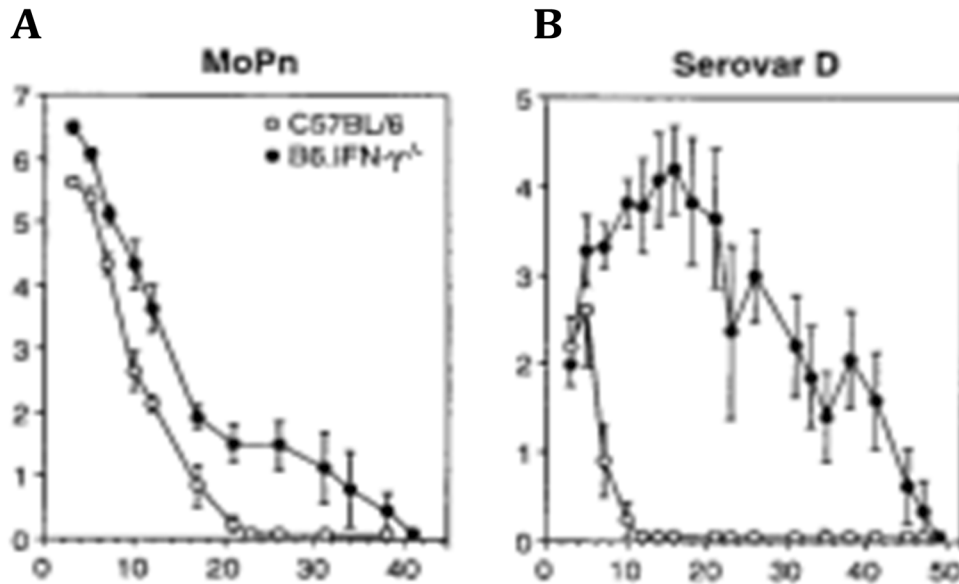
Fig. 5.1. *C. trachomatis* and *C. muridarum* **behave dissimilarly in mice.**
(A) *C. muridarum* (MoPn) infection of IFN-γ knockout mice (B6.IFN-γ$^{/-}$) does not significantly differ from MoPn infection in wild-type C57BL/6 mice. (B) *C. trachomatis* serovar D is cleared from C57BL/6 mice at around 10 days post inoculation. Course of infection in B6.IFN-γ$^{/-}$ of serovar D is more similar to that of MoPn.
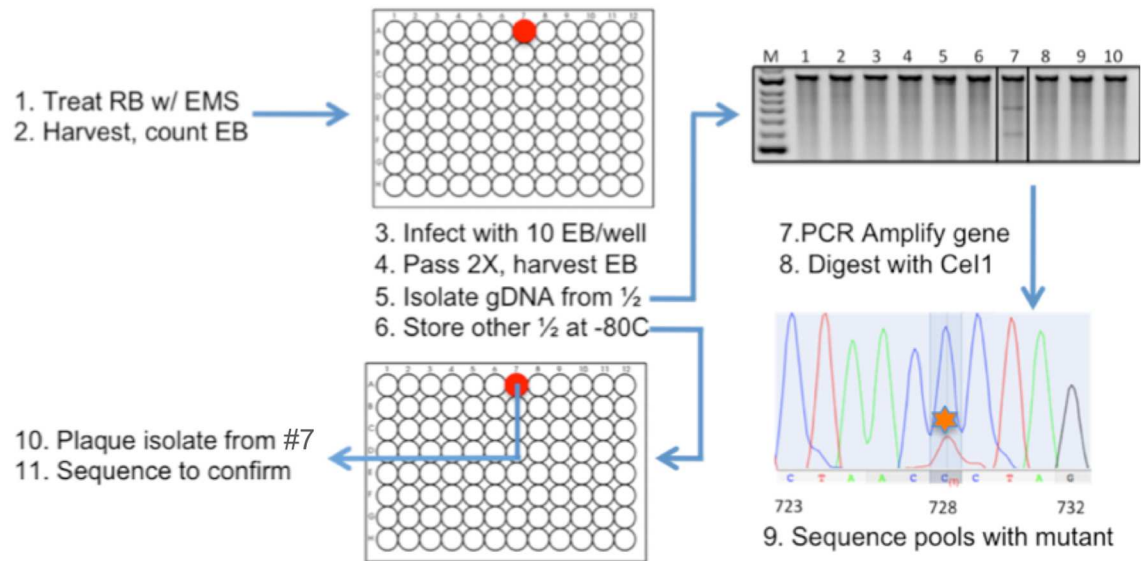
Fig. 5.2. Targeting Induced Local Lesions IN Genomes. Schematic description of the TILLING mutagenesis protocol.
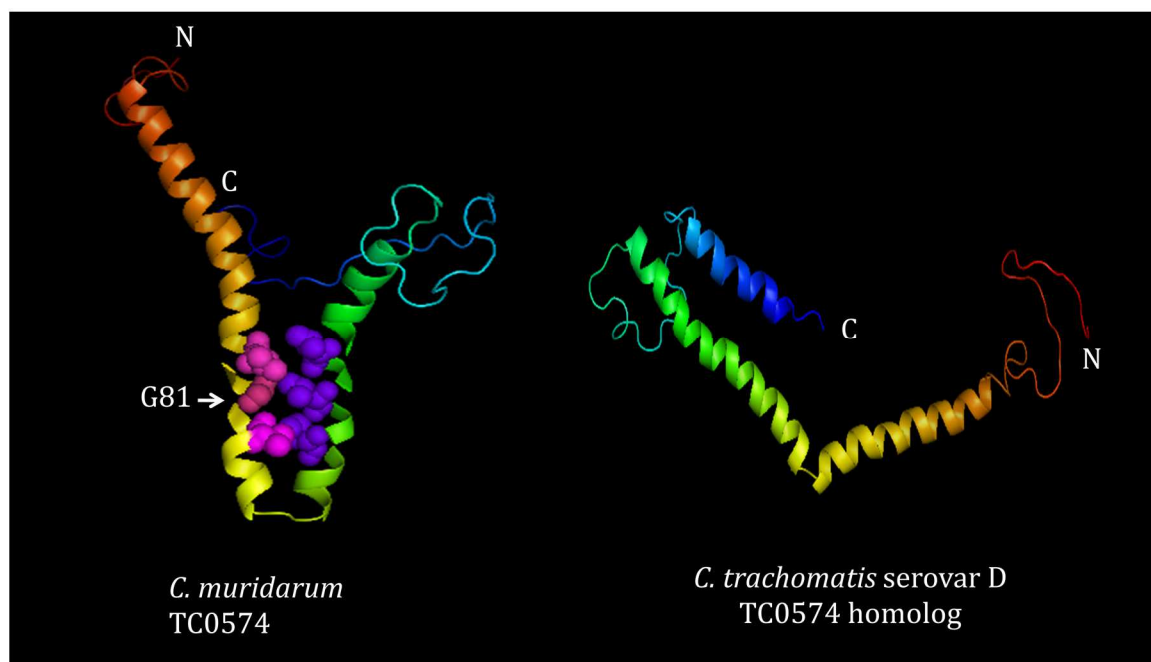
Fig. 5.3. Phyre2 modeling of *C. muridarum* TC0574 and its *C. trachomatis* homolog. *C. muridarum* TC0574 (left) contains two predicted α-helices. The mutated glycine residue in *igs4* and interacting neighboring residues are colored using PyMOL (The PyMOL Molecular Graphics System, Schrödinger, LLC). The α-helices in the *C. trachomatis* serovar D TC0574 homolog (right) are positioned away from each other. (N, N-terminal; C, C-terminal).

5.1 References

1. **Perry LL, Su H, Feilzer K, Messer R, Hughes S, Whitmire W, Caldwell HD.** 1999. Differential sensitivity of distinct *Chlamydia trachomatis* isolates to IFN-gamma-mediated inhibition. J. Immunol. **162:**3541-3548.

2. **Moulder JW.** 1991. Interaction of chlamydiae and host cells *in vitro*. Microbiol. Rev. **55:**143-190.

3. **Caldwell HD, Wood H, Crane D, Bailey R, Jones RB, Mabey D, Maclean I, Mohammed Z, Peeling R, Roshick C, Schachter J, Solomon AW, Stamm WE, Suchland RJ, Taylor L, West SK, Quinn TC, Belland RJ, McClarty G.** 2003. Polymorphisms in *Chlamydia trachomatis* tryptophan synthase genes differentiate between genital and ocular isolates. J. Clin. Invest. **111:**1757-1769.

4. **Fehlner-Gardiner C, Roshick C, Carlson JH, Hughes S, Belland RJ, Caldwell HD, McClarty G.** 2002. Molecular basis defining human *Chlamydia trachomatis* tissue tropism - A possible role for tryptophan synthase. J. Biol. Chem. **277:**26893-26903.

5. **Kari L, Goheen MM, Randall LB, Taylor LD, Carlson JH, Whitmire WM, Virok D, Rajaram K, Endresz V, McClarty G, Nelson DE, Caldwell HD.** 2011. Generation of targeted *Chlamydia trachomatis* null mutants. PNAS **108:**7189-7193.

6. **Stephens RS, Kalman S, Lammel C, Fan J, Marathe R, Aravind L, Mitchell W, Olinger L, Tatusov RL, Zhao QX, Koonin EV, Davis RW.**

1998. Genome sequence of an obligate intracellular pathogen of humans: *Chlamydia trachomatis*. Science **282:**754-759.

7.   **Read TD, Myers GSA, Brunham RC, Nelson WC, Paulsen IT, Heidelberg J, Holtzapple E, Khouri H, Federova NB, Carty HA, Umayam LA, Haft DH, Peterson J, Beanan MJ, White O, Salzberg SL, Hsia RC, McClarty G, Rank RG, Bavoil PM, Fraser CM.** 2003. Genome sequence of *Chlamydophila caviae* (*Chlamydia psittaci* GPIC): examining the role of niche-specific genes in the evolution of the Chlamydiaceae. Nuc. Ac. Res. **31:**2134-2147.

8.   **Read TD, Brunham RC, Shen C, Gill SR, Heidelberg JF, White O, Hickey EK, Peterson J, Utterback T, Berry K, Bass S, Linher K, Weidman J, Khouri H, Craven B, Bowman C, Dodson R, Gwinn M, Nelson W, DeBoy R, Kolonay J, McClarty G, Salzberg SL, Eisen J, Fraser CM.** 2000. Genome sequences of *Chlamydia trachomatis* MoPn and *Chlamydia pneumoniae* AR39. Nuc. Ac. Res. **28:**1397-1406.

9.   **Nelson DE, Virok DP, Wood H, Roshick C, Johnson RM, Whitmire WM, Crane DD, Steele-Mortimer O, Kari L, McClarty G, Caldwell HD.** 2005. Chlamydial IFN-gamma immune evasion is linked to host infection tropism. PNAS **102:**10658-10663.

10. **Al-Zeer MA, Al-Younes HM, Braun PR, Zerrahn J, Meyer TF.** 2009. IFN-gamma-Inducible Irga6 mediates host resistance against *Chlamydia trachomatis* via autophagy. PloS One **4**.

11. **Nelson DE, Taylor LD, Shannon JG, Whitmire WM, Crane DD, McClarty G, Su H, Kari L, Caldwell HD.** 2007. Phenotypic rescue of *Chlamydia trachomatis* growth in IFN-gamma treated mouse cells by irradiated *Chlamydia muridarum*. Cell. Microbiol. **9:**2289-2298.

12. **Voigt A, Schofl G, Saluz HP.** 2012. The *Chlamydia psittaci* genome: A comparative analysis of intracellular pathogens. PloS One **7**.

13. **Wang YB, Kahane S, Cutcliffe LT, Skilton RJ, Lambden PR, Clarke IN.** 2011. Development of a transformation system for *Chlamydia trachomatis*: restoration of glycogen biosynthesis by acquisition of a plasmid shuttle vector. PLoS Pathog. **7**.

14. **Johnson CM, Fisher DJ.** 2013. Site-specific, insertional inactivation of *incA* in *Chlamydia trachomatis* using a group II Intron. PloS One **8**.

15. **Belland RJ, Scidmore MA, Crane DD, Hogan DM, Whitmire W, McClarty G, Caldwell HD.** 2001. *Chlamydia trachomatis* cytotoxicity associated with complete and partial cytotoxin genes. PNAS **98:**13984-13989.

16. **Barron AL, White HJ, Rank RG, Soloff BL, Moses EB.** 1981. A new animal model for the study of *Chlamydia trachomatis* genital infections: infection of mice with the agent of mouse pneumonitis. J. Infect. Dis. **143:**63-66.

17. **Rank RG.** 2006. Chlamydial Diseases. The Mouse in Biomedical Research: Diseases**:**325-348.

18. **Cotter TW, Ramsey KH, Miranpuri GS, Poulsen CE, Byrne GI.** 1997. Dissemination of *Chlamydia trachomatis* chronic genital tract infection in gamma interferon gene knockout mice. Infect. Immun. **65:**2145-2152.

19. **Nagarajan UM, Prantner D, Sikes JD, Andrews CW, Jr., Goodwin AM, Nagarajan S, Darville T.** 2008. Type I interferon signaling exacerbates *Chlamydia muridarum* genital infection in a murine model. Infect. Immun. **76:**4642-4648.

20. **Fung KY, Mangan NE, Cumming H, Horvat JC, Mayall JR, Stifter SA, De Weerd N, Roisman LC, Rossjohn J, Robertson SA, Schjenken JE, Parker B, Gargett CE, Nguyen HP, Carr DJ, Hansbro PM, Hertzog PJ.** 2013. Interferon-epsilon protects the female reproductive tract from viral and bacterial infection. Science **339:**1088-1092.

21. **Hermant P, Michiels T.** 2014. Interferon-lambda in the context of viral Infections: Production, response and therapeutic implications. J. Innate Immun. **6:**563-574.

22. **Lutter EI, Martens C, Hackstadt T.** 2012. Evolution and conservation of predicted inclusion membrane proteins in Chlamydiae. Comp. Funct. Genomics **21:**362104.

23. **Kelley LA, Sternberg MJE.** 2009. Protein structure prediction on the Web: a case study using the Phyre server. Nature Protocols **4:**363-371.

Krithika Rajaram

Department of Microbiology and Immunology ♦ Indiana University-School of Medicine
Medical Science Building 409 ♦ 635 Barnhill Drive ♦ Indianapolis-46202
Cell: (812) 606-5801 ♦ Lab: (317) 278-4409 ♦ e-mail: rajaramk@indiana.edu

----

Education

February 2015	Ph.D., Department of Biology Indiana University, Bloomington, IN
May 2008	B.Tech., Department of Biotechnology Anna University, Coimbatore, India

----

Research Experience

2008 – present **Graduate Student**
Department of Biology, Indiana University, Bloomington, IN
Advisor: Dr. David Nelson
Thesis Project: Studies of host-chlamydial interactions mediated by interferon-γ and nitric oxide

2007 – 2008 **Undergraduate Research Assistant**
The Wellcome Trust Research Laboratory, Department of Gastrointestinal Sciences, Christian Medical College and Hospital, Vellore, India
Advisor: Dr. B.S. Ramakrishnan
Project: A study of curd microflora and its probiotic properties

Summer 2007 **Indian Academy of Sciences Summer Fellow**
Molecular Biophysics Unit, Indian Institute of Science, Bangalore, India
Advisor: Dr. P. Balaram
Project: Purification and unfolding studies on Triosephosphate Isomerase from *Methanocaldococcus jannaschii*

2006 – 2007 **Undergraduate Research Assistant**
Department of Biotechnology, Anna University, Coimbatore, India
Advisor: Dr. S. Shanmugam
Project: Bioremedial properties of *Ganoderma lucidum* and *Agaricus bisporus*

Publications
----

1. Kari L, Goheen M, Randall L, Taylor L, Carlson J, Whitmire W, Virok D, **Rajaram K**, Endresz V, McClarty G, Nelson D, and Caldwell H. Generation of targeted *Chlamydia trachomatis* null mutants. ***Proc Natl Acad Sci U S A.*** **2011**; 108:7189–7193.

2. Balamurugan R, Chandragunasekaran AS, Chellappan G, **Rajaram K**, Ramamoorthi G, Ramakrishna BS. Probiotic potential of lactic acid bacteria present in home made curd in southern India. ***Indian J Med Res.*** **2014**; 140:345-55.

Manuscripts
----

1. **Rajaram K**, Giebel A, Toh E, Hu S, Newman J, Morrison S, Laszlo K., Suchland R, Morrison R and Nelson D. Mutational analysis of the *Chlamydia muridarum* Plasticity Zone. Submitted.

2. Hu S, **Rajaram K**, Brothwell J, Toh E, Morrison S, Suchland R, Morrison R and Nelson D. A genetic screen reveals that *Chlamydia muridarum* IFN-γ resistance is a complex phenotype. In preparation.

3. **Rajaram K** and Nelson DE. Chlamydia muridarum infection elicits bactericidal nitric oxide production via reactive oxygen species and cathepsin B. In preparation.

Conference Presentations (Oral)

2013	**Chlamydia Basic Research Society** San Antonio, TX
2012	**European Society for Chlamydial Research** Amsterdam, Netherlands
2007	**Opportunities & Challenges in Biotechnology and Environmental Sciences** Erode, India
2007	**Regional Microbiology Symposium** Coimbatore, India

Conference Presentations (Poster)

2011	**Annual Midwest Microbial Pathogenesis Conference** Ann Arbor, MI
2011	**Microbial Pathogenesis and Host Response Meeting** Cold Spring Harbor Laboratory, NY

Awards and Scholarships

2013   **Floyd Travel Award**
Department of Biology, Indiana University

2009 – 2012   **Floyd Microbiology Summer Fellowship**
Department of Biology, Indiana University

2008   **Best Outgoing Student Award**
Anna University, Coimbatore, India

2006 – 2007   **Dr.A.P.J.Abdul Kalam Merit Scholarship**
Anna University, Coimbatore, India

2007   **Summer Research Fellowship**
Indian Academy of Sciences, Bangalore, India

2003   **Merit Scholarship**
CSIR Program on Youth for Leadership in Science, Karaikudi, India

----

Teaching Experience

2013   **Research Mentor** for Undergraduate STARS student
Department of Biology, Indiana University

2012   **Guest Lecturer**
L585 Genetics, Department of Biology, Indiana University

2011 – 2012   **Associate Instructor**
L211 Molecular Biology, Department of Biology, Indiana University

2010   **Associate Instructor**
L321 Immunology, Department of Biology, Indiana University